Synthesis and Antimalarial Evaluation of Gold Thiosemicarbazone Complexes and Polyamine-Thiosemicarbazone Dendrimers

Setshaba David Khanye

University of Cape Town

February 2010

Synthesis and Antimalarial Evaluation of Gold Thiosemicarbazone Complexes and Polyamine-Thiosemicarbazone Dendrimers

A thesis submitted to the University of Cape Town
in partial fulfillment of the requirements
for the degree of Doctor of Philosophy

By

Setshaba David Khanye

Thesis Supervisor: **Professor Kelly Chibale**
Co-supervisor: **Doctor Gregory Smith**

Department of Chemistry
University of Cape Town
Rondebosch, 7701
Cape Town

February 2010

DEDICATION

To the following late people:

Friend and a sister **Nswabiseng "Swabi" Skosana;** three important members of my community u**-Baba** no**-Mama Tshabalala** and their son **Sizwe "Bizo" Tshabalala;** my relatives **Puleng Khanye,** u-**Mkhulu** and no-**Gogo Masiteng** and their son **Makhehleni Masiteng;** my former principal in **Dedangifunde Senior Secondary School** Mr **W.A.L Mlambo.**

I will always remember you for your valuable words of encouragement and support throughout my studies.

ACKNOWLEDGEMENTS

I would like to thank my creator Almighty God for His blessings and protection throughout these years.

My heartfelt thanks go to my supervisor Prof. Kelly Chibale for his guidance, patience, support and encouragement. Many thanks also to my co-supervisor Dr. Gregory Smith for all his endless support. I would also like to extend my sincere thanks to Mrs Elaine Rutherfoord-Jones for her excellent administrative and academic support. My great appreciation and thanks to the non-academic staff in Department of Chemistry for their support.

Sincere thanks to my family: grandmother, mom, brother Yatiso Khanye, aunties, cousins especially Nthabuseng Tsotetsi, the little new fellows in our family Sandile and Lwethu Khanye for everything they have done for me and unconditional love. My family friends: Mr. and Mrs. Skosana, their daughters Tshepi, Petlele, Anna and Thandi for their support and encouragement.

I would like to thank Mr. Noel Hendricks, Mr. Pete Roberts, Mr. Pierro Benincasa and Dr. Nikoletta Báthori (University of Cape Town) for NMR experiments, microanalysis and X-ray crystallography data. Thanks are extended to Dr. Marietjie Stander (University of Stellenbosch) and Dr. Andreas Dinsmore (University of the Witwatersrand) for mass spectra data collection. I also thank the laboratories of Prof. Pete Smith (Division of Pharmacology, UCT), Prof. Phillip J. Rosenthal (University of California in San Francisco,

USA), and Dr. V. Yardley (London School of Hygiene Tropical Medicine, UK) for *in vitro* assays.

AuTEK Consortium members: Dr. Judy Coates, Dr. Mabel Coyanis and Dr. Frederik Kriel your contribution in one way or another is acknowledged.

It has been a blessing and privilege to occupy the laboratory with great individuals from my group (past and present) and all the best for your future endeavors. Other occupants in the laboratory whom I share both the East and West wing are also acknowledged for creating conducible working environment throughout these years.

Finally, it would not be possible to complete this project without AuTEK Biomed (Mintek and Harmony Gold), NRF and University of Cape Town for their financial support.

ABSTRACT

Malaria still remains one of the most dangerous widespread parasitic diseases in developing nations. Reported alarming figures of malaria infections annually highlight the 'gap' that remains to be filled to rid endemic of malaria. As cases of increasing spread of malaria and the emergence of resistance continue to exert pressure on health systems in most affected areas, novel antimalarial compounds are endlessly needed to overcome the problem of malaria infections.

This thesis presents research investigating a series of thiosemicarbazones (TSCs) and their novel gold complexes and dendrimers as potential antimalarial agents.

A series of TSCs were synthesised in one step using Schiff base chemistry. On the other hand pyrazoline analogues were obtained in two steps using both Mannich and Schiff base chemistries. A range of gold(I) TSC complexes were achieved by reacting TSCs with the starting gold(I) materials, [$Au^{I}(PEt_3P)Cl$] (**4.2**), [$Au^{I}(THT)Cl$] (**4.3**), [$Au^{I}(Ph_3P)Cl$] (**4.5**), [$Au^{I}(PTA)Cl$] (**4.24**), and $C_6F_5Au^{I}(THT)$ (**4.34**). Further reaction of TSCs with starting gold(III) complex **2.15** yielded the corresponding series of gold(III) TSC complexes. All the compounds were characterised by multinuclear NMR and FT-IR spectroscopies, mass spectrometry and elemental analysis. Gold(I) complexes **4.15** and **4.16** were further characterised by single X-ray crystallography.

The synthesised ligands and complexes were tested for their antiplasmodial activity against chloroquine-sensitive (D10, 3D7) and chloroquine-resistant (W2, K1) strains of the malaria parasite *Plasmodium falciparum*. These compounds were also evaluated for inhibitory activity against the malarial cysteine protease (falcipain-2). In most cases gold complexes showed enhanced antiplasmodial activities relative to their corresponding ligands. However, no correlation was found between antiplasmodial activities and the inhibition of falcipain-2 in respect of studied compounds.

Reaction of TSC thioesters **6.23** with branched dendritic polyamines (PAs) led to two series of polyamine-TSC dendrimers **6.24** and **6.25** whose chemical structures were elucidated using a range of techniques. Similarly, these dendritic TSCs were also tested for their antiplasmodial activity against the W2 strain. Generally, this class of compounds displayed improved antiplasmodial activities in the mid to low micromolar range. The most active compounds were **6.24c** (IC_{50} = 0.79 μM) and **6.24d** (IC_{50} = 0.67 μM), respectively.

TABLE OF CONTENTS

LIST OF ABBREVIATIONS

AIDS	Acquired immune deficiency syndrome
Ar	Aromatic/Aryl
ART	Artesiminin
^{13}C NMR	Carbon Nuclear Magnetic Resonance
$CDCl_3$	Deuterochloroform
CQ	Chloroquine
CQDP	Chloroquine disphosphate
Cp	Cyclopentadienyl
DCM	Dichloromethane
DMSO-d_6	Deuterodimethylsulfoxide
DMF	Dimethylformamide
DNA	Deoxyribonucleic acid
EtOAc	Ethyl acetate
EtOH	Ethanol
Et	Ethyl
ESI	Electrospray ionization
FAB	Fast Atomic Bombardment
Fc	Ferrocene
FQ	Ferroquine
FT-IR	Fourier Transform Infrared
^{1}H NMR	Proton Nuclear Magnetic Resonance
h	Hour
HCl	Hydrochloric acid
HNO_3	Nitric acid
Hex	Hexane
HIV	Human immunodeficiency virus
His	Histidine
IC_{50}	50% Inhibitory Concentration
kg	kilogram

m.p.	Melting point
m/z	Mass to charge ratio
mg	milligram
MeOH	Methanol
$MgSO_4$	Magnesium sulfate
MS	Mass spectrometry
mmol	Millimole
ml	Milliliter
nM	Nanomolar
NaOH	Sodium hydroxide
NADPH	Nicotinamide adenine dinucleotide phosphate
*µ*g	Micrograms
*µ*M	Micromolar
ppm	Parts per million
Ph	Phenyl
^{31}P NMR	Phosphorus Nuclear Magnetic Resonance
R_f	Retention factor
RR	Ribonucleotide reductase
SAR	Structure activity relationship
TB	Tuberculosis
THT	Tetrahydrothiophene
TLC	Thin layer chromatography
TSC	Thiosemicarbazone
TSCs	Thiosemicarbazones
TSCz	Thiosemicarbazide
UV	Ultraviolet
WHO	World Health Organization

PUBLICATION AND CONFERENCE PARTICIPATION

S.D. Khanye, N.B. Báthori, G.S. Smith, K. Chibale;
Gold(I) derived thiosemicarbazone complexes with rare halogen-halogen interaction-reduction of [Au(damp-C^1,N)Cl^2], *Dalton Transactions*, **2010**, 39, 2697-2700.

Conference Presentations

S.D. Khanye, G.S. Smith, K. Chibale;
Solvent dependent reactions: Synthesis of gold(I) and gold(III) thiosemicarbazone complexes, **September 2009**, Bloemfontein, **Poster**.

S.D. Khanye, G.S. Smith, K. Chibale;
Gold(I) thiosemicarbazone complexes as potential antimalarial cysteine protease inhibitors, Gordon Research Seminar (Bioinorganic Chemistry), **February 2010**, Ventura (CA), USA, **Data Blitz and a Poster**.

CHAPTER 1

INTRODUCTION AND LITERATURE REVIEW

1.1 HISTORY OF MALARIA AND ITS DISCOVERY

Malaria remains amongst the leading global health security threats worldwide.[1] It is one of the earliest diseases,[2] which has infected humans for many centuries.[3] It could be traced as far back as in 2700 BC, and evidence showing early documentations of the disease is found in recorded history in China, the Middle East and ancient Egypt.[4] The Romans named the disease "*mala aria*" – as at that time the disease was associated with "bad air" surrounding stagnant water.[4]

It was however, not until 1880 that the true cause of malaria became clear. Charles Louis Alphonse Laveran discovered the parasite in human blood, and was awarded a Nobel Prize in 1907.[3] Several years later the mode of transmission of the disease was demonstrated by Ronald Ross. He identified mosquitoes as being the vector of the protozoan parasite, and established the complete parasite life cycle. He was awarded the Nobel Prize in 1902 for his pioneering work.[3]

1.1.1 Malaria Today and Extent of the Problem

Malaria puts economic affairs of many affected countries in jeopardy. Despite years of research,[5,6] to date, malaria remains a major cause of illness. The burden of this disease remains a major concern as recent estimates stand well above 300 million infections annually.[7,8] The death

toll due to the disease is on the increase and more clinical cases are continuously being reported each year (Table 1.1).[9,10]

Table 1.1: Estimates of malaria cases and death by region.

Region	Global cases [%]	Global death [%]
Africa	71	85.7
Asia	26	9.4
The Americas	1	0.1
Middle East	<3	~5

Currently, between 1 and 3 million people are being killed by the disease each year.[11,12] More than 75% of the victims are African children under the age of five years and women during pregnancy.[12,13] About thirty high-burden countries in Africa and five in Asia contribute to 98% of the total deaths globally.

1.1.2 Malaria Distribution and Population at Risk

In many countries, malaria is widely accepted as a greater health problem. Fig. 1.1 below illustrates the geographical distribution of the disease worldwide.[14] The disease is prevalent in areas where environmental conditions are conducive for vector multiplication. It is estimated that over 40% of the world's population resides in malaria endemic areas, which are centred not only in tropical, but also in many temperate regions.[15] As malaria is a non-uniform disease due to many manifestations, its impact varies depending on the epidemiological setting. Some of the figures released by WHO are that 36% of the global population resides in areas where there is a significant

risk of malaria transmission, 7% is in areas where there has been non-existence of meaningful malaria control.[16] While regions which were once declared malaria free zones, 29% of the population in those areas is now experiencing resurgence of the disease.

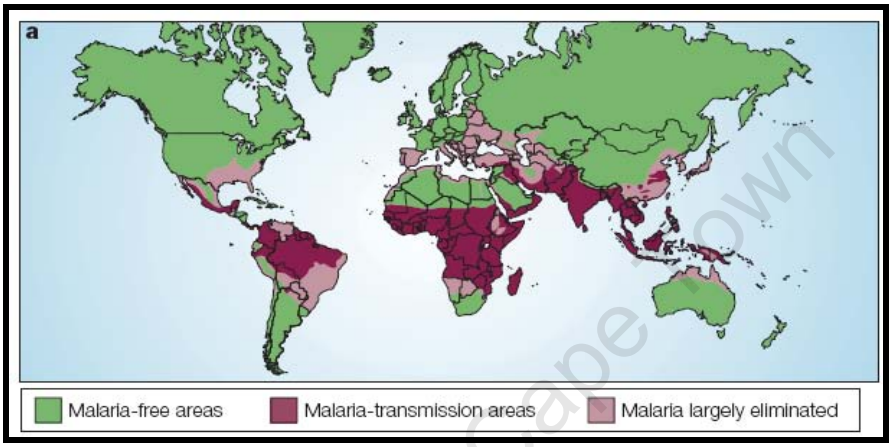

Figure 1.1: Geographical distribution of malaria.[14]

Whilst the development of new treatments to combat drug resistant strains is critical, it is equally essential to understand the biochemistry (*i.e.* the life cycle of *Plasmodium* species) of the parasite as it forms the basis for the discovery of new drugs.

1.2 BIOCHEMISTRY OF PLASMODIUM FALCIPARUM

1.2.1 The Life Cycle of the Parasite

P. falciparum is one of the four species of protozoan parasites (the other three are *P. vivax*, *P. malariae* and *P. ovale*), which are pathogenic in humans and also the most dangerous. The life cycle of the malaria parasite is depicted in Fig. 1.2.[17] It is comprised of the asexual and sexual phases. The former takes place in the host and the latter in the mosquito.[17,18]

1.2.1.1 Host: Asexual Phase

Malaria transmission to humans is initiated by the bite of an infected female *anopheles* mosquito during blood feeding. In the course of this event, the mosquito injects saliva into humans, which carries infective parasite cells called sporozoites **(1)**.

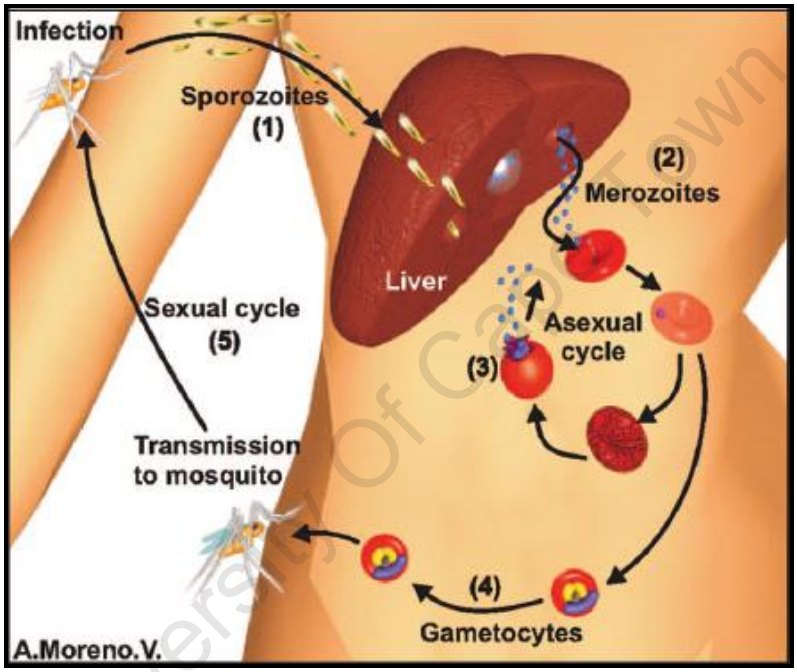

Figure 1.2: The life cycle of the malaria parasite.[17]

The sporozoites, after at least four hours at the injection site, find their way to the liver where they invade hepatocyte cells. Inside the cells, sporozoites develop into exo-erythrocytic schizonts in a period of 9–16 days.[7] Each schizont contains thousands of "daughter" parasites called merozoites **(2)**. Upon the release (coinciding with sharp increases in body temperature) from hepatocyte cells, they invade the red-blood cells (RBC) where each matures into a schizont containing 8 to 32 new merozoites. The

rupturing of the RBC results in the release of merozoites **(3)**, which are free to invade additional RBC. The rupturing of RBC is associated with intermittent fever, which signals the clinical onset of malaria.[17]

1.2.1.2 Mosquito: Sexual Phase

The parasite may differentiate into sexual forms called gametocytes **(4)**. Ingestion of gametocytes by the mosquito vector during its blood meal results in fusion of gametes (macro and microgametes) to form a zygote, enabling the parasite to escape from the erythrocytic host. The resulting zygote elongates and forms ookinetes, which develop in the oocysts once it has penetrated the cell wall of the mosquito vector. The oocyst is then multiplied asexually within the vector resulting in the production of sporozoites. Rupture of the mature oocysts releases thousands of sporozoites into the body cavity of the mosquito, which migrate to and invade the salivary glands, thus completing the life cycle. The *Plasmodium* life-cycle is initiated again when an infected mosquito bites a susceptible vertebrate host **(5)**.

1.2.2 Ingestion and Haemoglobin (Hb) Degradation

As merozoites intensely multiply within the RBC during the life cycle, a constant availability and/or supply of nutrients is required for parasite proliferation.[19] The parasite has limited capacity to synthesize its own amino acids, therefore, degradation of Hb is a viable option as a source of amino acids for protein synthesis.[20] In addition, the parasite uses Hb to make space for itself to maintain

osmotic stability within the RBC.[20a,21] During the life cycle, the *P. falciparum* trophozoite ingests and degrades approximately 75% of host cell Hb.[20a,22] This process occurs inside a specialized organelle called the food vacuole (FV, Fig. 1.3).[23]

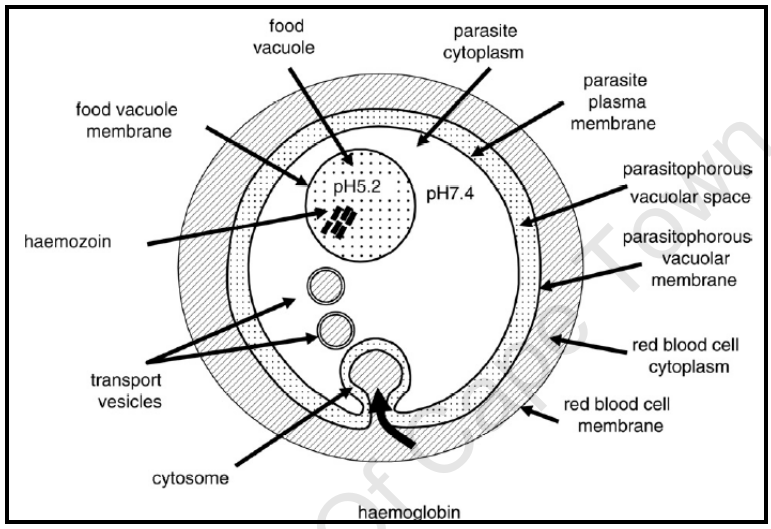

Figure 1.3: A schematic diagram of RBC showing the transport of Hb into the FV.[23]

During this event, Hb is ingested by means of cytosomes *via* endocytosis, an essential process occurring in all eukaryotic cells for uptake of external macromolecules (e.g. proteins), particles and fluids as nutrient sources to sustain their survival.[24] Vesicles from cytosome transport Hb to the acidic FV (pH~5.2-5.8) where the degradation occurs mediated by proteolytic enzymes. Essentially, degradation of haem-protein complex by the *P. falciparum* parasite during its life cycle results in the liberation of both haem and amino acids.

1.2.3 Haem Detoxification

During the process of Hb hydrolysis, free haem or Fe(II)-protoporphyrin-lX is released.[21,22,25] Haem, which leads to cell lysis is oxidized to haematin. Released haematin is detoxified to a cyclic dimer called ß-haematin. The crystallization of dimers gives rise to micrometer-sized crystals, haemozoin (malaria pigment),[26] which are harmless to the parasite. These crystals are considered markers of malaria infection in RBC assays.[15]

1.2.4 Proteolytic Enzymes

Several enzymes have been demonstrated to be involved in Hb proteolysis. These include: i) aspartic proteases namely: plasmepsins I, II, IV and a closely related histo-aspartic protease (HAP), ii) cysteine proteases namely: falcipain-2, -2′ and -3, iii) Zinc metalloprotease or falcilysin and dipeptidyl aminopeptidases (Fig. 1.4).[27]

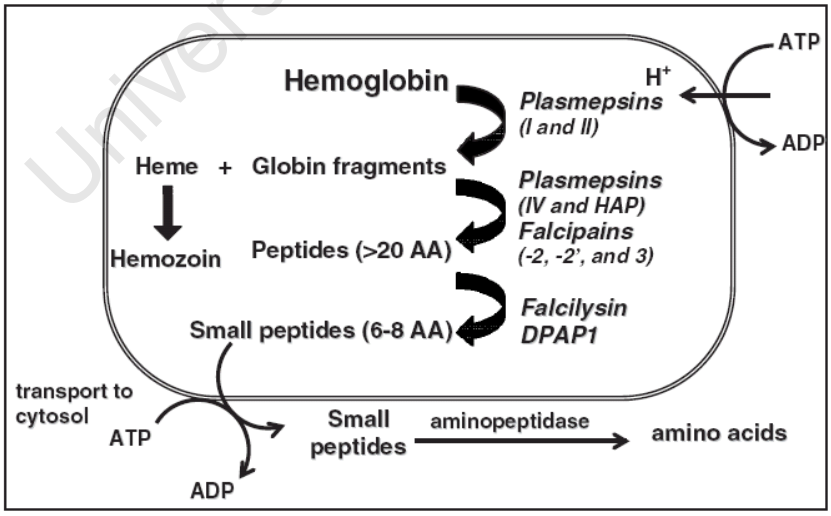

Figure 1.4: The general pathway for Hb metabolism in the Pf FV.[27]

1.2.4.1 Aspartic Proteases

Plasmepsins I and II have been postulated to initiate Hb digestion by cleaving preferentially the peptide bond between residues Phe33-Leu34 of Hb protein (Fig. 1.4).[27,28] Although plasmepsin IV is presumed to have weak proteolytic activity against the native protein, it appears to act synergistically with plasmepsins I and II as well as FP-2 and FP-3. However, the histo-aspartic protease is active against globin. In essence, these enzymes are responsible for splitting Hb into globin and haem (Fig. 1.4).

1.2.4.2 Cysteine Proteases

During the erythrocytic stage of the life cycle *P. falciparum* is reported to express three cysteine proteases: falcipain-1 (FP-1), identical copies of falcipain-2 (FP-2 and 2′) and falcipain-3 (FP-3) (Fig. 1.4).[27,29] FP-1, located on chromosome 14, shares approximately 40% sequence identity with FP-2 and FP-3. However, the function of FP-1 remains uncertain due to its low abundance in trophozoites and inadequate systems to produce recombinant protease. This enzyme has been suggested to play a role in oocyst production during parasite development in the mosquito midgut.[27]

On the other hand, FP-2 and FP-3 with 65% of amino acids identity are abundant trophozoidal proteases. The location of these enzymes in the FV is consistent with their roles in Hb digestion.[27] Although FP-2 and FP-3 show a high level of sequence homology, they differ in terms of substrate specificity. Moreover, FPs with the exception to FP-1 have

been suggested in the conversion of proplasmepsins into their active forms.[30]

1.2.4.3 Metalloproteases and Aminopeptidases

Falcilysin is a zinc metalloprotease, which is active in cleaving the smaller peptides into oligomers. These are hydrolyzed further into smaller fragments (amino acids) in the parasite cytoplasm by metallo-aminopeptidases.[31]

1.3 TREATMENT OF MALARIA: "OLD DRUGS"

The principal means to combat the disease remains chemotherapy.[32] Treatment of the disease with clinically established antimalarial drugs has been a success in fighting severe clinical cases. However, millions of people are still at risk of contracting malaria due to drug resistant parasites.[9,33] It is noteworthy that although the discussion is on "OLD DRUGS", antimalarial drugs which were discovered more than 50 years ago, there has been significant work done in terms of new chemical entities that are effective against the resistant parasite, and these are elegantly reviewed by *Mital et al.*[11] and *Kouznetsov et al.*[34]

1.3.1 Classification of Available Antimalarial Drugs

Antimalarial drugs can be classified into three main categories,[35,36] and these include i) the stage of the malaria parasite that they affect and the corresponding clinical objective. ii) the antimalarial activity, and iii) the common structural feature. Herein, the antimalarial drugs are grouped according to their chemical structures.[35a]

1.3.1.1 4-Aminoquinolines

The most common antimalarial drugs in this class include chloroquine (CQ, **1.1**) and amodiaquine (AQ, **1.2**) in Fig. 1.5. These agents are considered the main antimalarial drugs due to their proven success in both treatment and prophylaxis. However, the reputable agent has been **1.1**. Its initial success as the preferred drug to control malaria was mainly due to its safety, affordability and efficacy. The widespread emergence of chloroquine-resistant parasites however, has destabilized the usefulness of this drug.[37] This prompted the use of alternative antimalarial drugs such as **1.2**. This structurally related drug has been used as prophylaxis for several years,[38] but a degree of cross-resistance and potential hepatic toxicity are limiting the clinical use of **1.2**.[39]

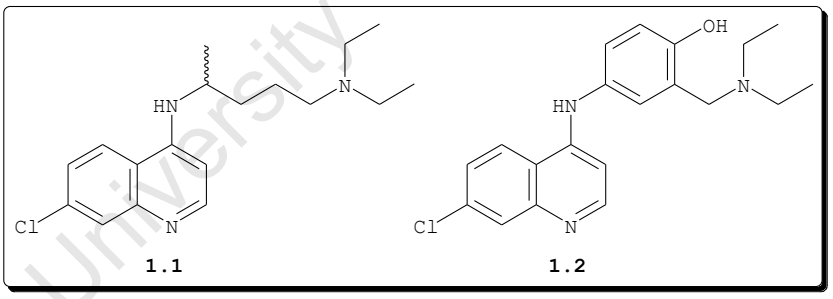

Figure 1.5: Chloroquine (**1.1**) and amodiaquine (**1.2**).

Whilst the 4-aminoquinolines, in particular **1.1**, have been effective for many decades, understanding their mechanisms of action and resistance remain a major challenge. The commonly accepted hypothesis is that quinoline-containing drugs act by binding to haematin, thus preventing the sequestration of haematin into haemozoin.[37]

Despite the partial understanding and complexity of resistance to quinolines, it is reported that resistance seems to be related to the appearance of gene mutations in two FV membrane proteins, which lower the concentration of quinoline drugs in the target.[40] This gene *pfcrt*, believed to function as a transporter in the parasite FV,[12] encodes a 424-amino acid protein commonly known as *P. falciparum* chloroquine resistance transporter (*PfCRT*).[40,41] Studies by Fidock and co-workers correlated the point mutations in *pfcrt* to CQ resistance *in vitro* using strains from Africa, South America and Asia.[42]

1.3.1.2 8-Aminoquinolines

The 8-aminoquinolines are comprised of drugs such as primaquine (PQ, **1.3a**) and pamaquine (**1.3b**), originally known as plasmoquine in Fig. 1.6.

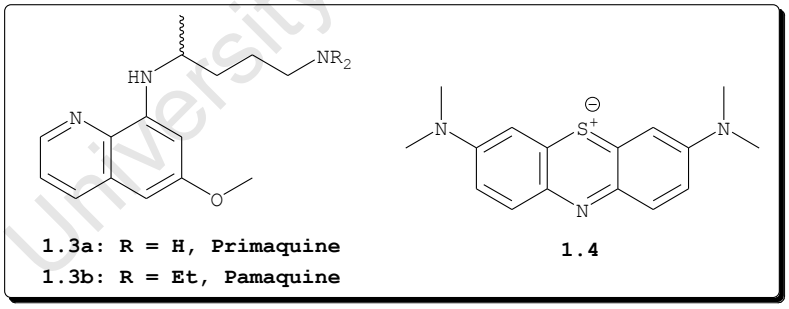

Figure 1.6: Primaquine (PQ, **1.3a**), pamaquine **(1.3b**) and methylene blue (MB, **1.4**).

Compound **1.3a** was developed after it was noted that the first synthetic drug, methylene blue (MB, **1.4**),[43] exhibited antimalarial properties. Although **1.3a** exhibited radical cure, its high toxicity led to the search for a milder drug, **1.3b**.[44,45] The mechanism of action for this group

appears to be different from those of 4-aminoquinolines. For example, **1.3b** is believed to radically cure *P. vivax* infections by acting on the gametocyte and hypnozoite (liver reservoirs) stages, and has been regarded as an ideal drug for this purpose. Other studies suggest that **1.3b** exerts its activity by interfering with mitochondrial functions.

1.3.1.3 Quinoline-Methanols

Arylamino alcohols, which also possess the quinoline scaffold, are a class of compounds with reputable history in the treatment of malaria. The first quinoline-methanols to be reported originating from the bark of the Cinchona bark tree are quinine (QN, **1.5**) and quinidine (QND, **1.6**), Fig. 1.7.[36]

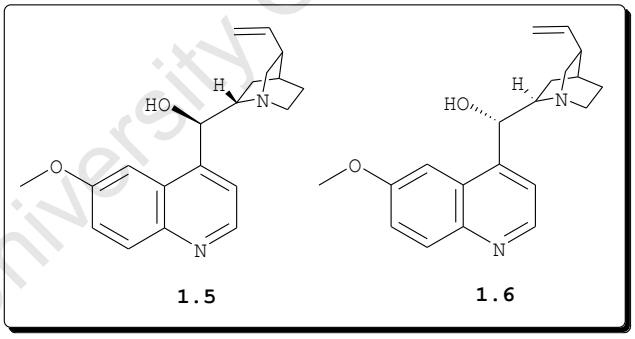

Figure 1.7: Quinine (**1.5**), quinidine (**1.6**).

For many years **1.5** was the only known effective treatment of malaria.[12,46] Although the clinical use of **1.5** and **1.6** have been in decline due to the low therapeutic index and toxicity, the advent of multi-drug resistant strains necessitated the use of **1.5** for treatment of severe cases. Both **1.5** and **1.6** remain important drugs in the therapy of

malaria, but **1.6** which is more potent than **1.5**, has higher incidences of cardiotoxicity.[46]

A second class of quinoline-methanols are synthetic analogues mefloquine (MQ, **1.7**) and halofantrine (**1.8**) in Fig. 1.8. Whilst **1.7** and **1.8** are effective against chloroquine resistant (CQR) strains, they are also vulnerable to the emergence of cross-resistance.[47] Additional limitations to these drugs include occasional neuropsychiatric disturbances for **1.7**, and strong contra-indicated effects in people with a history of heart disease for **1.8**.[47]

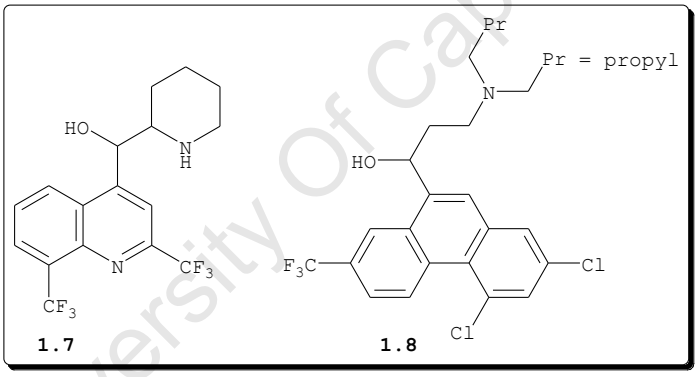

Figure 1.8: Mefloquine (**1.7**) and halofantrine (**1.8**).

Although compounds **1.7** and **1.5** are antagonistic in action with CQ, they primarily act on intraerythocytic asexual stages of the parasite as CQ. Reported cases of resistance to **1.7** and **1.5** are being associated with the *P. falciparum* multidrug resistance protein (PfMDR1). The protein PfMDR1 is reported to form a vacuolar channel and by means of its expression (through copy number) or mutations, modulates sensitivity to antimalarial molecules, including, compounds **1.7** and **1.5**.[48]

1.3.1.4 Pyrimidines, Amidines and Guanidines

This class of compounds is classified as type-2 antifolates:[49] pyrimethamine (**1.9**), cycloguanil (**1.10**), proguanil (**1.11**) and trimethoprim (**1.12**), Fig. 1.9.

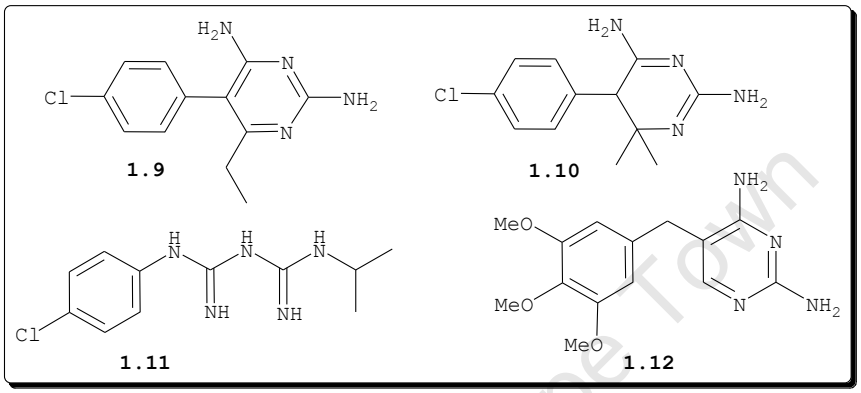

Figure 1.9: Pyrimethamine (**1.9**), cycloguanil (**1.10**), proguanil (**1.11**) and trimethoprim (**1.12**).

As the parasite requires folates for protein synthesis, pyrimethamine (**1.9**) and proguanil (**1.11**) inhibit the activity of dihydrofolate reductase (DHFR), an enzyme responsible for the synthesis of parasitic DNA. It is believed that DHFR inhibitors such as **1.9** inhibit parasitic DHFR *via* the active metabolite cycloguanil (**1.10**), thus resulting in the inhibition of tetrahydrofolic acid synthesis. These inhibitors mimic the pteridine ring of DHF, and thereby compete with DHF for the active site of the enzyme. Single mutations in the gene encoding for DHFR are believed to be the cause of resistance by the parasite.

1.3.1.5 Sulfonamides and Sulfones

A second class of antifolates, which are classified as type-1 antifolates, commonly known as sulfur compounds,

include sulfonamides and sulfones: sulfadoxine (**1.13**) and dapsone (**1.14**), Fig. 1.10, respectively.

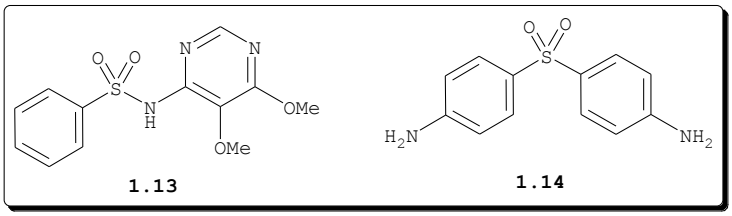

Figure 1.10: Sulfadoxine (**1.13**) and dapsone (**1.14**).

These compounds act by competing with para-aminobenzoic acid (PABA) for the active site of dihydropteroate synthase (DHPS), thereby, preventing the formation of dihydropteroate from hydroxymethyldihydropterin, a reaction catalysed by DHPS.[35] As in type-2, resistance to type-1 antifolates is conferred by single mutations of the gene encoding for the respective enzymes.

1.3.1.6 Hydroxynaphthoquinones

In this class the common drug is atovaquone (**1.15**) in Fig. 1.11. The antimalarial properties of these compounds were first noted in the early 1940s when hydrolapachol (**1.16**) was found to be active against avian malaria.[12,50] Atovaquone (**1.15**) is administered in a fixed combination with **1.11** (Fig. 1.9), Malarone®.[32]

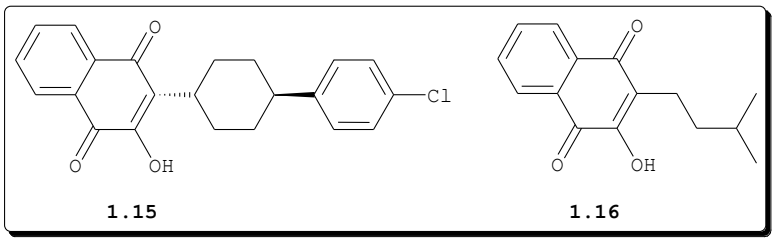

Figure 1.11: Atovaquone (**1.15**) and hydrolapachol (**1.16**).

Although it is known that **1.15** primarily acts on mitochondrial functions, the mechanism by which it acts, and its synergistic effect with **1.11** remain not fully understood. By and large, the consensus is that **1.15** acts on the mitochondria *via* an electron transfer chain. The activity and synergy of **1.15** have been attributed to its interference with mitochondrial membrane potential.

1.3.1.7 Tetracyclines

The tetracyclines (Fig. 1.12) are a class of compounds with pronounced history in the treatment of malaria.[18] The interest in tetracyclines (antibiotics) emerged from the appearance of CQ- and multidrug-resistant strains of *P. falciparum*.

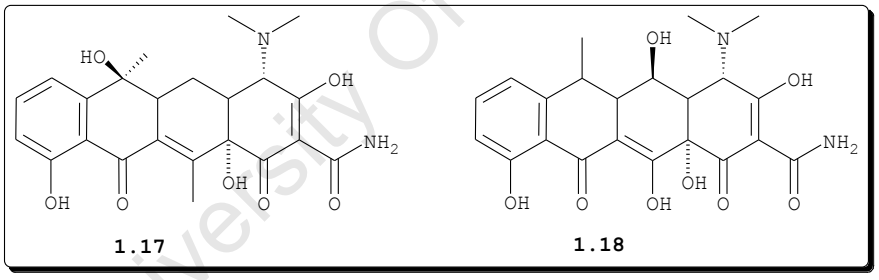

Figure 1.12: Tetracycline (**1.17**) and doxycycline (**1.18**).

These are well exemplified by **1.17** and **1.18** (Fig. 1.12). Tetracyclines are believed to act by inhibiting the parasite protein synthesis in the mitochondria and/or apicoplast (an organelle that is unique to apicomplexan parasites).[47] Relative slow action of these antimalarials warrants concurrent treatment with **1.5** (Fig. 1.7) for rapid control of parasitemia.

1.3.1.8 Sesquiterpene Lactones

Artemisinin (**1.19**, Fig. 1.13), a natural product derived from the Chinese herb 'qinghao' (*Artemisia annua*) represents this class of compounds. In China, it has been utilised to treat high fevers for many years including cases of multidrug-resistant *P. falciparum*.[51] However, artemisinin possesses low solubility in water and lipids. Consequently, the derivatives artemether (**1.20**), arteether (**1.21**) and artesunate (**1.22**) have been developed to improve its bioavailability (Fig. 1.13). Although resistance to these drugs has not been observed,[48] a few cases of decreased sensitivity have been reported in some areas, and evidence of resistance to artemisinin-based combination therapy (ACT) has been noted in Cambodia.[52]

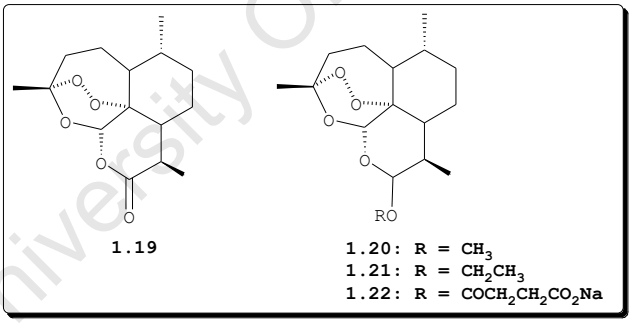

Figure 1.13: Artemisinin (**1.19**), artemether (**1.20**), arteether (**1.21**) and artesunate (**1.22**).

The mode of action of these drugs is not fully understood, but it is believed that the antimalarial action is as a consequence of reductive cleavage of intact peroxide by haem to form *C*-centred radicals. The resulting radicals alkylate haem to form haem-artemisinin adducts, which lead to the inhibition of haemozoin. The alkylation of proteins

by *C*-centred radicals has been put forward as a possible mode of action of artemisinins. Instead of heterolytic cleavage of the peroxide bridge, it has been hypothesised that the bridge undergoes homolytic cleavage to generate hydroperoxides, which might be converted into peroxy radicals or transfer oxygen to oxidizable substrates.[49,51] Other mechanisms of action that have been suggested include the inhibition of a Ca^{2+} ATPase (a protein which is not localized in the FV) together with inducible nitric oxide synthetase and nuclear factor NF-κB.[53]

1.3.2 Antimalarial Effects of Iron Chelators

Several studies have been conducted to evaluate the clinical potential of iron chelators.[12,54] Desferrioxamine (DFO, **1.23** in Fig. 1.14) and other iron chelators have been examined as therapeutic agents.

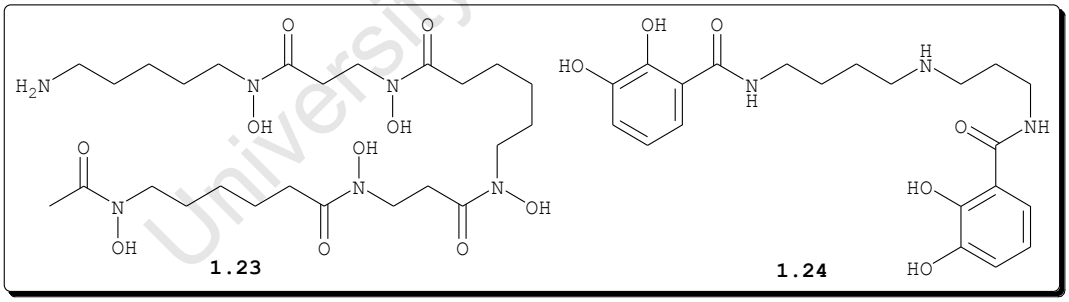

Figure 1.14: Iron chelators as antimalarial agents.

This compound inhibited the growth of *P. falciparum in vitro*. More importantly, clinical cases were resolved faster when **1.23** was used in combination with traditional antimalarial drugs. For example, **1.23** demonstrated fast clearance of the parasite and recovery from coma when it was used with quinine (**1.5**, in Fig. 1.7).[12,55]

The other extensively studied member of this group is a spermidine derivative (polyamine) **1.24** (Fig. 1.14), which displayed good activity against *P. falciparum* in culture. Although the mode of action of iron chelators remains unclear, it has been suggested that they may act by depriving iron for rapidly multiplying parasites or form complexes with iron that are toxic to the parasite.[55]

1.4 APPROACHES TO ANTIMALARIAL DRUG DEVELOPMENT

Amongst various approaches that have been adopted,[56] the most widely used is the development of chemically related analogs of existing drugs and identification of novel drug targets including the design of chemical entities acting on these targets.[57] Currently, there exists enough evidence suggesting that cysteine proteases are potential drug targets.[31] More importantly, these enzymes are found in viruses, bacteria, protozoa, plants, mammals and fungi,[58] which justify more research efforts to identify novel inhibitors. In this work FP-2, which is a member of cysteine proteases family is being pursued as one of targets for gold thiosemicarbazone (TSC) complexes (details in **Chapter 3**, **4** and **5**).

1.4.1 Parasitic Cysteine Proteases and Their Inhibitors

These enzymes are potential chemotherapeutic targets due to their role in the life cycle of protozoan parasites. In the malaria parasite, proteases appear to be useful in Hb hydrolysis, erythrocyte invasion and erythrocyte rupture.[56a] In humans these enzymes are implicated in various diseases relating to cardiovascular, inflammatory, neurological,

respiratory, viral, musculoskeletal, immunological, CNS disorders and cancer.[59] Since our focus in this work is on *P. falciparum*, discussion will be limited to cysteine proteases (falcipains) found in plasmodial species.

1.4.1.1 Classification

The first cysteine protease to be purified and characterised in 1879 originated from papaya fruit *Carica papaya*, and was then named papain.[60] Proteases exhibiting common sequences with papain have been referred to as 'papain-like'. The genome sequence of *P. falciparum* revealed that there exist over ninety proteases.[61] Cysteine proteases in *P. falciparum* are grouped according to their catalytic mechanism into five clans.

The active site comprises of two amino acid residues (i.e. Cys 25 and His 159), which are important in the hydrolysis of peptide bonds. Depending on sequence identities and similarities, clans are further divided into three main groups known as clan CA, CD and CE. Clan CA family C1 consists of falcipains, dipeptidyl peptidases, serine-rich antigen (proteins) and calpain homologs. Analysis of clan D and E have suggested members of these families to be corresponding to the *P. falciparum* genome.

1.4.1.2 Proteases and Binding Sites

For the hydrolysis of a peptide bond to occur, binding efficiency of a protease and the substrate is of great importance.[60] This is comprised of a combination of both chemical environments that the protease subsites (S) create

and the chemical nature of the substrates (P) that interact directly with the active site groove (Fig. 1.15).

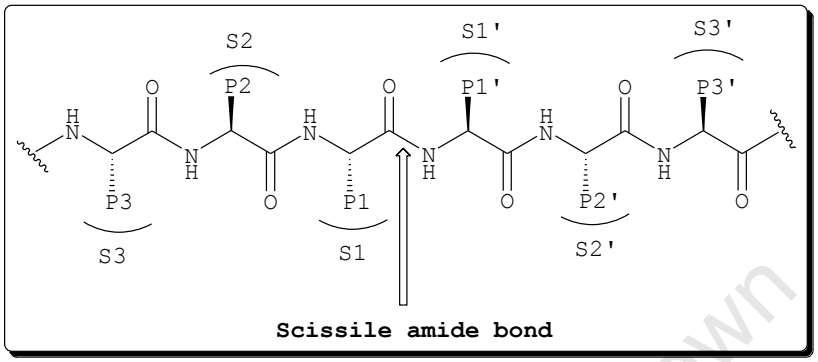

Figure 1.15: Nomenclature of substrate and protease subsite.

The limitation of substrates to interact with the available subsites may include factors such as size, polarity, charge, hydrophobicity and accessibility. The standard nomenclature to designate substrate residues and the enzyme subsites originated from the model described by Schechter and Berger, and is still commonly used to date.[62] The catalytic site is located within the substrate with the binding pockets (subsites) for amino acids N-terminal to the scissile amide bond are designated S (i.e. S1, S2...Sn), and S' (i.e. S1', S2'…Sn') for the C-terminal. Substituents of the corresponding substrate (or inhibitor) to interact with subsites are designated with P (i.e. P1, P2…Pn) and P' (i.e. P1', P2'…Pn'), respectively.

1.4.1.3 Proteolytic Mechanism of Cysteine Proteases

The proposed mechanism of peptide hydrolysis is illustrated in Scheme 1.1.[63]

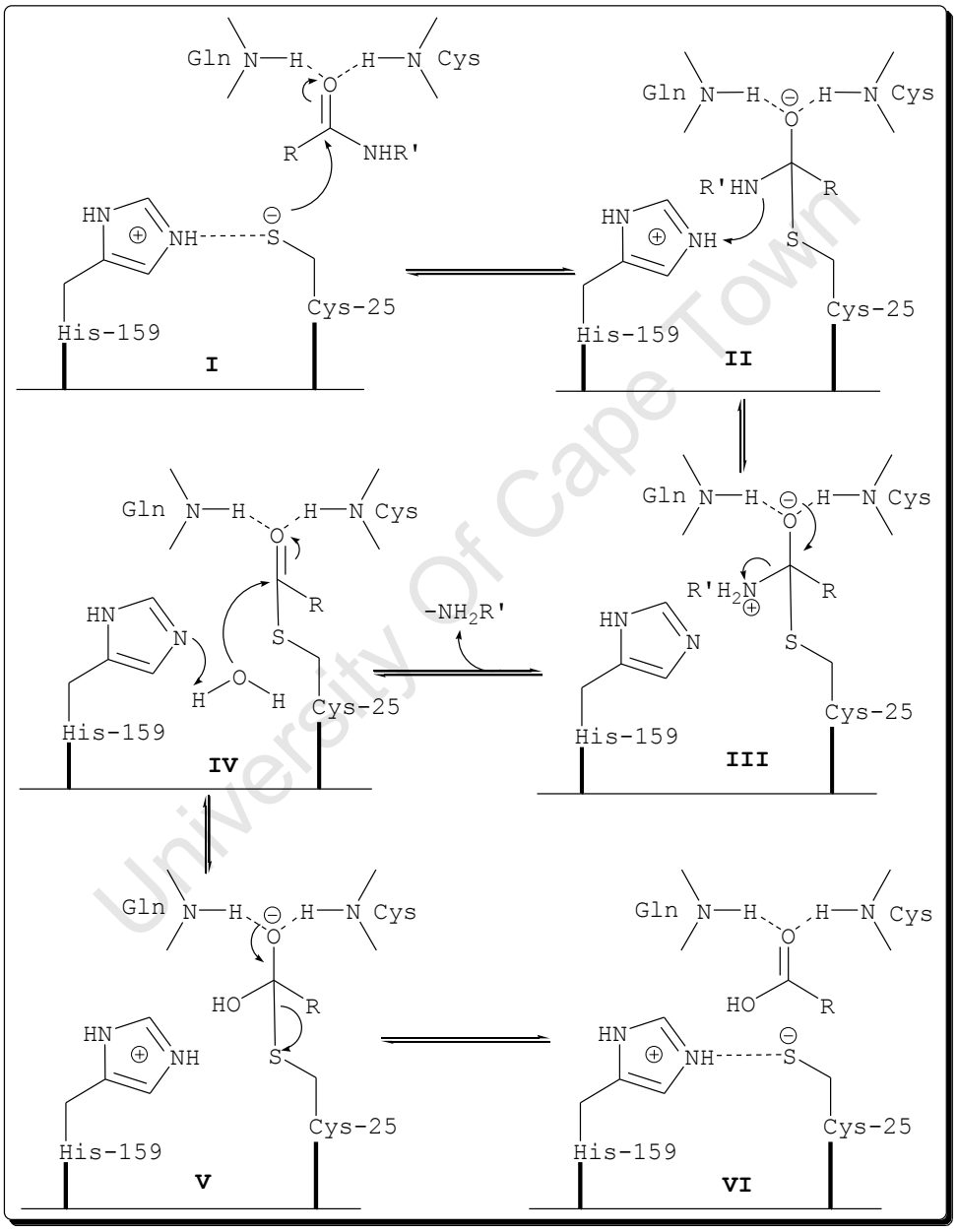

Scheme 1.1: Mechanism of peptide hydrolysis.

The catalytic process starts with imidazole moiety of the histidine residue whose close proximity to the sulfhydryl group polarises the 'SH' group. Deprotection of the latter give rise to a thiolate/imidazolium ion pair (**I**). The resulting nucleophilic thiolate attacks the carbonyl carbon of the scissile amide bond to produce a tetrahedral intermediate, which is stabilized by H bonding of both the backbone NH of Cys 25 and NH_2 group of the Gln 19 side chain (**II**). The tetrahedral intermediate transforms into an acyl enzyme (enzyme-substrate thiol ester) (**III**) and simultaneously releases the C-terminal portion of the substrate (deacylation). Subsequently, the hydrolysis of the acyl enzyme with water (**IV**) results in the formation of a second tetrahedral intermediate (**V**), which finally splits (**VI**) into free enzyme and N-terminal portion of the substrate (deacylation).

1.4.2 Falcipain Inhibitors

To date, many chemotypes have been identified as inhibitors of malarial cysteine protease FP-2. These include peptides (**1.25-1.27**), peptidomimetics (**1.28**), isoquinolines (**1.29**), chalcones (**1.30**) and TSCs (**1.31-1.35**) in Fig. 1.16.[27] These compounds inactivate the enzymes in a reversible or irreversible manner.

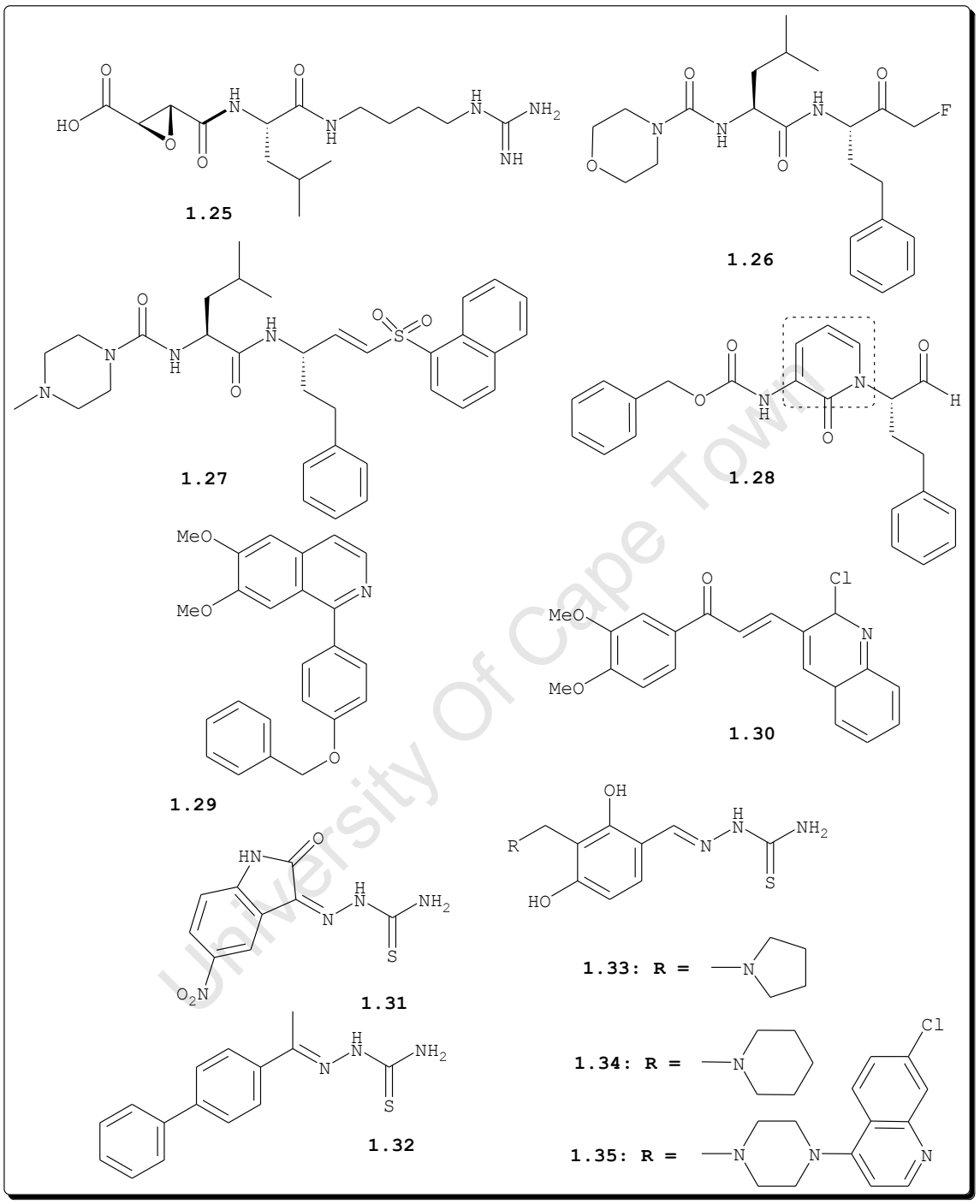

Figure 1.16: Falcipain inhibitors.

As part of ongoing research on novel inhibitors of FP-2, *Chiyanzu et al.*[64] designed TSCs as potential antimalarial agents. The most active and promising inhibitor in this

series was found to be compound **1.31.** In a subsequent study of *Greenbaum et al.*[65] compound **1.32** was the only TSC active against FP-2, but inactive against the whole parasite cultures at highest tested concentration (ED_{50} = 20 μM). More recently, TSCs with a phenolic Mannich base component were synthesised from our laboratory and screened for their activities against FP-2 and CQ-resistant *P. falciparum* W2 strain.[66] From the series, compounds **1.33-1.35** displayed good activity against FP-2. The study suggested that the activity of this series was not only due to the TSC side chain, but the combined effects of both Mannich base and TSC components.

A recent report by *De Oliveira et al.*[67] demonstrated the activity of some TSCs against the *P. falciparum* W2 strain, further lending support to some of observations made by others. In contrast, *Mallarai et al.*[68] concluded recently that TSCs do not represent promising antimalarial leads as some of the tested compounds in their library were virtually ineffective against the parasite.

1.4.3 Drug-Polyamine Conjugates

Given the role of PAs in key process such as cell growth, differentiation and macromolecular synthesis; enzymes involved in PA biosynthesis pathways have been suggested as targets in treatment of parasitic diseases.[57] However, an attractive approach which has been a success in cancer chemotherapy in recent years is the development of drug-polyamine conjugates, to target the polyamine transporter (PAT).[69] Drug-polyamine conjugation involves covalent appendage of a PA to a known cytotoxic agent. A PAT is

utilised by cells to import PAs from external sources. Due to their multivalent and cell recognition properties, branched PAs have been proposed as ideal scaffolds to covalently anchor TSCs (for details see **Chapter 6**, p 183). In this study, it was hypothesized that formation of TSC-PA conjugates could lead to enhanced antiplasmodial potency.

1.4.4 Metal-Based Antimalarial Agents

Due to the limited number of effective drugs and the emergence of drug resistance, there exists a need for increased efforts to search for new compounds with novel modes of action. Currently, new chemical entities are continuously being discovered and screened for their activities against the parasite;[34] and the category of metallodrugs is receiving considerable attention as potential antimalarial agents.

In this work, the approach of using metal-based compounds against *P. falciparum* will be exploited further due to the observed pharmacological properties of gold (**Chapter 2**) and TSCs (**Chapter 3**) against various diseases. *The real question behind this approach is whether gold complexation will enhance the antimalarial potency of TSCs against P. falciparum strains.* Briefly, **Chapter 2** reviews the role of starting metal complexes and ligands in the design of metal-based agents. The role of gold in medicine and its relevance in the fight against *P. falciparum* malaria, and other metalloantimalarial compounds which have been reported over the years, will be discussed.

1.10 REFERENCES

1. *A Safer Future: Global Public Health Security in the 21st Century, WHO Report* **2007**.
2. H.M. Gilles, A.O. Lucas, *Br. Med. Bull.*, **1998**, *54*, 269-280.
3. Africa Fighting Malaria (AFM)-http://www.nytimes.com
4. "Malaria," Microsoft® Encarta® Online Encyclopedia **2007** (http://encarta.msn.com © 1997-2007 Microsoft Corporation).
5. S.C. Oaks, Jr., V.S. Mitchell, G.W. Pearson, C.C.J. Carpenter, Malaria: *Obstacles and Opportunities*, National Academy Press, Washington, D.C., **1991**, p 39-44.
6. WHO. *Frequently Asked Question About Malaria* (http://www.who.int/malaria/faq.html).
7. R. Tuteja, *FEBS Journal*, **2007**, *274*, 4670-4679.
8. E. Gkrania-Klotsas, A.M.L. Lever, *Blood Rev.*, **2007**, *21*, 73-87.
9. *World malaria report* **2008**, WHO Geneva, Switzerland.
10. RBM. *Global Malaria Action Plan*, **2008**.
11. A. Mital, *Curr. Med. Chem.*, **2007**, *14*, 759-73.
12. D.A. Casteel, Antimalarial Agents. In *Burger's Medicinal Chemistry and Drug Discovery*, 6th ed., Vol. 5, *Chemotherapy Agents*, Ed. D.J. Abraham, John Wiley & Sons, Inc.: New York, **2003**, p 919-999.
13. (a) A.P. Dash, T. Adak, K. Raghavendra, O.P. Singh, *Curr. Sci.*, **2007**, *92*, 1571-1578. (b) J.G. Breman, *Am. J. Trop. Med. Hyg.*, **2001**, *64*, 1-11. (c) P.B. Bloland, *Drug Resistance in Malaria* (*WHO/CDR/CSR/DSR/2001.4 4*), **2001**, Geneva: World Health Organisation.

14. S.I. Hay, C.A. Guerra, A.J. Tatem, A.M. Noor, R.W. Snow, *Lancet Infect. Dis.*, **2004**, *4*, 327–336.
15. I. Weissbuch, L. Leiserowitz, *Chem. Rev.* **2008**, *108*, 4899-4914.
16. D.L. Hartl, *Nature Reviews*, **2004**, *2*, 15–22.
17. L.E. Rodriguez, H. Curtidor, M. Urquiza, G. Cifuentes, C. Reyes, M.E. Patarroyo, *Chem. Rev.* **2008**, *108*, 3656-3705.
18. M. Frederich, J.-M. Dogne, L. Angenot, P. De Mol, *Curr. Med. Chem.*, **2002**, *9*, 1435–1456.
19. (a) P.J. Rosenthal, *International Journal for Parasitology*, **2004**, *34*, 1489–1499. (b) B.L. Tekwani, L.A. Walker, *Comb. Chem. High Throughput Screening*, **2005**, *8*, 63–79.
20. (a) R. Banerjee, D.E. Goldberg, *Antimalarial Chemotherapy: Mechanism of Action, Reistance, and New Directions in Drug Discovery*, ed. P.J. Rosenthal, Human Press, Totowa, New Jersey, **2001**, p 43-63. (b) P.J. Rosenthal, P.S. Sijwali, A. Singh, B.R. Shenai, *Curr. Pharm. Des.*, **2002**, *8*, 1659–1672.
21. T.J. Egan, *Targets Rev.*, **2003**, *2*, 115-124.
22. T.J. Egan, *Drug Design Reviews-Online*, **2004**, *1*, 93–110.
23. S.M. Chemaly, C.-T. Chen, R.L. van Zyl, *J. Inorg. Biochem.* **2007**, *101*, 764-773.
24. H.C. Hoppe, D.A. van Schalkwyk, U.I.M. Wiehart, S.A. Meredith, J. Egan. B.W. Weber, *Antimicrob. Agents Chemother.*, **2004**, *48*, 2370-2378.
25. T.J. Egan, H.M. Marques, *Coord. Chem. Rev.*, **1999**, *190–192*, 493-517.

26. (a) D.C. Warhurst, *Current Science*, **2007**, *92*, 1556-1560. (b) T.J. Egan, *Mol. Biochem. Parasitol.*, **2008**, *157*, 127-136.
27. R. Ettari, F. Bova, M. Zappala, S. Grasso, N. Micale, *Med. Res. Rev.*, **2010**, *30*, 136-167 and references therein.
28. K.A. Werbovetz, *Curr. Med. Chem.*, **2000**, 7, 835–860.
29. L.J. Kaleta, D. Bromme, *Chem. Rev.*, **2002**, *102*, 4459–4488.
30. M.E. Drew, R. Banerjee, E.W. Uffman, S. Gilbertson, P.J. Rosenthal, D.E. Goldberg, *J. Biol. Chem.*, **2008**, *283*, 12870-12876.
31. J.H. McKerrow, P.J. Rosenthal, R. Swenerton, P. Doyle, *Curr. Opin. Infect. Dis.*, **2008**, *21*, 668-672.
32. A. Nzila, *Drug Discovery Today*, **2006**, *11*, 939–944.
33. B.L. Tekwani, L.A. Walker, *Combin. Chem. High Throughput Screening*, **2005**, *8*, 63–79.
34. V.V. Kouznetsov, A. Gómez-Barrio, *Eur. J. Med. Chem.*, **2009**, *44*, 3091–3113.
35. (a) P.M.S. Chauhan, S.K. Srivastava, *Curr. Med. Chem.*, **2001**, *8*, 1535–1542. (b) M. Frédérich, J.-M. Dogné, L. Angenot, P. De Mol, *Curr. Med. Chem.*, **2002**, *9*, 1435-1456. (c) P. Newton, N. White, *Annu. Rev. Med.*, **1999**, *50*, 179-192.
36. J.W. Tracy, L.T. Webster Jr., *Goodman and Gilman's The Pharmacological Basis of Therapeutics*, 9th ed., J. G. Hardman, A.G. Gilman, L.E. Limbird,McGraw-Hill, New York, **1996**, p 965–985.
37. R. Arav-Boger, T.S. Shapiro, *Annu. Rev. Pharmacol. Toxicol.*, **2005**, *45*, 565–585.

38. M.H. Gelb, *Curr. Opion. Cell Biol.*, **2007**, *11*, 440–445.
39. A. Robert, F. Benoit-Vical, O. Dechy-Cabaret, B. Meunier, *Pure Appl. Chem.*, **2001**, *73*, 1173–1188.
40. T.J. Egan, C.H. Kaschula, *Curr. Opin. Infect. Dis.*, **2007**, *20*, 598-604.
41 J.E. Hyde, *FEBS J. Minireview*, **2007**, *274*, 4688-4698.
42. D.A. Fidock, T. Nomura, A.K. Talley, R.A. Cooper, S.M. Dzekunov, M.T. Ferdig, L.M.N. Ursos, A.B.S. Sidhu, B. Naude, K.W. Deitsch, X.Z. Su, J.C. Wootton, P.D. Roepe, T.E. Wellems, *Mol. Cell*, **2000**, *6*, 861-871.
43. J. Wiesner, R. Ortmann, H. Jomaa, M. Schlitzer, *Angew. Chem. Int. Ed.*, **2003**, *42*, 5274–5293.
44. M. Foley, L. Tilley, *Pharmacol. Ther.*, **1998**, *79*, 55–87.
45. L.W. Kitchen, D.W. Vaughn, D.R. Skillman, *Rev. Anti-Infect. Agents*, **2006**, *43*, 67–71.
46. L. Tilley, P. Loria, M. Foley, *Antimalarial Chemotherapy: Mechanism of Action, Resistance, and New Directions in Drug Discovery*, ed. P.J. Rosenthal, Human Press, Totowa, New Jersey, **2001**, p 87-121.
47. R.G. Ridley, *Nature*, **2002**, *415*, 689–693.
48. B. Witkowski, A. Berry, F. Benoit-Vical, *Drug Resistance Updates*, **2009**, *12*, 42-50.
49. P. Olliaro, *Pharmacology and Therapeutics*, **2001**, *89*, 207–219.
50. N.H. Gokhale, S.B. Padhye, S.L. Croft, H.D. Kendrick, W. Davies, C.E. Anson, A.K. Powell, *J. Inorg. Biochem.*, **2003**, *95*, 249–256.
51. (a) D. Chaturvedi, A. Goswami, P.P. Saikia, N.C. Barua, P.G. Rao, *Chem. Soc. Rev.*, **2010**, *39*, 435-454.

(b) G.A. Gale, K. Kirtikara, P. Pittayakhajonwut, S. Sivichai, Y. Thebtaranonth, C. Thongpanchang, V. Vichai, *Pharmacol. Ther.*, **2007**, *115*, 307-351.

52. (a) H. Noedle, Y. Se, K. Schaecher, B.L. Smith, D. Socheat, M.M. Fukuda, *Engl. J. Med.*, **2008**, *359*, 2619-2620. (b) P. Lim, A.P. Alker, N. Khim, N.K. Shah, S. Incardona, S. Doung, P. Yi, D.M. Bouth, C. Bouchier, O.M. Puijalon, S.R. Meshnick, C. Wongsrichanalai, T. Fandeur, J. Le Bras, P. Ringwald, F. Ariey, *Malar. J.*, **2009**, *8*, 11. (c) W.O. Rogers, R. Sem, T. Tero, P. Chim, P. Lim, S. Muth, D. Socheat, F. Ariey, *Malar. J*, **2009**, *8*, 10.
53. C. Biot, K. Chibale, *Infectious Disorders-Drug Targets*, **2006**, *6*, 173-204.
54. G.F. Mabeza, M. Loyevsky, V.R. Gordeuk, G. Weiss, *Pharmacol. Ther.*, **1999**, *81*, 53-75.
55. M. Loyevsky, V.R. Gordeuk, *Antimalarial Chemotherapy: Mechanism of Action, Resistance and New Directions in Drug Discovery*, Ed. P.J. Rosenthal, Humana Press Inc., Totowa, NJ, **2001**, p 307–323.
56. (a) P.J. Rosenthal, *Antimalarial Chemotherapy: Mechanism of Action, Reistance, and New Directions in Drug Discovery*, ed. P.J. Rosenthal, Human Press, Totowa, New Jersey, **2001**, p 325-345. (b) P.J. Rosenthal, *International Journal for Parasitology*, **2004**, *34*, 1489–1499.
57. N.K. Sahu, S. Sahu, D.V. Kohli, *Chem. Biol. Drug Des.*, **2008**, *71*, 287-297.
58. H.-H. Otto, T. Schirmeister, *Chem. Rev.* **1997**, *97*, 133-171.

59. R. Leung-Toung, Y. Zhao, W. Li, T.F. Tam, K. Karimian, M. Spino, *Curr. Med. Chem.*, **2006**, *13*, 547-581.
60. M. Sajid, J.H. McKerrow, *Mol. Biochem. Parasitol.*, **2002**, **120**, 1-21.
61. G.E. García Liñares, J.B. Rodriquez, *Curr. Med. Chem.*, **2007**, *14*, 289-314.
62. I. Schechter, A. Berger, *Biochem. Bophys. Res. Commun.*, **1967**, *27*, 157–162.
63. K. Chibale, C.C. Musonda, *Curr. Med. Chem.*, **2003**, *10*, 1863–1889.
64. I. Chiyanzu, E. Hansell, J. Gut, P.J. Rosenthal, J.H. McKerrow, K. Chibale, *Bioorg. Med. Chem. Lett.*, **2003**, *13*, 3527-3530.
65. D.C. Greenbaum, Z. Mackey, E. Hansell, P. Doyle, J. Gut, C.R. Caffrey, J. Lehrman, P.J. Rosenthal, J.H. McKerrow, K. Chibale, *J. Med. Chem.*, **2004**, *47*, 3212-3219.
66. A. Chipeleme, J. Gut, P.J. Rosenthal, K. Chibale, *Bioorg. Med. Chem.*, **2007**, *15*, 273-282.
67. R.B. de Oliveira, E.M. de Souza-Fagundes, R.P.P. Soares, A.A. Andrade, A.U. Krettli, C.L. Zani, *Eur. J. Med. Chem.*, **2008**, *43*, 1983-1988.
68. J.P. Mallari, W.A. Guiguemde, R.K. Guy, *Bioorg. Med. Chem. Lett*. **2009**, *19*, 3546-3549,
69. (a) N. Kaur, J.-G. Delcros, J. Imran, A. Khaled, M. Chehtane, N. Tschammer, B. Martin, O. Phanstiel IV, *J. Med. Chem.*, **2008**, *51*, 1393-1401. (b) O. Phanstiel IV, H.L. Price, L. Wang, J. Jusola, M. Kline, S.M. Shah, *J. Org. Chem.*, **2000**, *65*, 5590-5599. (c) C. Wang, J.-G. Delcros, J. Biggerstaff, O. Phanstiel IV, *J. Med.*

Chem., **2003**, *46*, 2672-2682. (d) N. Kaur, J.-G. Delcros, B. Martin, O. Phanstiel IV, *J. Med. Chem.*, **2005**, *48*, 3832-3839.

CHAPTER 2

METALLOANTIMALARIALS: GOLD AND OTHER METAL COMPLEXES

2.1 INTRODUCTION

The advent of Cisplatin® (**2.1**, Fig.2.1) and its derivatives as potent anticancer metallodrugs (metal-based drugs) has prompted interest in using other metal-based compounds for the treatment of various diseases.[1] Although the utility of metallodrugs as antiparasitic agents is limited, there are some successes such as the clinical use of antimony-based compounds (e.g. Glucantime®, **2.2** in Fig. 2.1) to treat leishmaniasis.[2,3] Generally, metallodrugs can be described as chemically synthetic agents containing a metal or metal ion coordinated to a suitable ligand. On the other hand, a ligand is a molecule (in some cases biologically active) with sufficient donor atoms to hold a metal or metal ion.

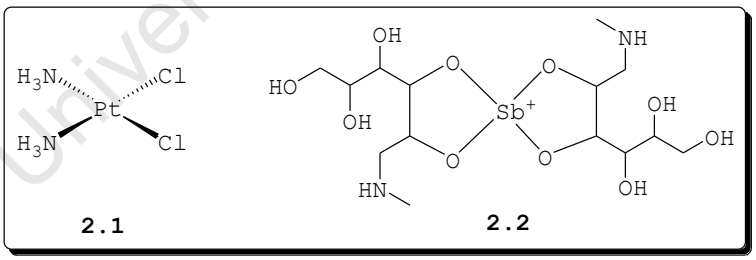

2.1 **2.2**

Figure 2.1: Cisplatin® (**2.1**) and Glucantime® (**2.2**).

Although some pharmaceutical companies have removed metal-based compounds from their libraries which are used in high-throughput screening programs,[4] there are some existing opportunities to exploit metal complexes in the development of pharmaceuticals for the treatment of various ailments,

especially malaria due to its prevalence in poor countries.[5] The potential toxicity of metals is often cited as one of the reasons for their exclusion in companies and some academic institutions.

2.2 METAL COMPLEXES

Metal complexes have been reported to compliment organic molecules as structural scaffolds for bioactive compounds.[5b] They can be designed such that instead of the metal assuming the structural role, it contains a vacant coordination site - in some cases with the loss of a labile ligand - to bind with amino acids (e.g. cysteine, histidine and tyrosine) in the target active sites.

A key feature in the design of metal complexes with desirable effects lies with suitable ligands to support metals directed towards a particular target. Different ligands are believed to impart various physical and chemical characteristics on a metal.[6] Metal complexes with suitable ligands exhibit unique properties that may be exploited for the development of probes to unravel the functioning of proteins, sensors, chemotherapeutics and diagnostic tools.[5b]

2.3 DESIGN AND THE ROLE OF LIGAND SYSTEMS

Apart from their role in traditional coordination chemistry, ligands are of greater importance in modification of biological effects of metal complexes.[6] Depending on the requirements (therapy or diagnosis), ligands are capable of: i) modifying the oral or systematic bioavailability of metals, ii) targeting specific tissues

or enzymes, iii) delivering, protecting or sequestering metal ions. They can also be involved in protecting tissues from toxic metals or enhance uptake of pharmacologically beneficial metals. Fine-tuning of ligands by appending substituents that bind membrane receptors or mimic naturally-occurring hormones, is believed to render metal complexes with target specificity to achieve the desired diagnostic or therapeutic effects.[6]

In some cases the strategy of using bioactive ligands to form metallodrugs has been widely used to form metal complexes with enhanced bioactivities.[5a] For example, bioactive ligands (Fig. 2.2) clotrimazole (**2.3**) and ketoconazole (**2.4**) formed effective anti-malarial and anti-trypanosomal complexes (compared to their free form) with copper(II), ruthenium(II) and gold(I) ions.[6,7]

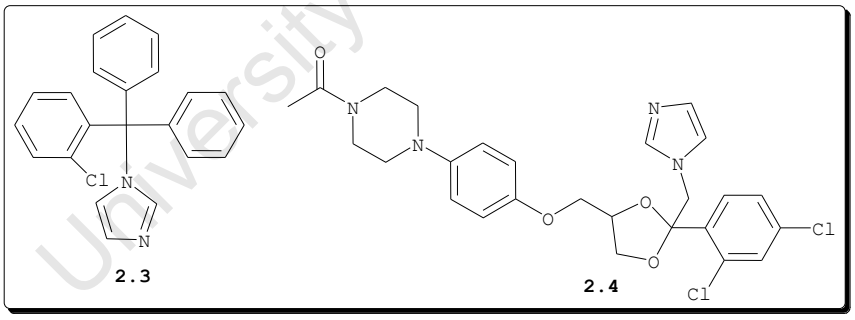

Figure 2.2: Clotrimazole (**2.3**) and ketoconazole (**2.4**).

2.4 GOLD IN MEDICINE

2.4.1 History

Medicinal use of gold dates back to antiquity when both Arabic and Chinese cultures used it to treat various ailments.[8] However, it was not until the early 1920s when the rational approaches of using gold in medicine began to

gain wide support. This followed the disclosure by Robert Koch (bacteriologist) in 1890 that the gold complex, $K[Au(CN)_2]$, was lethal against the micro-organism mycobacterium, a causative agent of tuberculosis (TB).[9] The introduction of gold thiolate complexes to treat TB came after it was observed that $K[Au(CN)_2]$ had significant side effects when applied in pulmonary TB. Concurrently, in the early 1930s Jacque Forenstier, a French physician, introduced gold thiolate complexes for the treatment of rheumatoid arthritis (RA), a condition then believed to be associated with TB.[8]

2.4.2 Antirheumatoid Arthritis Activity

RA is a painful and disabling disease characterised by inflammatory and progressive joint erosion. Fig. 2.3 shows some of anti-RA gold compounds (**2.5**–**2.7**) and indomethacin (**2.8**) representing nonsteroidal anti-inflammatory drugs (NSAIDS).

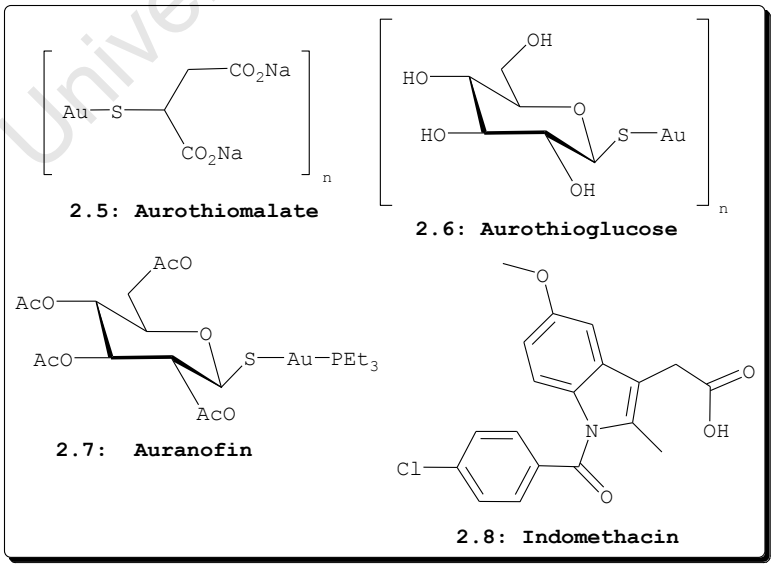

Figure 2.3: Anti-rheumatoid arthritis drugs.

The first injectable gold(I) thiolate complexes to be used clinically for treating RA are aurothiomalate (**2.5**) and aurothioglucose (**2.6**).[3] However, the toxic side effects observed (e.g. nephrotoxicity) with these compounds prompted the search for new and less toxic complexes. The primary objective during the search was to ensure that the proposed gold compound (drug) should be administered orally in low doses. This led to the development of auranofin (**2.7**), which was introduced in the clinic (1985) to treat severe cases of RA. Regrettably, its efficacy was found to be lower compared to that of polymeric gold(I) thiolate complexes; and some of the patients who were treated with this drug suffered from serious side effects.[8b] The use of **2.7** has been declining due to the popularity of NSAIDS such as indomethacin (**2.8**).[10]

Recently, *Sannella et al.*[11] demonstrated that **2.7** in combination with artemisinin (**1.19**) displays good activity against the malaria parasite 3D7 strain. This suggested that there is great potential for using **2.7** (since it is a clinically established drug) in combination therapy to counteract cases of drug resistance, a major limiting factor in most standard antimalarial drugs.

2.4.3 Antitumour Activity

Since the first report by *Simon et al.*[12] on the antitumour activity of **2.7** in 1979, gold(I) complexes have been considered in cancer chemotherapy due to the growing interest in non-platinum metal complexes with novel modes of action. Several studies conducted on gold(I) complexes

as antitumour agents mainly involved the modification of **2.7** to generate various analogous complexes.

Recently, *Ott et al.*,[13] *de Vos et al.*[14] and *Casas et al.*[15] reported gold(I) complexes **2.9**–**2.12** (Fig. 2.4) with pronounced antitumour activities against HeLa and A2780 (cisplatin resistant) cell lines. These compounds were prepared by replacing the carbohydrate ligand with naphthalimide, dithiocarbamate, azacoumarin and vitamin K3 derived TSC. These examples serve as a clear indication of embedded interest in utilising gold(I) complexes to treat various diseases.[8]

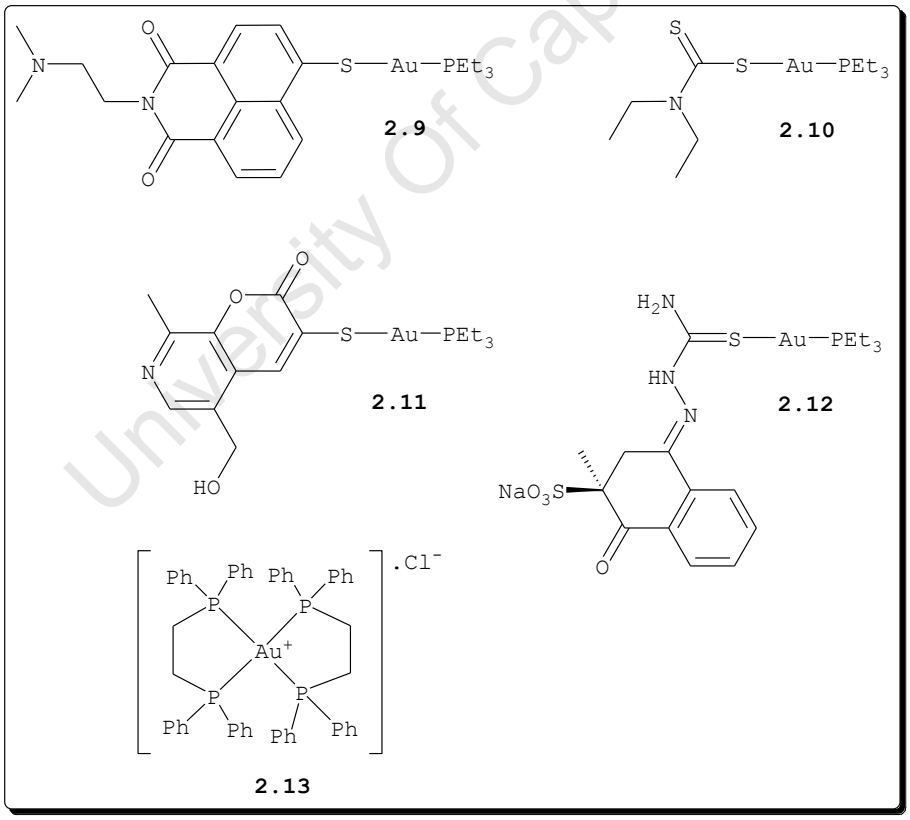

Figure 2.4: Antitumoural gold(I) complexes.

A second class of gold(I) complexes pursued in the 1980s is that of four coordinate gold complexes. The prominent complex is **2.13** (Fig. 2.4), reported in the mid 80s to be a promising compound against solid tumours.[16] Unlike complex **2.7**, this compound exhibited antitumour activities against a panel of human cell lines including leukaemia cells.[16] However, it failed to reach clinical trials due to cardiotoxicity problems encountered during pre-clinical toxicology studies.[17]

Owing to electronic and geometric similarities of gold(III) with platinum(II), gold(III) complexes have been reported to be amongst the first non-platinum complexes to be tested for antitumour activities.[18] However, the development of these compounds as therapeutic drugs has been questioned due to their instability under physiological conditions.[9,19] The design of better ligands such as PAs, cyclam, terpyridines, porphyrins, phenanthrolines, and *N*-benzyl-*N,N*-dimethylamine (damp) to stabilise gold(III) has renewed interest in the search for gold(III) complexes as potential anti-tumour agents.[20] As a result, a number of gold(III) compounds have been evaluated *in vitro* against a panel of tumour cells, and some exhibited superior activities compared to cisplatin.[18b,21]

2.4.4 Antimicrobial Activity

The early work by Robert Koch revealing that gold compounds were active against the *tubercucle bacillus*, prompted extensive utility of gold(I) thiolate complexes for the treatment of tuberculosis during the period 1925-1935, the "gold decade".[22] During this period, various gold(I)

compounds were found to be active against a broad spectrum of micro-organisms. Although there has been little novel work on the antimicrobial activity of gold compounds,[16] a number of different metal complexes have also been tested for antimicrobial activity against a panel of bacterial strains and clinical isolates of methicillin-resistant *S. aureus* (MRSA), methicillin-sensitive *S. aureus*, enterrococci, coagulase-negative staphylococci and streptococci. This came after it was realised that there is growing need for new antimicrobial agents such as vancomycin (**2.14**, Fig. 2.5), the drug of choice for these organisms, and other standard drugs are facing various limitations, including, problems of drug-resistance.[16a]

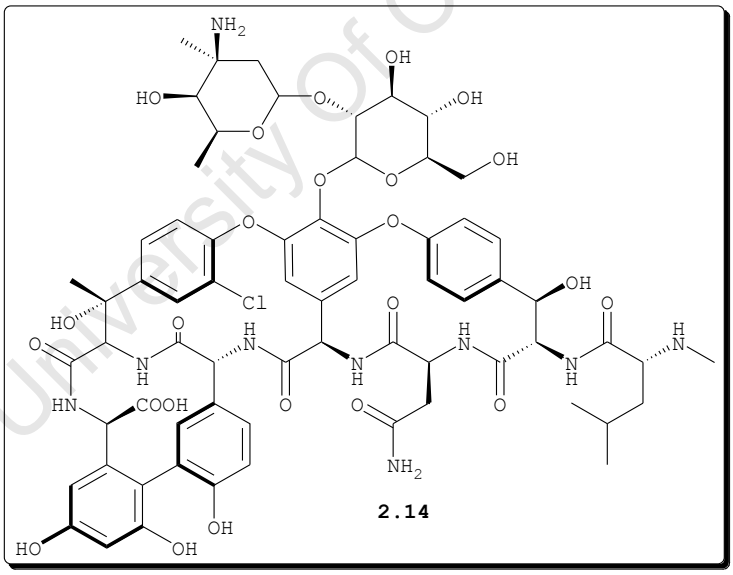

Figure 2.5: Chemical structure of vancomycin (**2.14**).

A gold(I) compound that has been demonstrated to be active against Gram positive bacteria and MRSA is the gold(I) thiocyanate complex, which has been found to be selective for bacteria over mammalian cells (CHO rodent cell line)

with MIC_{50} (minimum concentration inhibiting 50% of bacterial growth) of 0.33 and 0.77 against *Staphylococcus aureus* and *Enterococcus faecalis*. This study revealed that toxicity doses of at least ten times higher are required to kill CHO cells.[16a] In addition, *Nomiya et al.*[23] demonstrated the antimicrobial activity of some gold(I) complexes derived from heterocyclic, penicillamine and 'mercaptant' acids.

Further search for antimicrobial gold complexes led to the identification of gold(I) phosphonium dithiocarboxylate complexes, which exhibited activity against Gram positive bacteria and cocci.[16a] Recently, *Jackson-Rosario et al.*[24] reported the activity of **2.7** against *Clostridium difficile*, a selenium-dependent pathogen associated with severe diarrhea.

Figure 2.6: Gold(III) complexes **2.15** and **2.16**.

The antimicrobial activity of gold(III) complexes **2.15** and **2.16** has also been investigated (Fig. 2.6). These compounds exhibited broad spectrum activity against a range of organisms with a small degree of specificity against Gram positive bacteria *S aureus* and *E. faecalis*.[16a] These compounds also exhibited remarkable activities against an *in vitro* panel of human tumour cell lines.[16a]

2.4.5 Anti-HIV Activity

The observations made from clinical data of HIV+ patients not undergoing antiretroviral treatment, but treated with **2.7** (Fig. 2.3) for psoriesis experienced increasing CD4+ cells, have stimulated interest in gold compounds for the treatment of AIDS.[25] Consequently, various gold compounds have been evaluated for their ability to inhibit the HIV virus. Sodium aurothiomalate (**2.5**) and aurothioglucose (**2.6**) are amongst those gold(I) compounds, which have been tested for anti-HIV activity (Fig. 2.3).[26] Aurocyanide, $[Au(CN)_2]^-$, has been shown to inhibit the proliferation of HIV in cultured T-9 cells (strain of CD4+ T cells) with an IC_{50} value of 20 nM. This has prompted interest in its potential to treat HIV/AIDS in combination therapy. Gold(III) compounds containing a porphyrin ligand have also been reported to be potent against the reverse transcriptase (RT) enzyme, a target for anti-HIV drugs such as azidothymidine (AZT).[27]

2.5 ANTIMALARIAL ACTIVITY

As previously mentioned, malaria is a tropical disease which causes devastation in the populations residing in tropical regions. Although gold compounds have been studied extensively against other diseases (previous sections), their potential application as antimalarial agents has not been explored to a great degree. The first attempt to explore gold compounds against malaria was reported by Wasi and co-workers in 1987.[28] A metal-synergic effect approach reported as far back as 1976 prompted *Wasi et al.*[28] to prepare a number of metal complexes in which two were based

on gold(III).[29] These complexes were obtained by employing amodiaquine (**1.2,** Fig. 1.5) and primaquine (**1.3a,** Fig. 1.6) as ligands. The complexes were found to be active against *P. falciparum* to the same extent as the parent drugs.

2.5.1 Gold(I) Complexes

In the early 1990s, the group of Sánchez-Delgado conceived an approach of developing alternative agents against tropical diseases.[7] It was hypothesised that modification of bioactive compounds by chemically incorporating a transition metal into the molecular structure could yield antiparasitic agents with improved activity.

As a land mark in gold(I) chemistry, *Navarro et al.*[30] reported the first gold(I) CQ complex (**2.17,** Fig. 2.7), which was active against malaria parasites. Since then there has been growing interest in gold(I) complexes as potential antimalarial agents.[29] Complex **2.17** effectively inhibited *P berghei in vitro*, and it was also found to be effective against CQ-resistant FcB1 (IC_{50} = 5.1 nM) and FcB2 (IC_{50} = 2.3 nM) strains of *P. falciparum*. More importantly, it was 5-10 fold more active compared to the corresponding CQDP, thus lending support to the hypothesis that metal coordination results in a significant enhancement of the activity of the parent drug against resistant parasites. This observation prompted further investigations of gold(I) complexes as antimalarial agents. Analogous complexes **2.18** and **2.19** (Fig. 2.7), which were also several fold more active than CQDP against the CQ-resistant strain FcB1, were identified as potential antimalarial agents.[31] Similarly,

Sparatore et al.[32] reported gold(I) complex **2.20** (Fig. 2.7) with pronounced activity against the W2 strain.

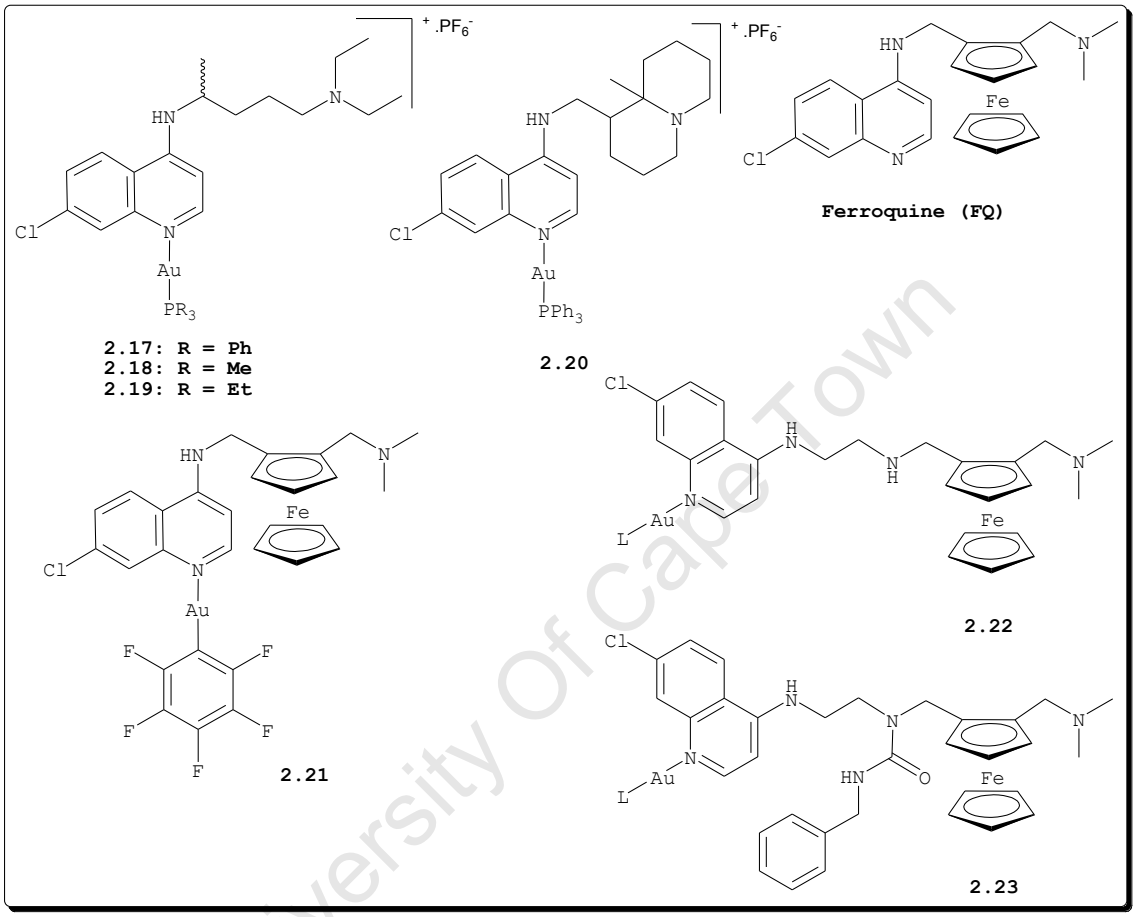

Figure 2.7: Antimalarial gold(I) complexes.

Motivated by their work on ruthenocene[33] and that of the Biot group on ferroquine (FQ, Fig. 2.7)[34] against the CQ-resistant parasite, *Blackie et al.*[35] investigated the approach of using heterobimetallic complexes obtained by reacting rhodium and gold-containing fragments with FQ instead of CQ. In the series, complexes **2.21–2.23** (L = triphenylphosphine or pentafluorobenzene co-ligands) were tested for antimalarial activity against the CQ-resistant strain of the parasite.[36] However, it was observed that the

presence of two metal centers [i.e. gold(III) and iron(II)] in one molecule had little effect on the overall efficacy of heterobimetallic compounds.[35]

2.5.2 Gold(III) Complexes

In an effort to develop improved antimalarial agents, *Navarro et al.*[37] demonstrated the activities of gold(III) complexes against several *P. falciparum* strains. Complex **2.24** (Fig. 2.8) proved to be more active compared to CQDP in both sensitive and resistant strains. Due to a limited number of compounds, the structure-activity relationship (SAR) for these compounds could not be extracted from the generated data.

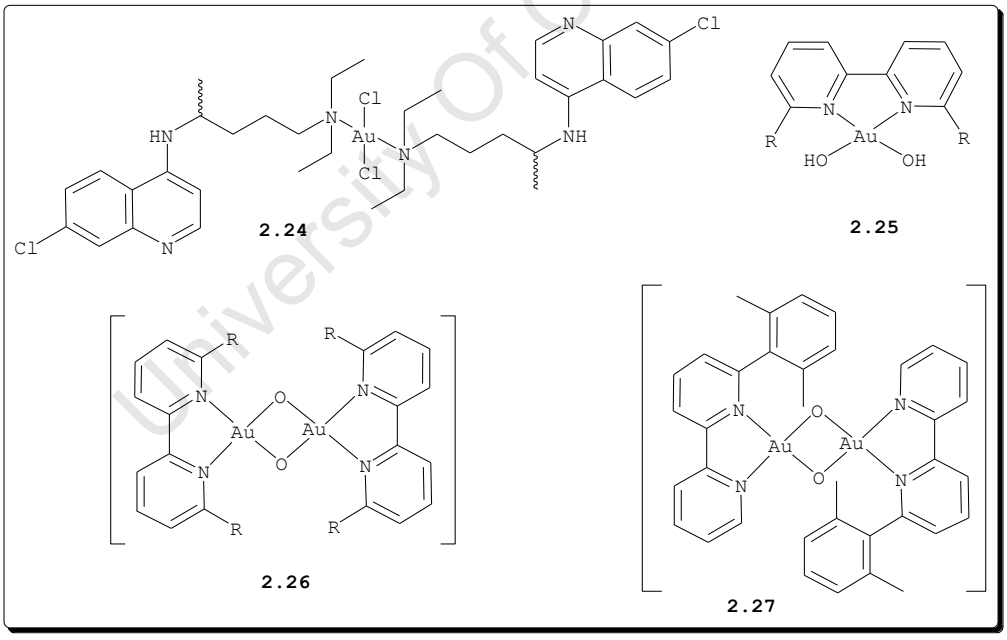

Figure 2.8: Antimalarial gold(III) complexes.

Recently, *Gabbiani et al.*[38] reported gold(III) complexes (**2.25–2.27**) with marked potency (IC_{50} values of 2.3–12.2 μM) against the 3D7 *P. falciparum* strain. However, these

compounds were found to be one order of magnitude less potent than gold(I) complex **2.7** (IC_{50} value of 0.142 μM).

2.6 GOLD COMPOUNDS: POSSIBLE MODES OF ACTION

Over the last several decades, mechanisms of action of gold complexes (antirheumatoid or antiproliferative) remain the subject of intense debate.[39] As a result, several hypotheses have been suggested,[40] but the exact molecular mechanism responsible for the pharmacological effects of gold compounds is unclear.[41,42] The available pharmacological data for a variety of these compounds has led to the identification of a few cellular processes, which are likely to be involved in their cytotoxicity.[40] These include direct DNA damage, modification of the cell cycle, mitochondrial damage, proteasome inhibition, modulation of specific kinases, and other cellular processes.

However, the molecular mechanism of action of gold complexes, which may well also account for their anti-malarial effects (the vast evidence emerged from studies mainly involving RA and solid tumour diseases) include DNA damage, inhibition of thioredoxin reductase, protein kinases (PK) and lysosomal cysteine proteases. These are further discussed in the sections hereafter.

2.6.1 DNA as a Target

Mechanistic studies of gold compounds have mostly focused on DNA and RNA as these biomolecules are primary targets for platinum anticancer drugs.[40] Several studies based on the weak interactions observed *in vitro* between gold(I) and DNA have suggested different cellular processes, which

might be involved in the cytotoxic mechanism of gold(I) drugs.

Similarly, extensive studies were conducted on the interaction of gold(III) with DNA based on consideration of the 'harder' character of the gold(III) center and its propensity to react with nucleobase nitrogens. However, these studies revealed that the *in vitro* interactions of several gold(III) compounds are often weak and reversible, thus suggesting that interactions are electrostatic in nature. The strong gold association with DNA observed in some gold(III) compounds is believed to be due to ligand dependent interactions, as in the case of porphyrins and terpyridines. This indicated that distinct cellular processes and targets may be responsible for their cytotoxicity.[40] The overall conclusion from various studies is that DNA is neither the primary nor the exclusive target for most gold(I) and gold(III) complexes.

2.6.2 Inhibition of Thioredoxin Reductase

Thioredoxin reductase (TrxR) is a homodimeric protein belonging to the family of glutathione reductase (GR)-like enzymes.[43] It catalyses the NADPH-dependent reduction of thioredoxin (Trx) disulfide and other related oxidised cell constituents. This enzyme has been identified in different species including the malaria parasite *P. falciparum*,[44] *Drosophila melanogaster* and humans.[43] It has broad substrate specificities and is involved in numerous metabolic pathways (antioxidant network, nucleotide synthesis) and pathophysiological conditions.[43] The active site of TrxR contains a selenocysteine (sec) Gly-Cys-Sc-Gly motif, which

is responsible for the catalytic mode of action of the enzyme.

The first study demonstrating the inhibitory effects of gold compounds (e.g. **2.6,** Fig. 2.3) on crude preparations of TrxR was conducted by *Hill et al*.[45] A year later, *Gromer et al*.[46] showed, in more detail, that complex **2.7** (Fig. 2.3) inhibited TrxR with high potency and selectivity over the other related enzymes (glutathione reductase and peroxidase). Consequently, several studies have demonstrated that **2.7** is a potent and specific inhibitor of both cytosolic and mitochondrial TrxR due to the affinity of gold for sulfur and selenium in thiol or selenol groups.[47] In addition, complex **2.7** and other gold(I) compounds have been found to induce, in the presence of Ca^{2+} ions,[48] mitochondrial permeability and membrane potential decrease, possibly due to interaction with the mitochondrial isoform of TrxR.[40] The release of cytochrome *c* triggers apoptosis, which is often accompanied by elevated production of reactive oxygen species (ROS).[43]

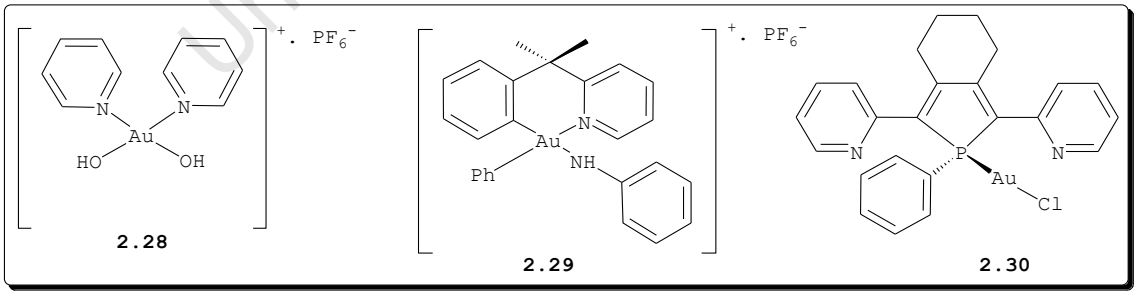

Figure 2.9: Aubipy (**2.28**), Aubipyxil (**2.29**) and GoPI (**2.30**) complexes.

In the mid 2000s, attention turned to a variety of gold(III) complexes for which relevant TrxR inhibitory properties were unambiguously established. *Rigobello et al.*[49] prepared several gold(III) compounds some of which inhibited mitochondrial TrxR2. Gold(III) compounds, especially Aubipy (**2.28**) and Aubipyxil (**2.29**, Fig. 2.9), also trigger mitochondrial swelling (but to some degree) compared to complex **2.7**.[49]

In a separate study, *Urig et al.*[50] demonstrated covalent binding of the gold phosphole complex (**2.30**, Fi.g 2.9) to cysteines in the active site of human glutathione reductase (hGR), which is structurally related to TrxR but lacks the selenol residue in the active site. The experimental (crystallography) data, which provided the first concrete evidence of gold(I) interacting with hGR, confirmed the binding of gold with two cysteine residues to the active site of the enzyme. This study suggested that the "undressing" – dissociation of surrounding phosphole and chloride ligands – of gold complexes might represent the general mode of interaction of almost all gold agents with cysteine or selenocysteine containing enzymes.[50,51]

2.6.3 Inhibition of Cysteine Proteases

Gold(I) salts have been shown to inhibit numerous thiol-dependent enzymes, including cysteine proteases *in vitro*.[52] The cathepsins, a family of homologous lysosomal cysteine proteases, have been extensively studied as biological targets of gold compounds by *Chircorian et al.*[53] and *Weidauer et al.*[54] The enzymes are involved in joint inflammation and destruction in RA and contain an activated

cysteine group in their active site. It is believed that coordination of gold(I) with an activated cysteine residue in the active site results in inactivation of the enzyme. Complexes **2.6**, **2.7** and Et_3PAuCl are amongst gold(I) complexes, which have been shown to moderately inhibit cathepsin B activity. *Weidauer et al.*[54] showed that complex **2.5** and **2.7** were moderately potent against cathepsin K and S, respectively.

2.6.4 Inhibition of Protein Kinases

Protein kinase C, belonging to a family of structurally related protein kinases, is a metalloenzyme containing Zn(II) bound to cysteine and histidine residues.[55] It plays an important role in intracellular signal transduction by phosphorylating other proteins, especially those with serine/threonine residues. The three widely used gold complexes, **2.5**, **2.6**, and **2.7** (Fig. 2.3) have been shown to inhibit protein kinase C.[40,55] This has been suggested as a possible mode of action for the therapeutic antirheumatic action of gold drugs.

2.7 ANTIMALARIAL ACTIVITY OF OTHER METAL COMPLEXES

2.7.1 Chloroquine-Based Metal Complexes

Metal-based compounds containing CQ have been considered as an ideal approach toward novel antimalarial agents over the past decade. In the early work of enhancing the pharmacological activity of CQ by incorporating metal-containing fragments, *Navarro et al.*[56] demonstrated that coordination of rhodium (**2.31** in Fig. 2.10) and ruthenium (**2.32**) led to improved activity against CQ-resistant

strains of *P. falciparum*. The same authors reported related iridium (Ir)-CQ derivatives, which were active *in vivo* against *P. berghei*.[57]

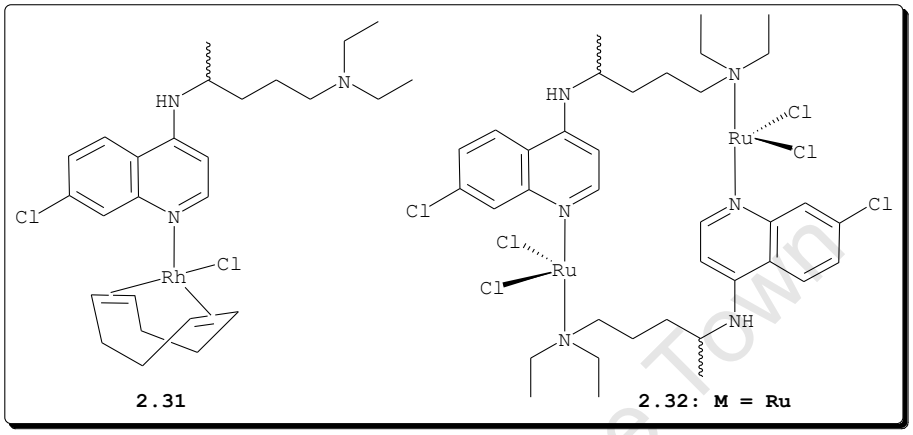

Figure 2.10: Antimalarial of platinum group metals with QC.

Recently, *Rajapakse et al.*[58] reported Ru-π-arene-CQ complexes, which were active against CQ-resistant strains of *P. falciparum in vitro*. In addition, these compounds were consistently more active compared to CQ, and this was found to be in agreement (qualitatively) with predictions made based on heam aggregation inhibition activity (HAIA) measured near water/*n*-octanol interfaces. Overall, the activity of these compounds against the resistant parasite has been ascribed to an alteration of the structure, basicity, and lipophilicity of CQ by the presence of metal.[59]

On the other hand, Biot and coworkers incorporated a ferrocenyl moiety into the side chain of the CQ structure through covalent linking to one of the cyclopentadienyl units to form an organometallic compound, FQ (Fig. 2.7).[34] This compound has been shown to be highly active and

selective against CQ-resistant *P. falciparum*.[60] A number of FQ analogues have been reported and in most cases they showed enhanced activities compared to CQ against CQ-resistant strains.[33,34,60,61]

2.7.2 Non-Chloroquine-Based Metal Complexes

Metal complexes bearing ligands with a non-chloroquine scaffold have also been reported. The overview of some of these complexes with antimalarial properties is provided below.

2.7.2.1 Bipyradyl and Phenanthroline-Based Complexes

In the late 1990s, *Koch et al.*[62] reported self-association (i.e. concentration-dependent) of a class of mixed-ligand cationic *N*-acyl-(*N'*,*N'*-dialkylthioureato)diimine-derived platinum(II) complexes in acetronitrile solution. Intrigued by these observations, *Egan et al.*[63] hypothesised that these complexes may associate with haem. A series of similar complexes were prepared and studied for their interactions with haematin.

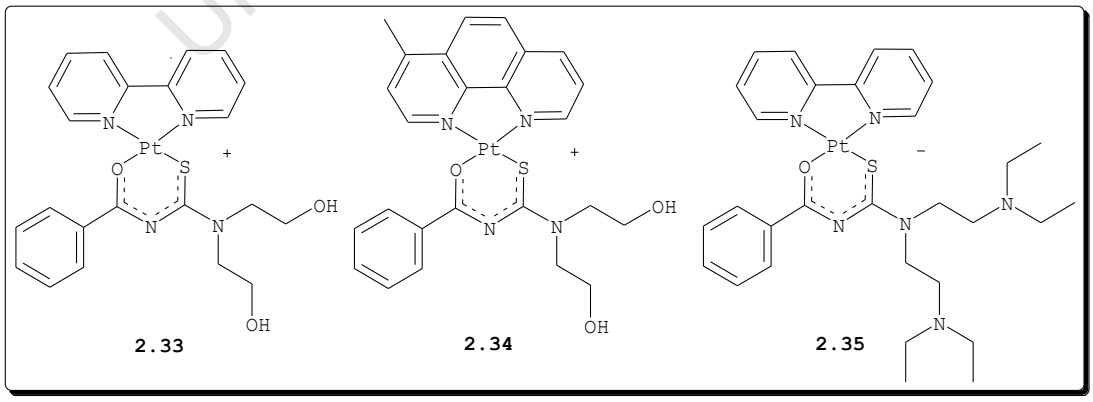

Figure 2.11: Antimalarial platinum(II) complexes.

Amongst those reported, complexes **2.33**–**2.35** were found to associate strongly with haem and inhibit β-haematin formation (Fig. 2.11). These complexes – except complex **2.35** which was moderately active - displayed good *in vitro* antiplasmodial activities (IC_{50} = 0.28–2.38 μM) although it was expected that such activities would be weak for two reasons. Firstly, since the complexes are cationic, they would not efficiently cross biological membranes without some specific uptake mechanisms. Secondly, with the exception of **2.35** they lack basic groups that are necessary for pH trapping in the food vacoule.[63] Although they interacted with haem, there could be no correlation found between their acitivity and ability to inhibit β-haematin formation, which suggested that they may act against other targets in the parasite.

2.7.2.2 Naphthoquinone Derived Complexes

In section **1.3.1.6** (p 15), the antimalarial properties of naphthoquinones have been discussed. The synthesis and investigation into the antimalarial properties of metal complexes, e.g. **2.36** (Fig. 2.12), of hydroxynaphthoquinones is being stimulated by fact that these compounds are capable of chelating biologically relevant ions, and thus the metal conjugation influences the redox properties of parent quinones.[64] The research group of Padhye reported several transition metal complexes derived from hydroxynaphthoquinone ligands. The copper(II) complex **2.36** (Fig. 2.12) was the most active compound against both *P. falciparum* 3D7 and K1 strains with ED_{50} values in the range 0.0002–1.97 μg/ml.[64] *In vivo*, this complex cleared 90% of

parasitemia at a dose of 15 mg/kg, while the standard drug, CQ, needed 10 mg/kg for 100% clearance. More importantly, complex **2.36** showed a several hundred-fold enhanced activity compared to the free ligand.

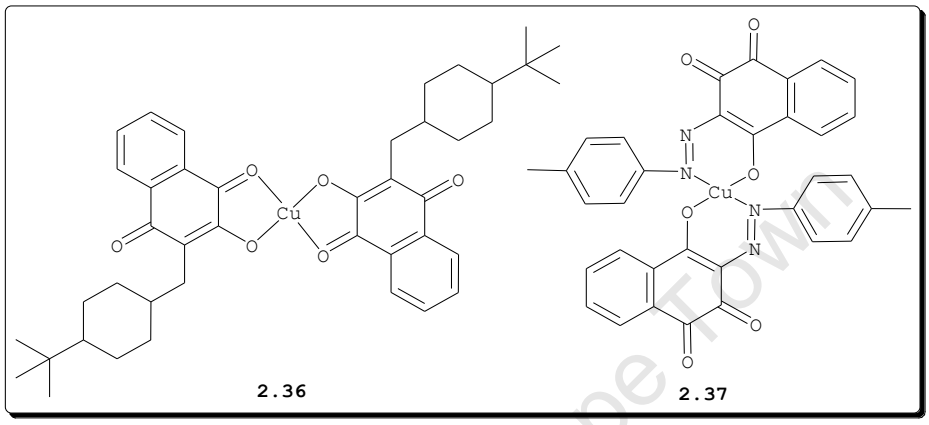

Figure 2.12: Antimalarial of copper(II) complexes.

Due to the promising antimalarial activity of copper(II) hydroxynaphthoquinone complex **2.36**, *Gokhale et al.*[65] reported the synthesis of copper(II) complex **2.37** (Fig. 2.12) derived from another class of naphthoquinone ligands, *viz*. 3-arylazo-4-hydroxy-1,2-naphthtoquinones. Within the series, complex **2.37** was found to be the most active against the 3D7 strain, and displayed approximately 170 fold enhancement in the antimalarial activity over the parent ligand.

2.7.2.3 Schiff-Base Metalloantimalarial Complexes

Schiff-base phenolate coordinated complexes (e.g. **2.38** and **2.39** in Fig. 2.13) - developed by Sharma and Piwnica-Worms – represent an unusual class of antimalarial agents targeted against haem aggregation.[66,67] More importantly, these compounds possess a favourable balance of

hydrophobicity and delocalized charge for enhanced cell membrane permeability. These *pseudo*-octahedral complexes with a N_4O_2 donor set, which were purposely designed for multidrug resistance in cancer cell lines,[68] have been found to possess antimalarial activities (IC_{50} = 1-3 μM) possibly by disrupting haem aggregation in *P. falciparum*.

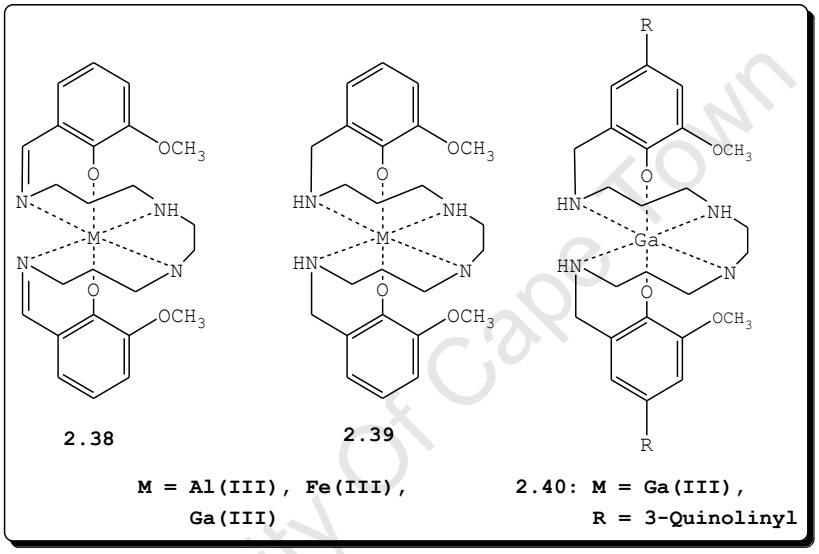

Figure 2.13: N_4O_2 Schiff-based metalloantimalarial complexes.

Several complexes were effective when evaluated against the CQ-sensitive and CQ-resistant clones. The efficacy of these complexes was found to correlate with their ability to inhibit haem dimerization.[68] This was further supported by experimental data showing that neither demetallation reactions, counter-ions, nor free ligands were responsible for the observed efficacy. This suggested that these complexes express activity in their fully intact form.

Further investigation of the possible mode of action has also shown that these complexes displayed no inhibition of plasmepsins and falcipains, suggesting that the N_4O_2-derived complexes act by disrupting the formation of haemozoin. Additionally others have suggested molecular conformation (e.g. **2.40**) of these complexes as being important for pharmacological activity.[68,69]

2.7.2.4 Thiosemicarbazone-Derived Complexes

In the early 1980s, *Scovill et al.*[70] investigated the ability of metal TSC complexes to cure mice infected with *P. berghei*. A small series of complexes of iron(III), copper(II) and nickel(II) with N^1,N^1-disubstituted TSC ligands such as **2.41** were prepared and evaluated for their antimalarial properties.

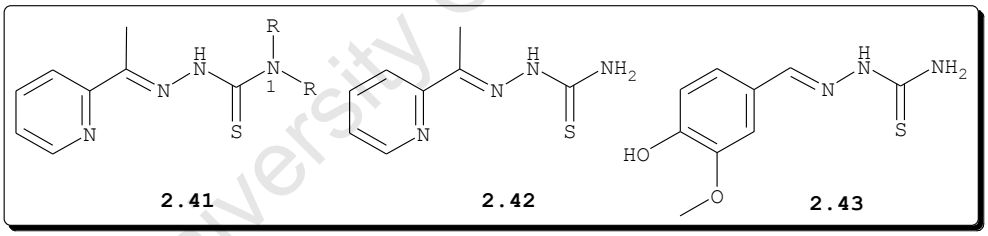

Figure 2.14: Antimalarial platinum(II) complexes.

However, it was noted that whereas antimalarial activity is retained in the series (i.e. TSCs) upon metal complexation, the resulting complexes offered no therapeutic advantage over the free ligands. In contrast, platinum(II) and ruthenium(III) chelates derived from 2-acetylpyridine (**2.42**) and *o*-vanillin (**2.43**) TSC ligands showed significant potency in mice infected with *P. berghei*.[71]

2.8 AIMS AND OBJECTIVES

Objective: The overall objective of current work is to identify novel gold complexes derived from TSC ligands as potential antimalarial agents.

Hypothesis: The underlying question and/or hypothesis to this research work we seek to address is whether it will be possible to enhance the *in vitro* antimalarial activity of TSCs by incorporating gold(I) and gold(III) containing fragments. Secondly, whether the incorporation of branched PA scaffolds to TSCs to form dendritic structures will enhance the *in vitro* antimalarial activity of TSCs, possibly due to increased cellular uptake

2.8.1 Specific Aims:

- to synthesise TSCs (**Chapter 3**) as bioactive ligands.
- to synthesise the corresponding gold(I) and gold(III) complexes (**Chapter 4**).
- to synthesise dendritic TSCs (**Chapter 6**) for potential postulated selective uptake by parasitic RBCs, possibly through polyamine transporters (PAT).
- to pharmacologically evaluate ligands (**Chapter 3**), metal complexes (**Chapter 5**) and dendritic TSCs (**Chapter 6**) *in vitro* against *P. falciparum* strains.
- to (in part) probe the mechanism of action of potent novel compounds with respect to the inhibition of malarial cysteine proteases, an important enzyme involved in Hb degradation.

2.9 REFERENCES

1. K.H. Thompson, C. Orvig, *Concepts and Models in Bioinorganic Chemistry*, Eds. H.-B. Kraatz and N. Metzler-Nolte, WILEY-VCH Verlag GmbH & Co. KGaA, Weinheim, **2006**, p 25-46.
2. S.P. Fricker, *J. Chem. Soc., Dalton Trans.*, **2007**, 4903-4917.
3. Z. Guo, P.J. Sadler, *Angew. Chem. Int. Ed.*, **1999**, *38*, 1512-1531.
4. P.C. Preusch, NIGMS Report Emanating from a meeting entitled, "*Metal in Medicine: Targets, Diagnostic, and Therapeutics*", June **2000**, in Bethesda, Maryland. www.nigms.nih.gov/news/meeting/metals.html.
5. (a) T.W. Hambley, *Dalton Trans.*, **2007**, 4929-4937. (b) E. Meggers, *Chem. Commun.*, **2009**, 1001-1010. (c) A special volume issue published in volume of **2008**, Metal-Based Drugs: *Metal-Containing Proteins, Macrocycles and Coordination Complexes in Therapeutic Application*, Editor-in-Chief, G. Sava, Hindawi Publishing, Italy.
6. K.H. Thompson, C. Orvig, *Dalton Trans.*, **2006**, 761-764.
7. R.A. Sánchez-Delgado, K. Lazardi, L. Rincón, J.A. Urbina, *J. Med. Chem.*, **1993**, *36*, 2041-2043.
8. (a) B.M. Sutton, *Gold Bull.*, **1986**, *19*, 15-16. (b) E.R.T. Tiekink, *Critical Reviews in Oncology/Hematology*, **2002**, *42*, 225-248. (c) V. Milacic, Q.P. Dou, *Coord. Chem. Rev.*, **2009**, *253*, 1649-1660. (d) W.F. Kean, I.R.L. Kean, *Inflammopharmacology*, **2008**, *16*, 112-125.

9. C.F. Shaw III, *Gold*: *Progress in Chemistry, Biochemistry and Technology*, Ed. H. Schimidbaur, John Wiley & Sons Ltd, **1999**, New York, p 260-298.
10. N. Farrel, "*Metal Complexes as Drugs and Chemotherapeutics*": *Comprehensive Coordination Chemistry II*, Vol. 9, Elsevier, Place, p 809-839.
11. A.R. Sannella, A. Casini, C. Gabbiani, L. Messori, A.R. Bililia, F.F. Vincieri, G. Majorie, C. Severini, *FEBS Lett.*, **2008**, *582*, 844-847.
12. T.M. Simon, D.H. Kunishima, G.J. Vibert, A. Lorber, *Cancer*, **1979**, *44*, 1965-1975.
13. I. Ott, X. Qian, Y, Xu, D.H.W. Vlecken, I.J. Marques, D. Kubutat, J. Will, W.S. Sheldrick, P. Jesse, A. Prokop, C.P. Bagowski, *J. Med. Chem.*, **2009**, *52*, 763-770.
14. D. de Vos, S.Y. Hoo, E.R.T. Tiekink, *Bioinorg. Chem. Appl.*, **2004**, *2*, 141-154.
15. (a) J.S. Casas, E.E. Castellano, M.D. Couce, O. Crespo, J. Elena, A. Laguna, A. Sanchez, J. Sordo, C. Taboada, *Inorg. Chem.*, **2007**, *46*, 6236-6238. (b) J.S. Casas, E.E. Catellano, M.D. Couce, J. Ellena, A. Sanchez, J. Sordo, C. Taboada, *J. Inorg. Biochem.*, **2006**, *100*, 1858-1860.
16. (a) S.P. Friker, *Gold Bulletin*, **1996**, *29*, 53-59. (b) S.J. Berners-Price, K. Christopher, C.K. Mirabelli, K.J. Randall, MR. Mattern, F.L. McCabe, *Cancer Research*, **1986**, *46*, 5486-5493. (c) C.K. Mirabelli, R.K. Johnson, D.T. Hill, L.F. Faucette, G.R. Girard, G.Y. Keu, C.M. Sung, S.T. Crooke, *J. Med. Chem.*, **1986**, *29*, 218-233.

17. G.D. Hoke, R.A. Macia, P.C. Meunier, P.J. Bugelski, C.K. Mirabelli, G.F. Rush, W.D. Mathews, *Toxicology and Applied Pharmacology*, **1989**, *100*, 293-306.
18. (a) E.R.T. Tiekink, *Inflammopharmacology*, **2008**, *16*, 138-142. (b) V. Milacic, Q.P. Dou, *Coord. Chem. Rev.*, **2009**, *253*, 1649-1660.
19. L. Ronconi, C. Marzano, P. Zanello, M. Corsini, G. Miolo, C. Macca, A. Trevisan, D. Fregona, *J. Med. Chem.*, **2006**, *49*, 1648-1657.
20. R. W.-Y. Sun, D.-L. Ma, E. L.-M. Wong, C.-M. Che, *Dalton Trans.*, **2007**, 4884-4892.
21. L. Messori, G. Marcon, P. Orioli, *Bioinorg. Chem. Appl.*, **2003**, *1*, 177-187.
22. P.J. Sadler, R.E. Sue, *Metal-Based Drugs*, **1994**, *1*, 107-144.
23. K. Nomiya, S. Yamamoto, R. Noguchi, H. Yokoyama, N.C. Kasuga, K. Ohyama, C. Kato, *J. Inorg. Biochem.*, **2003**, *95*, 208-220.
24. S. Jackson-Rosario, D. Cowart, A. Myers, R. Tarrien, R.L. Levine, R.A. Scott, W.T. Self, *J. Biol. Inorg. Chem.*, **2009**, *14*, 507-519.
25. C.F. Shaw III, *Chem. Rev.*, **1999**, *99*, 2589-2600.
26. D.L. Shapiro, J.R. Masci, *J. Rheumatol.*, **1996**, *23*, 1818-1820.
27. R. Wai-Yin, Y. Wing-Yu, S. Hongzhe, C. Chi-Ming, *ChemBioChem – Eur. J. Chem. Biol.*, **2004**, 5, 1293-1298.
28. N. Wasi, H.B. Singh, A. Gajanana, A.N. Raichowdhary, *Inorg. Chim. Acta*, **1987**, *135*, 133–137.
29. M. Navarro, *Coord. Chem. Rev.*, **2009**, *253*, 1619-1626.

30. M. Navarro, H. Pérez, R.A. Sánchez-Delgado, *J. Med. Chem.*, **1997**, *40*, 1937-1939.
31. M. Navarro, F. Vásquez, R.A. Sáchez-Delgado, H. Pérez, V. Sinou, J. Schrével, *J. Med. Chem.*, **2004**, *47*, 5204-5209.
32. A. Sparatore, N. Basilico, S. Parapini, S. Romeo, F. Novelli, F. Sparatore, D. Taramelli, *Bioorg. Med. Chem.*, **2005**, *13*, 5338-5345.
33. P. Beagley, M.A.L. Blackie, K. Chibale, C. Clarkson, J.R. Moss, P.J. Smith, *J. Chem. Soc., Dalton Trans.*, **2002**, 4426-4433.
34. C. Biot, G. Glorian, L.A. Maciejewski, J.S. Brocard, O. Domarie, G. Blampain, P. Millet, A.J. Georges, H. Abessolo, D. Dive, J. Lebibi, *J. Med. Chem.*, **1997**, *40*, 3715-3718.
35. M.A.L. Blackie, P. Beagley, K. Chibale, C. Clarkson, J.R. Moss, P.J. Smith, *J. Organomet. Chem.*, **2003**, *688*, 144-152.
36. M.A.L Blackie, **PhD Thesis**; *New Mono and Bimetallic Chloroquine Derivatives: Synthesis and Evaluation as Antiparasitic Agents*, University of Cape Town, **2002**.
37. M. Navarro, F. Vásquez, R.A. Sánchez-Delgado, H. Pérez, V. Sinou, J. Schrével, *J. Med. Chem.*, **2004**, *47*, 5204-5209.
38. C. Gabbiani, L. Messori, M.A. Cinellu, A. Casini, P. Mura, A.R. Sannella, C. Severini, G. Majori, A.R. Bilia, F.F. Vincieri, *J. Inorg. Biochem.*, **2009**, *103*, 310-312.

39. S.S. Gunatilleke, C.A.F. de Oliveira, J.A. McCammon, A.M. Barrios, *J. Biol. Inorg. Chem.*, **2008**, *13*, 555-561.
40. S. Nobili, E. Mini, I. Landini, C. Gabbiani, A. Casini, L. Messori, *Medicinal Research Reviews*, **2009**, *29*, doi: 10.1002/med.20168.
41. C. Gabbiani, A. Casini, L. Messori, *Gold Bulletin*, **2007**, *40*, 73-81.
42. H.E. Abdou, A.A. Mohamed, J.P. Fackeler Jr, A. Burini, R. Galassi, J.M. López-de-Luzuriaga, M.E. Olmos, *Coord. Chem. Rev.*, **2009**, *253*, 1661-1669.
43. I. Otto, *Coord. Chem. Rev.*, **2009**, *253*, 1670-1681.
44. (a) K. Chibale, *ARKIVOC*, **2002**, *ix*, 93-98. (b) S. Rahlfs, R.H. Schirmer, K. Becker, *Cell. Mol. Life Sci.*, **2002**, *59*, 1024-1041. (c) K. Becker, L. Tilley, J.L. Vennerstrom, D. Roberts, S. Rogerson, H. Ginsburg, *Int. J. Parasitol.*, **2004**, *34*, 163-189.
45. K.E. Hill, G.W. McCollum, M.E. Boeglin, R.F. Burk, *Biochem. Biophys. Res. Commun.*, **1997**, *234*, 293-295.
46. S. Gromer, L.D. Arscott, C.H. Williams, R.H. Schirmer, K. Becker, *J. Biol. Chem.*, **1998**, 273, 20096-20101.
47. (a) M.P. Rigobello, G. Scutari, A. Folda, A. Bindoli, *Biochem. Pharmacol.*, **2004**, *67*, 689-696. (b) M.P. Rigobello, A. Folda, B. Dani, R. Menabò, G. Scutari, A. Bindoli, *Eur. J. Pharmacol.*, **2008**, *582*, 26-34. (c) A. Bindoli, M.P. Rigobello, G. Scutari, C. Gabbiani, A. Casini, L. Messori, *Coord. Chem. Rev.*, **2009**, *253*, 1692-1707.
48. M.P. Rigobello, G. Scutari, R. Boscolo, A. Bindoli, *Br. J. Pharmcol.*, **2002**, *136*, 1162-1168.

49. M.P. Rigobello, L. Messori, G. Marcon, M.A. Cinellu, M. Bragadin, A. Folda, G. Scutari, A. Bindoli, *J. Inorg. Biochem.*, **2004**, *98*, 1634-1641.
50. S. Urig, K. Fritz-Wolf, R. Reau, C. Herold-Mende, K. Toth, E. Davioud-Charvet, K. Becker, *Angew. Chem. Int. Ed.*, **2005**, *45*, 1881-1886.
51. M. Deponte, S. Urig, L.D. Arscott, K. Fritz-Wolf, R. Reau, C. Herold-Mende, S. Konkarevic, M. Meyer, E. Davioud-Charvet, D.P. Ballou, C.H. Williams, K. Becker, *J. Biol. Chem.*, **2005**, *280*, 20628-20637.
52. S.S. Gunatilleke, C.A.F. de Oliveira, J.A. McCammon, A.M. Barrios, *J. Biol. Inorg. Chem.*, **2008**, *13*, 555-561.
53. (a) A. Chircorian, A.M. Barrios, *Bioorg. Med. Chem. Lett.*, **2004**, *14*, 5113-5116. (b) S.S. Gunatilleke, A.M. Barrios, *J. Med. Chem.*, **2006**, *49*, 3933-3937. (c) S.S. Gunatilleke, A.M. Barrios, *J. Inorg. Biochem.*, **2008**, *102*, 555-563.
54. E. Weidauer, Y. Yasuda, B.K. Biswal, M. Cherny, M.N.G. James, D. Brömme, *Biol. Chem.*, **2007**, *388*, 331-336.
55. S.L. Best, P.J. Sadler, *Gold Bulletin*, **1996**, *29*, 87-93.
56. R.A. Sachez-Delgado, M. Navarro, H. Perez, J.A. Urbina, *J. Med. Chem.*, **1996**, *3*, 1095-1099.
57. M. Navarro, S. Pekerar, H. Pérez, *Polyhedron*, **2007**, *26*, 2420-2424.
58. C.S.K. Rajapakse, A. Martínez, B. Naoulou, A.A. Jarzecki, L. Suárez, C. Deregnaucourt, V. Sinou, J. Schrevel, E. Musi, G. Ambrosini, G.K. Schwartz, R.A. Sáchez-Delgado, *Inorg. Chem.*, **2009**, *48*, 1122-1131.

59. A. Martínez, C.S.K. Rajapakse, D. Jalloh, C. Dautriche, R.A. Sáchez-Delgado, *J. Biol. Inorg. Chem.*, **2009**, *41*, 863-871.

60. C. Biot, *Curr. Med. Chem. -Anti-Infective Agents*, **2004**, *3*, 135-147.

61. (a) K. Chibale, J.R. Moss, M.A.L. Blackie, D. Van Schalkwyk, P.J. Smith, *Tetrahedron Lett.*, **2000**, *41*, 6231-6235. (b) M.A.L. Blackie, K. Chibale, *Metal-Based Drugs*, **2008**, *Article ID*: 495123.

62. K.R. Koch, C. Sacht, C. Lawrence, *J. Chem. Soc., Dalton Trans.*, **1998**, 689-695.

63. T.J. Egan, K.R. Koch, P.L. Swan, C. Clarkson, D.A. Van Schalkwyk, P.J. Smith, *J. Med. Chem.*, **2004**, *47*, 2926-2934

64. N.H. Gokhale, S.B. Pdhaye, S.L. Croft, H.D. Kendrick, W. Davies, C.E. Anson, A.K. Powell, *J. Inorg. Biochem.*, **2003**, *95*, 249-258.

65. N.H. Gokhale, K. Shirisha, S.B. Padhaye, S.L. Croft, H.D. Kendrick, V. Mckee, *Bioorg. Med. Chem. Lett.*, **2006**, *16*, 430-432.

66. (a) V. Sharma, D. Piwnica-Worms, *Chem. Rev.*, **1999**, *99*, 2545-2560. (b) J. Ziegler, R. Linck, D.W. Wright, *Curr. Med. Chem.*, **2001**, *8*, 171-189. (c) V. Sharma, *Mini-Rev. Med. Chem.*, **2005**, *5*, 337-3351.

67. D.A. Casteel, Antimalarial Agents in *Burger's Medicinal Chemistry and Drug Discovery*, 6th ed, Vol. 5: *Chemotherapeutic Agents*, Ed. D.J. Abraham, Wiley & Sons, Inc, **2003**, p 920-999.

68. D.E. Goldberg, V. Sharma, A. Oksman, I.Y. Gluzman, T.E. Wellems, *J. Biol. Chem.*, **1997**, *272*, 6567-6572.

69. J.A. Ochesky, S.E. Harpstrite, A. Oksman, D.E. Goldberg, V. Sharma, *Chem. Commun.*, **2005**, 1622-1624.

70. J.P. Scovill, D.L. Klayman, C.F. Franchino, *J. Med. Chem.*, **1982**, *25*, 1261-1264.

71. H. Beraldo, D. Gambino, *Mini-Rev. Med. Chem.*, **2004**, *4*, 31-39.

CHAPTER 3

SYNTHESIS AND BIOLOGICAL EVALUATION OF THIOSEMICARBAZONES AND RELATED PYRAZOLINE ANALOGUES

ABSTRACT: As important scaffolds on which to base the development of potential antiparasitic agents, TSCs are also vital N,S donor ligands in coordination chemistry. A vast array of metal complexes of TSCs has been reported. This chapter describes the synthesis, characterization and antiplasmodial evaluation of a focused series of TSCs **3.28a–h** and pyrazoline analogues **3.37a–f**, respectively. The discussion is preceded by a brief introduction and a survey of biological activities of TSCs, and subsequently the rationale behind their synthesis.

3.1 THIOSEMICARBAZONES: GENERAL OVERVIEW

TSCs are a class of compounds belonging to the Schiff base family historically discovered as by-products from reactions involving organic analysis for identification of aldehydes and ketones.[1] These compounds have played a significant role as N,S donor ligands in traditional coordination chemistry. Up to now, a number of transition and main group metal complexes have been reported.[2] In general, they are broadly classified as mono-TSCs (**3.1**), *bis*-TSCs (**3.2**) and *di*-TSCs (**3.3**). The general structures of different types of TSCs are depicted in Fig. 3.1.

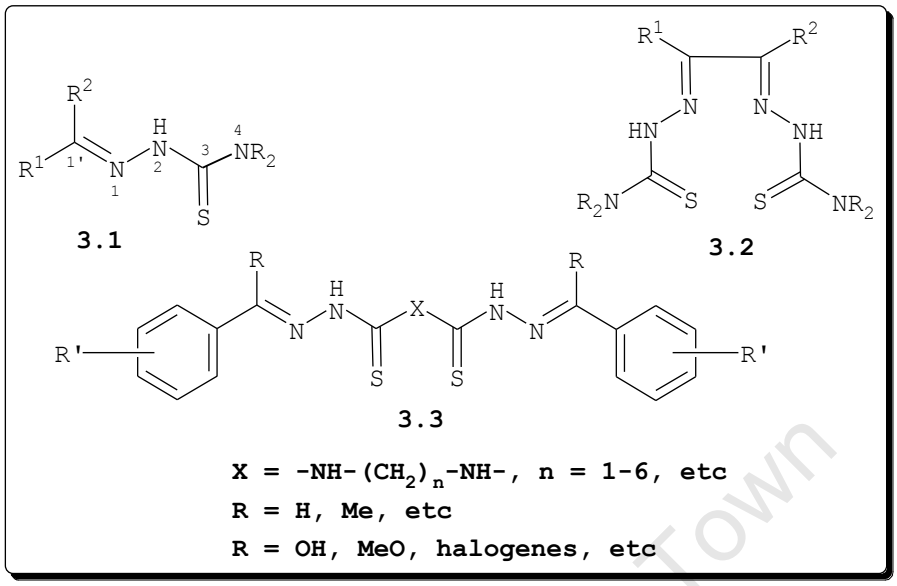

Figure 3.1: General structures of types of TSCs.

However, for the purpose of this thesis, only mono-TSCs will be described although a number of *bis*-TSCs are of great interest as delivery agents for radioactive copper in copper-based radiopharmaceuticals.[3]

3.1.1 Mono-TSCs: Substitution Pattern and Stability

Mono-TSCs are often grouped into two categories. The first category involves aldehyde-based derivatives, which have a hydrogen atom (R^2) at the iminic carbon (C1′), while R^1 may be an alkyl, aryl or a heterocyclic moiety. The substituents at ^{4}N may be similar (e.g. hydrogen atoms, alkyl) or a combination of hydrogen atom, alkyl, aryl, or cyclic.[2a] SAR studies revealed that cyclic structures possess significant antimalarial activities than their non-cyclic counterparts.[4] The second category, however, constitutes a ketonic moiety with the R^1 and R^2 either exhibiting similar or different alkyl and aryl groups.

Due to their ability to delocalise charge as shown in Scheme 3.1, TSCs are considerably stable in comparison to other imine counterparts. Delocalization decreases the δ^+ charge on the carbon atom (C1′) of the imine (C=N) double bond, and by so doing C1′ becomes less susceptible to nucleophilic attack.[5] Theoretically, this suggests that TSCs are by far more resistant to nucleophilic attack and/or hydrolysis than primary imines.

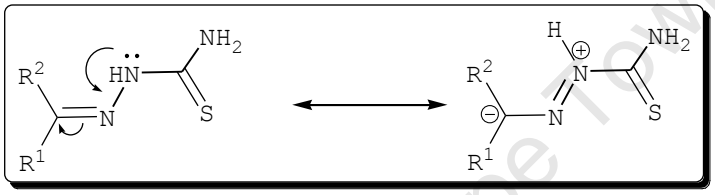

Scheme 3.1: Charge stabilisation in TSCs.

3.1.2 Binding Modes of TSCs with Metal Centers

Several studies have shown that the non-hydrogen atoms in TSC template are nearly planar.[6] In solution, these ligands exist as both tautomers [thione(**A**)-thiol(**B**)],[2,7] hence they can bind to a metal center (M) in the neutral (**A**) and/or the anionic (**C**) form after the loss of the ^{2}NH or SH proton.

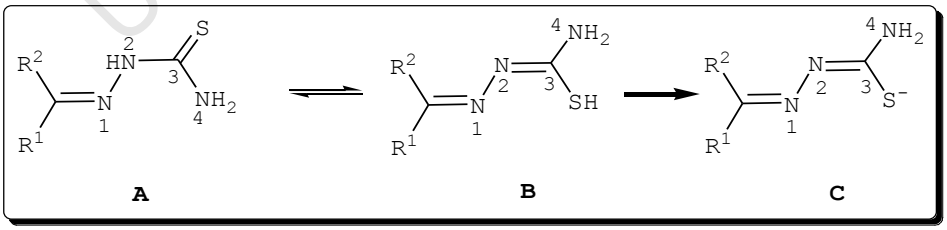

Scheme 3.2: Thione-thiol tautomers.

A number of intriguing bonding modes have been observed.[2a] In neutral form (**A**), bonding with a metal center occurs through the S donor atom and/or N,S chelation. A third

coordinating donor atom often gives rise to ONS (e.g. 2-hydroxybenzaldehyde TSC) or NNS (e.g. 2-acetylpyridine TSC) tridentate ligating systems.[2a] The same argument regarding the binding mode can be extended to the anionic form (**C**). However, there have been some reported cases where heterocyclic (third atom) and azomethine N donor atoms are involved in bidentate coordination with metal centers instead of normal tridentate NNS/ONS ligating systems exhibited by these ligands. The sulfur atom in these cases is considered to be either not coordinated, or weakly coordinated to the same metal center or coordinated to an adjacent metal center.[8]

3.2 MEDICINAL APPLICATIONS OF THIOSEMICARBAZONES

It has been reported that a number of known TSCs have poor aqueous solubility.[8] As a result oral administration of TSCs in clinical practice is extremely limited. However, the biological importance of this class of compounds is well established. The available biological data reveal a wide spectrum of pharmacological properties,[8,9,10] and some of these properties, including examples of different types of TSCs, are described below.

3.2.1 Antitubercular Activity

In the mid 1940s, *Domagk et al.*[11] reported for the first time the biological properties of TSCs. In the study, they demonstrated that TSCs exhibited some antitubercular activities *in vitro*. Amongst the leading clinically established agents to treat TB is the relatively inexpensive TSC drug, thioacetazone (**3.4**, Fig. 3.2).[12,13]

However, **3.4** suffers from a range of side effects and the development of resistance to the drug by the organism. To overcome these problems, compound **3.4** was recommended for use in combination with other antitubercular drugs (e.g. isoniazid **3.5**), and this approach is widely used in developing countries.[14] The clinical success of **3.4** has broadened further interest in TSCs as anti-TB agents.[15] Analogues of **3.4**, compounds **3.6** and **3.7** (Fig. 3.2) have been developed and found to be more active compared to **3.4** *in vitro* and *in vivo* against *Myocobacterium avium*.[16]

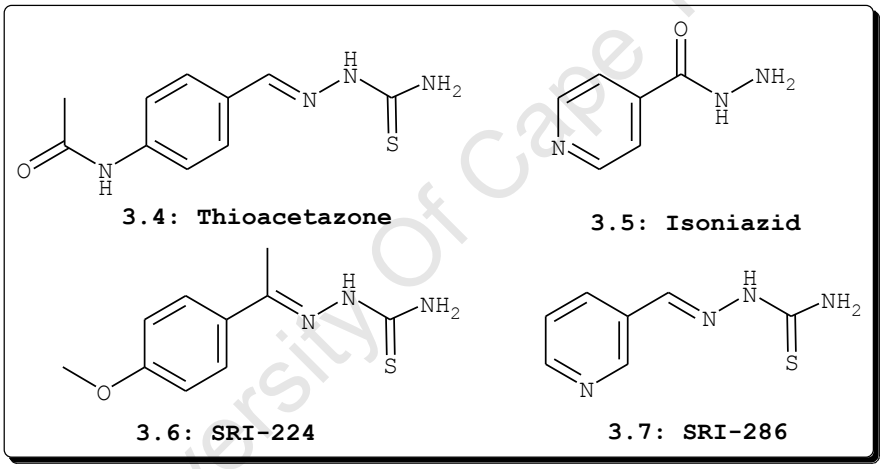

Figure 3.2: Examples of antitubercular TSCs and isoniazid.

3.2.2 Antifungal Activity

In the 1960s, a series of TSCs derived from aldehydes and ketones (aliphatic and aromatic), was tested for antifungal activity against *Chaetomium globosum* and *Aspergillus niger*.[17] Some of these compounds included *p*-anisaldehyde (**3.8**) and pyridine-2-aldehyde (**3.9**) TSCs (Fig. 3.3), which were screened for antifungal activity against *Alternarai sp*, *Paecilomyces sp*, *Pestalotia sp*.

However, the corresponding metal complexes were far more active compared to the free TSC ligand against fungi.

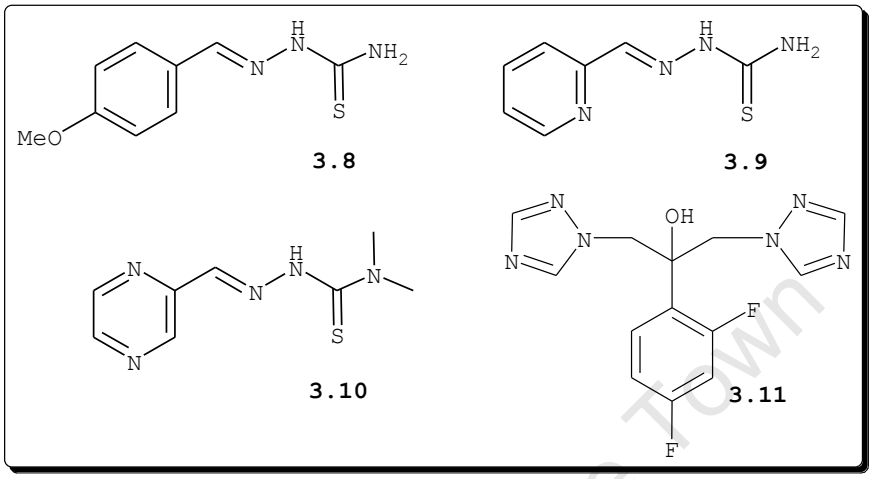

Figure 3.3: Antifungal TSCs and fluconazole (**3.11**).

Recently, acetylpyrazine TSCs were tested against a panel of fungal strains.[18] The most potent compound was **3.10** (Fig. 3.3), which exhibited comparable efficacy to the clinically used agent, **fluconazole** (**3.11**), against *C. albicans* ATCC 44859, *C. tropicalis* 156, and *T. asahii* 1188. This compound also showed greater potency than **3.11** when tested for antifungal activity against *C. krusei* E 28, *C. glabrata* 20/I, *A. fumigatus*, *A. corymbifera* 272, and *T. mentagrophytes* 445.[18]

3.2.3 Antiviral Activity

Following the first report on the antiviral activity of benzaldehyde TSC against neurovaccinal infection in mice,[19] a number of TSC derivatives have been evaluated for their activities against viral infections.[10] The classic example representing these compounds is *N*-methyl-β-isatin TSC (Methisazone, **3.12**, Fig. 3.4), which was found to be potent

against smallpox during clinical trials conducted in India.[9] In addition, compound **3.12** has also been used to treat individuals infected with the Herpes Simplex Virus (HSV). Its derivatives have been shown to inhibit Moloney leukaemia virus and HIV.

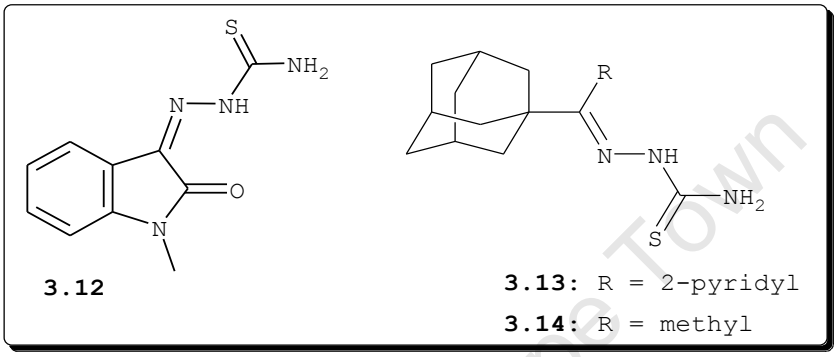

Figure 3.4: Chemical structures of antiviral TSCs.

In a separate study, *Kolocouris et al*[20] investigated adamantane TSC derivatives **3.13** and **3.14** (Fig. 3.4) for their ability to inhibit HIV-1 and HIV-2, respectively. Regrettably, these compounds displayed no activity against these viruses. On the other hand, the purine-6-carboxaldehyde, 2-acetylpyridine, 2-acetylquinoline and 1-acetylisoquonile derivatives were found to be highly active against type 1 and 2 HSV.[20]

3.2.4 Antitumour Activity

To date, α-*N*-heterocyclic TSC derivatives are by far the largest group of TSC compounds studied as antitumour agents.[9] Following reports by *Domagk et al.*[11] and *Hamre et al.*[19] on antitubercular and antiviral activities of TSCs in the mid 1950s, *Brockman et al.*[21] reported the antitumour effects of TSCs. Amongst the reported compounds exhibiting

antitumour activities, **3.9** (Fig. 3.3) was found to be the most effective compound. Consequently, several novel TSCs were investigated as potential antitumour agents. The hypothesis by *French et al.*[22] about the mode of action of α-*N*-heterocyclic TSCs necessitated further investigations into these compounds for biological benefits.

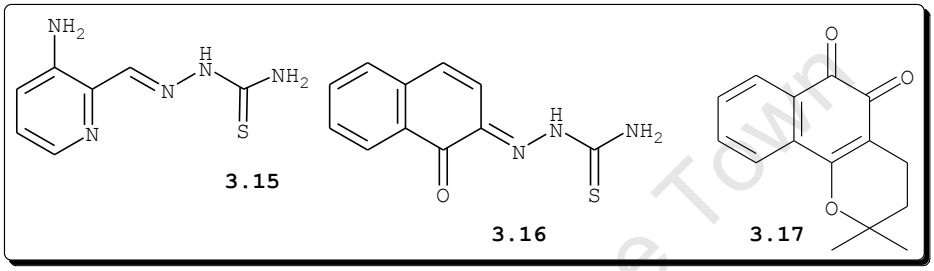

Figure 3.5: Triapine (**3.15**), NQTS (**3.16**) and *β*-lapachone (**3.17**).

The most successful compound in this group however, is 3-aminopyridine-2-carboxaldehyde TSC **3.15** (Triapine™, Fig. 3.5),[9,23] which has reached Phase I and II clinical trials. It has been demonstrated that **3.15** is able to cure mice inoculated with L1210 leukemia. More importantly, compound **3.15** has been shown to be potent against hydroxyurea (clinical established RR inhibitor) resistant cells, and inhibited a wide range of tumour xenografts in mice.

Further investigations led to *Afrasiabi et al.*[24] disclosing non-heterocyclic TSC derivative 1,2-napthaquinone TSC (**3.16**, NQTS, Fig. 3.5) containing a naphthaquinone scaffold from a natural product *β*-lapachone (**3.17**). The *in vitro* evaluation of **3.16** against cancer cell lines revealed that appending of the thiosemicarbazide (TSCz) pharmacophore to the parent scaffold quinone enhanced its antiproliferative activity against human breast cancer cell line MCF7.[25] A

similar observation was made by *Adsule et al.*[26] when the TSCz scaffold was attached to the parent quinoline pharmacophore.

3.2.5 Antiparasitic Activity

Globally, the most important infectious diseases threatening humankind are caused by protozoan parasites.[27] The leading three diseases: malaria, leishmaniasis and trypanosomiasis (Chagas' disease), which are associated with intense morbidity and extensive mortality mostly in resource poor countries, remain a huge public health challenge. The individuals with compromised immune systems are under severe threat from protozoan parasites.[27] TSCs have been shown to be important scaffolds for designing potent antiparasitic agents against a wide range of protozoan parasites.[28] In the context of TSCs, the most studied parasitic diseases are trypanosomiasis and malaria.

3.2.5.1 Antitrypanosomal

The first literature report on *in vitro* and *in vivo* antitrypanosomal activities of TSCs came to light in 1974.[1] From the reported series most effective compounds are best represented by **3.18** and **3.19** (Fig. 3.6).

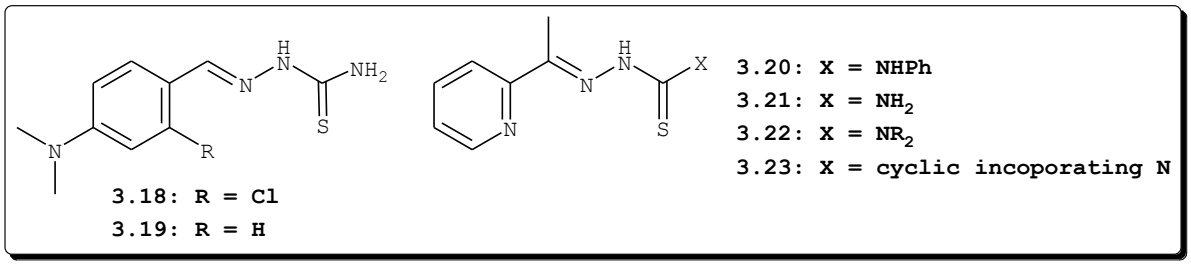

Figure 3.6: Chemical structures of antitrypanosomal TSCs.

In 1980, *Casero et al.*[29] reported on *in vitro* biological evaluation of 2-acetylpyridine TSCs (**3.20**–**3.23**) against *Trypanosoma rhodesience*. In both studies, it was suggested that marked antitrypanosomal activities of TSCs may be due to the inhibition of protein synthesis as had been shown for the antiviral activity of **3.12** (Fig. 3.4).

Following what could be described as an "abandoned study" of TSCs due to previous perceptions about their toxicity; *Du et al.*[30] identified a library of TSCs, which displayed significant activities against cruzain, the cysteine protease of *Trypanosoma cruzi*.[31] The compound **A**[1] (Fig. 3.7) was found to be the most active TSC. Intrigued by these observations, Du and co-workers explored the SAR around this lead compound. This renewed interest into this class of compounds as parasitic cysteine protease inhibitors.[28]

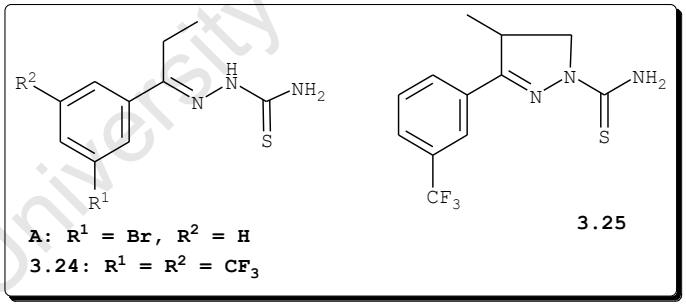

Figure 3.7: TSCs as inhibitors of cruzain.

A series of **A** analogues represented by **3.24** and **3.25** were synthesized and evaluated for their ability to inhibit cysteine proteases (Fig. 3.7). Compound **3.24** and **3.25** effectively inhibited cruzain. More importantly, some of these compounds displayed no significant toxicity against

[1]Compound **A** is **3.24h** in Table 3.1.

the host cells. This study led to the synthesis of a second series of TSCs, which were evaluated against *Trypanosoma brucei* and *cruzi*, respectively.[32] The deduced SAR study resulted in novel TSCs, which displayed greater trypanocidal activity.[33,34] The recent report by *Porcal et al.*[35] further illustrates the growing interest in TSCs as potential antitrypanosomal agents.

3.2.5.2 Antimalarial Activity

As mentioned in previous chapters, the antimalarial activity of TSCs was first demonstrated by *Klayman et al.*[36] three decades ago. Klayman and co-workers studied the antimalarial effects of these compounds on mice infected with *P. berghei*. Initially, it was observed that the ^{4}N monosubstituted analogues **3.20** (Fig. 3.6) cured mice at doses below 200 mg/kg/day. However, further investigation revealed that the activity was enhanced when ^{4}N is disubstituted (**3.22,** Fig. 3.6) or part of a ring system (**3.23,** Fig. 3.6).[4] This led to extensive investigations into antimalarial properties of TSCs.

In recent years a substantial amount of work has also been conducted in our laboratory to exploit the antimalarial and antitrypanosomial effects of TSCs including their ability to inhibit parasitic cysteine proteases, FP-2, cruzain and rhodesain.[28a,37]

3.3 THIOSEMICARBAZONES: POSSIBLE MODE OF ACTION

A number of studies have suggested various modes of action of TSCs,[35,38] but up to now the most common mechanisms on which consensus exists include the inhibition of

ribonucleotide reductase (RR),[22] cysteine proteases[30] and the creation of lesions (through the inhibition of polymerase α) in DNA strands.[8]

3.3.1 Iron Chelation

Iron is an essential element for the biological action of a number of proteins and other Fe dependent enzymes.[39] Since TSCs (e.g. **3.15** in Fig. 3.5 and **3.20–3.23** in Fig. 3.6) are also members of a class of iron chelators, it has been suggested that these ligands may act by sequestering iron,[22,40] thus interfering with supply of nutrients for protein proliferation. It has also been suggested that these compounds act by inhibiting RR through binding iron, which is involved in stabilising a tyrosol radical in the active site of the enzyme, ultimately, preventing the production of nucleotide precursors essential for DNA synthesis.[39,41]

Although this mechanism could not be pursued in this work, the recent study of *Richardson et al.*[18] clearly demonstrates that non-α-(N)-heterocyclic TSCs are poor iron chelators compared to α-(N)-heterocyclic TSC counterparts, which possess the NNS tridentate ligating system. This suggests that non-α-(N)-heterocyclic TSCs act by mechanisms independent of iron chelation, and one of those is the inhibition of cysteine proteases (section **3.3.2**).[30]

Alternatively, TSCs can bind iron (from the iron pool) to form lethal complexes which intracellularly may be involved in redox cycle, ultimately, the generation of cytotoxic

free radical species, which could be important for their potential activity.

3.3.2 Inhibition of Cysteine Proteases

As previously mentioned, proteases are essential for living organisms to fulfil virtually all biological functions. Fig. 3.8 illustrates the proposed interaction with cysteine proteases *via* nucleophilic attack.[28a,30]

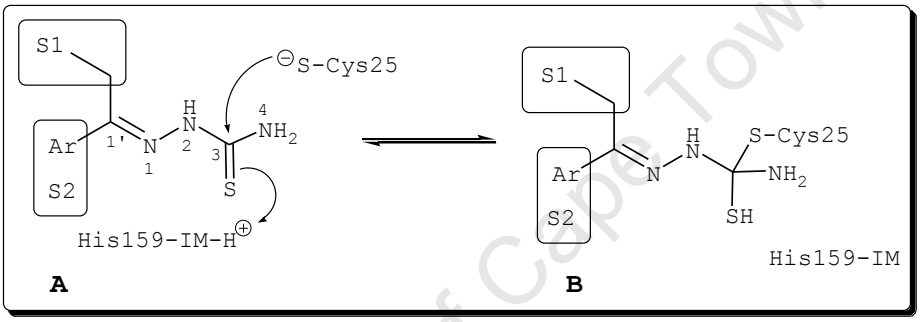

Figure 3.8: Reversible inhibition of cysteine proteases by TSCs.[30]

Due to inherent electrophilic centres (i.e. C=N, and C=S) in the chemical structures of TSCs, *Du et al.*[30] demonstrated through experimental and computational approaches that TSCs are susceptible to nucleophilic attack by the thiolate anion (**A**) to produce a tetrahedral intermediate (**B**). Thus, this reversible process resulted in the inhibition of the cysteine protease cruzain. Moreover, the homology model suggested the C=S group as a favorable position of nucleophilic attack by thiolate anion compared to C=N. This was attributed to incompatible separation between ^{1}N and proton of His159 for covalent bonding.

3.4 RATIONALE: SYNTHESIS OF THIOSEMICARBAZONES

Fig. 3.9 indicates structural consequences on the potency of TSCs against cysteine proteases by varying each position.[32] In summary, *Du* and co-workers showed that while modification of each position [i.e. **(i)**, **(ii)** and **(iv)**] was important for cruzain and rhodesain, it was however, not tolerated by the malarial cysteine protease FP-2. The comparative data from this study unravelled the important differences in the active sites of these three enzymes.[32]

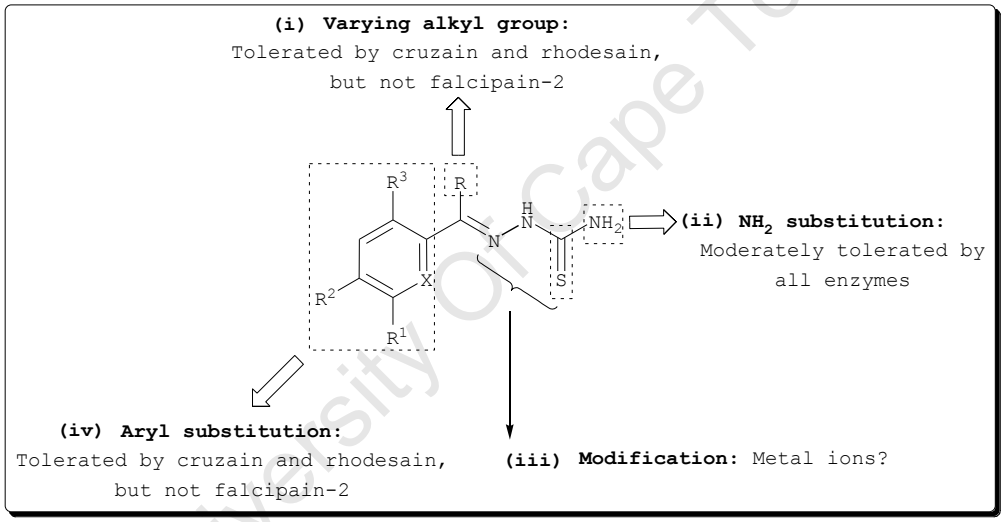

Figure 3.9: Rationale design of TSCs.

As our main focus in this study is on malaria, it was of interest to exploit the effects of coordinating gold containing fragments with already studied TSCs as cysteine protease inhibitors against FP-2. An attendant hypothetical reasoning was that coordination of gold with TSCs may lead to gold complexes in which the ligands are "locked" in an orientation that is favourable for maximum interactions of TSCs with enzyme pockets, thus enhancing their potency against FP-2.

Herein, we opted to synthesise selected ligands which have been shown to exhibit inhibitory effects against cruzain and tryponosomal cultures,[28a,30] but with no reports on their antimalarial activities with respect to their corresponding gold complexes. The rationale for the synthesis of these ligands was based on utilizing the existing coordinating sites **(iii)** in the ligands to access novel gold compounds (see **Chapter 4**) with potential antiplasmodial activities against *P. falciparum* strains (**Chapter 5**) presumably through the inhibition of the cysteine protease FP-2.

3.5 RESULTS AND DISCUSSION

3.5.1 Retrosynthetic Analysis

Retrosynthetic analysis of TSC targets is shown in Scheme 3.3.

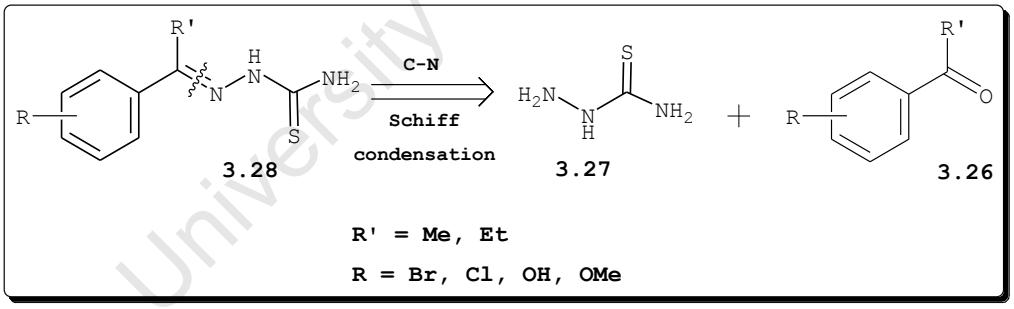

Scheme 3.3: Retrosynthetic analysis of TSCs.

The synthesis of TSCs (**3.28**) was envisaged as achievable from commercially available TSCz (**3.27**) and various ketones **3.26.** The starting materials employed for ferrocenyl-based ligands were ferrocene carboxaldehyde (**3.29**) and acetylferrocene (**3.30**), which are also accessible commercially. Similarly, compound **3.28h** could be obtained

from the condensation of **3.27** and the aldehyde, 3-methoxy-4-hydroxybenzaldehyde (**3.31**).

3.5.2 Synthesis of Mono-Thiosemicarbazone Ligands

The desired ligands were synthesised as illustrated in the general reaction scheme (Scheme 3.4).

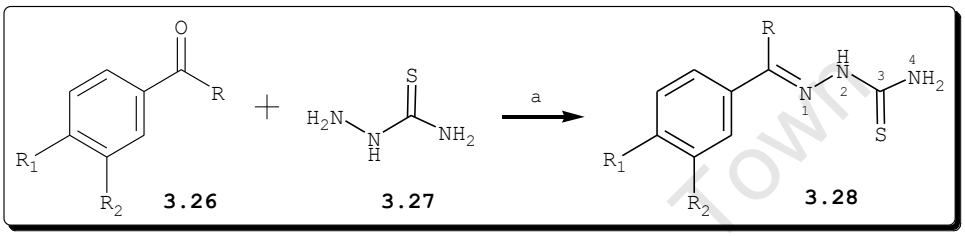

Scheme 3.4: *Reagents and conditions* a) MeOH/EtOH, 1% AcOH, reflux, 24 h.

A series of commercially accessible ketones (**3.26**) were each reacted with **3.27** in the presence of a catalytic (1%) amount of acetic acid in a 1:1 ratio in refluxing methanol to yield the corresponding TSCs **3.28a-e** (Table 3.1).[30] The reactions were allowed to reflux for 24 h. The reaction progress was monitored by thin layer chromatography (TLC). Despite leaving the reaction mixture to reflux for 24 h, TLC revealed the presence of unreacted starting material, which indicated that reaction did not fully converted into products. The desired TSCs and isolated yields are summarised in Table 3.1.

Table 3.1: Yields of isolated TSC **3.28a-h.**

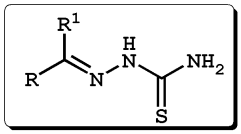

Entry	Code	Product	R	R^1	Yield/[%]
1	**DK-1R**	**3.28a**	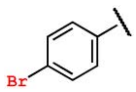	CH_3	49
2	**DK-2RD**	**3.28b**	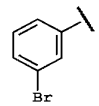	CH_3	60[30]
3	**DK-3G**	**3.28c**	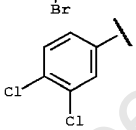	CH_3	74[30]
4	**DK-8D**	**3.28d**	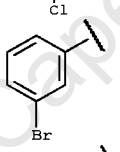	CH_3CH_2	30[30]
5	**DK-9D**	**3.28e**	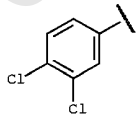	CH_3CH_2	54[30]
6	**DK-11B**	**3.28f**	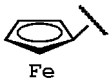	H	81[42]
7	**DK-25D**	**3.28g**		CH_3	70[43a]
8	**DK-69**	**3.28h**	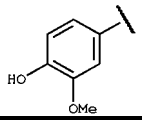	H	100[44]

Similarly, compounds **3.28f**, **3.28g** and **3.28h** were synthesised according to the reported method.[42,43,44] As can be seen from Table 3.1, the compounds were isolated in poor to excellent yields. The low yield of compound **3.28d** may be due to the fact that as most compounds crystallised on cooling, in some cases during refrigeration, to ambient temperature some of the product remained in solution.

3.5.3 Characterisation of Compounds 3.28a-h

The prepared compounds were characterised using ^{1}H, ^{13}C NMR and infrared (IR) spectroscopic techniques. Melting points were employed to assess the purity of targeted compounds relative to literature reported values (Table 3.2).

Table 3.2: Melting points of isolated compounds.

Compound	Meting point (°C)	
	Observed	**Literature**
3.28a	193-194	190-192[45]
3.28b	170-172	174-175[30]
3.28c	193-194	196-198[30]
3.28d	134-135	144-145[30]
3.28e	180-182	185-186[30]
3.28f	175-176	175[46]
3.28g	170-172	169-171[43a]
3.28h	193-194	187-189[47]

Typically, the ^{1}H and ^{13}C NMR (selected important regions) spectra for compound **3.28a** are shown in Fig 3.10. The ^{1}H NMR spectra of phenyl containing TSCs **3.28a-e** revealed diagnostic ^{3}NH proton signals as broad singlets in the range δ 10.15-10.35 ppm. These proton signals showed not only the formation of these ligands, but also unequivocally demonstrated the predominant thione form of all compounds in solution state. This is inconsistent with the reported mixture of tautomeric forms often observed in solution. The ferrocenyl analogues **3.28f** and **3.28g** showed chemical shifts of ^{3}N protons at δ 11.13 and 9.91 ppm, respectively. A

similar pattern was also observed from the ^{1}H NMR spectrum of compound **3.28h.**

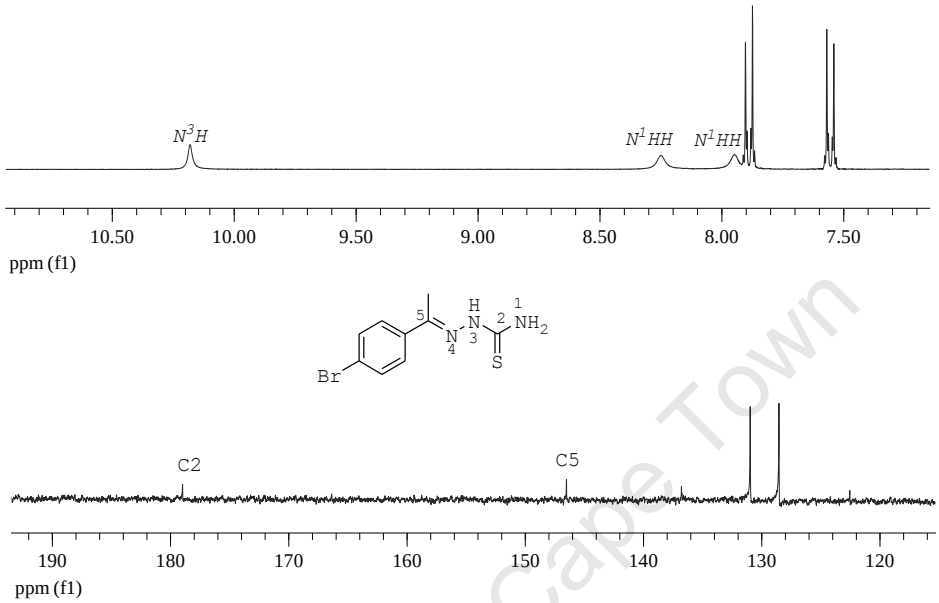

Figure 3.10: ^{1}H and ^{13}C NMR spectra of **3.28a** in DMSO-d_6.

The ^{1}N protons (i.e. ^{1}NHH) gave rise to two non-equivalent resonances in the ^{1}H NMR spectra of all synthesised compounds. This phenomenon, which is a common feature in TSC structures,[48] is attributed to the partial double bond character exhibited in the thioamide bond (C-N), ultimately restricting rotation about the C-N bond (Scheme 3.5).

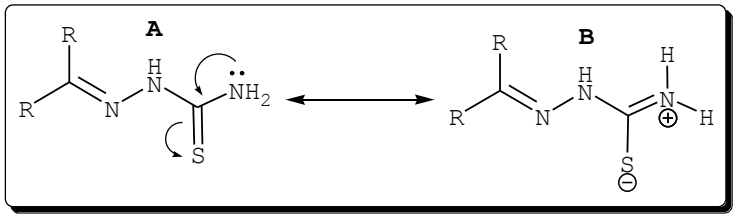

Scheme 3.5: Mesomeric behaviour of the thioamide group.

The ^{1}H NMR results were supported by those of the ^{13}C NMR spectra, which showed the chemical shifts of imine (C=N) carbons (C5) at δ 143.1-150.6 ppm, thus unambiguously confirming the formation of an imine functionality. The presence of thiocarbonyl (C=S) group in all of the proposed structures was also evident in the ^{13}C NMR spectra at δ 176.4-179.4 ppm.

The IR spectra of all compounds showed diagnostic bands in the regions 3138-3190, 1585-1599 and 805-850 cm^{-1}, which were assigned to ν(NH), ν(C=N) and ν(C=S) stretches, respectively (Fig. 3.11). From the spectra of all compounds, the bands at approximately 2200-2500 cm^{-1}, indicating the thiol form (SH) could not be observed, thus suggesting that these compounds existed predominantly in their thione form (**A**, in Scheme 3.2, p 69) in the solid state. This was also in agreement with observations made in the ^{1}H NMR spectra.

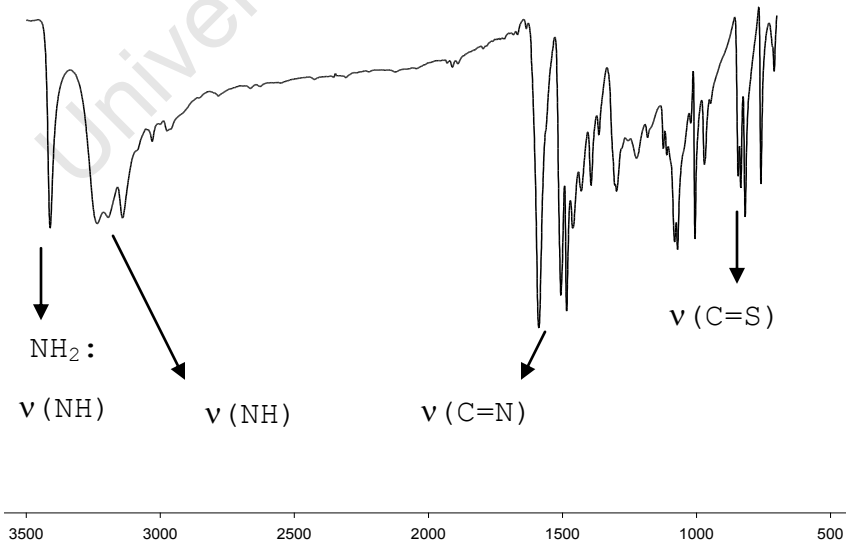

Figure 3.11: IR spectrum of **3.28a** as KBr pellet.

3.5.4 Synthesis of Pyrazoline TSC Analogues

A second series of TSCs, which was deemed suitable for the synthesis of novel gold complexes are pyrazoline analogues. This class of compounds are accessible in two reaction steps. The first step involves the Mannich reaction,[30] while the second step involves Schiff-base chemistry to access the cyclised pyrazoline TSC analogues. The Mannich reaction is widely applied in organic chemistry to form carbon-carbon and carbon-nitrogen bonds;[49] and the components required for this reaction include: a) a compound with an acidic methylene moiety (**I**), b) formaldehyde (**II**) [a non-enolizable aldehyde] and c) ammonia, a primary or secondary amine (**III**), Scheme 3.7.[50]

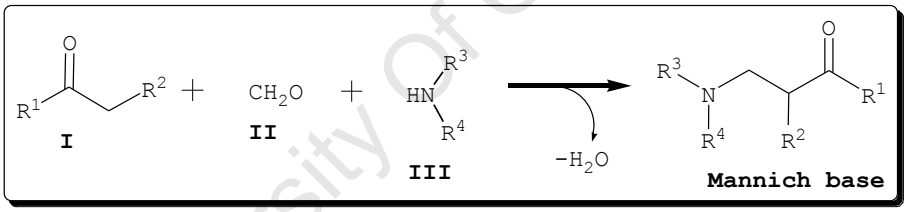

Scheme 3.6: Essential component in Mannich reaction.

Selected ketones (**3.26**) were each reacted under reflux (EtOH) with formaldehyde and a secondary amine salt in the presence of HCl (Scheme 3.7) to form the Mannich base.

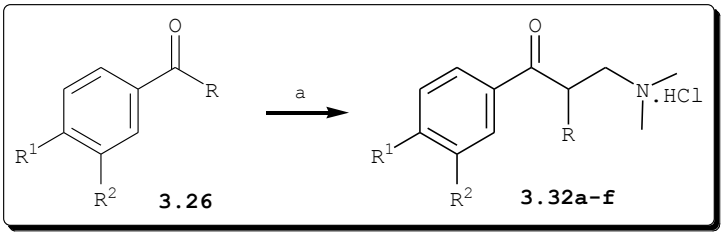

Scheme 3.7: *Reagents and conditions* a) $(HCHO)_n$, $(H_3C)_2N.HCl$, 32% HCl, Reflux, EtOH, 2 h.

The formation of Mannich base compounds **3.32** was evident from characteristic white precipitates upon cooling, and was isolated by means of filtration to give the desired products. It is noteworthy that compounds **3.32d** and **3.32e** were obtained as oil products.

3.5.4.1 Reaction Mechanism of Mannich Base Formation

The mechanism by which Mannich base products formed is illustrated in Scheme 3.8.

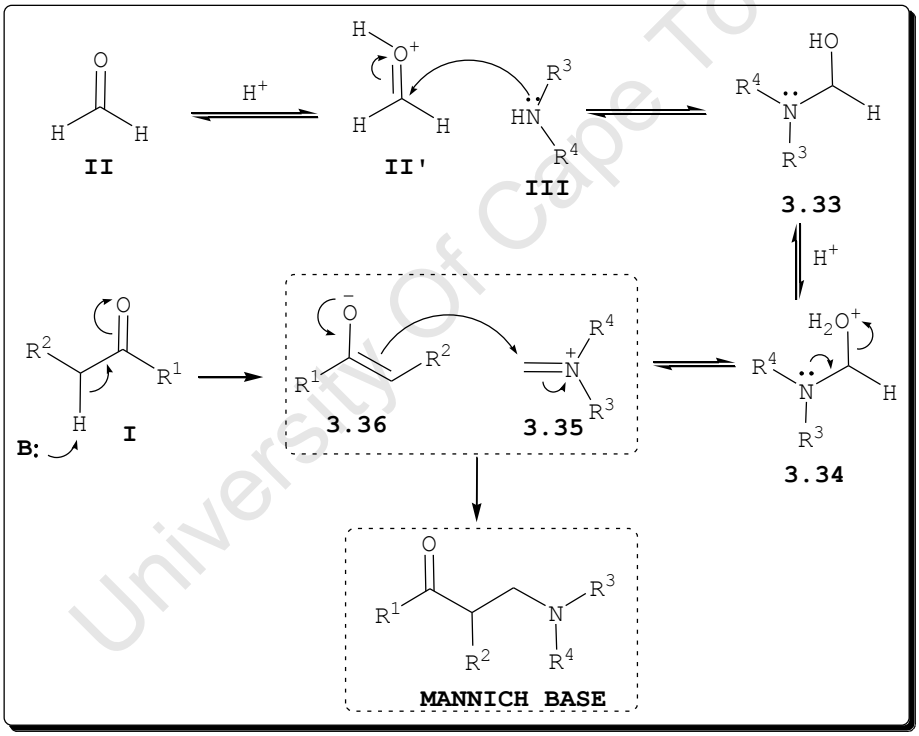

Scheme 3.8: Mechanism of Mannich base formation.

Nucleophilic attack of the secondary amine (**III**) onto the electrophilic carbonyl center of formaldehyde (**II'**) yields an alcohol intermediate (**3.33**). This intermediate under acid-dehydration conditions gives rise to the iminium salts (**3.35**). Finally, nucleophilic addition of enolate **3.36** to

the iminium ion **3.35** yields the Mannich base product (**3.32**).

^{1}H NMR spectroscopy was used to confirm the Mannich base products. The new chemical shifts corresponding to the CH_2 appeared in the range δ 3.39-3.40 ppm and δ 3.62-3.65 ppm, respectively. The observed signals were consistent with those of the same compounds reported in the literature.[30] Having synthesized **3.32,** the second step was to prepare the corresponding targeted cyclized TSCs. The Mannich products **3.32a-f** were each condensed with **3.27** in a 1:1 molar ratio in refluxing MeOH in a basic medium for 48 hours (Scheme 3.9).[51] In contrast to the adopted synthetic approach, *Du et al.*[30] reported that these reactions were completed within 1 h. However, in this case it was observed from TLC that the starting materials were still predominant within the first 2 h of the reaction.

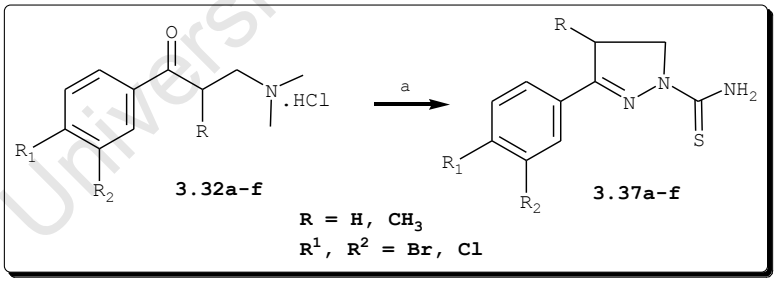

Scheme 3.9:[2] *Reagents and conditions* a) 50% NaOH, MeOH, reflux, N_2, 48 h.

The resulting reaction products contained unreacted starting materials (TLC) and some unidentifiable side products. The product mixture was purified by means of silica gel column chromatography eluting with DCM-MeOH

[2]Mannich base **3.32d** and **3.32e** are oils.

(98:2) to afford crystalline solid compounds in low to moderate yields. *Du et al.*[30] and *Abid et al.*[52] obtained these ligands in yields ranging 20-62% and 35-51%, respectively. A summary of the corresponding TSCs **3.37a-f** is provided in Table 3.3.

Table 3.3: Yields of isolated pyrazoline TSCs **3.37a-f**.

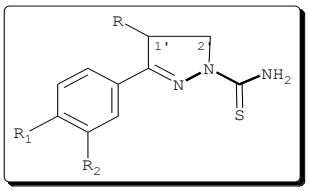

Entry	Code	Product	R	R^1	R^2	Yield/[%]
1	**DK-20**	**3.37a**	H	H	Br	10[30]
2	**DK-38**	**3.37b**	H	Cl	Cl	20[30]
3	**DK-39**	**3.37c**	H	Br	H	41
4	**DK-45**	**3.37d**	CH_3	Cl	Cl	31[30]
5	**DK-47**	**3.37e**	CH_3	H	Br	69[30]
6	**DK-134**	**3.37f**	H	Cl	H	24

3.5.5 Spectroscopic Characterisation of Pyrazolines 3.37a-f

The pyrazoline derivatives were characterised using ^{1}H NMR, IR and mass spectroscopic techniques. The purity of all compounds was determined *via* melting point (Table 3.4) and microanalyses. *Abid et al.*[52] reported melting point for 3.37a and 3.37e to be 141 °C and 92 °C, respectively. In the ^{1}H NMR spectra, the pyrazoline protons (CH_2) at C_1, and C_2, carbons in compounds **3.37a-c** and **3.37f** appeared as triplets resonating at δ 3.26-3.28 and δ 4.37-4.39 ppm, respectively.

On the other hand, the chemical shifts of CH_2 protons ($C_{2'}$) of compounds **3.37d** and **3.37e** resonated as a doublet at δ 4.37 ppm (J = 11.6 Hz) and doublet of doublets at δ 4.15 ppm (J = 4.8 and 11.6 Hz). The CH proton at $C_{1'}$ appeared as multiplet in the region 3.65-3.71 ppm.

Table 3.4: Melting points of isolated pyrazoline ligands.

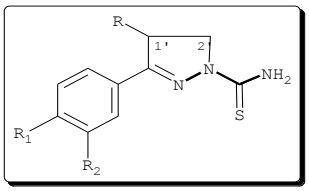

Entry	Compound	Melting point (°C)	
		Observed	Literature
1	**3.37a**	143-145	173-175[30]
2	**3.37b**	195-197	199-201[30]
3	**3.37c**	86-88	-
4	**3.37d**	173-174	171-172[30]
5	**3.37e**	120-122	107-109[30]
6	**3.37f**	162-164	-

The IR spectra of these compounds showed intense bands at 807-914 cm^{-1}, which were assigned to the ν(C=S) stretch of the thiocarboxamide moiety. The absorption bands due to the ν(C=N) stretch of the azomethine group appeared in the region 1571-1595 cm^{-1}. The bands in the region 3364-3477 cm^{-1} were assigned to the ν(NH) stretching frequencies.

The mass spectra of compounds **3.37a-f** are summarised in Table 3.5. The ESI (high resolution) mass spectrometry confirmed the molecular ion peaks of compounds **3.37a-c** consistent with $^{81}Br/^{37}Cl$ isotopic distribution. Whereas compounds **3.37e-f** showed ion peaks consistent with *m/z*, (M+H).

Table 3.5: Mass spectrometric data of **3.37a-f.**

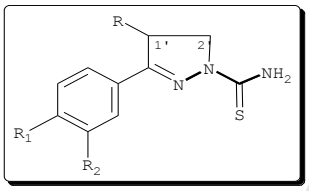

Compound No.	m/z	
	Found	Calcd
3.37a	285.9825	282.9779
3.37b	276.0067	272.9894
3.37c	285.9991	282.9779
3.37d	288.010	287.0051
3.37e	297.9979	296.9935
3.37f	240.0340	239.0284

3.6 BIOLOGICAL RESULTS AND DISCUSSION

The biological activities of synthesized TSCs were evaluated *in vitro* against *P. falciparum* CQ-sensitive strains (D10 and 3D7) and CQ-resistant strains (W2 and K1). In all assays, CQ was used as control. The cytotoxicity tests of all compounds were conducted in human nasopharynx carcinoma cell line (KB) and podophyllotoxin (POD) used as

a control drug. The compounds were also evaluated for their ability to inhibit the activity of the plasmodial cysteine protease FP-2. The biological tests were carried out in collaboration with various institutions: 1) Department of Medicine, San Francisco General Hospital, University of California in San Francisco (UCSF) - Professor P.J. Rosenthal (W2 and FP-2), 2) Department of Medicine, Division of Pharmacology, University of Cape Town - Professor P.J. Smith (D10) and 3) London School of Hygiene and Tropical Medicine (LSHTM) – Drs V. Yardley and Livia Vivas (3D7, K1 and KB).

3.6.1 *In vitro* Antiplasmodial Activity of 3.28a-h

The antiplasmodial activities of compounds **3.28a-h** against D10, W2 and recombinant FP-2 were determined and the results are displayed in Table 3.6. From the data (Table 3.6), it is clear that TSCs displayed no activities against D10 and W2 strains at the highest concentration tested. Generally, none of the compounds showed potency below 10 μM against the D10 strain, except compound **3.28d** which was moderately active against W2 was **3.28d** with an IC_{50} value of 4.94 μM. The rest of compounds did not show any significant inhibitory effects against the whole parasites at the maximum concentration tested (IC_{50} > 20 μM).

To probe the ability of these compounds to inhibit a malarial cysteine protease, hence their antimalarial activities, the compounds were tested against recombinant FP-2 (Table 3.6).

Table 3.6: *In vitro* antiplasmodial and FP-2 activities of TSCs.

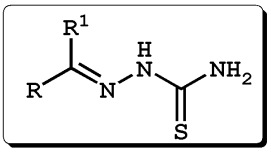

Entry	Cmp. No.	R	R^1	IC_{50} / μM		
				D10	W2	rec FP-2
1	3.28a	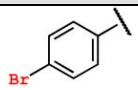	CH_3	31.1	>20	>100
2	3.28b	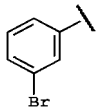	CH_3	>10	4.94	>100
3	3.28c	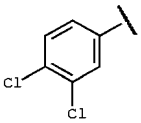	CH_3	95.8	>20	>100
4	3.28d	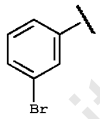	CH_3CH_2	18.2	>20	>100
5	3.28e	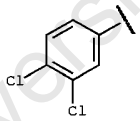	CH_3CH_2	26.9	>20	>100
6	3.28f		H	31.0	>20	36.8
7	3.28g		CH_3	>10	>20	18.2
8	3.28h	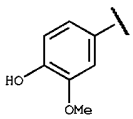	H	382.2	>20	>100
9	CQ	–	–	0.017	0.097	ND
10	E64	–	–	ND	~3.0	0.049

ND = not determined

The majority of the compounds were not effective against FP-2 at the highest concentration tested (IC_{50} > 100 μM). These results suggest that the moderate inhibitory effect of compound **3.28b** against W2 may be due to other mechanisms that exclude inhibition of FP-2. Despite the lack of inhibitory effects against the growth of cultured parasites, ferrocenyl TSCs **3.28f** and **3.28g** displayed modest activity against FP-2 with IC_{50} values of 36.2 and 18.2 μM, respectively. Previously, the potencies of compounds **3.28f** and **3.28g** have been reported.[37d]

In separate experiments, compounds **3.28a-h** were evaluated for their activities against 3D7, K1 and KB assays and the results are summarised in Table 3.7. The antiplasmodial activities were generally in mid to higher micromolar range (16.8-68.8 μM and 35.7-72.1 μM) against both 3D7 and K1 strains, respectively. In most cases, the IC_{50} values of these compounds against K1 were higher (except **3.28a**) than those against 3D7. This suggested that *P. falciparum* parasites are likely to develop resistance against these compounds.

In vitro cytotoxicity was evaluated against the KB cell line. From the data, these compounds exhibited no toxicity against KB cells; the IC_{50} values were generally well above 100 μM, with the exception of compound **3.28d** with an IC_{50} value of 87.5 μM, independent of their antiplasmodial activities. Ferrocenyl TSCs **3.28f** and **3.28g**, whose antiplasmodial activities were moderate against 3D7, exhibited no significant toxicity against KB cells

suggesting that these compounds are selective towards 3D7, with selectivity indices of 14 and 11, respectively. Compounds **3.28f** and **3.28g** also showed selectivity towards K1 strain parasites.

Table 3.7: Antiplasmodial and cytotoxicity data of TSCs.

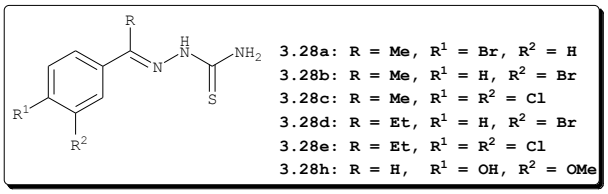

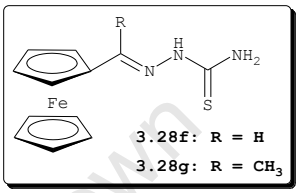

Entry	Cmp. No.	IC_{50} / μM			*RI*[a]	*SI*[b]
		3D7	K1	KB		
1	**3.28a**	68.8	59.4	>100	0.9	>1.45
2	**3.28b**	39.5	62.3	>100	1.6	>2.53
3	**3.28c**	43.1	72.1	>100	1.7	>2.32
4	**3.28d**	55.5	62.8	87.5	1.1	1.58
5	**3.28e**	23.8	38.9	>100	1.6	>4.20
6	**3.28f**	20.4	44.2	276.8	2.2	13.6
7	**3.28g**	16.8	35.7	181.4	2.1	10.8
8	**3.28h**	35.7	>20	>100	ND	>2.80
9	**CQ**	0.019	1.03	-	54.2	ND
10	**POD**	-	-	<0.003	-	ND

[a]**Resistance index calculated as [IC_{50} (K1)]/[IC_{50} (3D7)]**

[b]***Selectivity calculated as [IC_{50}KB/IC_{50}3D7]***

3.6.2 *In vitro* Antiplasmodial Activity of Pyrazolines

In the second series of synthesised TSCs, it was envisaged that the pyrazolines **3.37a–f** (Table 3.3) may exhibit interesting antimalarial activities. Thus, the

antiplasmodial activities of pyrazolines **3.37a-f** were also evaluated against 3D7 and K1 strains, along with their cytotoxicity against the KB cell line (Table 3.8). Although the activities remained in low to mid micromolar range, the results indicated that in moving from acyclic TSCs (**3.28**) to cyclic counterparts (**3.37**) there is a 1-5 fold improvement in the overall activity against 3D7 and K1, respectively. The pyrazoline TSCs were found to exhibit no toxicity against KB cell lines, with compound **3.37b** displaying significant selectivity towards both strains.

Table 3.8: Biological activities of pyrazoline TSCs.

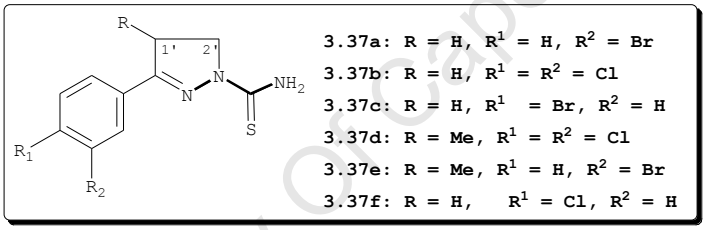

Entry	Cmp. No.	IC_{50} / μM			*RI*	*SI*
		3D7	K1	KB		
1	**3.37a**	27.5	32.5	>100	1.2	>3.64
2	**3.37b**	16.4	40.9	318.1	2.5	19.4
3	**3.37c**	16.4	15.7	>100	0.9	>6.10
4	**3.37d**	11.1	10.1	>100	0.9	>9.01
5	**3.37e**	48.1	>20	72.0	ND	1.50
6	**3.37f**	54.3	76.5	214.0	1.4	3.94
7	**CQ**	0.019	1.03	-	54.2	ND
8	**POD**	-	-	<0.003	-	ND

3.6.3 Discussion

The observed antiplasmodial activity of compound **3.28b** against cultured W2 parasites was independent of the inhibition of FP-2, suggesting that FP-2 is not the primary target. The same conclusion has been made by others on analogous TSCs that were modest against FP-2 but active against a drug resistant *P. falciparum* strain.[33] Recently, *de Oliveira et al.*[47] reported the antiplasmodial activities of TSCs illustrated in Fig. 3.12. As in our case, compound **3.28h** was not active against *P. falciparum* although it showed a lack of toxicity against human peripheral blood mononuclear cells (PBMC). The non-aromatic TSCs (Fig. 3.12) showed moderate antiplasmodial activities against the *P. falciparum* W2 strain.

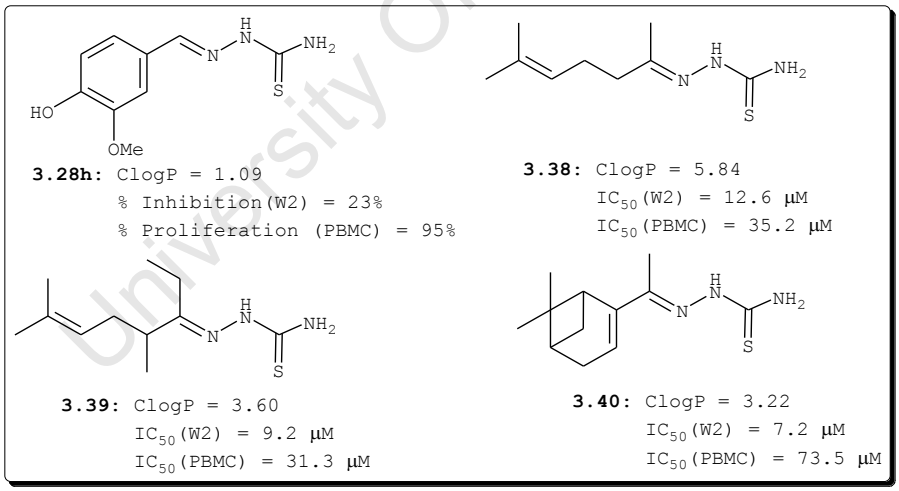

Figure 3.12: Antimalarial potency of TSCs reported in literature.[47]

On close examination of active compounds **3.38-3.40,**[47] it was observed that these compounds exhibit similar lipophilicity. Thus, it may be possible that the

ineffectiveness of compounds **3.28a-h** may be due to their poor solubility, an important physicochemical property of a compound, such that they hardly reach the target in sufficient concentration.[53] Since compounds **3.38-3.40** possess non-aromatic moieties it may tentatively be concluded that activities of **3.38-3.40** over **3.28a-e** may be due to selective uptake of these compounds by the parasitic erythrocytes.[54] More importantly, compounds **3.38-3.40** and **3.28b** (Table 3.6) lack the NNS tridentate ligating system, which preclude the assumption that their activities may be due to iron chelation.[40]

Unlike the W2 cultured parasites, mono-TSCs displayed modest activity against the K1 (resistant) strain. A similar trend was also noted in cyclic analogues, but more importantly the data suggests that the antiplasmodial activity against both 3D7 and K1 strains is enhanced when TSCs are converted to pyrazoline counterparts. Although these compounds were generally selective towards malaria parasites, further structural modifications are important to attain some physicochemical properties that may lead to an improved potency.

3.7 CONCLUSION

In conclusion, a focused series of mono-TSCs and cyclic analogues was evaluated for antiplasmodial activity against *P. falciparum* strains and inhibitory effects against the FP-2 enzyme. Most of the compounds showed no cytotoxicity towards the KB cell line, but displayed modest activities against 3D7 and K1 strains of *P. falciparum*. Although the activities were in the mid micromolar range, cyclization of

TSCs to form the corresponding pyrazoline derivatives resulted in beneficial effects against both 3D7 and K1 strains. Compound **3.28b** was the only TSC which exhibited moderate activity (below 10 μM) against W2 without any inhibition of the enzyme (IC_{50} > 10 μM). From the data, there was no correlation observed between the antiplasmodial activity and the inhibition of FP-2.

3.8 REFERENCES

1. H.R. Wilson, G.R. Revankar, R.L. Tolman, *J. Med. Chem.*, **1974**, *17*, 760–761.
2. (a) T.S. Lobana, R. Sharma, G. Bawa, S. Khanna, *Coord. Chem. Rev.*, **2009**, *253*, 977-1055. (b) J.S. Casas, M.S. García-Tasende, J. Sordo, *Coord. Chem. Rev.*, **2000**, *209*, 197-261. (c) M.J.M. Campbell, *Coord. Chem. Rev.*, **1975**, *15*, 279-319.
3. (a) Y. Fujibayashi, H. Taniuchi, Y. Yonekura, H. Ohtani, J. Konishi, A. Yokoyama, *J. Nucl. Med.*, **1997**, *38*, 1155-1160. (b) A.R. Cowley, J.R. Dilworth, P.S. Donnelly, E. Labisbal, A. Sousa, *J. Am. Chem. Soc.*, **2002**, *124*, 5270-5271.
4. D.L. Klayman, J.P. Scovill, J.F. Bartosevich, C.J. Mason, *J. Med. Chem.*, **1979**, *22*, 1367–1373.
5. J. Clayden, N. Greeves, S. Warren, P. Wothers, *Organic Chemistry*, Oxford University Press, New York, **2001**, p 351.
6. P. Domiano, G.F. Gasparii, M. Nardelli, P. Sgarabotto, *Acta Crystallogr.* 25B, **1969**, 343-349. (b) G.D.

Andretti, P. Domiano, G.F. Gasparii, M. Nardelli, P. Sgarabotto, *Acta Crystallogr*. 26B, **1970**, 1005-1009.

7. S. Padhye, *Coord. Chem. Rev*., **1985**, *63*, 127–160.
8. D.X. West, S.B. Padhaye, P.B. Sonawane, *Structure and Bonding*, ed. M.J. Clarke, Springer-Verlag, Berlin Heidelberg, **1991**, Vol. 76, p 4-50.
9. I. Kizilcikli, Y.D. Kurt, B. Akkurt, A.T. Genel, S. Birteksöz, G. Ötuk, B. Ülküseven, *Folia Microbiol*., **2007**, *52*, 15-25, and references cited therein.
10. H. Beraldo, D. Gambino, *Min. Rev. Med. Chem*., **2004**, *4*, 31–39.
11. D. Domagk, R, Behnisch, F. Mietzsch, H. Schimidt, *Naturwissenschaften*, **1946**, *33*, 315.
12. P. Sensi, G.G. Grassi, *Burger's Medicinal Chemistry and Drug Discovery*, 6th Ed. *Vol. 5*: *Chemotherapeutic Agent*, Ed. D.J. Abraham, John Wiley & Sons, Inc. **2003**, p 807-866.
13. B.G. Benns, B.A. Gingras, C.H. Bayley, *Appl. Microbiology*, **1960**, *8*, 353-356.
14. P. Sensi, *Antimyobacterial Agents*, *In Burger's Medicinal Chemistry and Drug Discovery* 6th Ed., Vol. 5: *Chemotherapeutic Agents*, Ed. D.J. Abraham, John Wiley & Sons, Inc., **2003**, p 832-833.
15. (a) Ö. Güzel, N. Karali, A. Salman, *Bioorg. Med. Chem*., **2008**, *16*, 8976-8987. (b) M.I. Merlani, L.Sh. Amiranashvili, K.G. Mulkidzhanyan, A.R. Shelar, F.V. Manvi, *Chem. Nat. Comp*., **2008**, *44*, 618-620. (c) D. Sriram, P. Yogeeswari, P. Dhakla, P. Senthilkumar, D. Banerjee, *Bioorg. Med. Chem. Lett*., **2007**, *17*, 1881-1891. (d) D. Sriram, P. Yogeeswari, R. Thirumurugan,

R.K. Pavana, *J. Med. Chem.*, **2006**, *49*, 3448-3450. (e) D. Sriram, P. Yogeeswari, J.S. Basha, D.R. Radha, V. Nagaraja, *Bioorg. Med. Chem.*, **2005**, *13*, 5774-5778. (f) L.E. Bermudez, R. Reynolds, P. Kolonoski, P. Aralar, C.B. Inderlied, L.S. Young, *Antimicrob. Agents Chemother.*, **2003**, *47*, 2685-2687. (g) A.S. Dobek, D.L. Klayman, E.T. Diskson, Jr., J.P. Scovill, E.C. Tramont, *Antimicrob. Agents Chemother.*, **1980**, *18*, 27-36.

16. L.E. Bermudez, R. Reynolds, P. Kolonoski, P. Aralar, C.B. Inderlied, *Antimicrob. Agents Chemother.*, **2003**, *47*, 2685-2687.
17. B.G. Benns, B.A. Gingras, C.H. Bayley, *Appl. Microbiology*, **1960**, *8*, 353-356.
18. V. Opletlová, D.S. Kalinowski, M. Vejsová, J. Kuneš, M. Pour, J. Jampílek, V. Buchta, D.R. Richardson, *Chem. Res. Toxicol.*, **2008**, *21*, 1878-1889.
19. D. Hamre, J. Bernstein, R. Donovick, *Proc. Soc. Exp. Biol. Med.*, **1950**, *73*, 275-278.
20. A. Kolocouris, K. Dimas, C. Pannecouque, M. Witvrouw, G.B. Foscolos, G. Stamatiou, G. Fytas, G. Zoidis, N. Koocouris, G. Andrei, R. Snoek, E. De Clercq, *Bioorg. Med. Chem. Lett.*, **2002**, *12*, 723-727.
21. R.W. Brockman, J.R. Thomson, M.J. Bell, H.E. Skipper, *Cancer Res.*, **1956**, *16*, 167-170.
22. F.A. French, E.J. Blanz, Jr., *J. Med. Chem.*, **1970**, *13*, 1117-1124.
23. M.-C. Liu, T.-S. Lin, A.C. Sartorelli, *J. Med. Chem.*, **1992**, *35*, 3672-3677.

24. Z. Afrasiabi, E. Sinn, J. Chen, Y. Ma, A.L. Rheigold, L.N. Zakharov, N. Rath, S. Padhaye, *Inorg. Chim. Acta*, **2004**, *357*, 271-278.
25. A. Garoufis, S.K. Hadjikakou, N. Hadjiliadis, *Coord. Chem. Rev.*, **2009**, *253*, 1384-1397.
26. S. Adsule, V. Barve, D. Chen, F. Ahmed, Q.P. Dou, S. Padhaye, F.H. Sarkar, *J. Med. Chem.*, **2006**, *49*, 7242-7246.
27. P.J. Rosenthal, *Advances in Parasitology*, Academic Press, New York, Vol. 43, **1999**, p 105-159.
28. (a) F.E. Cohen, X. Du, C. Guo, J.H. McKerrow, US 6,897,240 B2, **2005**. (b) K. Chibale, D.C. Greenbaum, J.H. McKerrow, WO2005/087211 A1, **2005**.
29. R.A. Casero, Jr., D.L. Klayman, G.E. Childs, J.P. Scovill, R.E. Desjardins, *Antimicrob. Agents Chemother.*, **1980**, *18*, 317-322.
30. X. Du, C. Guo, E. Hansell, P.S. Doyle, C.R. Caffrey, T.P. Holler, J.H. McKerrow, F.E. Cohen, *J. Med. Chem.* **2002**, *45*, 2695-2707.
31. K. Chibale, C.C. Musonda, *Curr. Med. Chem.*, **2003**, *10*, 1863-1889.
32. D.C. Greenbaum, Z. Mackey, E. Hansell, P. Doyle, J. Gut, C.R. Caffrey, J. Lehman, P.J. Rosenthal, J.H. McKerrow, K. Chibale, *J. Med. Chem.*, **2004**, *47*, 3212-3219.
33. N. Fujii, J.P. Mallari, E.J. Hansell, Z. Mackey, P. Doyle, Y.M. Zhou, J. Gut, P.J. Rosenthal, J.H. McKerrow, R.K. Guy, *Bioorg. Med. Chem. Lett.*, **2005**, *15*, 121-123.

34. R. Siles, S.-E. Chen, M. Zhou, K.G. Pinney, M.L. Trawick, *Bioorg. Med. Chem. Lett.*, **2006**, *16*, 4405-4409.
35. W. Porcal, P. Hernández, L. Boiani, M. Boiani, A. Ferreira, A. Chidichimo, J.J. Cazzulo, C. Olea-Azar, M. González, H. Cerecetto, *Bioorg. Med. Chem.*, **2008**, *16*, 6995-7004.
36. D.L. Klayman, J.F. Bartosevich, T.S. Grffin, C.J. Mason, J.P. Scovill, *J. Med. Chem.*, **1979**, *22*, 855–862.
37. (a) A. Chipeleme, **PhD Thesis**, University of Cape Town, **2004**. (b) I. Chiyanzu, **MSc Thesis**, University of Cape Town, **2004**. (c) F.M. Muganza, **MSc Thesis**, University of Cape Town, **2006**. (d) C.C. Musonda, Jr., **PhD Thesis**, University of Cape Town, **2006**.
38. L. Adane, P.V. Bharatam, *Curr. Med. Chem.*, **2008**, 15, 1552-1569.
39. D.S. Kalinowski, D.R. Richardson, *Pharmacol. Rev.*, **2005**, *57*, 547–583.
40. D.S. Kalinowski, Y. Yu, P.C. Sharpe, M. Islam, Y.-T. Liao, D.B. Lovejoy, N. Kumar, P.V. Bernhardt, D.R. Richardson, *J. Med. Chem.*, **2007**, *50*, 3716-3729.
41. D.B. Lovejoy, D.R. Richardson, *Curr. Med. Chem.*, **2003**, *10*, 1035–1049.
42. M. Martiño, E. Gayoso, J.M. Antelo, L.A. Adrio, J.J. Fernández, J.M. Vila, *Polyhedron*, **2006**, *25*, 1449-1456.
43. (a) J.S. Casas, M.V. Castano, M.C. Cifuentes, A. Sanchez, J. Sordo, *Polyhedron*, **2002**, *21*, 1651-1660. (b) B.J.A. Jeragh, A. El-Dissouky, *J. Coord. Chem.*, **2005**, *58*, 1029-1038.

44. P. Ren, T. Liu, J. Qin, C. Chen, *Spectrochimica Acta Part A*, **2003**, *59*, 1095-1101.
45. J. Liu, W. Yi, Y. Wan, L. Ma, H. Song, *Bioorg. Med. Chem.*, **2008**, *16*, 1096-1102.
46. J.S. Casas, M.V. Castaño, M.C. Cifuentes, J.C. García-Monteagudo, A. Sánchez, J. Sordo, U. Abram, *J. Inorg. Biochem.*, **2004**, *98*, 1009-1016.
47. R.B. de Oliveira, E.M. de Souza-Fagundes, R.P.P. Soares, A.A. Andrade, A.U. Krettli, C.L. Zani, *Eur. J. Med. Chem.*, **2008**, *43*, 1983-1988.
48. M.S. Bakkar, M.Y. Siddiqi, M.S. Monshi, *Synth. React. Inorg. Met.-Org. Chem.*, **2003**, *33*, 1157–1169.
49. M.Arend, B. Westermann, N, Risch, *Angew. Chem. Int. Ed.*, **1998**, *37*, 1044-1070.
50. J.J. Li, *Name Reactions: A collection of Detailed Reactions Mechanisms*, 3rd ed, Springer, Heildelberg, **2006**, p 361.
51. M. Abid, A.R. Bhat, F. Athar, A. Azam, *Eur. J. Med. Chem.*, **2009**, *44*, 417-425.
52. M. Abid, A. Azam, *Bioorg. Med. Chem. Lett.*, **2006**, *16*, 2812-2816.
53. E.H. Kerns, L. Di, *Drug-like Properties: Concepts, Structure Design and Methods: from ADME to Toxicity Optimization*, Academic Press, San Diego, **2008**, p 443.
54. I. Chiyanzu, C. Clarkson, P.J. Smith, L. Lehman, J. Gut, P.J. Rosenthal, K. Chibale, *Bioorg. Med. Chem.*, **2005**, *13*, 3249-3261.

CHAPTER 4

SYNTHESIS OF NOVEL GOLD COMPLEXES OF THIOSEMICARBAZONE AND PYRAZOLINE ANALOGUES

ABSTRACT: A series of gold(I) and gold(III) TSC complexes have been prepared from the reaction of gold(I) precursors **4.2, 4.3, 4.5, 4.27** and **4.37** as well as gold(III) **2.15** with various TSCs **3.28a-h** including pyrazoline analogues **3.37a-c** and **3.37f.** Crystal structures of complexes **4.15** and **4.16** were obtained as solvates with no evidence found of aurophilic Au(I)…Au(I) interactions contributing to the stability of their molecular structures.

4.1 THE CHEMISTRY OF GOLD

Gold as an element has been known to mankind since it was first discovered since earliest civilisation. Special interest in gold was connected with its value as a metal.[1] Naturally, gold exists in its native metallic form (oxidation number 0).[1,2] It is chemically unreactive and stable in the presence of oxygen and sulfur, but reacts readily with halogens or solutions containing and/or generating chlorine such as aqua regia. It dissolves in cyanide solutions in the presence of air or hydrogen peroxide to form $[Au(CN)_2]^-$.[3]

To date, a number of oxidation states of gold (−I, +I, +II, +III, +IV and +V) are known.[4] However, gold chemistry is dominated by the +I and +III oxidation states.[5] Gold complexes in the +II oxidation state have been reported,[6] but the medicinal application of gold in this form is yet

to be disclosed.[4b] Gold compounds in the oxidation states –I, +IV and +V are rare in the literature.[7]

4.1.1 Gold(I)

Gold(I) has a closed-shell $5d^{10}$ electron configuration and exhibits linear, trigonal or tetrahedral geometry (Fig. 4.1). Most gold(I) complexes have a linear two coordinate geometry, L-Au-X, where L is a 2-electron donor ligand, e.g. R_3P, R_2S, CO, and X is often a halogen or pseudohalogen.[7,8] The phosphine complexes are generally stable, whereas R_2S is more labile and renders some gold(I) complexes useful preparative intermediates.[8]

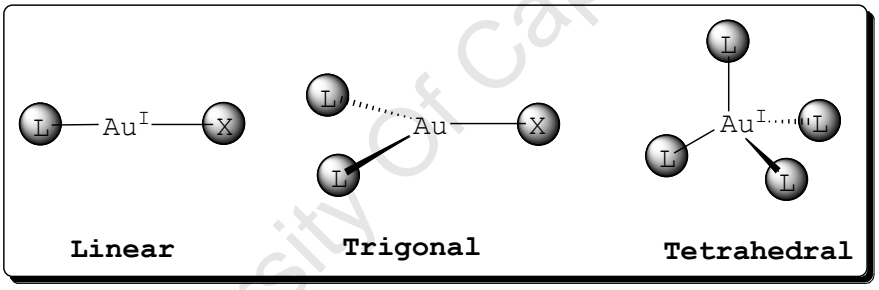

Figure 4.1: Possible geometries of gold(I) complexes.

Gold(I) complexes in their three and four coordination numbers require the participation of the energetically high lying orbitals $6p_y$ and $6p_z$ resulting in high promotion energy.[9] Consequently, complexes of the general formula L_nAuX, $n > 1$, are less common and often occur with S- and/or P-donor ligands known to form strong covalent bonds with gold(I). A few examples are also known with N-donor ligands. More importantly, stabilization of gold in higher coordination numbers occurs with chelating ligands such as bisphosphine.[9]

4.1.1.1 Aurophilicity and Aurophilic Interactions

Aurophilicity and aurophilic interactions are terms widely used to describe Au(I)…Au(I) intra- and inter-molecular interactions in gold compounds.[10] Aurophilicity is defined as the tendency of closed-shell gold(I) atoms to aggregate at distances shorter than the sum of van der Waals radii (2.884-3.60 Å).[11] The energy involved in aurophilic interactions is comparable in strength to that of a hydrogen bond of 30 $kJ.mol^{-1}$.[11,12] These interactions are commonly encountered in monovalent gold complexes occurring perpendicular to the axis of the linearly two coordinate gold(I) atoms. In compounds exhibiting coordination numbers greater than two, these aurophilic interactions are by far less common.[10]

4.1.2 Gold(III)

Gold(III), isoelectronic with platinum(II), has a $5d^8$ electronic configuration and can adopt a square planar (most common), square pyramidal or an octahedral coordination geometry, and it forms stable complexes with a variety of ligands. Gold(III) is considered as a "harder" acid than gold(I), hence it is more likely to form stable compounds with donor atoms such as nitrogen and oxygen. These types of ligands prevent reduction of gold(III) to gold(I). Gold(I) on the other hand exhibits a distinct preference for softer sulfur and phosphorus donor atoms.[13]

4.1.3 Organogold Compounds

Gold(I) and gold(III) ions also form σ-bonds with carbon.[14] The gold complexes derived from olefin, carbene and carbonyl compounds are some of the many well-known examples of organogold compounds.[7] This class of compounds also includes alkyl complexes of the form R-Au-L, where L is a donor ligand such as Me_2S, R_3P or isocyanide, $[R\text{-}Au\text{-}R]^-$ and $(RAu)_2$.

Another interesting class of organogold(I) complexes are binuclear ylid complexes $[Au_2\{\mu\text{-}(CH_2)_2PR_2\}_2]$, which reversibly react with halogens to give Au-Au bonded gold(II) alkyls with further oxidation leading to gold(III) compounds.[7] Organogold(III) compounds are also well-known and mainly form square-planar complexes of the types, R_3AuL, $[R_2AuL_2]^+$ and R_2AuXL. As in gold(I), gold(III) organometallic compounds based on ylid structures have been reported.[7]

4.1.4 Gold TSC Complexes

TSCs have attracted increasing attention due to their bonding versatility. Since the early 1960s when the first report on their complexes was published, the number of reports on coordination chemistry of these ligands has expanded significantly.[15,16] Currently, the chemistry of main group and transition metal TSC complexes with intriguing geometries is well established.[16,17] In the context of gold chemistry, however, there are a few examples of gold(I) complexes which have been reported.[18] A significant number of gold TSC complexes, which have received greater attention are gold(III) derivatives.[19] A brief overview of

these complexes, which are also encountered in this work, is provided below.

4.1.4.1 Gold(I)-Based TSC Complexes

In the late 1990s, *Ainscough et al.*[20] reported the reaction involving gold(I) $[Au^{I}ClS(CH_2CH_2OH)_2]$ and 2-formylpyridine TSC (**3.9**, Fig. 3.3, p 72) to form gold(I) complex of the form **4.1** (Scheme 4.1). Although the resulting complex **4.1** could not be fully characterised, microanalysis data suggested the molecular composition of atoms consistent with the chemical structure **4.1**.

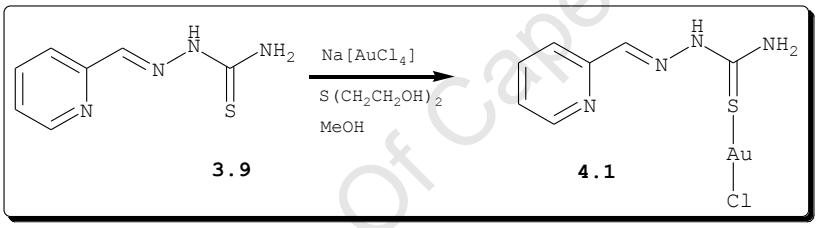

Scheme 4.1: Typical reaction of TSC with gold(I).

In view of the wide interest in the pharmacological properties of TSCs and their complexes, *Casas et al.*[18a] recently explored the chemistry of gold(I) with TSC ligands. As a result the gold(I) complex **2.12** (Fig. 2.4, p 39) was synthesised by reacting Menadione sodium bisulfide (MSB) TSC with $[Au^{I}(PEt_3)Cl]$ (**4.2**). This became the first gold(I) TSC complex to be reported and its molecular structure elucidated by single crystal X-ray diffraction. The molecular structure of the complex revealed that $[Au^{I}(PEt_3)Cl]$ reacts with MSB TSC to form **2.12** exhibiting a linear (P-Au-S) coordination geometry.

Recently, Lobana and co-workers observed that in gold(I) chemistry the common starting materials of gold(I) are $[Au^{I}(THT)Cl]$ (**4.3**), $[Au^{I}(SMe_2)Cl]$ (**4.4**) and $[Au^{I}(PPh_3)Cl]$ (**4.5**), respectively.[18b] In light of this observation they investigated direct reaction of gold(I) chloride (AuCl) with N,S-donor ligands. Thus, direct (1:1 molar) reaction of AuCl with 3-nitrobenzaldehyde TSC (**4.6**) in CH_3CN in the presence of one mole of PPh_3 resulted in the formation of ionic gold(I) TSC complex **4.7** (Fig. 4.2).

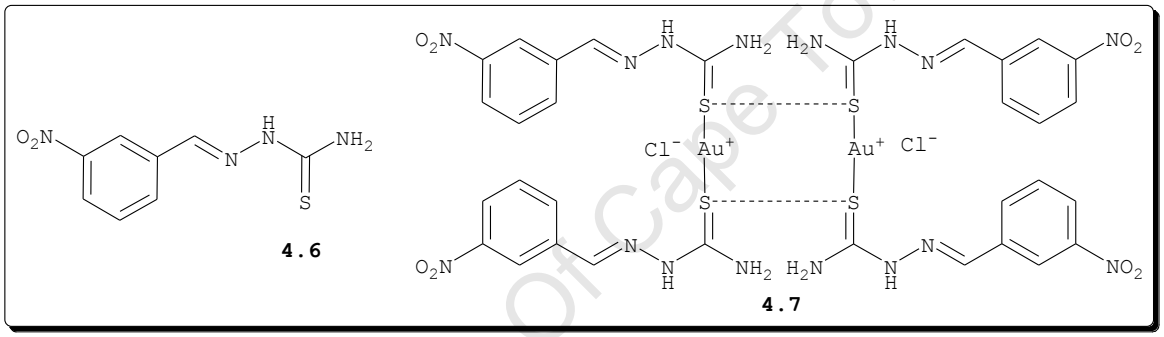

Figure 4.2: Chemical structure of gold(I) TSC complexes.

The molecular structure of **4.7** showed that the two monomeric molecules are linked to each other by Au(I)…Au(I) and S…S interactions to form the dimeric structure with a six membered cavity in the center. The S-Au-S bond angle deviates from linearity with an angle of 172.70 (16)°.

More recently, *Castiñeiras et al.*[18c] reported a binuclear gold(I) complex **4.9** (Fig. 4.3), which was isolated from a reaction employing the starting gold(III) complex **2.15** (Fig. 2.6, p 42) and bis{3-hexamethylene-iminyl TSC} (H_2Plhexim), **4.8**, in methanol. Although studies have shown that the reaction of **2.15** with TSCs affords gold(III) TSC complexes,[18a] (see **4.1.3.2**), reduction of **2.15** to gold(I) in

the presence of thiols other than TSCs have been noted.[21] Castiñeiras and co-workers concluded that the formation of **4.9** is due to the reduction of gold(III) in methanol.[18c] The same observation has been noted in our case (encountered in section **4.6.1**) when **2.15** was reacted with TSCs to form gold(III) complexes also resulted in the formation of gold(I) complexes (see **4.3.1.2**).

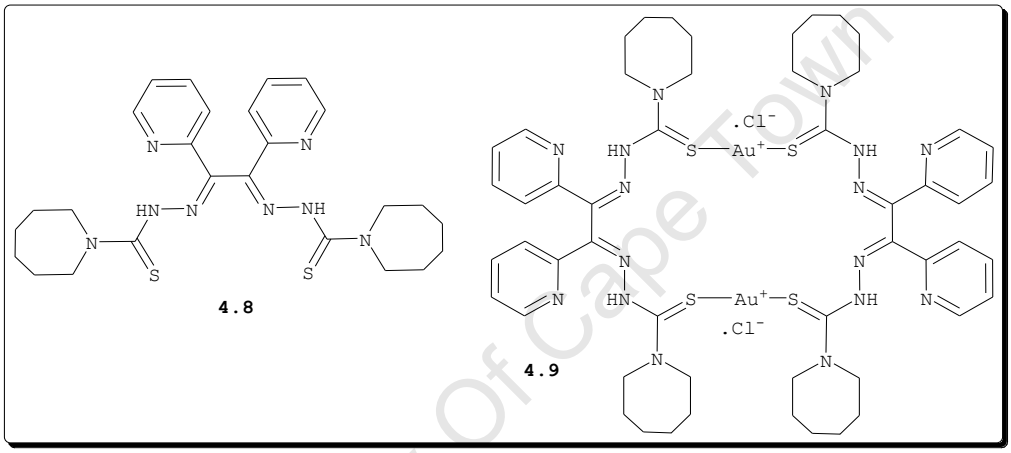

Figure 4.3: Binuclear gold(I) bis-TSC complex.

The molecular structure of **4.9** revealed a distorted linear coordination geometry with an S-Au-S bond angle of 167.1(11)° around gold atoms. Due to the steric crowding produced by pyridyl and hexamethyleneiminyl rings, the structure exhibited a Au(I)…Au(I) distance of 6.0141(9) Å, which is an exceedingly large separation to suggest the possible Au(I)…Au(I) interactions within the structure.

4.1.4.2 Gold(III)-Based TSC Complexes

In the early 1990s, Zheng-Zhi and Yong-Xiang reported reactions involving 5-nitro-2-furful and 2-acetylpyridine TSCs and $AuCl_3$ to form gold(III) complexes.[22] However, there

were no suitable single X-ray crystals to ascertain the molecular structures of the complexes in order to support the data from microanalysis. In the late 1990s, *Ortner et al.*[19e] reported the first crystal structures of square planar gold(III) TSC complexes represented by **4.10** and **4.11** (Fig. 4.4). As a result, a significant number of gold(III) complexes with TSCs exhibiting NS, PNS and NNS ligating systems were reported.[17] *Castiñeiras et al.*[18c] also reported a gold(III) complex resulting from the reaction of **2.15** with **4.8** in acetone.

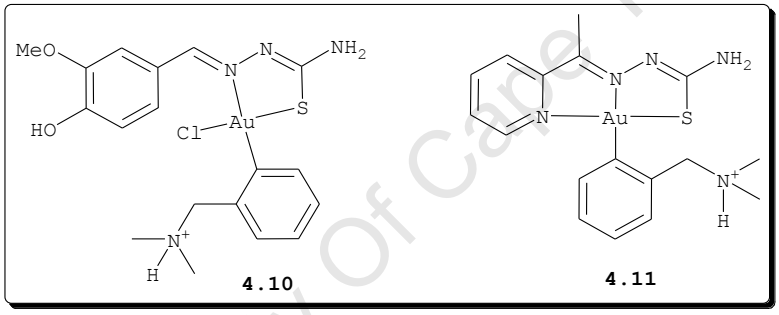

Figure 4.4: Chemical structures of gold(III) TSC complexes.

4.2 RATIONALE: SYNTHESIS OF GOLD TSC COMPLEXES

The structural features described previously (**Chapter 3**), showed that structural modifications on the TSC scaffold had no beneficial biological effects on the malaria parasite cysteine protease FP-2. However, a series of TSC derived metal complexes have been shown to be potent against the cysteine protease FP-2 and FP-3.[23]

On the other hand, the cathepsin family of lysosomal cysteine dependent enzymes have been shown to be attractive targets of auranofin (**2.7** in Fig. 2.3, p 37) and analogous complexes.[24] Thus, it was envisaged that investigating the

effects of gold TSC complexes on the malaria parasite cysteine protease FP-2, and hence their antiplasmodial activities, would be a worthwhile effort.

4.3 RESULTS AND DISCUSSION

SECTION A: GOLD(I) TSC COMPLEXES

Apart from the envisaged pharmacological effects which necessitated the search for new gold complexes, it was thought that the synthesis of these compounds would also contribute to the limited number of gold(I) TSC complexes previously reported in the literature.

4.3.1 Synthesis of gold(I) TSC complexes: $[Au(TSC)_2]Cl$

Scheme 4.2 shows the synthetic route for the target gold(I) TSC complexes. Thus, treatment of starting gold(I) complex $[Au^{I}(THT)Cl]$ (**4.3**) with individual TSCs (**3.28a-g**) in MeOH in a ratio of 1:2 mol for 2 h readily led to the substitution of the labile THT ligand to produce S-coordinated **4.12-4.19** complexes. Complex **4.19** was obtained by allowing the reaction mixture to reflux for 3 h in MeOH.

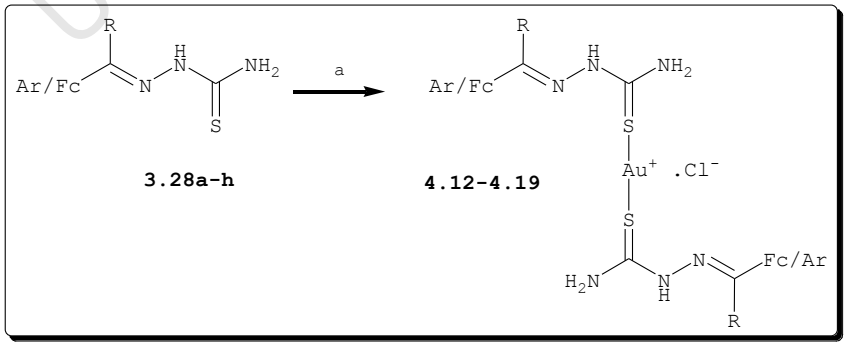

Scheme 4.2: *Reagents and conditions* a) 0.5 mol **4.3**, MeOH, reflux, 2 h.

The reaction mixtures were filtered through celite and evaporated to complete dryness. The resulting tan to red-brown complexes are mainly soluble in DMSO, MeOH, CH_3CN and insoluble in water. Although these complexes are generally stable, after prolonged periods in solution at ambient temperature, a fine dark-brown solid was often observed suggesting the possible decomposition. The desired gold(I) TSCs and isolated yields are summarised in Table 4.1.

Table 4.1: Yields of isolated gold(I) complexes **4.12-4.19**.

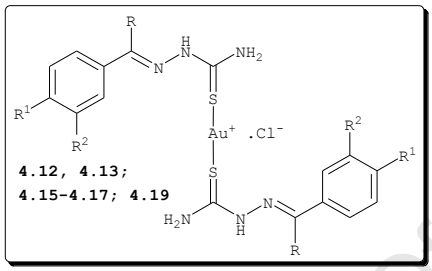

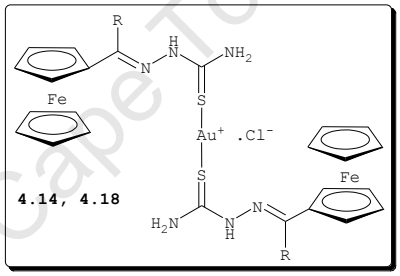

Entry	Code	Comp. No	R	R^1	R^2	Yield/[%]
1	DK-10	4.12	CH_3	H	Br	96
2	DK-12	4.13	CH_3CH_2	H	Br	83
3	DK-13	4.14	H	Ferrocene		89
4	DK-15	4.15	CH_3	Br	H	96
5	DK-16	4.16	CH_3	Cl	Cl	97
6	DK-17	4.17	CH_3CH_2	Cl	Cl	96
7	DK-42	4.18	CH_3	Ferrocene		95
8	DK-84	4.19	H	OH	CH_3O	97

4.3.1.1 Characterisation of Compounds 4.12-4.19

The synthesised gold(I) complexes were characterised using ^{1}H, and ^{13}C NMR; IR and MS. The molecular structures of these complexes were elucidated using single X-ray diffraction. The purity of all compounds was established using microanalysis. As a general example, Table 4.2 displays the ^{1}H and ^{13}C chemical shifts of the ligand **3.28b** and those of the corresponding of gold(I) complex **4.12.**

Table 4.2: Chemical shifts of the ligand and gold complex.

^{1}H and ^{13}C NMR (d_6-DMSO)			
Comparison	**Comp. No**	***$N^{2}H$***	***C=S***
Ligand	**3.28b**	10.15	179.0
Complex	**4.12**	10.99	173.6

As can be seen from the Table 4.2, the ^{1}H-NMR data for gold(I) TSC complex **4.12** revealed the NH proton chemical shift downfield with respect to that of the free ligand **3.28b**. More importantly, the presence of NH signals suggested coordination of TSCs to gold(I) in their thione form.[17] The appearance of different signals of NH_2 at δ 9.12 and 8.69 ppm indicated the non-equivalence of these protons due to the double bond character created around the C-N thioamide bond (see Scheme 3.5).

The ^{13}C spectrum of complex **4.12** showed an upfield shift of the thiocarbonyl (C=S) compared to **3.28b**. Similar trends on coordination of TSCs have been observed by Lobana and co-workers for a mercury(II) complex derived from acetophenone

TSC ligand,[25] and recently for the gold(I) complex **4.7** (Fig. 4.2).[18b]

The FT-IR spectra of the synthesised gold(I) complexes showed characteristic bands in ranges 3062-3251, 1587-1600 and 796-845 cm^{-1}, which can be assigned to ν(NH), ν(C=N) and ν(C=S) stretching frequencies, respectively. On gold coordination, the ν(C=S) stretch of all resulting complexes appeared at lower frequencies (shifted *ca*. 6–72 cm^{-1}) compared to the free ligands.

Laly et al.[26] proposed a silver(I) complex with vanillin TSC (VTSC) as a ligand binding through the S-donor atom. The ν(C=N) band of the silver complex displayed no shift in comparison to that of the VTSC ligand, while the ν(C=S) stretching frequency shifted *ca.* 30 cm^{-1} to lower frequencies. This supported our deduction that TSCs coordinated with the softer gold(I) through S-donor atoms.

The positive-ion FAB-MS spectra of all complexes contained molecular ion peaks at *m/z* 740.80 (**4.12**), 768.93 (**4.13**), 770.95 (**4.14**), 740.93 (**4.15**), 720.87 (**4.16**), 748.97 (**4.17**) and 798.7 (**4.18**). Electron-spray ionization (ESI) mass spectrometry revealed a molecular ion peak for **4.19** at *m/z* 647.0819. The fragmentation signals arising from the loss of a TSC moiety was also apparent in each spectrum of proposed structures. Microanalysis data showed atom composition consistent with the proposed structures.

4.3.1.2 Crystal Structures of Compounds 4.15 and 4.16

The single X-ray crystals of **4.15** (Fig. 4.5) and **4.16** (Fig. 4.6) were grown from their CH_3CN solutions by the slow evaporation method.[27] The crystal structures of these complexes contain a solvent molecule in a 2:1 ratio and a Cl^- counter anion. The complexes **4.15** and **4.16** are isostructural[28] and crystallize in centrosymmetric, monoclinic *C* centered space group, *C*2/c.[29]

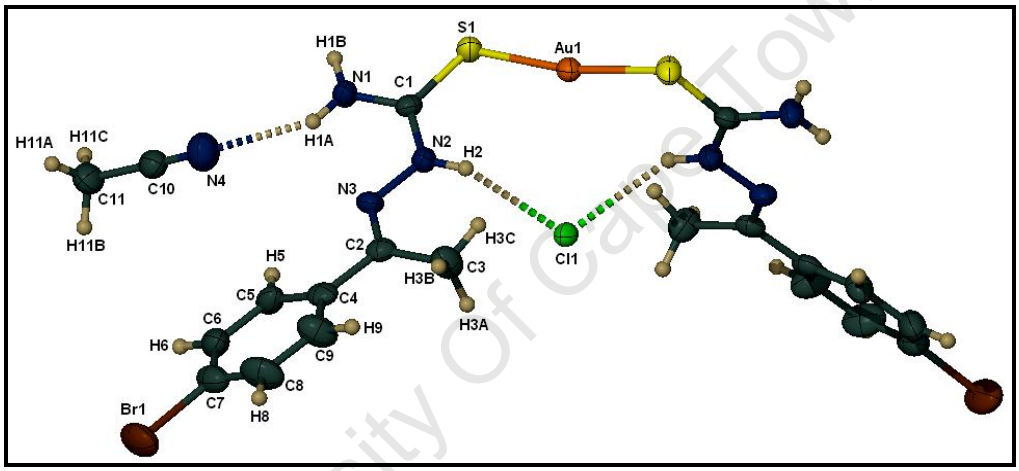

Figure 4.5: Molecular structure of **4.15** with a hydrogen bonded solvent molecule. Thermal ellipsoids of the asymmetric unit are shown at 50% probability level.

The Au1-S1 bond distances are similar in both structures: 2.2825(13) Å (**4.15**) and 2.2818(13) Å (**4.16**).[27] The Au-S distances in **4.15** and **4.16** are comparable to the bond distances of 2.278(4) and 2.279(5) Å in $[Au_2(3\text{-}NO_2Hbtsc)_4]Cl_2$,[18b] but relatively short compared to 2.319(1) Å in $[Au^IPEt_3(K_3TSC)]$, **2.12**.[18a] The Au-S distances of binuclear gold(I) complex **4.9** (see Fig. 4.9) are in agreement with those of **4.15** and **4.16** with a value of 2.282(2) Å.[18c]

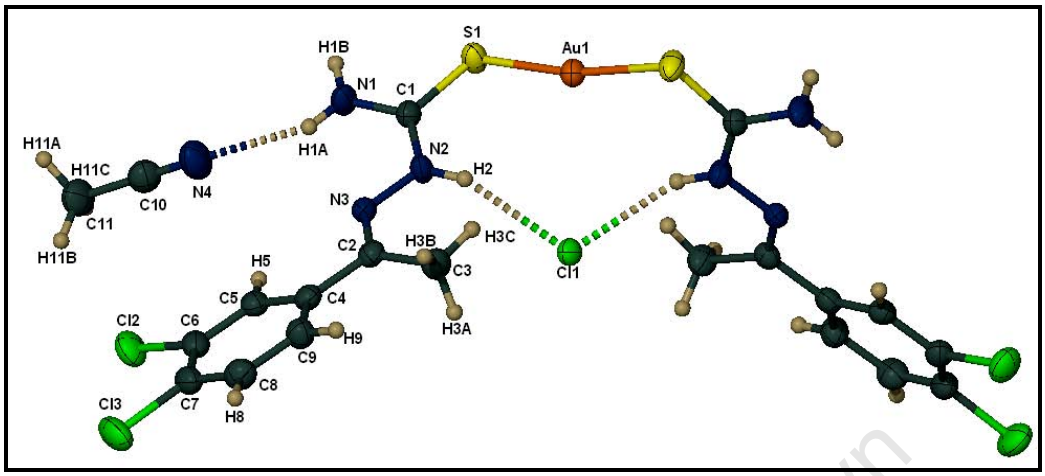

Figure 4.6: Molecular structure of **4.16** with a hydrogen bonded solvent molecule. Thermal ellipsoids of the asymmetric unit are shown at 50% probability level.

The gold atoms exhibit distorted linear coordination geometries with an S-Au-S angle of 170.24° in **4.15** and 169.66° in **4.16**. The literature reported gold(I) complexes **4.7** (Fig. 4.2) and **4.9** (Fig. 4.3) also showed distorted linear coordination geometries with an S-Au-S angle of 172.70° and 167.07°, respectively.[18b,18c] The relative angle of the two aromatic rings is 72.86° (**4.15**) and 73.47° (**4.16**).

The chloride counter anion is on a two fold rotational axis and hydrogen bonded to four amide groups which are arranged in a distorted tetrahedral arrangement. The nitrogen atom of the acetonitrile molecule is hydrogen bonded to the amide group through N1-H1A···N4 (Fig. 4.5 and 4.6), while the methyl hydrogen of the solvent molecule is involved in C-H···π interaction with the neighbouring aromatic ring (Fig. 4.7).[27]

a)

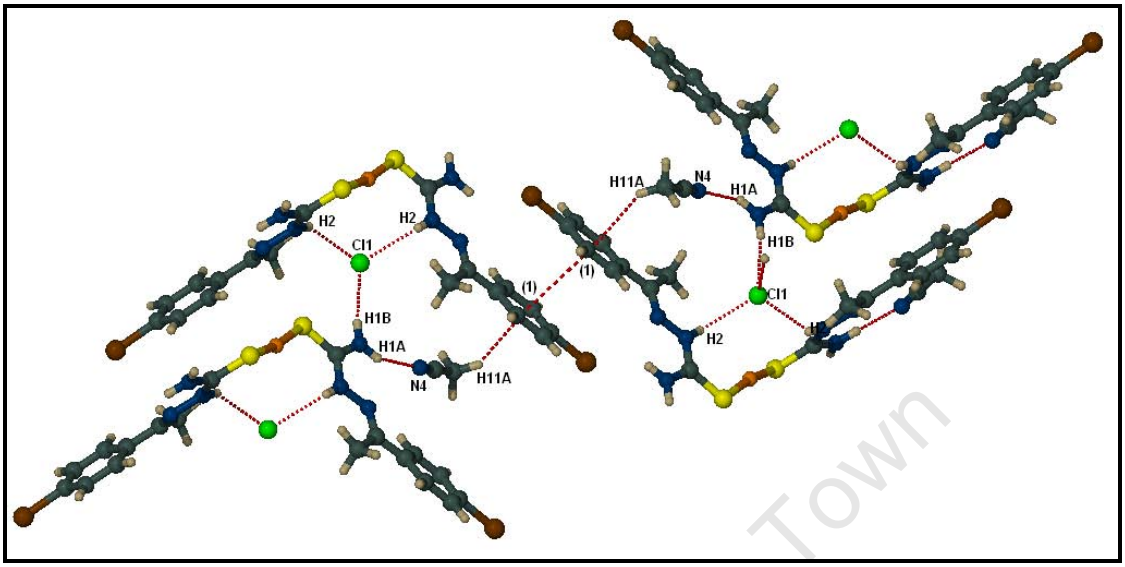

b)

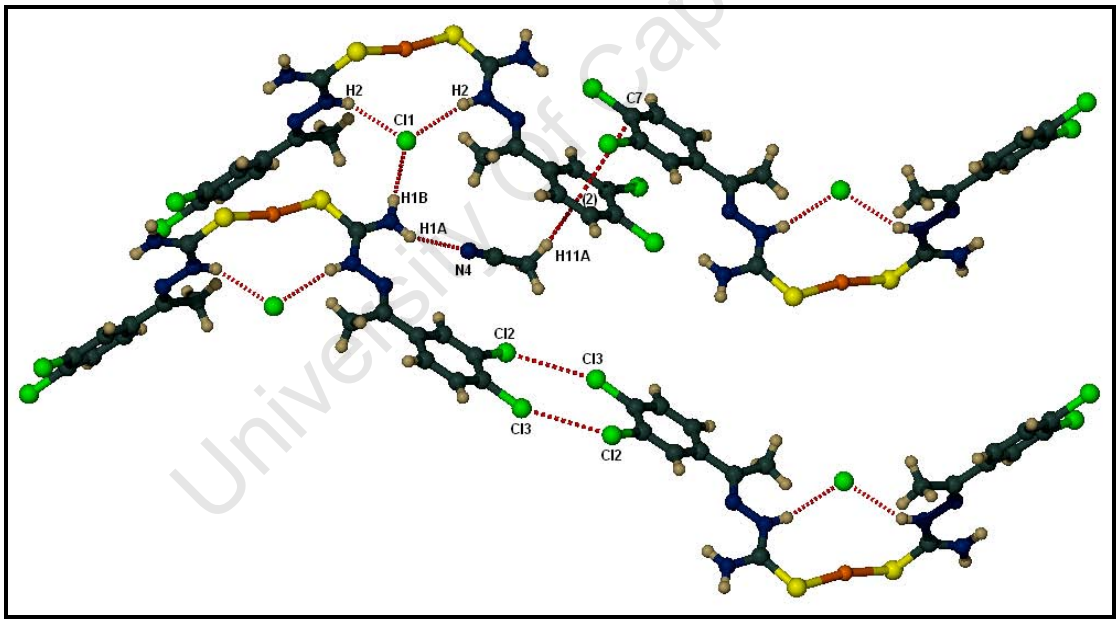

Figure 4.7: Molecular arrangement and significant intermolecular interactions in molecular structures **4.15** (**a**) and **4.16** (**b**).

Unlike gold(I) complex **4.7** (Fig. 4.2), no aurophilic Au(I)···Au(I) and S···S interactions were observed in both molecular structures of **4.15** and **4.16.** The crystal structures of these complexes also revealed aromatic

interactions between the phenyl rings of the symmetry generated molecular pairs. The two rings (C4…C9) are parallel with the neighbouring molecule and separation distances of 3.733 Å (**4.15**) and 3.489 Å (**4.16**). The brominated phenyl groups in **4.15** are in close to perfect overlap (Fig. 4.7a), while in **4.16** the dichlorinated aromatic rings are in off-set (Fig. 4.7b).[27]

To study weak interactions involved in both crystal structures, Hirshfeld surfaces were generated with the aid of CrystalExplorer,[30] a tool commonly utilised to describe packing arrangements and intermolecular interactions in molecular crystals.[31] By comparing the two fingerprint plots (Fig. 4.8) it can be seen that the intermolecular interactions are largely similar in the two structures, but some significant differences are also visible.[27]

In both compounds two spikes are related to short contacts between H2 and H1B to the Cl anion (①) and the hydrogen bonded solvent molecule (H1A…N4, ②). The plot of **4.15** revealed two symmetrical spikes, which are related to H…Br and Br…H weak interactions (③ and ④, Fig. 4.8a) between the halogen negatively polarized region and the methyl hydrogen atoms of neighbouring molecules.[27] A remarkable difference is observed on the plot of **4.16** indicated by the middle red region, which is related to the overlap of the π…π interaction between the aromatic rings (⑤) and the Cl…Cl contacts (⑥) in the crystal (Fig. 4.8b).[27]

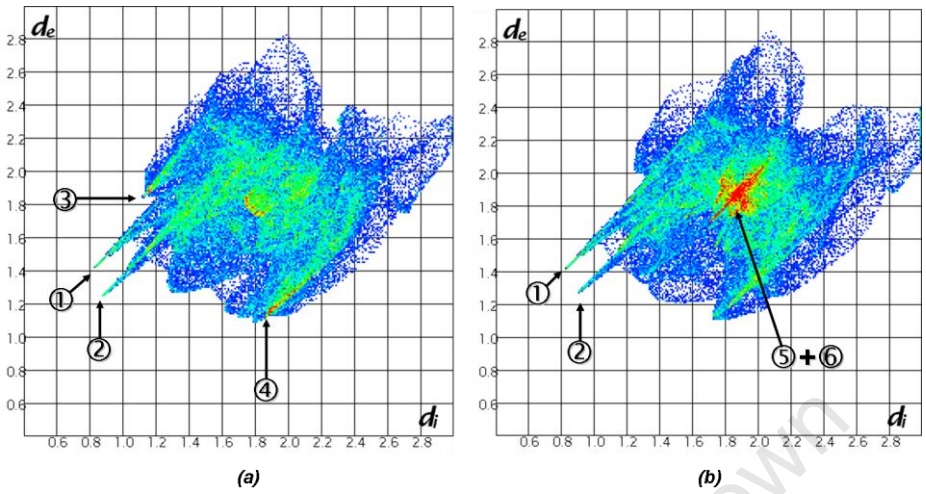

Figure 4.8: Fingerprint plots of the coordinated TSC gold(I) complex **4.15** (a) and **4.16** (b). The labels are referred to in the text.

Having observed the Cl···Cl contacts (⑥), it was also worth determining the type of chlorine-chlorine interactions existing in complex **4.16**. Although halogen-halogen contacts is a well known phenomenon, in the context of gold chemistry these interactions are rare. The interactions are dependent on the polarity of the C-X bond. Generally, in organic based compounds they are classified into two types, depending on the C-X…X' angle (Θ1 = C-X…X' and Θ2 = X…X'-C) within the C-X…X'-C' distance. Type I (Θ1 = Θ2 = 140-180°) interactions are driven by dispersion forces, while type II (Θ1 = 150-180°, Θ2 = 90-120°) are stabilized by Coulombic electrophile-nucleophile pairing. The observed geometric parameters for structure **4.16** suggest type I (Θ1 = 136.4°, Θ2 = 157.7°, Cl2…Cl3' = 3.43Å) (Fig. 4.9) driven by weak electrostatic attractions and dispersion forces.

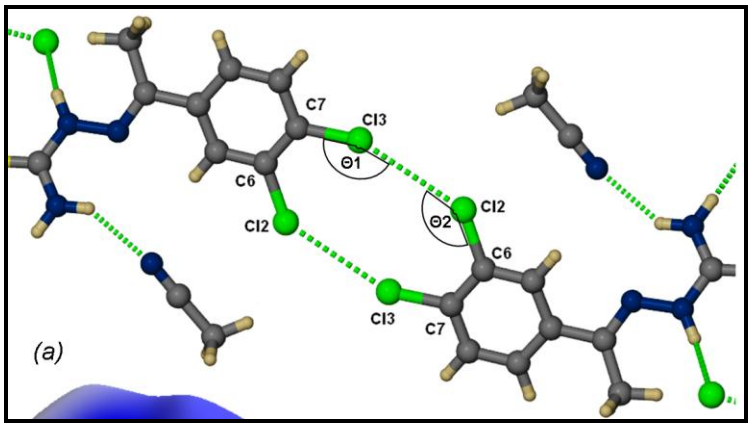

Figure 4.9: The centrosymmetric pair of Cl···Cl interaction analysed geometrically.

4.3.2 Synthesis of gold(I) Pyrazoline Complexes

The synthesis of pyrazoline gold(I) complexes **4.20-4.23** is illustrated in Scheme 4.3. Treatment of **4.3** with pyrazoline TSC analogues (**3.37a-c** and **3.37f**) in MeOH in a ratio 0.5:1 mol for 2 h readily produced the bis(PyTSC) gold(I) complexes as yellow to tan solids in moderate to good yields (Table 4.3).

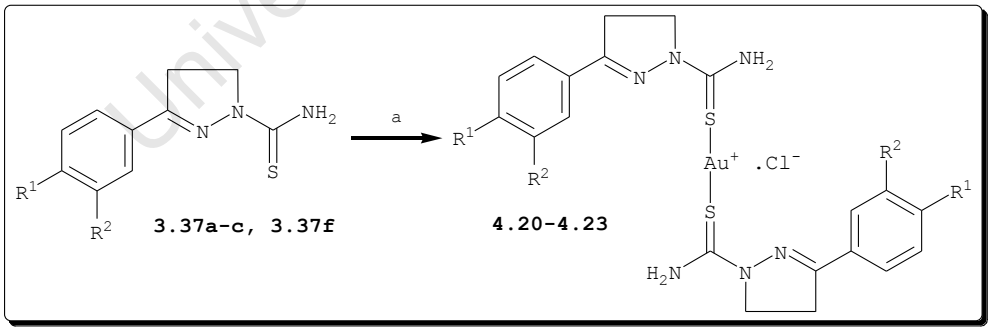

Scheme 4.3: *Reagents and conditions* a) 0.5 mol **4.3**, MeOH, reflux, 2 h.

Table 4.3: Yields of isolated gold(I) pyrazoline complexes

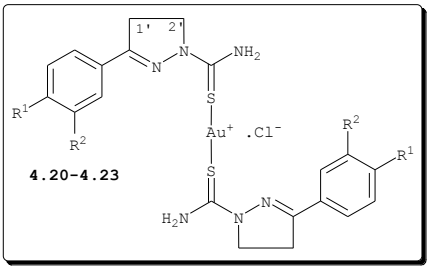

Entry	Code	Compound No	R^1	R^2	Yield/[%]
1	**DK-33**	**4.20**	H	Br	77
2	**DK-40C**	**4.21**	Cl	Cl	51
3	**DK-41**	**4.22**	Br	H	91
4	**DK-135**	**4.23**	Cl	H	55

4.3.2.1 Characterisation of Compounds 4.20-4.23

The synthesised complexes were characterised using ^{1}H and ^{13}C NMR, IR, MS and microanalysis. The ^{1}H NMR spectra of complexes **4.20-4.23** showed a slight shift in chemical shifts of methylene protons of $C_{1'}$ and $C_{2'}$ carbons relative to the free ligands. In the ^{13}C NMR spectra there was no significant shifts observed except the signals of C=S carbons appearing upfield. The FT-IR spectra also confirmed the coordination of pyrazoline ligands with the gold(I) centre through the S-donor atom.

ESI mass spectra of resulting complexes gave intense signals of molecular ion peaks at *m/z* 764.90(**4.20**), 744.94(**4.21**), 764.92(**4.22**) and 975.02(**4.23**). The fragmentation peaks at *m/z* 750.93(**4.20**), 730.95(**4.21**), 750.93(**4.22**) and 663.03(**4.23**) appeared consistent with the loss of the methylene group in the five membered ring.

4.4 SYNTHESIS OF TWO COORDINATE GOLD(I) COMPLEXES

An overwhelming majority of phosphine ligands used in gold(I) coordination chemistry are monodentate tertiary phosphines of the type R_3P.[14] Synthetically, phosphine ligands are of great importance in coordination chemistry due to the fact that they are easily modified by varying organic substituents to introduce properties such as aqueous solubility.[32] This has received greater application in areas such as catalysis and medicine where water soluble compounds are generally a prerequisite.[32] The ease of accessibility of these compounds, e.g. [$Au^I(Ph_3P)Cl$] (**4.5**), has rendered them attractive as starting materials for the synthesis of a wide range of novel gold(I) complexes. The following sections describe the synthesis of two coordinate gold(I) derivatives using [$Au^I(Et_3P)Cl$] (**4.2**), [$Au^I(Ph_3P)Cl$] (**4.5**) and [Au^I(PTA)Cl] (**4.24**) as gold(I) sources.

4.4.1 Gold(I) TSC Complexes Derived from [$Au^I(Ph_3P)Cl$]

Scheme 4.4, illustrates our synthetic approach to gold(I) complexes, [$Au^I(Ph_3P)$TSC]SO_3CF_3, **4.26a-f.**

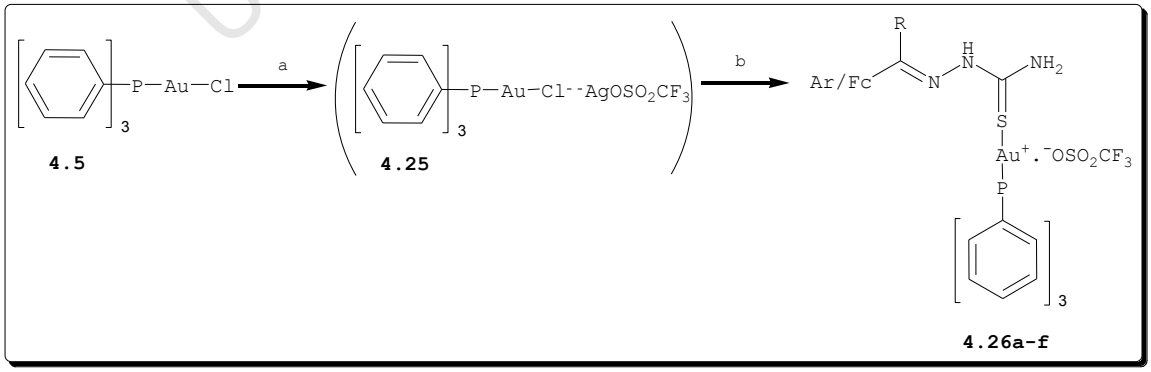

Scheme 4.4: *Reagents and conditions* a) $AgOSO_2CF_3$, MeOH, r.t., 1 h, N_2. b) **3.28a-f**, MeOH, r.t., 4 h, N_2.

Initially, treatment of the gold(I) precursor **4.5** with TSCs in MeOH at ambient temperature and under reflux yielded no desired products. Instead the starting material **4.5** was recovered and confirmed by ^{31}P NMR spectroscopy. On the other hand, metathesis of **4.5** with silver triflate ($AgOSO_2CF_3$), presumably proceeding *via* the intermediate **4.25**, led to the formation of complexes **4.26a-f**. The reaction products were all filtered (to remove AgCl precipitate) through celite and evaporated *in vacuo* to complete dryness. The resultant complexes were generally soluble in polar organic solvents. However, attempts to obtain suitable crystals for X-ray analysis were unsuccessful. Isolated compounds and respective yields are displayed in Table 4.4.

Table 4.4: Yields of isolated gold(I), $[Au^{I}(Ph_3P)TSC]SO_3CF_3$, complexes.

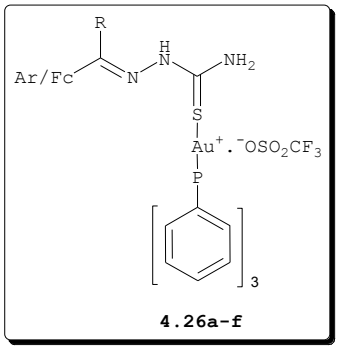

4.26a-f

Entry	Code	Product	Ar/Fc	R^1	Yield/[%]
1	**DK-32G**	**4.26a**	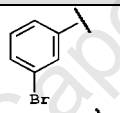	CH_3	72
2	**DK-52**	**4.26b**	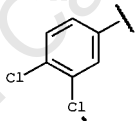	CH_3	66
3	**DK-53**	**4.26c**	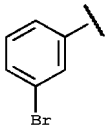	CH_3CH_2	76
4	**DK-54**	**4.26d**	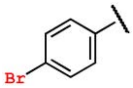	CH_3	73
5	**DK-55**	**4.26e**	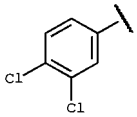	CH_3CH_2	76
6	**DK-56**	**4.26f**	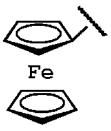	H	85

4.4.1.1 Characterization of Compounds 4.26a-f

The synthesised complexes were characterised using ^{1}H and ^{13}C NMR, IR and MS. The purity of these compounds was determined using microanalysis. The ^{1}H NMR spectra of complexes **4.26a-f** showed broad singlet peaks in the region

δ 11.20–12.12 ppm due to the NH protons, thus suggesting that TSCs bind with gold(I) predominantly in thione form.[18] The NH_2 protons in the resulting complexes appeared as two separate broad peaks in the range δ 9.53–9.01 and δ 9.05–8.26 ppm, due to restricted rotation about the C–N bond of the thioamide group (see Scheme 3.5).[18a] These signals also showed downfield shifts in comparison to those of the free ligands.

The ^{13}C NMR spectra of all complexes revealed an upfield shift of C=S (*ca.* 168.5–171.6 ppm) on gold(I) complexation. The observed trends are consistent with gold(I) MSB TSC complex **2.12** (Fig. 2.4, p 39) reported by *Casas et al.*[18a] The ^{31}P spectra of the complexes showed singlet resonances in the region δ 36.8–38.5 ppm. The peaks are also in agreement with those of **4.5** coordinated with sulfur-containing ligands to form $[Au^{I}(Ph_3P)SR)]$.[33,34]

In addition to the structural features described above, the FT-IR spectra of complexes **4.26a–f** showed ν(C=S) bands in the range 791–831 cm^{-1}, which shifted by 3–62 cm^{-1} towards lower frequencies relative to the ligands.

The molecular ion peaks of complexes (positive-ion FAB) appeared as intense signals at *m/z* 731.9 (**4.26a**), 719.9 (**4.26b**), 746.1 (**4.26c**), 732.1 (**4.26d**), 734.1 (**4.26e**) and 746.2 (**4.26f**). A fragmentation peak at *m/z* 459.1 was assigned to $[Au^{I}(Ph_3P)]^{+}$ due to the loss of the TSC ligand in each complex.

4.4.2 Gold(I) TSC Complexes Derived from [Au^{I}(PTA)Cl]

A second series of phosphine gold(I) TSC complexes involved the synthesis of compounds of the type [Au^{I}(PTA)TSC]Cl with 1,3,5-triaza-7-phosphaadamantane (PTA).[32] The ligand PTA (**4.28**) is well-known in terms of enhancing the aqueous solubility of metal complexes. It has accordingly attracted interest in biphasic catalysis.[32] Recently, *Grguric-Sipka et al.*[35] reported a novel PTA ruthenium(II)-TSC complex with noticeable aqueous solubility.

Since complex **4.26a-f** exhibited poor aqueous solubility, it was envisaged that replacement of the triphenylphosphine (TPP) ligand by **4.28** would lead to gold(I) TSC complexes with improved solubility. Scheme 4.5, below, outlines the synthesis of **4.28** and its conversion into the starting material [Au^{I}(PTA)Cl] (**4.24**).[36]

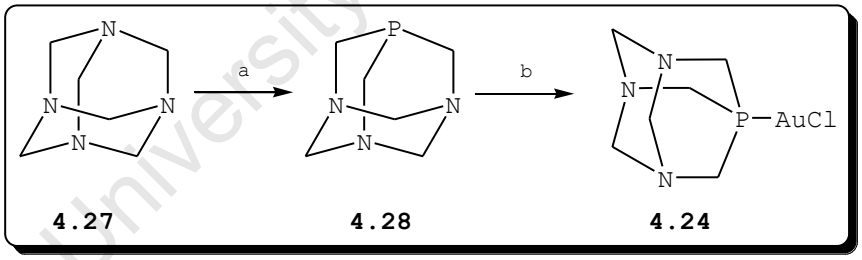

Scheme 4.5: *Reagents and conditions* a) THPC, aqu. NaOH, $(HCHO)_n$, r.t., 17 h; b) 4.3, $CHCl_3$, r.t., 2 h.

The condensation of trishydroxymethylphosphine [$P(CH_2OH)_3$], generated *in situ* from tetrahydroxymethylphosphine chloride (THPC), with formaldehyde and hexamethylenetetraamine (**4.27**) afforded **4.28** in 37% yield. Recrystallisation of the solid residue from ethanol led to the isolation of **4.28** in analytically pure form. The reaction of **4.3** with **4.28** at

ambient temperature afforded linear two-coordinate gold(I) precursor **4.24.** The formation of both **4.24** and **4.28** was confirmed by both ^{1}H and ^{31}P NMR spectroscopy in which the observed chemical shifts were consistent with the values reported in the literature.[36]

Having synthesised **4.24,** the subsequent step was to generate a series of PTA-based gold(I) complexes. Thus, treatment of equimolar amounts of the starting material gold(I) **4.24** with individual TSCs (**3.28a–h**) readily effected the displacement of the chloride ligand to produce cationic S-coordinated complexes **4.29a–h** (Scheme 4.6).

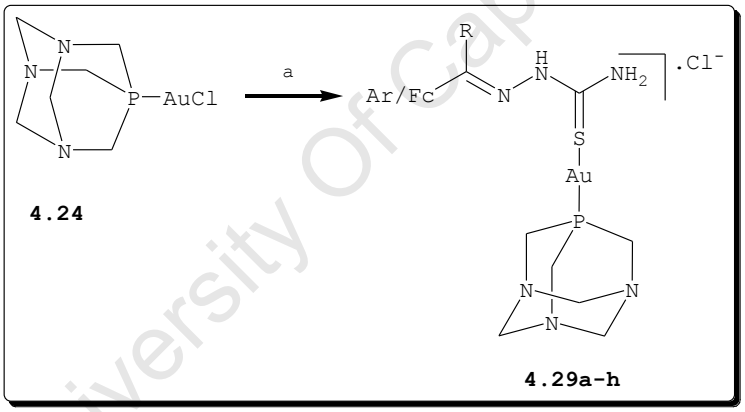

Scheme 4.6: *Reagents and conditions* a) **3.28a-h**; MeOH, r.t, 1½ h.

Reaction mixtures were filtered through celite to remove solid contaminants and dried *in vacuo* to give tan and/or yellow solids, which were soluble in polar organic solvents. The move to ascertain molecular structures of resulting complexes by X-ray was hampered by the poor quality of crystals. In some cases attempted methods for obtaining suitable X-ray crystals (e.g. cooling the solution and solvent diffusion) yielded no crystals. A

summary of isolated gold(I) complexes is displayed in Table 4.5.

Table 4.5: Yields of isolated PTA gold(I) TSC complexes.

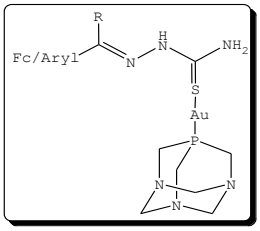

Entry	Code	Product	Ar/Fc	R	Yield/[%]
1	DK-109	4.29a	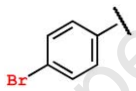	CH_3	87
2	DK-112	4.29b	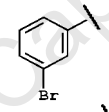	CH_3	84
3	DK-113	4.29c	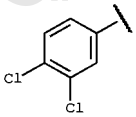	CH_3	81
4	DK-114	4.29d	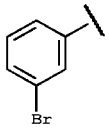	CH_3CH_2	83
5	DK-115	4.29e	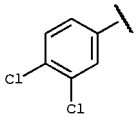	CH_3CH_2	80
6	DK-116	4.29f	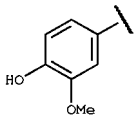	H	98
7	DK-117	4.29g	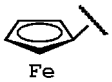	H	96
8	DK-118	4.29h		CH_3	70

4.4.2.1 Characterization of Compounds 4.29a-h

The synthesised complexes were characterised using ^{1}H and ^{13}C NMR, IR, MS and microanalysis. The ^{1}H NMR spectra revealed that the gold(I) centre coordinates with TSC ligands through the S-donor atom to form the desired complexes. The ^{31}P NMR spectral data of all compounds showed one singlet phosphorus signals at *ca* δ -50.9 ppm. A similar observation has been noted by Forward and co-workers when thiolate ligands are reacted with **4.24**.[37]

The infrared spectra of complexes showed a shift of ν(C=S) absorption bands to lower frequencies, thus lending support to the coordination of TSCs to the gold(I) center through S-donor atoms. The presence of NH (^{1}H NMR) and absence of SH bands (IR) indicated TSCs coordination predominantly in their thione form.

ESI mass spectral data of the complexes showed strong molecular ion peaks at *m/z* 625.0206 (**4.29a**), 625.0221 (**4.29b**), 615.0338 (**4.29c**), 639.0355 (**4.29d**), 629.0517 (**4.29e**), 579.1021 (**4.29f**), 641.0628 (**4.29g**) and 677.0770 (**4.29h**), which were in agreement with calculated values. The elemental analysis data appeared consistent with the observed molecular ion peaks of anticipated compounds.

4.4.3 Gold(I) Pyrazoline Complexes Derived from [Au^{I}(PTA)Cl]

Using a similar synthetic approach to that used for compounds **4.29a-h**, pyrazoline TSC analogues **3.37b**, **3.37c** and **3.37f** were employed as ligands to access complexes **4.30a-c** in moderate yields (Table 4.6).

Table 4.6: Yields of isolated PTA gold(I) pyrazoline complexes.

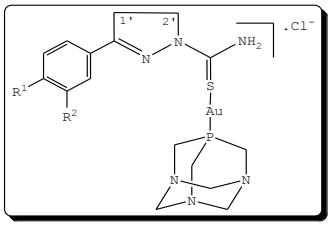

Entry	Code	Product	R^1	R^2	Yield/[%]
1	**DK-136**	**4.30a**	Br	H	50
2	**DK-137**	**4.30b**	Cl	H	67
3	**DK-138**	**4.30c**	Cl	Cl	60

4.4.3.1 Spectroscopic Characterisation of Compounds 4.30a-c

In the ^{1}H NMR spectra, the pyrazoline protons at C_1, and C_2, carbons in complexes **4.30a-c** resonated as triplets at δ 3.27-3.29 and δ 4.15-4.18 ppm, respectively. The appearance of new PTA protons in each spectrum further confirmed the proposed structures. In the ^{13}C NMR spectra, the C_1, and C_2, carbons, including those of characteristic signals (e.g. C=S, C=N, PTA, etc) were observed, further supporting the ^{1}H NMR spectral data. As in compounds **4.29a-h**, the chemical shifts in the ^{31}P NMR spectra also showed one singlet phosphorus signals at δ -51.1 ppm.

The mass spectra (ESI) of pyrazoline derivatives exhibited strong molecular ion peaks that confirmed the proposed structures at *m/z* 637.0228 (**4.30a**), 593.0714 (**4.30b**) and 627.0307 (**4.30c**).

4.4.4 Gold(I) TSC Complexes Derived from [$Au^{I}(Et_3P)Cl$]

The gold thioglucose derivative **2.7** (see also Fig. 2.3, p 37), an orally active gold(I) drug, is considered the lead structure for the development of analogous antiproliferatively active gold(I) compounds.[38] As mentioned previously, this complex has been shown to inhibit the *in vitro* growth of *P. falciparum*.[39] Fig. 4.11 illustrates our rationale behind the synthesis of gold(I) complexes **4.31a-f**, **4.32** and **4.33**.

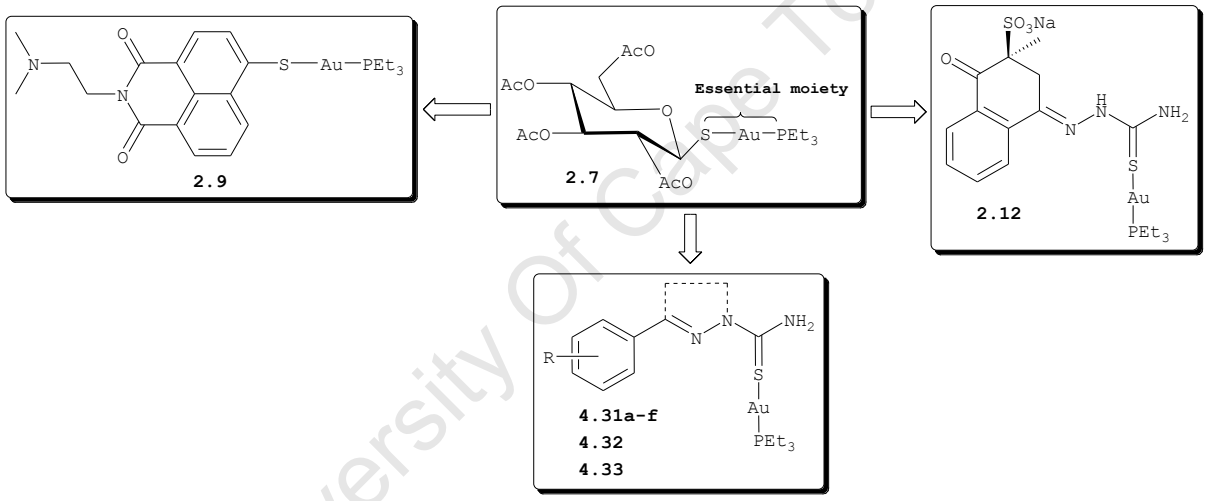

Figure 4.10: The effects of retaining Et_3P-Au-S moiety.

Early SAR studies derived from **2.7** and its analogues revealed that complexes lacking the R_3P-Au-S moiety (Fig. 4.11) display reduced antitumour activities.[40] Currently, in order to design agents with biological properties beyond complexes with simple the central gold atom or gold ions, replacement of thioglucose by bioactive compounds as ligands and retention of the triethylphosphine (Et_3P) moiety is considered an ideal approach to develop novel gold compounds.[38] This prompted *Otto et al.*[41] and *Casas et al.*[18a] to develop novel pharmacologically active gold(I) complexes

2.9 and **2.12** (Fig. 4.10) with pronounced antiproliferative effects in cultured tumour cells. In this regard, we envisaged that replacement of thioglucose ligands with TSCs and related pyrazoline analogues could be beneficial in addressing problems of antimalarial drug resistance.

By employing a similar synthetic approach to that used for compounds **4.29a-h** and reaction conditions reported by *Casas et al*.[18a] the synthesis of Et_3P gold(I) TSC complexes **4.31a-f** was pursued as shown in Scheme 4.7.

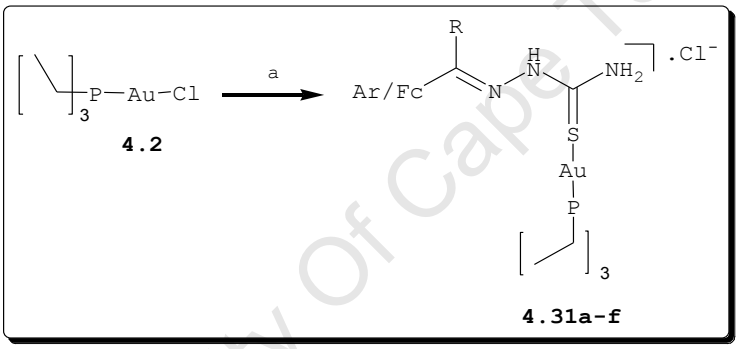

4.2

4.31a-f

Scheme 4.7: *Reagents and conditions* a) **3.28a-f,** MeOH, r.t, 4 h, N_2.

Treatment of equimolar amounts of gold(I) **4.2** with ligands **3.28a-f** readily afforded gold(I) complexes **4.31a-f** after a simple work-up. The resultant compounds were soluble in polar organic solvents. A summary of these complexes and isolated yields is provided in Table 4.7.

Table 4.7: Yields of isolated Et_3P gold(I) TSC complexes.

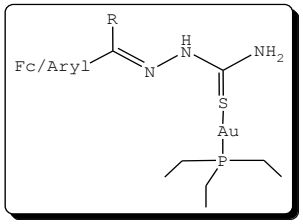

Entry	Code	Product	Ar/Fc	R	Yield/[%]
1	DK-151	4.31a	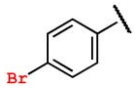	CH_3	92
2	DK-152	4.31b	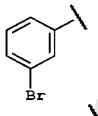	CH_3	94
3	DK-160	4.31c	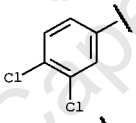	CH_3	96
4	DK-161	4.31d	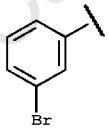	CH_3CH_2	98
5	DK-162	4.31e	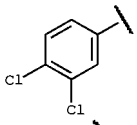	CH_3CH_2	95
6	DK-163	4.31f	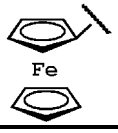	H	90

4.4.4.1 Characterisation of Compounds 4.31a-f

The ^1H and ^{31}P NMR spectra recorded in d_6-DMSO provided good evidence of the formation of coordinated complexes **4.31a-f.** In the ^1H NMR spectra of **4.31a-f,** the NH signals appeared downfield (relative to free ligands) as broad singlets at δ 10.33-11.19 ppm. The NH_2 protons gave rise to two broad singlets, which also appeared downfield at δ 7.61-8.36 and 8.01-8.68 ppm. The chemical shifts which appeared as multiplets at 1.09 and 1.92 ppm provided evidence of the

presence of the Et_3P moiety. The ^{31}P NMR spectra of each complex showed a singlet resonance at δ 35.1 ppm from the δ 38.5 ppm chemical shift of the starting gold(I) complex **4.2**.

The ESI mass spectra of complexes **4.31a-f** are summarised in Table 4.8. The spectral data showed molecular ion peaks of each complex and characteristic fragmentation signals due to the loss of TSC ligand from the complexes. The elemental analysis confirmed atomic composition in these compounds.

Table 4.8: Mass spectroscopic data for compounds **4.31a-f**.

Entry	Compound	*m/z* (%)	
		$\{[M]\}^+$	$\{[Et_3PAu]\}^+$
1	**4.31a**	586.0344(8)	315.0520(58)
2	**4.31b**	586.0396(27)	315.0531(33)
3	**4.31c**	576.0489(53)	315.0546(23)
4	**4.31d**	602.0474(70)	315.0550(35)
5	**4.31e**	590.0621(55)	315.0584(29)
6	**4.31f**	602.0744(100)	315.0255(20)

4.4.5 Pyrazoline Gold(I) Complexes based on $[Au^I(Et_3P)Cl]$

Using a similar synthetic approach to that used for compounds **4.31a-f**, pyrazoline derivatives **4.32** and **4.33** were synthesised by treating equivalent amounts of **4.2** with ligands **3.37c** and **3.37f**. The isolated compounds and respective yields are tabulated in Table 4.9.

Table 4.9: Yields of isolated Et_3P gold(I) pyrazoline complexes.

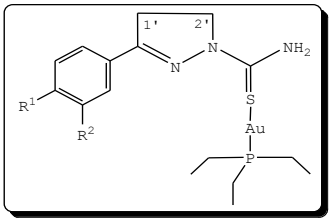

Entry	Code	Product	R^1	R^2	Yield/[%]
1	**DK-165**	**4.32**	Cl	H	90
2	**DK-166**	**4.33**	Br	H	95

4.4.5.1 Characterisation of Compounds 4.32 and 4.33

In the ^1H NMR spectra recorded in d_6-DMSO, the pyrazoline protons at C_1, and C_2, carbons in complexes **4.32** and **4.33** showed the expected two triplets with chemical shifts at δ 3.27-3.29 and δ 4.13-4.15 ppm. The chemical shifts appearing as multiplets at 1.07-109 and 1.90-192 ppm are due to Et_3P in the Et_3PAu fragment. As found in **4.31a-f**, the ^{31}P NMR spectra showed the shifting of ^{31}P resonances by *ca* 3.0 ppm to 35.1 ppm in **4.32** and **4.33**.

ESI mass spectra of Et_3P gold(I) pyrazoline complexes exhibited molecular ion peaks that confirm the proposed structures at *m/z* 554.0851 (**4.32**) and 598.0349 (**4.33**). The diagnostic fragmentation signals at *m/z* 315.0549 $\{(Et_3PAu)\}^+$ indicated the loss of TSCs in both **4.32** and **4.33**, respectively. Microanalysis data revealed the molecular composition of each complex consistent with the proposed structures.

4.5 SYNTHESIS OF ORGANOGOLD TSC COMPLEXES

The chemistry of organogold compounds has been known for almost a century,[42] and it has grown quite considerably over the past few decades. Several examples of organogold complexes are known, but the commonly used organogold precursor is pentafluorobenzene gold(I) complexes [Au(C_6F_5)THT], **4.34**. Reactions involving **4.34** with S-donor ligands to form gold(I) complexes such as **4.35**[43] and **4.36**[44] including other organogold derivatives have been reported.[45]

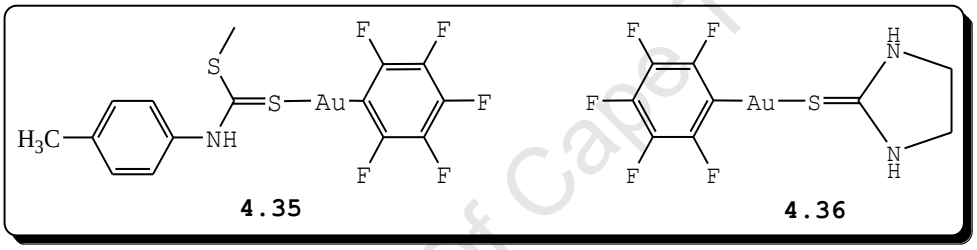

Figure 4.11: Neutral methyl dithiocarbamate gold(I) complexes

As part of our campaign to identify gold TSC complexes with potential antiplasmodial activities, we became interested in exploring the influence of other gold(I) compounds containing different moieties, e.g. pentafluorobenzyl, against plasmodial species.

4.5.1 Pentafluorobenzene Gold(I) TSC Complexes

Scheme 4.8 illustrates the synthesis of pentafluorophenyl gold(I) TSC complexes. Thus, the starting material gold(I) **4.34** was prepared according to the published method from **4.37**.[46] Simple substitution of the labile ligand (THT) from **4.34** by ligands **3.28a-f** readily afforded neutral gold(I) complexes **4.38a-f** as yellow to orange solids.

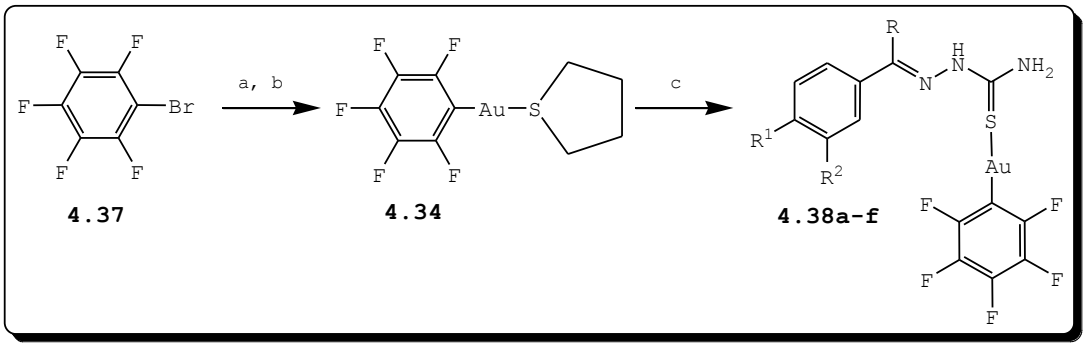

Scheme 4.8: *Reagents and conditions* a) *n*-BuLi, Et_2O, -78 °C, 1 h, N_2; b) **4.3**; c) **3.28a-f**, DCM, r.t., 1 h.

The resulting gold(I) compounds are mainly soluble in DCM, DMSO and slightly in MeOH and CH_3CN. A summary of proposed structures (in the absence of X-ray crystallographic evidence) and their isolated yields is provided (Table 4.10)

Table 4.10: Pentafluorophenyl gold(I) TSC complexes.

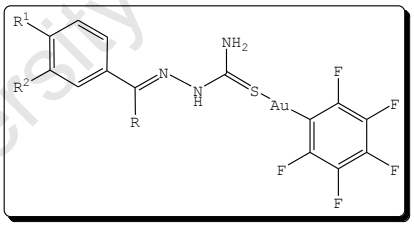

Entry	Code	Product	R	R^1	R^2	Yield/[%]
1	DK-74	4.38a	CH_3	Br	H	100
2	DK-75	4.38b	CH_3	H	Br	100
3	DK-76	4.38c	CH_3	Cl	Cl	100
4	DK-77	4.38d	CH_3CH_2	H	Br	86
5	DK-78	4.38e	CH_3CH_2	Cl	Cl	100
6	DK-79	4.38f	H	OH	CH_3O	69

4.5.1.1 Characterisation of compounds 4.38a-f

The ^{1}H NMR spectra of these complexes showed a downfield shift of the NH and NH_2 signals of the ligands on gold(I) complexation. The non-equivalence of the NH_2 proton chemical shifts was also clearly evident in ^{1}H NMR spectra of all complexes. Infrared spectra of all the complexes revealed the ν(C=S) bands at lower frequencies compared to those of corresponding ligands.

The molecular ion peaks of **4.38a**, **4.38b** and **4.38e** were not observed in the mass spectra, only *m/z* values consistent with resulting fragments at 467.75 (**4.38a**), 469.94 (**4.38b**), 471.97 (**4.38e**). The ESI mass spectral analysis of complex **4.38d** exhibited a weak molecular ion peak at *m/z* 650.97(4%) and a fragmentation signal *m/z* at 483.96. Microanalyses data confirmed atomic composition of these compounds.

SECTION B: THE CHEMISTRY OF GOLD(III) TSC COMPLEXES

4.6 SYNTHESIS OF ORGANOGOLD(III) TSC COMPLEXES

Although a number of gold(III) TSC complexes have been reported,[17,19] to our knowledge there are no reports dealing with their antimalarial evaluation. In view of antitumour activities of the gold(III) complex **2.15** (Fig. 2.6, p 42) and its analogues,[4c,47] it seemed a worthwhile endeavour to investigate the influence of **2.15** on TSCs against *P. falciparum* strains. Thus, we pursued the synthesis and *in vitro* antiplasmodial evaluation of this class of compounds.

4.6.1 Synthesis of Gold(III) TSC Complexes

The reaction of *N,N*-dimethylaminomethylbenzene (damp) **4.39** with *n*-BuLi produced an organolithium intermediate *in situ*, which was subsequently treated with $HgCl_2$ to give complex **4.40** (Scheme 4.9).[48] The formation of **4.40** was confirmed by both ^1H NMR spectroscopy and microanalysis.

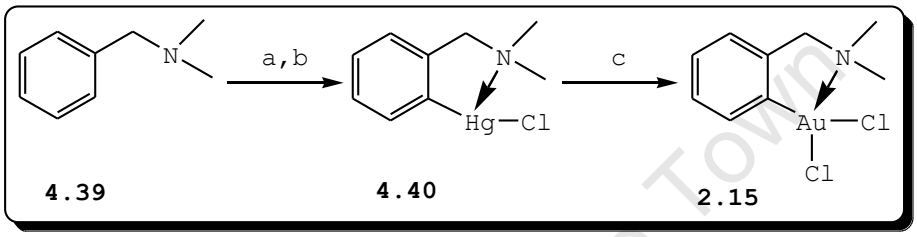

Scheme 4.9: *Reagents and conditions* a) n-BuLi, Et_3O, 0 °C→r.t, 24 h, N_2. b) $HgCl_2$, THF, -90 °C, 24 h, N_2. c) **$Me_4N[AuCl_4]$**/Me_4NCl, CH_3CN, r.t., 24 h.

Treatment of **4.40** with the gold(III) precursor $Me_4N[AuCl_4]$ (**4.41**) in anhydrous acetonitrile afforded a yellow solid residue, which was extracted with DCM to produce complex **2.15** as an analytically pure yellow solid.[49] ^1H and ^{13}C NMR spectroscopy, and microanalysis confirmed the formation of **2.15**.

Having synthesised **2.15**, the subsequent step was to prepare gold(III) TSC complexes **4.42a-f**. By employing conditions reported by *Ortner et al.*[19e], reaction of complex **2.15** with **3.28a-f** and **3.28h** in methanol resulted in the formation of products as a mixture of **4.42a-f** and gold(I) bis(TSC) complexes due to the *in situ* reduction of gold(III) to gold(I).[21] This appeared unusual since **2.15** and analogous complexes are known to be stable in the presence of thiols

due to the electron-rich phenyl group of the damp ligand stabilising the gold(III) center.[50] It was later established that in order to circumvent the reduction of gold(III) to gold(I), the reactions should be conducted in polar aprotic solvents such as acetone.[18c] The polar protic solvent, MeOH, is believed to be responsible in varying the redox behaviour of gold(III), thus favouring its reduction to gold(I), and hence the formation of gold(I) complexes.[18c]

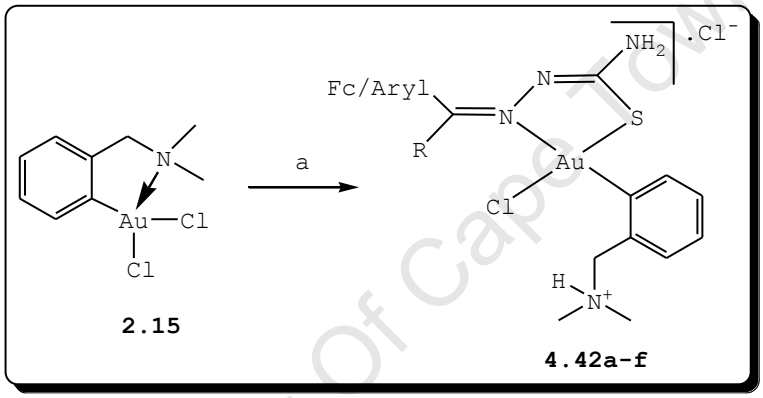

2.15 **4.42a-f**

Scheme 4.10 *Reagents and conditions*: (a) **3.28a-f** and **3.24h**, Acetone, reflux 1 h, r.t., 5 h.

Treatment of complex **2.15** with TSCs **3.28a-f** and **3.28h** in acetone led to the formation of complexes **4.42a-f** (Scheme 4.10) without any evidence (ESI mass spectroscopy) of the formation of competing gold(I) complexes being observed. These complexes were obtained as yellow, orange-yellow and dark-red solids after solvent evaporation and drying of the products *in vacuo*. In general complexes **4.42a-f** are soluble in polar organic solvents and insoluble in non-polar solvents and water. Table 4.11 summarises isolated compounds and their respective yields.

Table 4.11: Yields of isolated Gold(III) complexes.

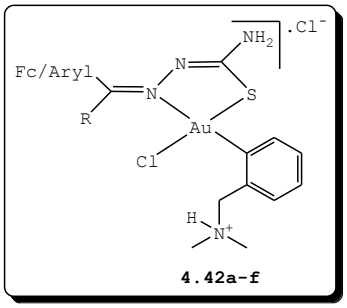

4.42a-f

Entry	Code	Product	Ar/Fc	R	Yield/[%]
1	**DK-46M**	**4.42a**	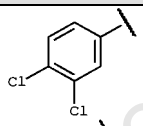	CH_3	98
2	**DK-51F**	**4.42b**	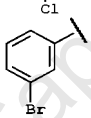	CH_3	96
3	**DK-62**	**4.42c**	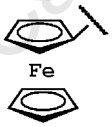	H	98[19a]
4	**DK-63F**	**4.42d**	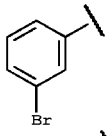	CH_3CH_2	93
5	**DK-64F**	**4.42e**	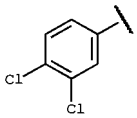	CH_3CH_2	90
6	**DK-65F**	**4.42f**	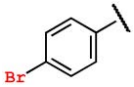	CH_3	91
7	**DK-70**	**4.42g**	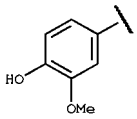	H	96[19e]

4.6.1.1 Characterisation of Gold(III) Compounds 4.42a-g

The complexes were characterised by means of ^{1}H NMR, FT-IR, MS, and elemental analysis. The ^{1}H spectra of **4.42a-g** in deuterated DMSO showed chemical shifts at δ 10.35-10.83 ppm, which were assigned to the protonated tertiary amine

(NH^+) group of damp ligand.[19] Coordination of the damp ligand was also supported by the appearance of signals at δ 4.30-5.40 ppm and δ 2.65-3.20 ppm, which were assigned to the $-CH_2$ and $-N(CH_3)_2$ groups, respectively. The ^1H NMR spectra showed no chemical shifts corresponding to NH. This suggests that TSCs bond with gold(III) to give **4.42a-f** in their thiol form.[19]

The FT-IR spectra of complexes **4.42a**, **4.42c**[19a], **4.42d**, **4.42e** and **4.42g**[19e] displayed weak bands at 2664-2683 cm^{-1} due to NH^+ stretches. These bands revealed that during the reaction, cleavage of the Au-N (**2.15**) bond is accompanied by protonation of the tertiary amine group in the damp ligand.[19] Evidence of S-coordination of TSCs to the gold(III) was provided by a decrease in the ν(C=S) frequencies to lower streching frequencies. The absorption bands due to ν(C=N) appeared in the range 1580-1700 cm^{-1}.

The formation of cationic complexes **4.42a-f** was supported by detection of molecular ion peaks in the ESI and FAB mass spectra at *m/z* 627.028 (**4.42a**), 637.0118 (**4.42b**), 653.1 (**4.42c**), 651.025 (**4.42d**), 641.036 (**4.42e**), 637.011 (**4.42f**), 591.0 (**4.42g**). The intense fragmentation peaks at *m/z* 555.0-617.1 suggested the loss of a chloride anion (i.e. M^+-Cl) in each complex. Microanalytical data of all the compounds appeared consistent with atomic composition of proposed structures.

4.7 CONCLUSION

In conclusion, we have demonstrated the synthesis of novel gold(I) and gold(III) TSC complexes from previously investigated bioactive ligands. The available experimental data showed that TSCs coordinate to gold(I) through the S-donor atom. The data suggests that coordination of TSCs to gold(III) involve both sulfur and nitrogen donor atoms.

The crystal structure of **4.15** revealed that the structure of this complex is partly held together by secondary interactions including H…Br and Br…H weak interactions. In both the crystal structures of **4.15** and **4.16**, however, no inter- and intra-molecular aurophilic interactions were found, which is a common phenomenon in linear gold(I) compounds. In addition, complex **4.16** exhibited π…π interactions between the aromatic rings and the Cl…Cl contacts in the crystal.

Although the formation of two coordinate gold(I) and gold(III) complexes has been supported by most analytical techniques, greater insight into their molecular structures could have been gained if crystals suitable for analysis had been successfully obtained in all or most cases.

4.8 REFERENCE

1. (a) B.F.G. Johnson, R. Davis, *Comprehensive Inorganic Chemistry*, Vol. 3, Ed. J.C. Bailer Jr et al., Pergamon Press, New York, **1973**, p 129-186. (b) G.J. Hutchings, M. Brust, H. Schmidbaur, *Chem. Soc. Rev.*, **2008**, *37*, 1759-1765.
2. C.F. Shaw III, *In Gold*: *Progress in Chemistry, Biochemistry and Technology*, Ed. H. Schmidbaur, John Wiley & Sons Ltd., Chichester, **1999**, p 261–308.
3. F.A. Cotton, G. Wilkinson, C.A. Murillo, M. Bochmann, *Advanced Inorganic Chemistry*, 6th Ed, John Wiley & Sons, Inc., New York, **1999**, p 1087.
4. (a) S. Nobili, E. Mini, I. Landini, C. Gabbiani, A. Casini, L. Messori, Medicinal Research Reviews, **2009**, *29*, doi: 10.1002/med.20168. (b) C.F. Shaw III, *Chem. Rev.*, **1999**, *99*, 2589-2600.
5. R.J. Puddephatt, *Comprehensive Organometallic Chemistry*, Vol. 2, eds. G. Wilkinson, F.G.A. Stone, E.W. Abel, Pergamon Press, Oxford, **1982**, p 765.
6. A. Laguna, M. Laguna, *Coord. Chem. Rev.*, **1999**, *193-195*, 837-856.
7. F.A. Cotton, G. Wilkinson, C.A. Murillo, M. Bochmann, *Advanced Inorganic Chemistry*, 6th Ed, John Wiley & Sons, Inc., New York, **1999**, p 1098-1107.
8. M.C. Gimeno, A. Laguna, *Chem. Rev.*, **1997**, *97*, 511-523.
9. J. Strahle, *In Gold: Progress in Chemistry, Biochemistry and Technology*, ed. H. Schmidbaur, John Wiley & Sons, Chichester, **1999**, p 314.

10. H. Schmidbaur, A. Schier, *Chem. Soc. Rev.*, **2008**, *37*, 1937-1951.
11. A. Codina, E.J. Fernández, P.G. Jones, J.M. López-de-Luzuriaga, M. Monge, M.E. Olmos, J. Pérez, M.A. Rotriäguez, *J. Am. Chem. Soc.*, **2002**, *124*, 6781-6786.
12. (a) H. Schmidbaur, W. Graf, G. Müller, *Angew. Chem. Int. Ed.*, **1988**, *27*, 417-419. (b) P. Pyykkö, *Angew. Chem. Int. Ed.*, **2004**, *43*, 4412-4456.
13. E.R.T. Tiekink, *Gold Bulletin*, **2003**, *36*, 117-124.
14. A. Grohmann, H. Schmidbaur, *In Comprehensive Organometallic Chemistry* II, Pergamon, Oxford, **1995**, p 1-56.
15. S. Padhye, *Coord. Chem. Rev.*, **1985**, *63*, 127–160.
16. J.S. Casaa, M.S. Garcia-Tasende, J. Sordo, *Coord. Chem. Rev.*, **2000**, *209*, 197–261.
17. T.S. Lobana, R. Sharma, G. Bawa, S. Khana, *Coord. Chem. Rev.*, **2009**, *253*, 977-1055.
18. (a) J.S. Casas, E.E. Castellano, M.D. Couce, J. Ellena, A. Sanchez, J. Sordo, C. Taboada, *J. Inorg. Biochem.*, **2006**, *100*, 1858–1860. (b) T.S. Lobana, S. Khanna, R.J. Butcher, *Inorg. Chem. Commun*. 11, **2008**, 1433-1435. (c) A. Castiñeiras, S. Dehnen, A. Fuchs, I. García-Santos, P. Sevillano, *Dalton Trans.*, **2009**, 2731-2739.
19. (a) J.S. Casas, M.V. Castaño, M.C. Cifuentes, J.C. García-Monteagudo, A. Sánchez, J. Sordo, U. Abram, *J. Inorg. Biochem.*, **2004**, *98*, 1009-1016. (b) I.G. Santos, A. Hagenbach, U. Abram, *Dalton Trans.*, **2004**, 677-682. (c) A. Sreekanth, H.-K. Fun, M.R.P. Kurup, *Inorg. Chem. Commun.* 7, **2004**, 1250-1253. (d) U. Abram,

K. Ortner, R. Gust, K. Sommer, J. *Chem. Soc., Dalton Trans.*, **2000**, 735-744. (e) K. Ortner, U. Abram, *Inorg. Chem. Commun*. 1, **1998**, 251-253.

20. E.W. Ainscough, A.M. Brodie, W.A. Denny, G.J. Finlay, J.D. Ranford, *J. Inorg. Biochem.*, **1998**, *70*, 175-185.
21. U. Abram, J. Mack, K. Ortner, M. Müller, *J. Chem. Soc., Dalton Trans.*, **1998**, 1011-1019.
22. Z. Zheng-Zhi, M. Yong-Xiang, *Chem. Papers*, **1991**, *45*, 373-378.
23. E.M.R. Kiremire, K. Chibale, P.J. Rosenthal, L.S. Daniel, A.M. Negonga, F.M. Munyololo, *Biosci. Biotech. Res. Asia*, **2007**, *4*, 399-402.
24. S.S. Gunatilleke, C.A.F. de Oliveira, *J. Biol. Inorg. Chem.*, **2008**, *13*, 555-561.
25. T.S. Lobana, A. Sanchez, J.S. Casas, M.S. Garcia-Tasende, J. Sordo, *Inorg. Chim. Acta*, **1998**, *267*, 169–172.
26. S. Laly, G. Parameswaran, *Asian J. Chem.*, **1993**, *5*, 712-718.
27. S.D. Khanye, N.B. Báthori, G.S. Smith, K. Chibale, *Dalton Trans.*, **2010**, *39*, 2697-2700.
28. (a) A. Kálmán, L. Párkányi, G. Argay, *Acta Crystallogr.*, **1993**, *B49*, 1039-1049. (b) J.S. Rutherford, *ACH Models Chem.*, **1997**, *134*, 395-405. (c) L. Fábián, A. Kálmán, *Acta Crystallogr.*, **1999**, *B55*, 1099-1108.
29. (a) COLLECT, Data Collection Software, Nonius, Delft, The Netherlands, **1999**. (b) Z. Otwinowski, W. Minor, DENZO and SCALEPACK. In International Tables of Crystallography, Vol F. ed.: M.G. Rossman, M.G.; E.

Arnold, Kluwer, Dordrecht, **2000**. (c) G.M. Sheldrick, SHELXS-97 and SHELXL-97 Programs for crystal structure determination and refinement. University of Gottingen, **1997**. (d) XSeed-A software tool for "Supramolecular Crystallography", L.J. Barbour, *J. Supramol. Chem.*, **2001**, *1*, 189-191. (e) Platon , A multipurpose crystallographic tool, A.L. Spek, *J. Appl. Crystallogr*. **2003**, *36*, 7-13. (f) C.F. Macrae, I.J. Bruno, J.A. Chisholm, P.R. Edgington, P. McCabe, E. Pidcock, L. Rodriguez-Monge, R. Taylor, J. van de Streek, P.A. Wood, *J. Appl. Cryst.*, **2008**, *41*, 466-470.

30. (a) M.A. Spackman, P.G. Byrom, *Chem. Phys. Lett.*, **1997**, *267*, 215-220. (b) J.J. McKinnon, A.S. Mitchell, M.A. Spackman, *Chem. Eur. J.*, **1998**, *4*, 2136-2141. (c) S.K. Wolff, D.J. Grimwood, J.J. McKinnon, D. Jayatilaka, M.A. Spackman, CrystalExplorer 2.1, **2007**, University of Western Australia, Perth. http://hirshfeldsurface.net/CrystalExplorer.
31. M.A. Spackman, D. Jayatilaka, *CrystEngComm.*, **2009**, *11*, 19-32.
32. A.D. Phillips, L. Gonsalvi, A. Romerosa, F. Vizza, M. Peruzzini, *Coord. Chem. Rev*. **2004**, *248*, 955-993.
33. (a) A.A. Isab, M. Fettouhi, S. Ahmad, L. Ouahab, *Polyhedron*, **2003**, *22*, 1349-1354. (b) C.L.L. Chai, D.C.R. Hockless, K.D.V. Weersuria, *Polyhedron*, **1997**, *16*, 1577–1580.
34. M.C. Gimeno, E. Jambrina, E.J. Fernández, A. Laguna, M. Laguna, P.G. Jones, F.L. Merchán, R. Terroba, *Inorg. Chim. Acta*, **1997**, *258*, 71-75.

35. S. Grguric-Sipka, C.R. Kowol, S.-M. Valiahdi, R. Eichinger, M.A. Jakupec, A. Roller, S. Shova, V.B. Arion, B.K. Keppler, *Eur. J. Inorg. Chem.* **2007**, 2870-2878.

36. (a) D.J. Daigle, A.B. Pepperman Jr., S.L. Vail, *J. Heterocycl. Chem.*, **1974**, *11*, 407-409. (b) D.J. Daigle, A.B. Pepperman Jr., *J. Heterocycl. Chem.* **1975**, *12*, 579-580. (c) D.J. Daigle, T.J. Decuir, J.B. Robertson, D.J. Darensbourg, *Inorg. Synth.*, **1998**, *32*, 40-45.

37. J.M. Forward, D. Bohmann, J.P. Fackler, R.J. Staples, *Inorg. Chem.*, **1995**, *34*, 6330-6336.

38. I. Ott, *Coord. Chem. Rev.*, **2009**, *253*, 1670-1681.

39. A.R. Sannella, A. Casini, C. Gabbiani, L. Messori, A.R. Bilia, F.F. Vincieri, G. Majorie, C. Severini, *FEBS Lett.*, **2008**, *582*, 844-847.

40. C.K. Mirabelli, R.K. Johnson, D.T. Hill, L.F. Faucette, G.R. Girard, G.Y. Kuo, C.M. Sung, S.T. Crooke, *J. Med. Chem.*, **1986**, *29*, 218-223.

41. I. Otto, X. Qian, Y. Xu, D.H.W. Vlecken, I.J. Marques, D. Kubutat, J. Will, W.S. Sheldrick, P. Jesse, A. Prokop, C.P. Bagawski, *J. Med. Chem.*, **2009**, *52*, 763-770.

42. E.J. Fernández, A. Laguna, M. E. Olmos, *Coord. Chem. Rev.*, **2008**, *252*, 1630–1667.

43. M. Bardají, A. Laguna, M. Laguna, *Inorg. Chim. Acta*, **1994**, *215*, 215-218.

44. T.K. Hagos, **MSc. Thesis**, University of Stellenbosch, April **2006**.

45. S. Cronje, H.G. Raubenheimer, H.S.C. Spies, C. Esterhuysen, H. Schmidbaur, A. Schier, G.J. Kruger, *Dalton Trans.*, **2003**, 2859-2866.
46. R. Uson, A. Laguna, M. Laguna, *Inorg. Synth.*, **1989**, *26*, 86–87.
47. R.V. Parish, B.P. Howe, J.P. Wright, J. Mack, R.G. Pritchard, *Inorg. Chem.*, **1996**, *35*, 1659-1666.
48. (a) O. Bumbu, C. Silvestru, M.C. Gimeno, A. Laguna, *J. Organomet. Chem.*, **2004**, *689*, 1172-1179. (b) P.-A. Bonnardel, R.V. Parish, *J. Organomet. Chem.*, **1996**, *515*, 221-232.
49. (a) J. Vicente, M.T. Chicote, M.D. Bermúdez, *J. Organomet. Chem.*, **1984**, *268*, 191-195. (b) P.A. Bonnardel, R.V. Parish, R.G. Pritchard, *J. Chem. Soc., Dalton Trans.*, **1996**, 3185–3193.
50. W. Henderson, *Advances in Organometallic Chemistry*, Vol. 4, Ed. R. West, A.F. Hill, Academic Press, Amsterdam, **2006**, p 208.

CHAPTER 5

ANTIPLASMODIAL EVALUATION OF GOLD THIOSEMICARBAZONE COMPLEXES

ABSTRACT: The main aim of this project was to identify antimalarial gold compounds based on the TSC scaffold. All the synthesised gold TSC complexes described in **Chapter 4** were evaluated for *in vitro* growth inhibitory activity against *P. falciparum* strains, and in selected cases for the inhibition of FP-2 activity. This chapter will discuss the biological results.

5.1 INTRODUCTION

The target compounds were principally generated in order to assess their ability to inhibit plasmodial growth by determining the IC_{50} values. The IC_{50} is the drug concentration required to cause the measured parameter to fall to 50% of its original value. The term is used throughout this chapter to express the biological activity of each compound. The lower the IC_{50} value of a compound, the better is its efficacy.

However, a good drug should exhibit good selectivity.[1] The more selective a drug for its target, the less chance that it will interact with different targets, which may lead to undesirable side effects. Thus, a compound displaying good efficacy (low IC_{50}) will not be a good drug if it has poor selectivity between host and the parasite. All experimental details relating to biological tests are given in the experimental section.

5.2 BIOLOGICAL RESULTS AND DISCUSSION

The synthesised gold compounds and corresponding precursors were evaluated *in vitro* against *P. falciparum* chloroquine-sensitive (D10 and 3D7) and chloroquine-resistant (W2 and K1) strains. In all assays, chloroquine (CQ) and artemisinin (ART) were used as control drugs. The cytotoxicity tests of some of the compounds were conducted in human nasopharynx carcinoma cell line (KB). This was carried out in this study to gain an insight on toxicity of gold complexes towards human cell line (i.e. normal cells). Podophyllotoxin (POD) was used as a control drug. Some of the compounds were also evaluated for their ability to inhibit the malarial cysteine protease FP-2.

The biological tests were carried out in collaboration with the following institutions: 1) Department of Medicine, San Francisco General Hospital, University of California in San Francisco (UCSF) - Professor P.J. Rosenthal, 2) Department of Medicine, Division of Pharmacology, University of Cape Town - Professor P.J. Smith and 3) London School of Hygiene and Tropical Medicine (LSHTM) – Drs V. Yardley and L. Vivias.

5.2.1 *In Vitro* Antiplasmodial Activity of Gold Precursors

Consistent with the objectives of this project, gold precursors (Table 5.1) were evaluated along with target compounds against D10, W2 and FP-2 to investigate the role of gold(I) and gold(III) starting materials as well as TSCs (**Chapter 3**) towards the overall activity of resulting gold complexes. The ability of gold precursors to inhibit the

growth of chloroquine sensitive (D10, 3D7) and chloroquine-resistant (W2, K1) strains as well as FP-2 inhibition were determined and results are shown in Table 5.1.

Table 5.1: *In vitro* antiplasmodial, cytotoxicity and FP-2 inhibitory activities of gold precursors

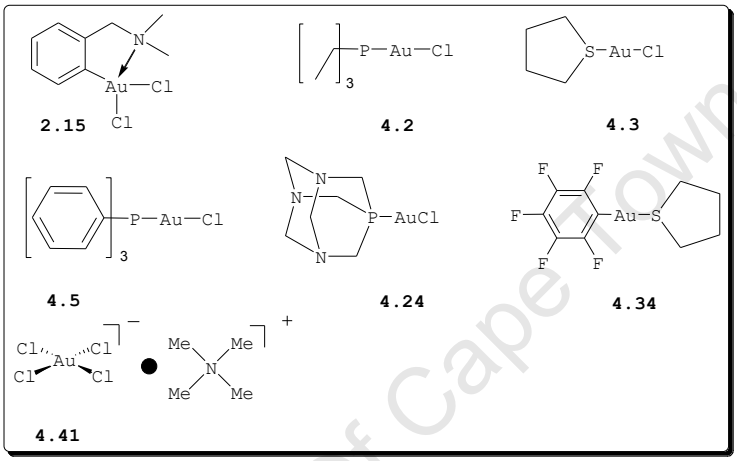

Comp.	IC_{50} / μM						^{a}SI
	3D7	D10	K1	W2	KB	FP-2	
2.15	15.7	10.5	5.94	1.88	36.2	>100	2.3
4.2	^{b}ND	ND	ND	8.04	ND	ND	ND
4.3	16.4	193.7	34.6	>20	66.3	>100	4.0
4.5	2.45	3.13	11.4	>20	2.51	25.0	1.0
4.24	22.2	26.9	4.62	>20	20.9	>100	0.9
4.34	11.3	31.0	12.4	>20	8.54	20.9	0.7
4.41	ND	>10	ND	>20	ND	>100	ND
CQ	0.019	0.029	1.03	0.097	ND	ND	ND
ART	0.003	ND	0.003	0.019	104.4	ND	34794
E64	ND	ND	ND	~2.00	ND	0.049	ND
POD	ND	ND	ND	ND	<0.007	ND	ND

^{a}Selectivity index calculated as [IC_{50}KB/IC_{50}3D7]; ^{b}ND = not determined

These complexes displayed moderate to poor activities against D10. The most active complex against D10 was **4.5** with an IC_{50} value of 3.13 μM. Whereas gold(III) **2.15** and **4.2** were the most active compounds against W2, with IC_{50} values of 1.88 and 8.04 μM, respectively. However, these complexes were less active than the control drugs (i.e. CQ and ART). The rest of complexes displayed no activities against W2 at highest concentration tested (IC_{50} > 20 μM).

Alternatively, the gold precursors were also evaluated against different strains (3D7, K1) of *P. falciparum* (Table 5.1). It is noteworthy that some of the literature reported gold compounds have been tested for their antiplasmodial activities using these strains.[2,3] All compounds showed antiplasmodial activities in the mid micromolar range. While most complexes showed better activity against 3D7 than K1, compounds **2.15** (IC_{50} = 5.94 and 15.7 μM) and **4.24** (IC_{50} = 4.62 and 22.2 μM) were generally active against K1 compared to 3D7.

Compounds **2.15**, **4.3** and **4.24** showed low cytotoxicity towards human KB cell line. Although compounds **2.15** and **4.3** showed some degree of selectivity (SI = 2.3 and 4.0), complexes **4.5** and **4.24** were not selective in favour of the parasite.

Since thiol-containing molecules have been hypothesised as molecular targets of gold compounds, gold(I) (e.g. **4.2**) and gold(III) (e.g. **2.15**) complexes have been evaluated for their ability to inhibit cysteine proteases such as cathepsin B.[4,5] Herein, we examined the efficacy of these

compounds (Table 5.1) against the malaria cysteine protease FP-2. Although some of these compounds have been evaluated for growth inhibition of *P. falciparum*,[3] no information is available on the inhibition of FP-2.

From Table 5.1, it can be seen that gold complexes showed weak inhibition of FP-2. IC_{50} values of **4.5** and **4.34** were 25.0 and 20.9 μM, respectively. Although compound **2.15** showed activity against W2 (IC_{50} = 1.88 μM), it was not effective against the inhibition of FP-2. This suggests that the observed antiplasmodial activity was independent of enzyme inhibition. It is possible that the *in vitro P. falciparum* growth inhibition may be due to direct interaction of the gold center with specific parasitic molecular targets such as thioredoxin reductase,[3,6] and/or other cysteine proteases.

5.2.2 *In Vitro* Antiplasmodial Activity of Gold(I) Compounds

The following sections discuss evaluation of various types of gold(I) TSC complexes for their ability to inhibit the growth of *P. falciparum*. These were tested on four different strains D10, 3D7, W2 and K1 as well as the inhibition of FP-2 activity. Cytotoxicities of compounds were determined against human KB cell line.

5.2.2.1 Gold(I) TSC Complexes 4.12-4.17 and 4.19

The *in vitro* antiplasmodial activity data of synthesised gold(I) TSC complexes **4.12–4.17** (also see Table 4.1, p 115) is shown in Fig. 5.1. The results revealed that gold(I) complexes were generally more effective (with the exception

to **4.19** which showed no activity at highest concentration tested) compared to the corresponding free ligands (see **Chapter 3**) against D10 and W2 strains. In this series the tested compounds **4.12–4.17** displayed antiplasmodial activity in the range 1.28–6.92 μM. Whereas the gold(I) complex **4.19** (not shown in Fig. 5.1) showed poor activity against both D10 (IC_{50} > 10 μM) and W2 (IC_{50} > 20 μM) strains. These compounds were less effective compared to CQ, which displayed antiplasmodial activity against D10 and W2 with IC_{50} values of 0.0174 μM and 0.065 μM, respectively.

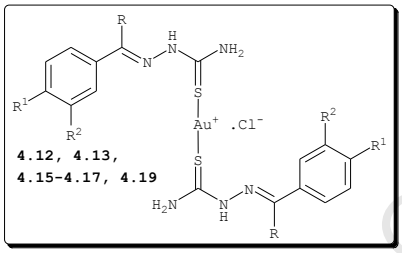

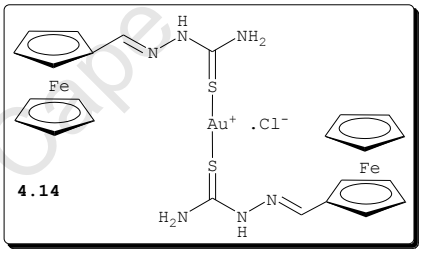

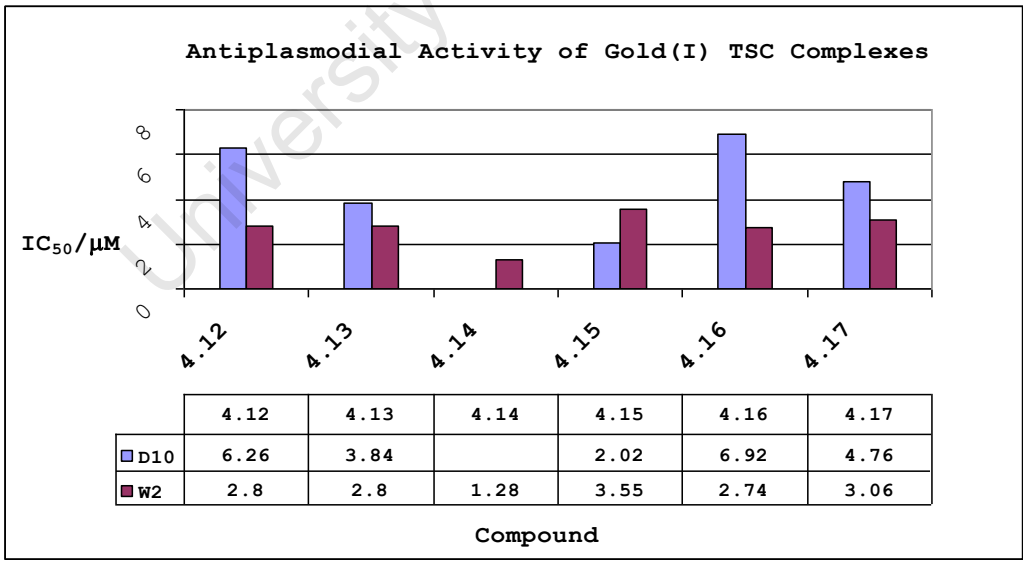

	4.12	4.13	4.14	4.15	4.16	4.17
D10	6.26	3.84		2.02	6.92	4.76
W2	2.8	2.8	1.28	3.55	2.74	3.06

Figure 5.1*: In vitro* screen of gold(I) TSC complexes against *P. falciparum* parasite strains

On the other hand, these compounds were also assessed against *P. falciparum* 3D7 and K1 strains. The *in vitro* data (Table 5.2) showed that the complexes have low to moderate activity against the malaria parasite strains 3D7 and K1. The IC_{50} values for growth inhibition of *P. falciparum* were in the low to mid micromolar (5.02-24.2 μM) range. Some of the reported gold(I) complexes in the literature exhibited their antiplasmodial activities on the same strains within this range.[7] Nevertheless, complexes **4.12**, **4.14-4.18** and **4.20-4.23** were 1-8 fold more active compared to their parent ligands in the 3D7 and K1 strains.

By comparing complexes bearing similar substitution patterns (e.g. **4.16** against **4.21**), pyrazoline-based gold(I) complexes **4.20-4.23** were approximately 3-fold better than their non-cyclic analogues (**4.12** and **4.14-4.18**) when tested against 3D7 and K1 strains (Table 5.2). Although gold precursors (Table 5.1) displayed comparable activities as **4.12-4.23**, their coordination to TSCs and pyrazoline analogues seemed to be beneficial to the antiplasmodial activities of these ligands. In the absence of complexes **4.16** and **4.17**, these compounds showed lower cytotoxicity against human KB cell line. In addition, these compounds showed poor to moderate selectivity towards parasite.

Table 5.2: Antiplasmodial activities and cytotoxicity of gold(I) TSC complexes

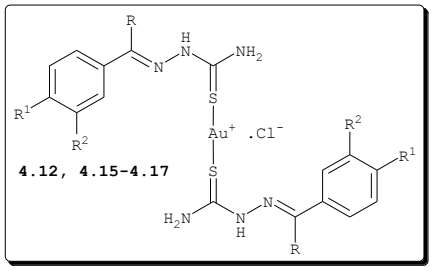

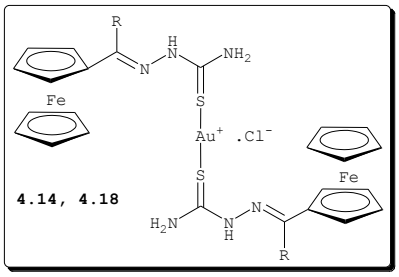

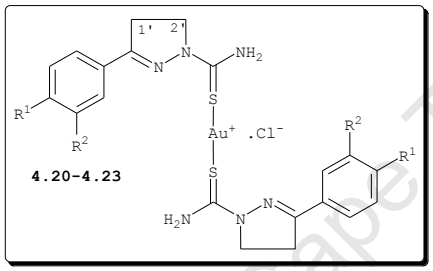

Compound	Substituent			IC_{50} / μM			SI
	R	R^1	R^2	3D7	K1	KB	
4.12	CH_3	H	Br	12.9	23.2	32.2	2.5
4.14	H	Ferrocene		8.48	14.3	22.0	2.6
4.15	CH_3	Br	H	7.42	7.68	28.9	3.9
4.16	CH_3	Cl	Cl	14.7	24.2	7.27	0.5
4.17	CH_3CH_2	Cl	Cl	19.2	12.2	7.23	0.4
4.18	CH_3	Ferrocene		10.4	16.0	18.3	1.8
4.20	-	H	Br	10.1	10.2	73.5	7.4
4.21	-	Cl	Cl	5.09	9.17	22.7	4.5
4.22	-	Br	H	9.22	10.6	82.3	8.9
4.23	-	Cl	H	9.83	18.1	19.1	1.9
CQ	-	-	-	0.019	1.03	ND	ND
ART	-	-	-	0.003	0.003	104.4	34794
POD	-	-	-	ND	ND	<0.007	ND

5.2.2.1.1 Assessment of Falcipain-2 Inhibition

In order to establish the likely targets of **4.12-4.17** against *P. falciparum*, the compounds were tested for their ability to inhibit the activity of the enzyme FP-2. The results are summarized below (Fig. 5.2).

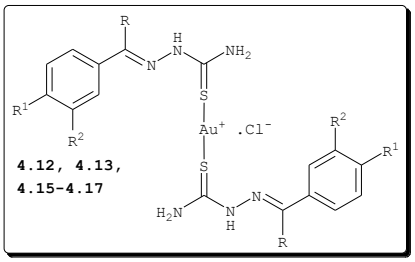

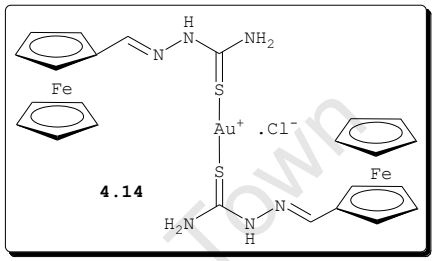

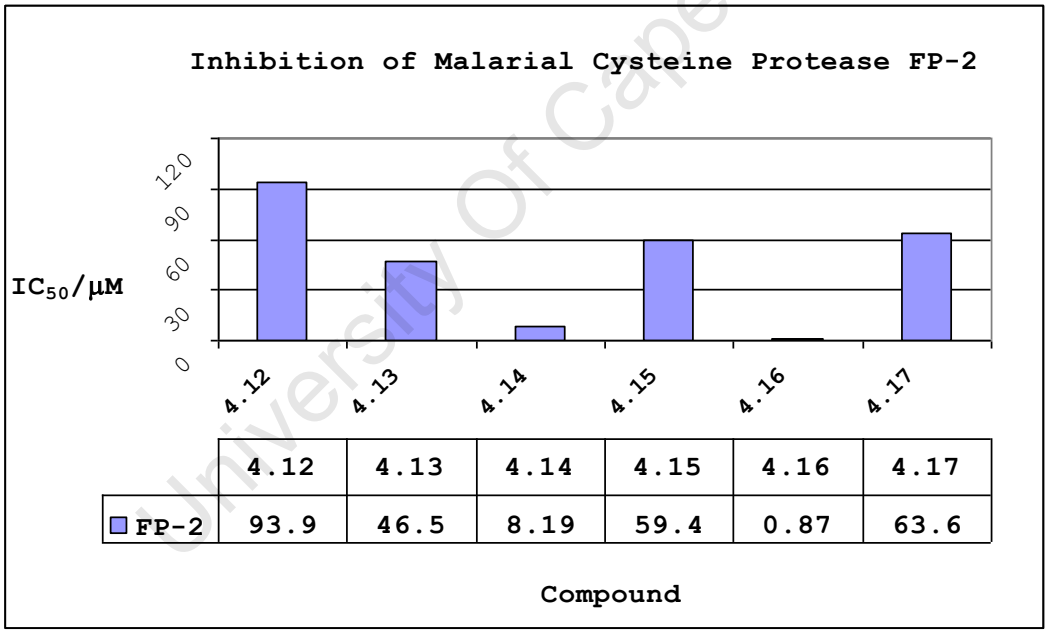

	4.12	4.13	4.14	4.15	4.16	4.17
FP-2	93.9	46.5	8.19	59.4	0.87	63.6

Figure 5.2*: In vitro* screening of gold(I) complexes against FP-2

As mentioned previously (**Chapter 3**, p 93), the free ligands, with the exception to ferrocenyl analogues **3.28f** and **3.28g** (see section **3.6.1**, p 93), displayed no inhibitory effects against FP-2 at maximum concentration (IC_{50} > 100 µM) tested. Interestingly, gold(I) complexes

showed enhanced potency against FP-2. The most effective compound was **4.16** with an IC_{50} value of 0.87 μM. The structural modification of these complexes, e.g. replacing the methyl groups in **4.12** and **4.16** with the ethyl as in **4.13** and **4.17**, lowered their efficacy against FP-2. However, substitution of Cl for Br atom, as in complexes **4.12**, **4.13** and **4.15**, was tolerated by the enzyme.

The enhanced activity of TSCs on complexation could be the ability of the gold(I) center to hold TSCs in a geometry that allows favourable interaction of TSCs with the target.[8] On the other hand, due to the ability of gold(I) to undergo facile ligand exchange and its affinity for S ligands,[9] it could be possible that the inhibition of FP-2 involves direct interaction with the sulfhydryl groups in the active site. *Urig et al*.[10] demonstrated direct interaction of gold(I) with sulfhydryl groups in the active site of human glutathione reductase (hGR) following a stepwise ligand displacement by these groups. These enzymes and other antioxidant enzymes have been shown to be potential targets for antimalarial chemotherapy.[11] Overall, there was no correlation found between the antiplasmodial activity and FP-2 inhibition. This suggests that FP-2 is not the primary target for these compounds.

5.2.2.2 Triphenylphosphine Gold(I) TSC Complexes 4.26a-f

The *in vitro* antiplasmodial activity data of this series is shown in Table 5.3. The compounds displayed moderate antiplasmodial activities against both strains, with IC_{50} values in the range 2.15-7.89 μM. The least active compound was complex **4.26c** with the IC_{50} value of 7.89 μM. As with

compounds **4.12-4.17,** these complexes also displayed enhanced activity compared to their free ligands. It is worth noting that although the gold(I) starting material **4.5** (Table 5.1) displayed poor activity (IC_{50} > 20 µM) against the W2 resistant strain, replacing the chloro ligand in [Au(PPh_3)]Cl with TSCs led to compounds with improved *in vitro* activity against *P. falciparum*.[12]

Table 5.3: *In vitro* antiplasmodial, cytotoxicity and FP-2 activities of complexes **4.26a-f**

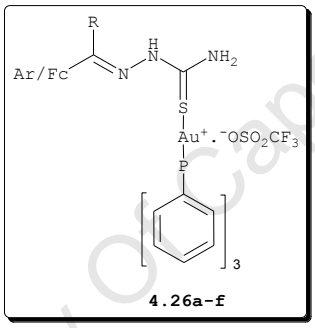

4.26a-f

Compound	IC_{50} / µM						SI
	3D7	D10	K1	W2	KB	FP-2	
4.26a	3.26	2.37	7.89	2.15	1.91	11.6	0.6
4.26b	2.74	5.0	2.87	5.89	7.73	21.1	2.8
4.26c	ND	2.77	ND	7.89	ND	15.5	ND
4.26d	1.44	3.12	2.01	6.38	5.49	14.3	3.8
4.26f	ND	3.44	ND	3.63	ND	10.7	ND
CQ	0.019	0.029	1.03	0.097	ND	ND	ND
ART	0.003	ND	0.003	0.019	104.4	ND	34794
E64	ND	ND	ND	~2.00	ND	0.049	ND
POD	ND	ND	ND	ND	<0.007	ND	ND

The compounds were also tested for the inhibition of FP-2 to gain insight into their possible antiplasmodial mode of actions. From the data (Table 5.3), it can be seen that complexes **4.26a-f** exhibited significant activity against the enzyme compared to the parent ligands (see Table 3.6 in **3.6.1**, p 94). The gold(I) precursor **4.5** (Table 5.1) and complex **4.26a** displayed similar activity against FP-2, while the rest of compounds were more active than **4.5**.

Apart from the presumed enhanced lipophilicity of resulting complexes, the improved activities of these compounds against FP-2 could be due to the presence of Ph_3PAu, which has been suggested to bring complexes in close proximity to the active site.[7] In this series, there was also no correlation found between the antiplasmodial activity and the inhibition of the enzyme. This suggests that the observed antiplasmodial activities may be due to the inhibition of other cysteine proteases or thioredoxin reductase.[12] This is assuming compounds reach the site of action. Alternatively, the compounds may not possess the physicochemical properties to cross the various membranes to reach the presumed target in the acidic food vacuole (FV) of the parasite.

On the other hand, complexes **4.26a-b** and **4.26d** displayed moderate antiplasmodial activities against both 3D7 and K1 (Table 5.3). The IC_{50} values were in the range 1.44-7.89 μM. The three compounds displayed cytotoxic activity towards human KB cell line used as well as poor selectivity.

5.2.2.3 PTA Gold(I) TSC Complexes 4.29a-h and 4.30a-c

Replacing the PPh_3 with PTA led to a new series of gold(I) compounds **4.29a-h**, which was also evaluated against W2 and the inhibition of FP-2 (Table 5.4). Although most compounds displayed no activity against W2 at highest concentration tested, IC_{50} > 20 µM, half of these complexes retained the antiplasmodial activity below 10 µM. Comparing the two series (i.e. **4.26** and **4.29**), no marked difference in activity against the W2 strain was evident. This data suggests that replacing the PPh_3 moiety with PTA was not beneficial against this particular strain of the drug resistant parasites.

Similarly, the compounds were tested for their ability to inhibit the activity of FP-2. From the three selected compounds **4.29b** and **4.29d-e**, which exhibited moderate activity against W2 (IC_{50} = 3.98-7.85 µM), the most active compounds against FP-2 were **4.29d** and **4.29e** with the latter being the most potent compound against the enzyme with an IC_{50} value of 0.94 µM. Comparing the data of **4.29b** with that of **4.29d** and **4.29e**, it can be seen that a single mode of action is unlikely to exist for these complexes.

The PTA-derived complexes **4.29a-h** and **4.30a-c** were evaluated *in vitro* against 3D7 and K1 strains (Table 5.4). These complexes displayed *in vitro* antiplasmodial activity against 3D7 (IC_{50} = 4.40-18.4 µM) and K1 (IC_{50} = 5.59-32.7 µM). However, these compounds were slightly less active compared to Ph_3P-derived complexes **4.26a-b** and **4.26d** (Table 5.3). Furthermore, the compounds showed lower cytotoxicity

against the human KB cell line compared to compounds **4.26a-b** and **4.26d.**

Table 5.4: Antiplasmodial and FP-2 activities of complexes **4.29a-h**

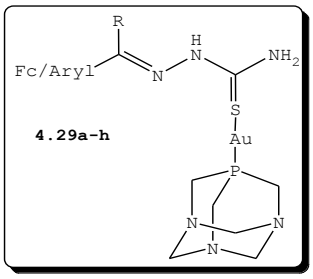

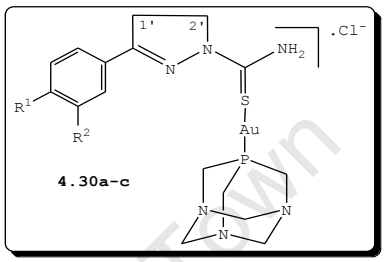

Compound	IC_{50} / μM					SI
	3D7	W2	K1	KB	FP-2	
4.29a	9.09	>20	13.1	21.5	ND	2.4
4.29b	10.3	3.98	8.97	21.8	>100	2.1
4.29c	ND	>20	ND	ND	ND	ND
4.29d	4.40	6.69	16.5	23.6	27.9	5.4
4.29e	20.9	7.85	10.8	25.1	0.94	1.2
4.29f	17.1	>20	32.7	36.0	ND	2.1
4.29g	9.53	>20	13.7	33.9	ND	3.6
4.29h	13.8	>20	9.11	32.1	ND	2.3
4.30a	4.51	ND	5.59	29.1	ND	6.5
4.30b	18.4	ND	17.3	40.1	ND	2.2
4.30c	5.30	ND	16.4	33.2	ND	6.3
CQ	0.019	0.097	1.03	ND	ND	ND
ART	0.003	0.019	0.003	104.4	ND	34794
E64	ND	~2.00	ND	ND	0.049	ND
POD	ND	ND	ND	<0.007	ND	ND

5.2.2.4 Triethylphosphine Gold(I) TSC Complexes 4.31a-c, 4.31e-f and 4.32-4.33

The rationale behind the synthesis of these complexes has been provided in **Chapter 4** (see section **4.4.4,** p 134) and will not be repeated in this chapter. This series was evaluated for antiplasmodial activity against the W2 strain and data is shown in Fig. 5.3. The compounds displayed moderate antiplasmodial activities against W2 strain, with activity averaging below 8 μM.

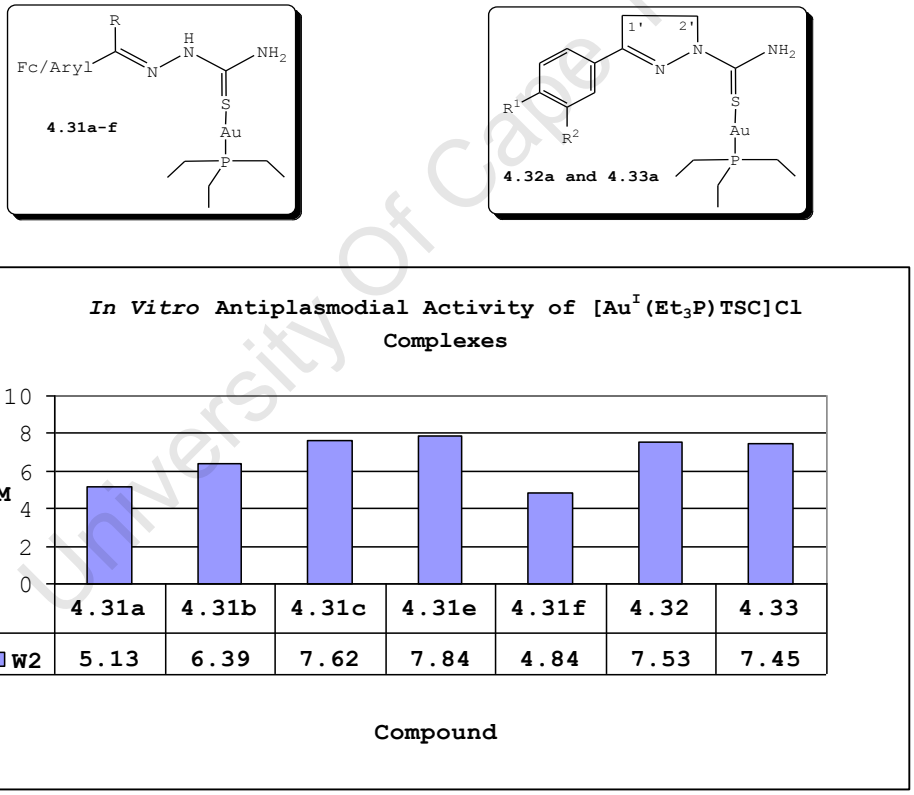

Figure 5.3*: In vitro* antiplasmodial data of gold(I) complexes

Comparing this series (Fig. 5.3) with other phosphine-based complexes $[Au^{I}(Ph_3P)TSC]O_3SCF_3$ (**4.26a-d** and **4.26f**) and $[Au^{I}(PTA)TSC]Cl$ (**4.29a-h**), it can be seen that complexes

4.31a-c, 4.31e-f, 4.32 and **4.33** had similar activity (Table 5.5) against the W2 strain of the malaria parasite. The results suggest that introduction of different phosphine containing moieties had no effect on the antiplasmodial activity.

Table 5.5: *In vitro* antiplasmodial activities range of phosphine based gold(I) TSC complexes against W2

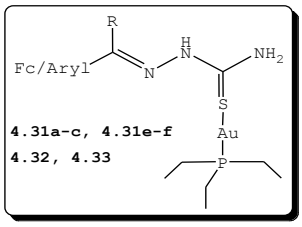

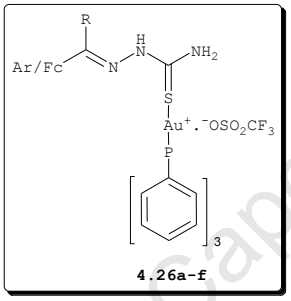

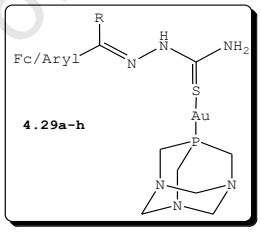

IC_{50} / µM		
$[Au^{I}(Et_3P)TSC]Cl$	**$[Au^{I}(Ph_3P)TSC]O_3SCF_3$**	**$[Au^{I}(PTA)TSC]Cl$**
2.15-7.89	3.98-7.85	4.84-7.84

5.2.2.5 Pentafluorobenzene Gold(I) TSC Complexes 4.38a-f

All six pentaflourobenzyl gold(I) TSC complexes displayed enhanced *in vitro* antiplasmodial activities against D10 and W2 strains (Table 5.6). Excluding data on W2 for **4.38a,** compounds **4.38b-d** were modestly active against W2. The least active compounds were **4.38e** and **4.38f** with IC_{50} values of 10.3 and 16.1 µM, respectively.

Table 5.6: Antiplasmodial and FP-2 activities of complexes **4.26a-d** and **4.26f**

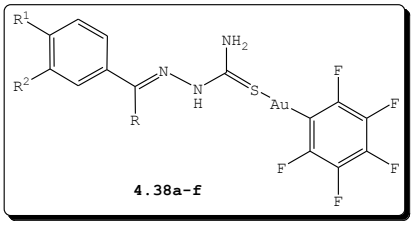

4.38a-f

Compound	IC_{50} / µM						SI
	D10	W2	3D7	K1	KB	FP-2	
4.38a	2.81	>20	5.15	9.37	5.18	ND	1.0
4.38b	4.09	4.93	2.23	4.46	9.19	4.54	4.1
4.38c	1.82	6.20	4.58	29.3	4.76	2.48	1.0
4.38d	5.11	7.66	4.69	14.8	10.8	5.94	2.3
4.38e	3.03	10.3	3.70	10.9	7.45	2.35	2.0
4.38f	3.92	16.1	ND	ND	ND	3.31	ND
CQ	0.029	0.097	0.019	1.03	ND	ND	ND
ART	ND	0.019	0.003	0.003	104.4	ND	34794
E64	ND	~2.00	ND	ND	ND	0.049	ND
POD	ND	ND	ND	ND	<0.007	ND	ND

These complexes showed significant enzyme inhibition (Table 5.6). In fact, the gold(I) TSC complexes derived from **4.34** displayed better enzyme inhibition, IC_{50} = 2.35-4.54, than those derived from **4.5** (IC_{50} = 25.0 µM, Table 5.3) and **4.24** (IC_{50} > 100 µM, Table 5.6), with the exception to complex **4.29e** whose activity against the enzyme was far superior (IC_{50} = 0.94 µM) to the rest of compounds.

On the other hand, compounds **4.38a-e** showed modest *in vitro* antiplasmodial activity against 3D7 (IC_{50} = 2.23-4.69 μM) and K1 (IC_{50} = 4.46-29.3 μM). The compounds generally showed low cytotoxicity against KB cell line.

5.2.3 *In Vitro* Antiplasmodial Activities of Gold(III) TSC Complexes

In view of the antitumour activities of square planar gold(III) TSC complexes of the type [Au(Hdamp-C^1)Cl(TSC)]X and starting complex **2.15** (Fig. 2.6, p 42) against the human MCF-7 breast cancer cell line,[13] analogous complexes reported in **Chapter 4** (p 113) were evaluated for *in vitro* growth inhibition of *P. falciparum* and their ability to inhibit FP-2. Table 5.7 shows the results obtained against D10 and W2 strains as well as FP-2. From the data (Table 5.7), it is apparent that complexes **4.42b** [IC_{50} (W2) = 3.04 μM] and **4.42g** [IC_{50} (D10) = 3.12 μM] were the most active compounds.

Complexes **4.42a**, **4.42d** and **4.42e** were moderately active, with IC_{50} values in the range 7.17-7.22 μM. The remaining compounds were inactive at the maximum concentration tested (IC_{50} > 20 μM). The only complex evaluated against the inhibition of the enzyme was **4.42g**, which showed no activity at highest concentration tested (IC_{50} > 100 μM).

Table 5.7: Antiplasmodial and FP-2 activities of gold(I) TSC complexes **4.26a-d** and **4.26f**

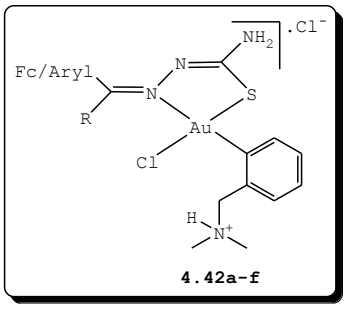

4.42a-f

Entry	Compound No.	IC_{50} / μM		
		D10	W2	FP-2
1	**4.42a**	ND	7.17	ND
2	**4.42b**	ND	3.04	ND
3	**4.42c**	10.5	>20	ND
4	**4.42d**	ND	7.22	ND
5	**4.42e**	ND	7.22	ND
6	**4.42f**	3.12	>20	ND
7	**4.42g**	>10	>20	>100
8	**CQ**	0.0293	0.049	ND
9	**ART**	ND	0.0082	ND
10	**E64**	ND	~2.00	0.0494

5.3 CONCLUSION

A series of gold TSC complexes have been demonstrated to exhibit antiplasmodial activity against the *P. falciparum* strains. From the data, it is evident that coordination of gold ions to TSC ligands has beneficial antiplasmodial

effect. Although there was no noticeable difference in potencies of gold precursors and gold TSC complexes, regardless of the gold ion and nature of the complex, the resulting complexes generally displayed enhanced efficacy against *P. falciparum* compared to parent ligands.

Whereas gold(I) TSC complexes inhibited FP-2, there could be no correlation found between their antiplasmodial activity and the ability to inhibit FP-2. The data suggest that these complexes exhibit their antiplasmodial activities against *P. falciparum* through the inhibition of more than one target. This implied that FP-2 is not the primary target for these compounds. On the other hand, it could be possible that the compounds do not possess suitable physicochemical properties to cross various membranes to reach the presumed target (FP-2) in the acidic FV. Most of these complexes showed low cytotoxicity towards human KB cell line as well as poor to moderate selectivity.

5.4 REFERENCES

1. G.L. Patrick, *An Introduction to Medicinal Chemistry*, 3rd Ed., Oxford University Press, New York, **2005**, p 165.
2. A.R. Sannella, A. Casini, C. Gabbiani, L. Messori, A.R. Bilia, F.F. Vincieri, G. Majori, C. Severini, *FEBS Lett.*, **2008**, *582*, 844-847.
3. C. Gabbian, L. Messori, M.A. Cinellu, A. Casini, P. Mura, A.R. Sannella, C. Severini, G. Majori, A.R. Bilia, F.F. Vincieri, *J. Inorg. Chem.*, **2009**, *103*, 310-312.
4. S.S. Gunatilleke, C.A.F. de Oliveira, J.A. McCammon, A.M. Barrios, *J. Biol. Inorg. Chem.*, **2008**, *13*, 555-561.
5. S.P. Fricker, R.M. Mosi, B.R. Cameron, I. Baird, Y. Zhou, V. Anastassov, J. Cox, P.S. Doyle, E. Hansell, G. Lau, J. Langille, M. Olsen, L. Qin, R. Skerlj, R.S.Y. Wong, Z. Santucci, J.H. McKerrow, *J. Inorg. Biochem.*, **2008**, *102*, 1839-1845.
6. I. Otto, *Coord. Chem. Rev.*, **2009**, *253*, 1670-1681.
7. E. Schuh, S.M. Valiahdi, M.A. Jakupec, B.K. Keppler, P. Chiba, F. Mohr, *Dalton Trans.*, **2009**, 10841-10845.
8. E. Meggers, *Chem. Commun.*, **2009**, 1001-1010.
9. C.F. Shaw III, *Chem. Rev.*, **1999**, *99*, 2589-2600.
10. S. Urig, K. Fritz-Wolf, R. Réau, C. Herold-Mende, K. Tóth, E. Davioud-Charvet, K. Becker, *Angew. Chem. Int. Ed.*, **2006**, *45*, 1881-1886.
11. K. Becker, L. Tilley, J.L. Vennerstrom, D. Roberts, S. Rogerson, H. Ginsburg, *Int. J. Parasitol.*, **2004**, *34*, 163-189.

12. I. Ott, X. Qian, Y. Xu, D.H.W. Vlecken, I.J. Marques, D. Kubutat, J. Will, W.S. Sheldrick, P. Jesse, A. Prokop, C.P. Bagowski, *J. Med. Chem.*, **2009**, *52*, 763-770.
13. T.S. Lobana, R. Sharma, G. Bawa, S. Khana, *Coord. Chem. Rev.*, **2009**, *253*, 977-1055 and the references therein.

CHAPTER 6

SYNTHESIS OF NOVEL POLYAMINE-THIOSEMICARBAZONE DENDRIMERS AND THEIR ANTIPLASMODIAL EVALUATION

ABSTRACT: High proliferating and differentiating cells have been shown to exhibit elevated polyamine (PA) levels and an active polyamine transport system (PAT) to import exogenous polyamines (PAs). This and the tolerance of the PAT for non-native PAs have led to the design of PA conjugates, which mimic native PAs and enter cells through the PAT. This chapter describes an exploratory series of novel PA-TSC dendrimers **6.24a-f** and **6.25a-e**. These were obtained from commercially available dendritic PAs **6.16** and **6.17** as well as thioesters **6.23a-g**. All of the synthesised dendrimers were evaluated for *in vitro* antiplasmodial activity against chloroquine-resistant (W2) strain.

6.1 INTRODUCTION

The majority of non-α-*N*-heterocyclic TSC derivatives have been found to exhibit low activity when evaluated *in vitro* against *P. falciparum* strains.[1] This was also noted for the series **3.24a-g** (see section **3.6.1**, p 93) when profiled for *in vitro* antiplasmodial activity against D10 and W2 strains. On the other hand, α-*N*-heterocyclic TSCs have been shown to display potent antimalarial activities.[2] In the current work, the important question and/or hypothesis we intended to probe is whether non-α-*N*-heterocyclic TSCs are inherently inactive against cultured parasites or if their

ineffectiveness can be attributed to insufficient cellular accumulation.

Since natural PAs and unnatural analogues are recognised by PAT,[3] it was hypothesized that conjugation of PAs with TSCs might lead to enhanced antiplasmodial activity of series **3.24a-g** presumably due to selective uptake by parasitic red-blood cells (RBCs). Anchoring of chemotherapeutic drugs to PAs has been shown to result in enhanced potency and selectivity against tumour cells.[4] However, this approach is yet to deliver promising clinical candidates for cancer treatment.[5]

6.1.1 Polyamines

PAs such as putrescine (**6.1**), cadavarine (**6.2**) spermidine (**6.3**) and spermine (**6.4**) are widely distributed in nature, ranging from the plants to animals (Fig. 6.1).[6] These are involved in diverse processes, including cell proliferation and differentiation, regulation of gene expression, translation, modulation of cell signalling and membrane stabilisation.[6a,7,8]

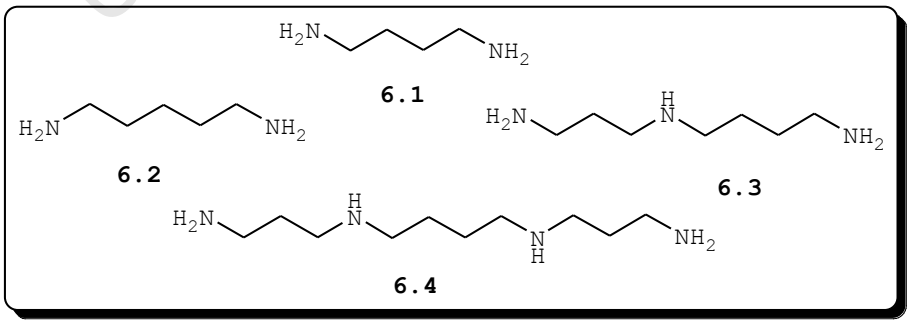

Figure 6.1: Biogenic polyamines.

These aliphatic bases occur both in free polycationic form and in conjugation with other biomolecules such as sugars,[9] steroids,[10] alkaloids,[11] phospholipids[12] and peptides.[13] In recent years, a vast array of synthetic PAs and conjugated analogues has been synthesised in an effort to find PA-based compounds with potential pharmaceutical application.[14] Hence, a significant number of symmetrical and asymmetrical linear alkyl PAs as well as chemotherapeutic drug-PA conjugates have been evaluated for antitumour activity.[15]

More importantly, high proliferating and differentiating cells (e.g. tumour and parasitic) have been found to exhibit elevated PA levels and an activated PAT system for growth factors and importing of exogenous PAs.[16] This prompted the design of PA-drug conjugates to selectively target tumour cells.[4a,17] Several antitumour experiments showed that PAT tolerates large modification of PA structures.[18] Consequently, a wide range of PA analogues has been demonstrated to target PAT to enter tumour cells.

6.2 BIOSYNTHESIS OF POLYAMINES

The biosynthetic pathways (Scheme 6.1) for the PAs are conserved from bacteria to animals including plants.[6a] These involve the conversion of L-arginine (**6.5**) to L-ornithine (**6.6**) by enzyme arginase.[6a,18] The decarboxylation of **6.6** catalysed by ornithine decarboxylase (ODC) leads to the synthesis of the diamine **6.1**. This is then converted to spermidine (**6.3**) by spermidine synthase (SpdS) and further to spermine (**6.4**) by spermine synthase (SpmS). The aminopropyl moieties in **6.3** and **6.4** are transferred from decarboxylated S-adenosyl methioine (dcSAM), which is

derived from L-methione in two sequential reactions of methionine adenosyltransferase and S-adenosyl methionine decarboxylase.

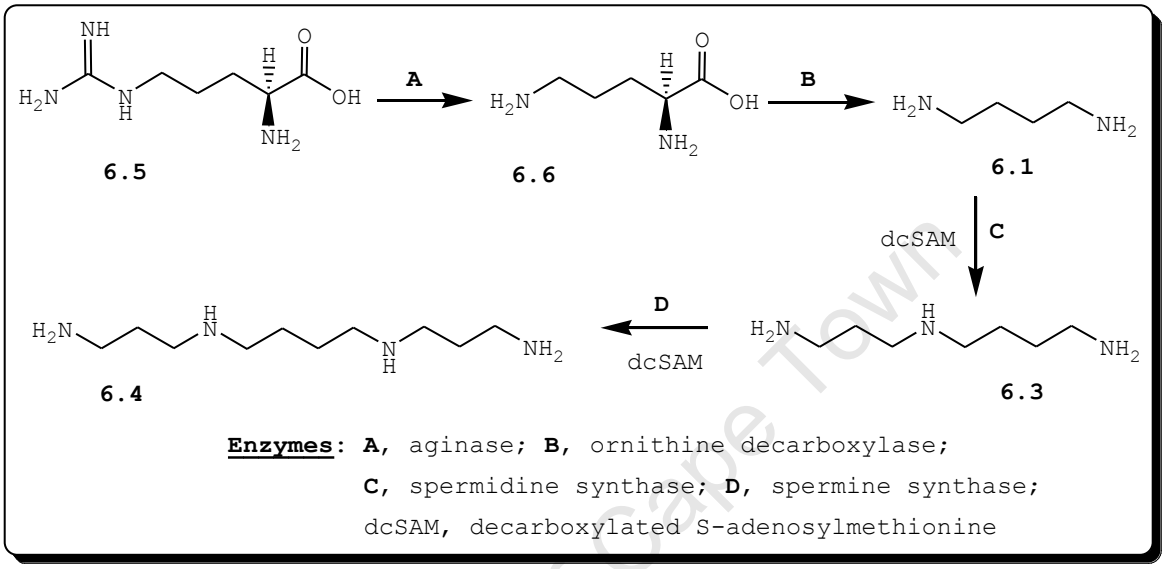

Scheme 6.1: Biosynthetic pathway of PAs.

The biosynthetic pathway of PAs has been an important target for therapeutic intervention during the last decades.[19] However, compensatory upregulation mechanisms in biosynthesis and induction of PAs uptake during the blockade of biosynthetic enzymes have shifted the focus to compounds that produce cellular effects.[8,20]

6.3 BIOLOGICAL SIGNIFICANCE OF SYNTHETIC PA CONJUGATES

PA conjugates possessing biological properties have been isolated from natural resources (e.g. spiders, wasps, plants and marine organisms).[14] On the other hand, synthetic analogues have been found to exhibit a multitude of biological functions, and show promise as antiparasitic,[8] antimalarials,[7] antidiarrhoeals,[21] anti-HIV agents,[22] metal

chelators[14] and gene delivery agents.[14] More importantly, the synthetic PA conjugates are designed to exhibit improved biological activity (in particular against cellular targets) compared to the parent molecules.[14] To illustrate the importance of PA conjugates, a few examples of synthetic PA conjugates are discussed below.

6.3.1 Conjugates with Nucleosides

Polyamines conjugated to nucleosides have been synthesised and evaluated as inhibitors of PA biosynthesis. For example, adenosyl-SPD conjugate **6.7** (Fig. 6.2) was found to be a potent inhibitor of the anabolic enzyme SPD aminopropyl transferase, an enzyme that catalyses the reaction leading to the formation of **6.4**.

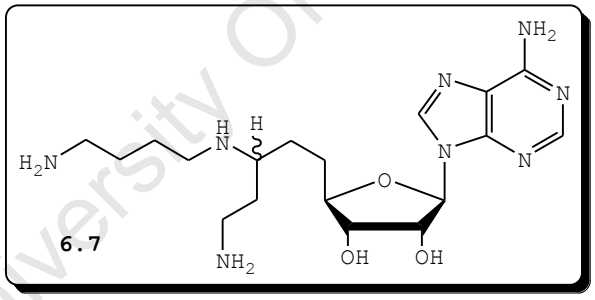

Figure 6.2: Example of PA conjugate with a nucleoside.

6.3.2 Conjugates with Cytotoxic Agents

In this group PAs are conjugated to known cytotoxic agents. A typical example includes the conjugation of branched PA with chlorambucil, a well-known cross-linker of DNA helices, to form conjugate **6.8** (Fig. 6.3).[23] This conjugate showed enhanced activity compared to chlorambucil in forming interstrand cross-links with DNA.[24] On the other hand, the naturally occurring anticancer agent paclitaxel

and its derivatives are well-known drugs for treatment of solid tumours,[25] but their selectivity remains a great challenge. *Battaglia et al.*[26] reported the synthesis of PA-paclitaxel conjugate **6.9** with the primary objective of improving the selectivity of paclitaxel towards tumour cells.

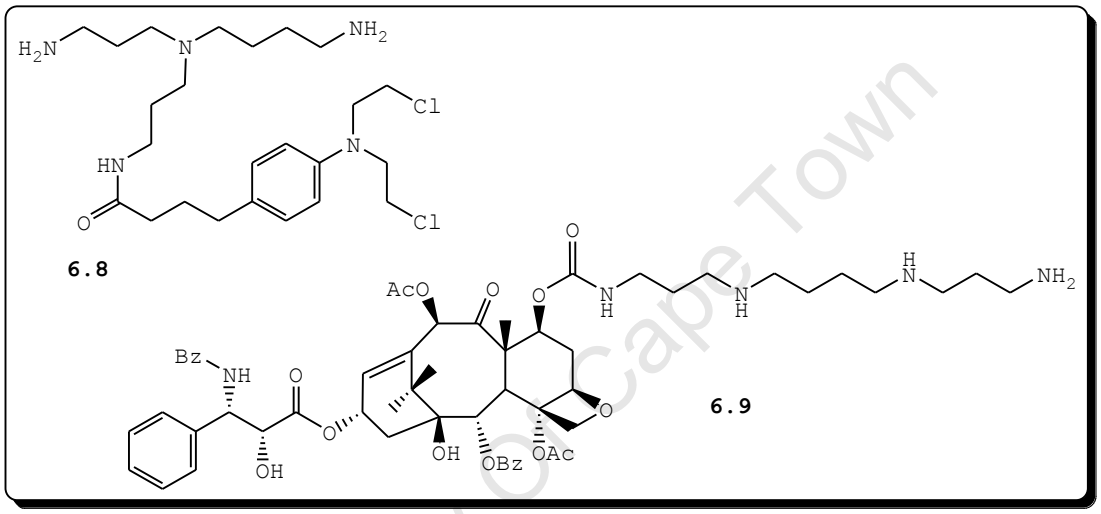

Figure 6.3: PA conjugates with cytotoxic agents.

6.3.3 Conjugates with Amino Acids

Invertebrate venom toxins (e.g. **6.10** in Fig. 6.4) are spider and wasp PA conjugates.

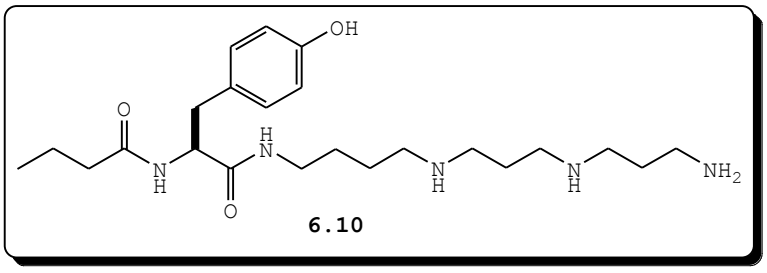

Figure 6.4: Example of PA conjugate with amino acids.

These act as potent antagonists of the mammalian neuroexcitatory glutamic acid receptors. Analogous conjugates have been synthesised to explore their biological activities. From the delineated SARs, it was found that longer PA chains often lead to increased affinity for these receptors.[14]

6.3.4 Conjugates with Steroidal and Fatty Acids

In this category conjugates of PAs with cholesterol and bile acids have been synthesised to introduce polynucleic acids into cells.[14] These are best represented by PA conjugate **6.11** (Fig. 6.5).

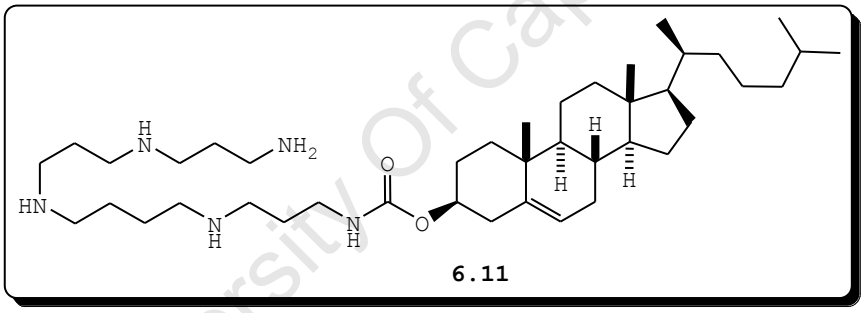

6.11

Figure 6.5: Example of PA conjugate with steroid.

6.4 DENDRITIC POLYAMINES

PAs (in particular branched PAs, see **6.6**) are used in the synthesis of dendrimers, e.g. polypropylene imine (PPI) **6.12** in Fig. 6.6.[27] Dendrimers are highly branched macromolecules with 'arms' emanating from the central core.[28] This class of compounds are unique from traditional linear polymers due to several attractive properties: 1) regular and highly branched, 2) narrow polydispersity, 3) multivalency, 4) nano-sized scale, 5) globular architecture and well-defined molecular weights.[29] Dendrimer molecules

constitute three features; namely multifunctional core, inner generations, which consist of repeating branched units and exterior surface groups where the outermost generations or functionalities are attached.

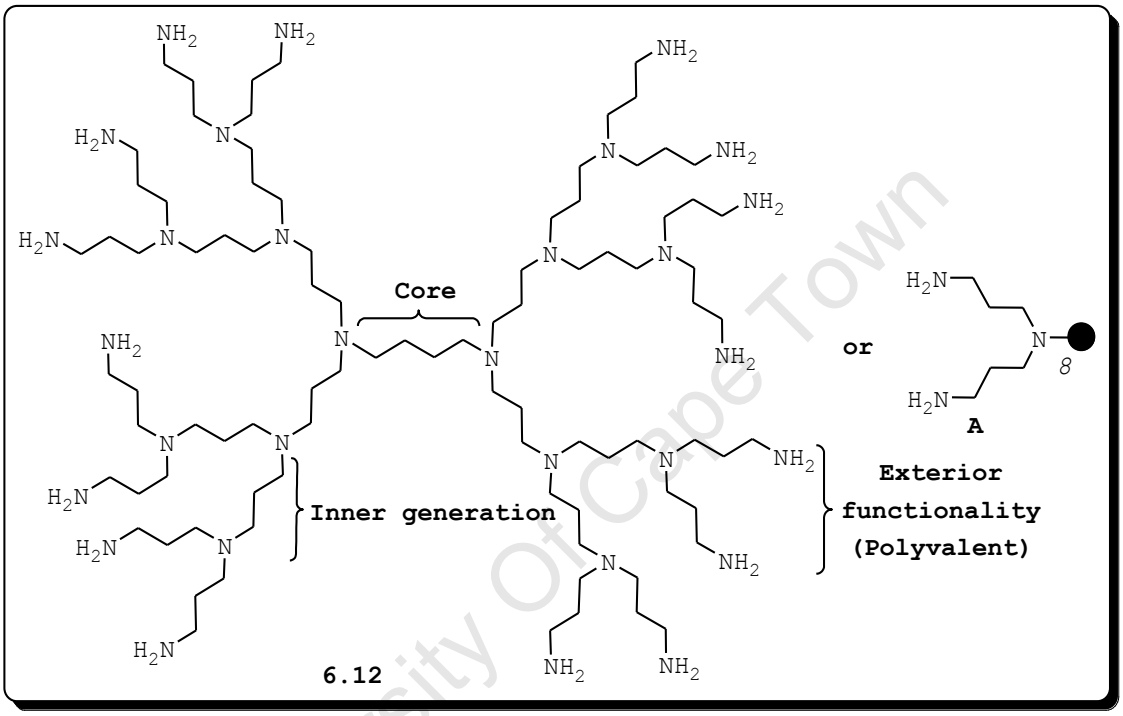

Figure 6.6: Polyamine dendrimer. The complete dendrimer **6.12** is also represented by the structure **A.** Inner shells are depicted as a black 'ball' and the number of functional groups on the surface are depicted by an italic number beneath the ball.

The synthetic strategies for accessing these compounds are either convergent or divergent.[30] In the convergent strategies, the synthesis starts from the exterior with the molecular structure that ultimately becomes the outer-most arm of the final dendrimer. Whilst in the divergent strategy the molecule is constructed radially outwards starting from the core by repeated addition of building units in a step-wise manner.

6.4.1 Dendrimer and Multivalency

The most exploited property of dendrimers is multivalency.[31] Multivalency can be described as the interaction of a dendritic array of ligands and/or drug molecules with a cell or target bearing multiple receptors.[32] Multivalent interaction is widely found in nature.[33] Multivalency has been shown to lead to strongly increased activity compared to the monomeric interaction.

Dendrimer multivalency is believed to enhance the affinity of substrates to complementary receptors mainly by co-operative effect.[34] This is referred to as a cluster or dendritic effects.[33] One of the implications of multivalency is that by attaching multiple drugs on the periphery (i.e. exterior surface groups) of the dendritic structure this may in part address problems relating to drug dosing (e.g. frequent dosing and higher dosages), and ultimately patient compliance.

6.5 ANTIMALARIAL ACTIVITY OF SYNTHETIC POLYAMINES AND CONJUGATES

As in mammalian cells, infection with *Plasmodial* species has been shown to exhibit both increased PA content and an activated PAT system.[8] The transport system has been suggested to meet the demand of PAs by the parasite.[7] In the late 1990s, *Singh et al.*[35] demonstrated that *P. knowlesi* infected erythrocytes acquire PAs through the putruscine transport (PuT) system. It has also been found that higher demand for PAs in intraerythrocytic malarial parasites is accompanied by a compensatory mechanism that induces PuT

synthesis. This suggested that in addition to biosynthesis of PAs, parasitic erythrocytes obtained PAs externally for growth and multiplication of the parasite.[7,36] Greater understanding of PAT in tumour cells has led to the design of PA analogues and conjugates that selectively target tumour cells through PAT.[3-6]

Singh et al.[35] reported the design of putrescine conjugate (**6.13**, Fig. 6.7), which inhibited the influx of putrescine *via* the PuT (K_i = 43.2 μM) in *P. knowlesi* infected erythrocytes. The conjugate displayed improved inhibitory effect *in vitro* against the growth of *P. knowlesi* (IC_{50} = 7.64 ± 0.97 ng/ml) compared to the chloroquine (IC_{50} = 10.8 ± 0.45 ng/ml). Intraperitoneal administration of **6.13** (24 mg/kg body weight twice a day for four days) cured the Swiss mice infected with multidrug resistant infection of *P. yoelli*.[35]

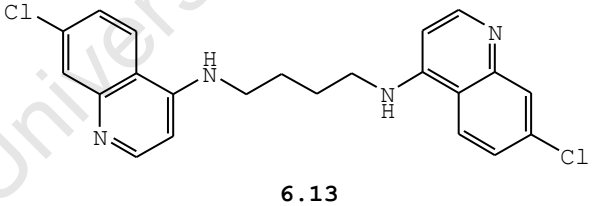

6.13

***N*^{1},*N*^{4}-bis(chloroquine-4-yl)butane-1,4-diamine (BCBD)**

Figure 6.7: Dendritic polyamine structures.

However, an increasingly successful approach to interfere with PA biosynthesis in the context of malaria chemotherapy is the use PA analogues to manipulate and/or disrupt intracellular concentration of natural PAs.[16,37] Increasing the displacement of natural PAs from their binding sites

with toxic synthetic PA analogues has been suggested to lead to the shortage of PAs for cell growth, hence parasite death. In addition to a decrease in PA synthesis, PA analogues lead to an increase in PA catabolism and export.[16] This approach has been considered an effective strategy for the development of chemotherapeutic molecules.

A series of bis(benzyl)polyamine analogues such as **6.14** (Fig. 6.8) with marked antimalarial activity against both CQ-sensitive and CQ-resistant *P. falciparum in vitro* has been reported.[7,38,39] Bis(benzyl)diamine (**6.15**) displayed ten-fold enhanced effect on the growth of cultured *P. falciparum*.[7]

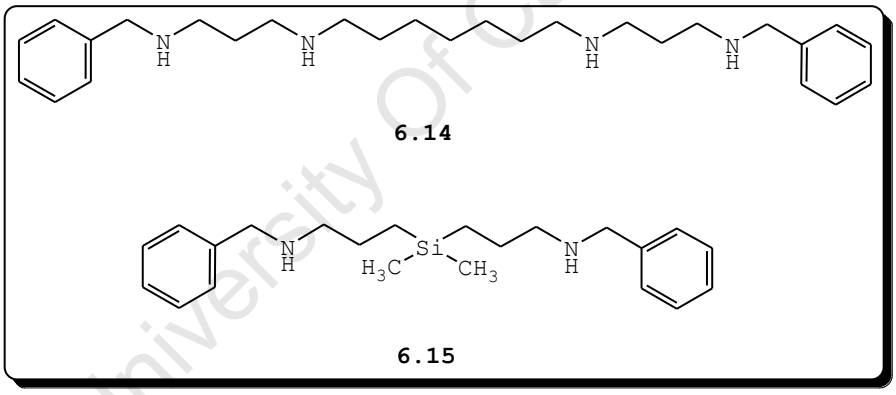

Figure 6.8: Chemical structure of PA analogues.

6.6 RATIONALE: POLYAMINE-TSC CONJUGATES

The rationale for the design of PA-TSC dendrimers is based on combining the properties of PAs (cell recognition) and dendrimers (multivalency), Fig. 6.9. Branched PAs **6.16** and **6.17** (Fig. 6.9) display natural PA backbones namely spermine and cadavarine. The latter the $-CH_2-$ is being replaced by –NR-, where R is an ethyl substituent.

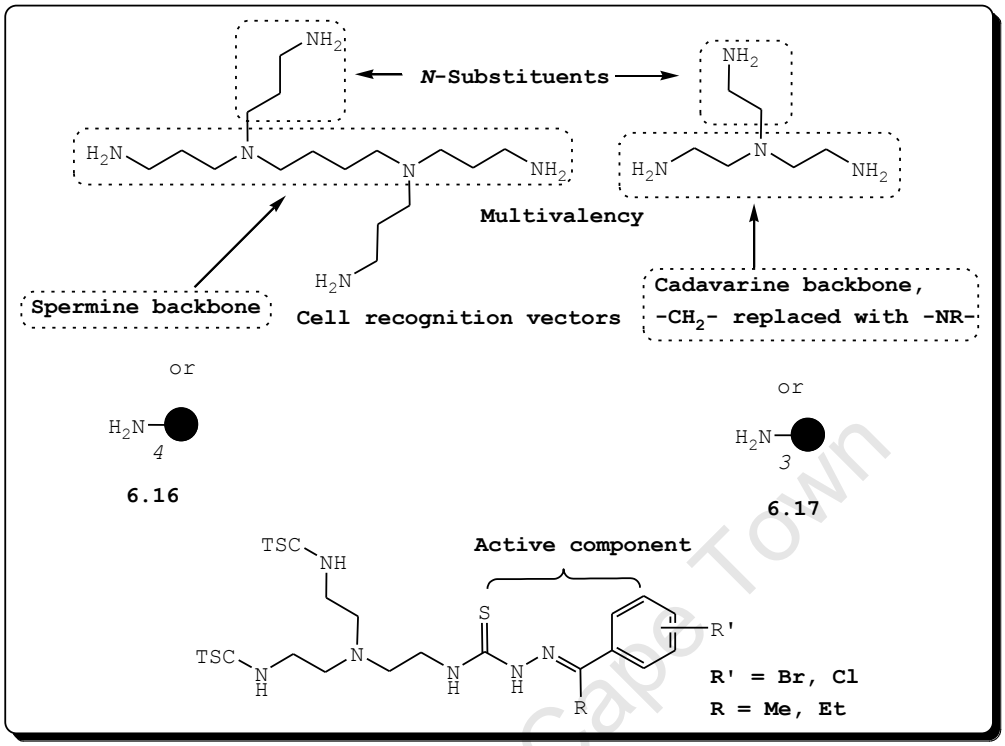

Figure 6.9: Dendritic polyamine structures.

Herein, covalent linking of the branched PA framework with TSCs is envisioned to enhance accumulation of dendritic TSCs into the malaria parasite RBCs presumably due to the recognition of PA backbones by specific transporters. *Wang et al.*[40] reported that conjugates closely resembling natural PAs are more likely to be recognised by the PAT system in tumour cells. Natural PAs putrescine (**6.1**) and spermidine (**6.3**) have been demonstrated to be transported by PA transporters into the malaria parasite infected RBCs.[35,36] Hence, it is hypothesised that motifs **6.16** and **6.17** could be recognised by these PA transporters.

The multivalency of dendritic PA scaffolds **6.16** and **6.17** is hypothesised to enhance the antiplasmodial activities of TSCs due to their multiple attachments. Our hypothesis to

enhance the antiplasmodial activity of TSCs by increasing the number of TSC moieties is supported by the recent work of *Yingyongnarongkul et al.*[41] on antibacterial activities of dihydrocaffeoyl-polyamine conjugates **6.18** and **6.19** (Figure 6.10). This research group demonstrated that increasing the number of dihydrocaffeoyl moieties from mono analogue **6.18** to tetra(dihydrocaffeoyl)polyamine **6.19** led to enhanced antibacterial activity against methicillin resistant *Staphylococcus aureus* (MRSA) and vancomycin-resistant *S. aureus* (VRSA) strains.

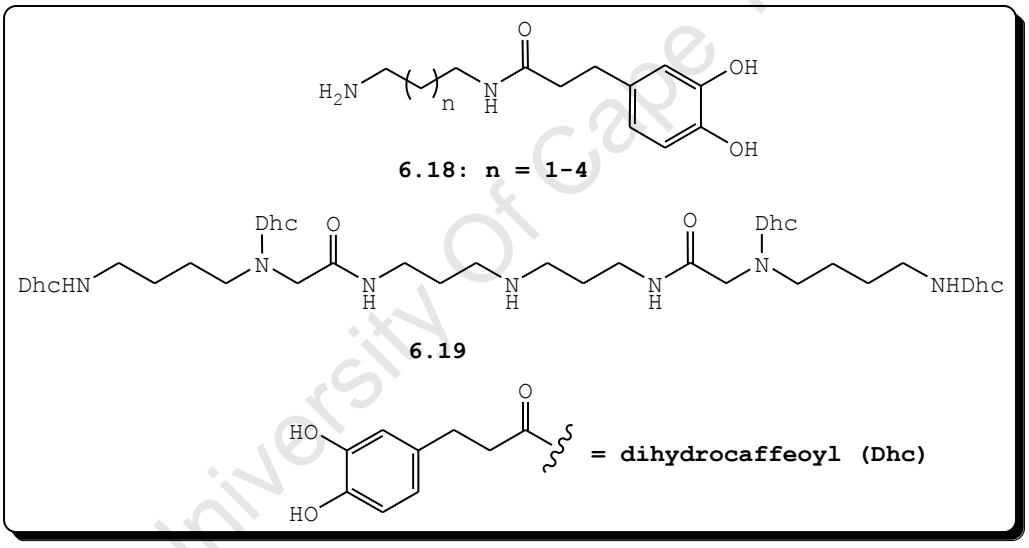

Figure 6.10: Structures of dihydrocaffeoyl-diamine (**6.18**) and tetra(dihydrocaffeoyl)polyamine conjugate (**6.19**).

6.7 RESULTS AND DISCUSSION

6.7.1 Retrosynthetic Analysis

The synthesis of dendritic TSCs was envisaged according to the retrosynthetic analysis illustrated in Scheme 6.2.

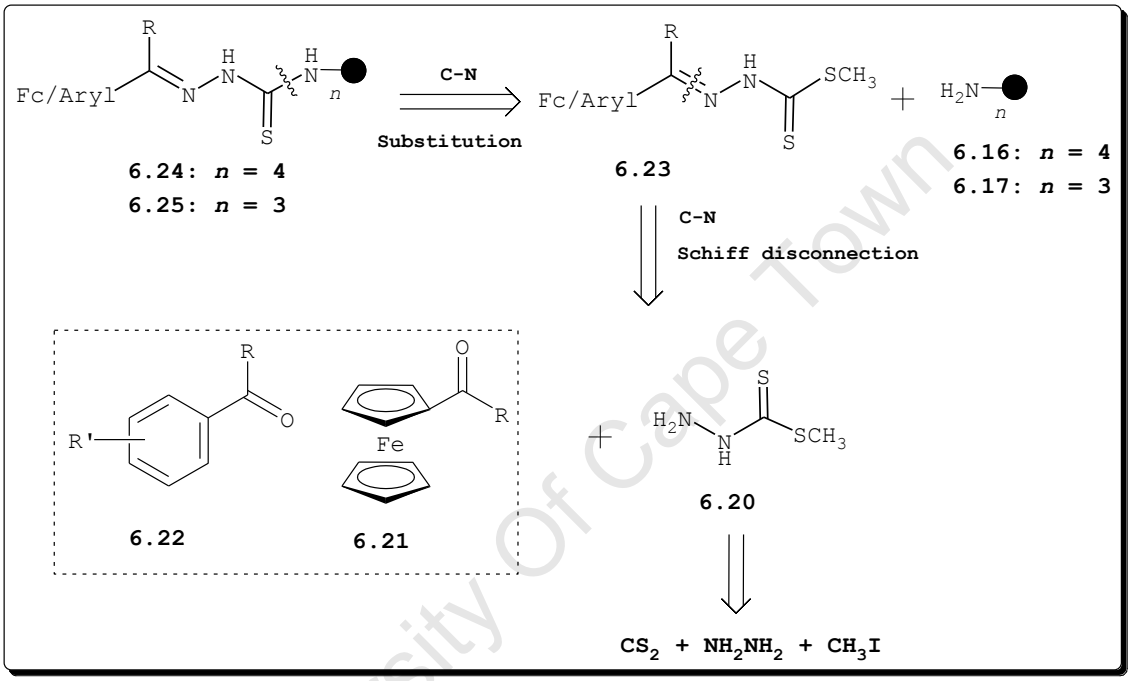

Scheme 6.2: Retrosynthetic analysis of TSC thioesters.

The C-N disconnection in **6.24** and **6.25** leads to dendritic PAs **6.16** and **6.17** as well as the key ferrocenyl and/or aryl TSC thioester motifs **6.23**. Further analysis of **6.23** leads to commercially accessible carbonyl compounds (**6.21** and **6.22**) and thiosermicarbazide thioester **6.20**. Compound **6.20** is easily obtained from carbon disulfide (CS_2), hydrazine (NH_2NH_2) and methyl iodide (CH_3I), which are all available commercially.

6.7.2 Synthesis of TSC Thioesters

The thioester **6.20** was synthesised according to the method described in the literature (Scheme 6.3).[2] The reaction of CS_2 with $NH_2NH_2.H_2O$ in an aqueous KOH-*i*PrOH solution and CH_3I afforded **6.20** in 37% yield after recrystallisation of the resultant residue from chloroform. The ^1H NMR spectroscopy in deuterated DMSO confirmed the formation of **6.20.**

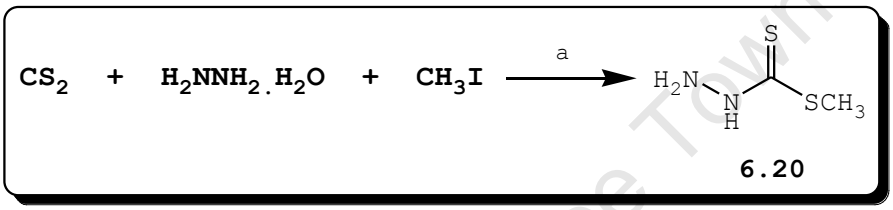

Scheme 6.3: *Reagents and condition* a) KOH, <10 °C, 6 h, *i*PrOH.

The subsequent step was to synthesise a series of TSC thioester derivatives **6.23**. Thus, condensation (Scheme 6.4) of **6.20** with a selected series of carbonyl compounds (**6.21** and **6.22**) in *i*PrOH at ambient temperature resulted in thioesters **6.23a-g** in low to good yields (Table 6.1). The compounds were isolated by gravity filtration of precipitates and obtained as brown, red and yellow solids.

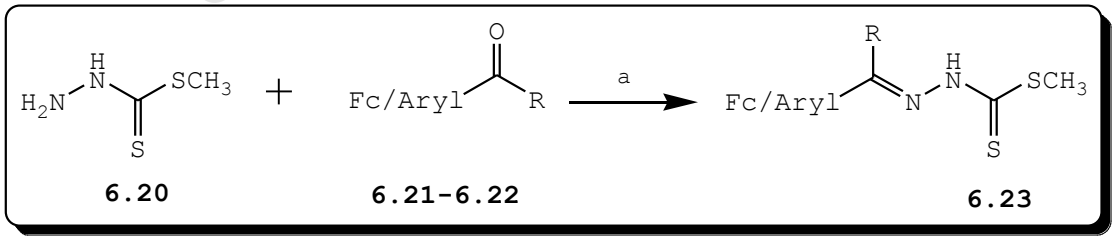

Scheme 6.4: *Reagents and condition* a) *i*PrOH, ambient temperature, 4-24 h.

Table 6.1: Isolated yields of TSC **6.23a-g.**

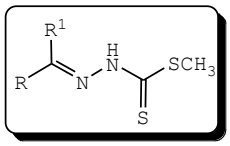

Entry	Code	Product	R	R^1	Yield/[%]
1	DK-87	6.23a	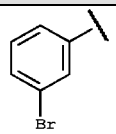	CH_3	68
2	DK-88	6.23b	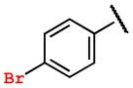	CH_3	56
3	DK-89	6.23c	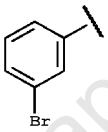	CH_3CH_2	58
4	DK-90	6.23d	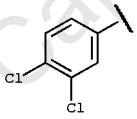	CH_3	41
5	DK-91	6.23e	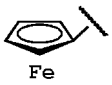	H	86
6	DK-92	6.23f		CH_3	58
7	DK-93	6.23g	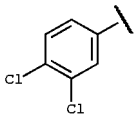	CH_3CH_2	50

6.7.2.1 Characterisations of Compounds 6.23a-b

The prepared compounds were characterised using ^{1}H NMR and FT-IR spectroscopic techniques. The structures were identified (^{1}H NMR) by downfield chemical shifts of NH, which appeared within the range δ 12.45-12.99 ppm. The presence of SCH_3 was confirmed (^{1}H NMR) by singlet chemical shifts at δ 2.47-2.52 ppm integrating for three hydrogens.

The FT-IR confirmed characteristic features (i.e. C=N, C=S, C-S) of each compound.

6.7.3 Chemical Synthesis of Tetrathiosemicarbazones

Since thiosemicarbazide and carbonyl compounds are key starting materials in the synthesis of TSCs, *Wiles et al.*[42] reported the synthesis of di(TSCs) through the ethylene dithiosemicarbazide intermediate. This method has been widely used in the synthesis of a number of di(TSC) motifs.[43] Initially, it was thought that the synthesis of tetrathiosemicarbazide (**6.26,** Scheme 6.5) intermediate would lead to the formation of tetra(TSC) dendrimers **6.24.** This approach was considered ideal since it is shorter than the synthesis of the same compounds *via* intermediate **6.23.**

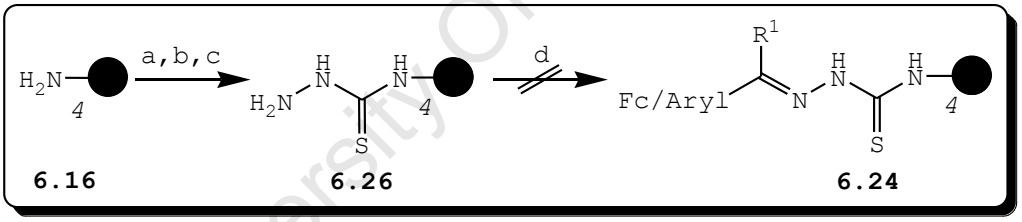

Scheme 6.5: *Reagents and conditions* a) CS_2, aqu. NaOH, ambient temp., 4 h. b) $ClCH_2CO_2Na$, ambient temp. c) HCl, $H_2NNH_2.H_2O$, 90 °C, 2h. d) Carbonyl precursors, EtOH/DMF, reflux, AcOH, 24 h.

Sequential treatment (Scheme 6.5) of dendritic PA **6.16** ("one pot" reaction) with a slight excess of CS_2 in aqueous NaOH solution and four equivalents of sodium chloroacetate led to a brown reaction mixture. This mixture was acidified and on further treatment with excess hydrazine monohydrate generated **6.26** (Fig. 6.11) as a yellow solid in 65% yield. This compound is soluble only in DMSO and DMF.

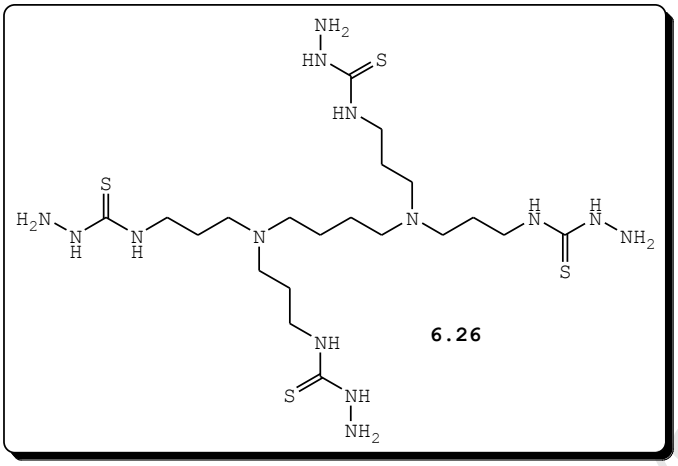

Figure 6.11: Chemical structure of tetrathiosemicarbazide **6.26.**

Evidence for the formation of **6.26** was obtained from ^{1}H and ^{13}C NMR spectra analysis as well as ESI-MS. The ^{1}H NMR spectrum revealed the presence of all aliphatic chain protons including thiourea and hydrazide NH_2 protons. The presence of five aliphatic carbons (CH_2) in ^{13}C NMR spectrum at δ 24.0, 26.3, 41.9, 51.3 and 53.3 ppm as well as the carbonyl carbon at δ 181.0 ppm confirmed the carbon skeleton of **6.26**. The ESI-MS showed a single peak at *m/z* 613.3143 [$(M + H)^+$, calc. mass 612.3069].

However, reaction of **6.26** with carbonyl compounds under refluxing EtOH for 24 h led to the isolation of starting materials only. Repeating the reaction by mixing EtOH with minimal DMF, since **6.26** dissolves in DMF and DMSO, as well as changing the reaction conditions also led to the same result. TLC plate analysis following the reaction in DMF revealed a new spot on the base line plus the spots corresponding to carbonyl starting materials. However, isolation of the desired compounds was unsuccessful.

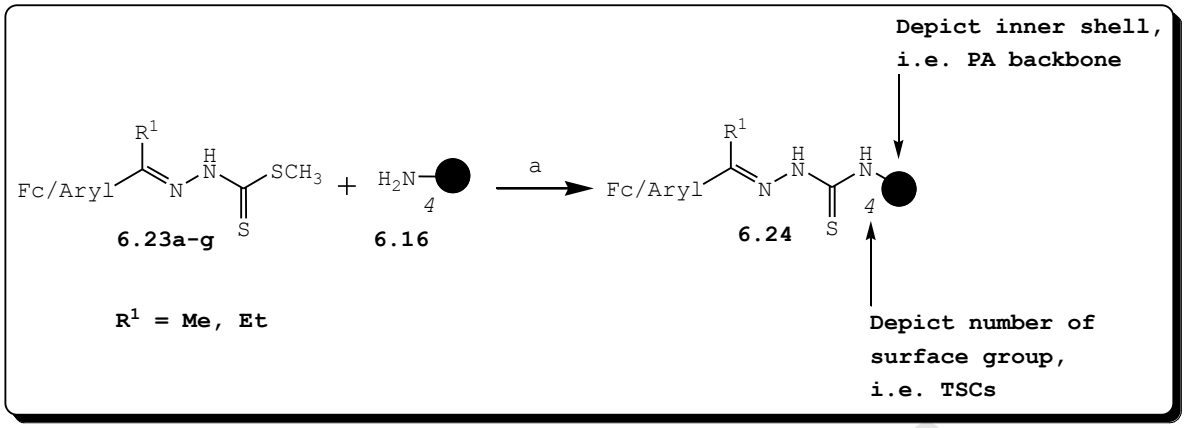

Scheme 6.6: *Reagents and conditions* a) MeOH, Reflux, 24 h.

A three reaction sequence successfully used by *Klayman et al.*[2] and other groups to synthesise *N*-terminal derivatised TSCs was employed despite being one step longer in comparison to the unsuccessful synthetic route (Scheme 6.5). Having obtained key compounds **6.23a-g,** the next step was to couple (Scheme 6.6) this series with dendritic PA motifs **6.16** and **6.17** (Fig. 6.10) to generate an exploratory series of dendritic TSCs.

Thus, treatment of **6.16** with four equivalents of **6.23a-g** in refluxing MeOH for 24 h generated novel compounds **6.24a-g** in good yields (Table 6.2). These compounds were obtained as orange, yellow and red-brown solids and were soluble in DCM, DMSO and partially in alcohols. These compounds are insoluble in aqueous solution. A summary of isolated compounds and corresponding yields is displayed in Table 6.2.

Table 6.2: Isolated dendritic TSCs and yields.

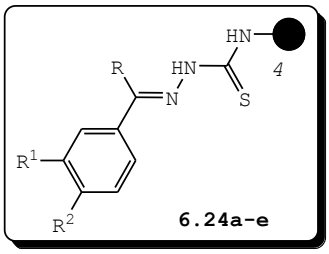

6.24a-e

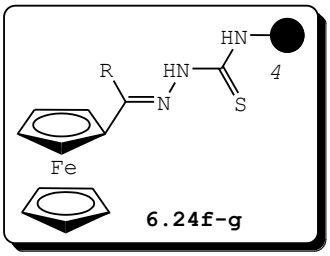

6.24f-g

Entry	Code	Cmp. No.	R	R^1	R^2	Yield/[%]
1	**DK-142E**	**6.24a**	CH_3	Cl	Cl	78
2	**DK-143C**	**6.24b**	CH_3	Br	H	94
3	**DK-144**	**6.24c**	CH_3	H	Br	63
4	**DK-145**	**6.24d**	CH_3CH_2	Br	H	82
5	**DK-146**	**6.24e**	CH_3CH_2	Cl	Cl	85
6	**DK-148**	**6.24f**	H	-	-	85
7	**DK-149**	**6.24g**	CH_3	-	-	66

6.7.3.1 Characterisations of Compounds 6.24a-g

The ^1H and ^{13}C NMR, FR-IR, MS, and elemental analysis were used to characterise compounds **6.24a-g**. The ^1H NMR spectra of all compounds revealed chemical shifts consistent with the presence of aliphatic chains (PA backbone) and thiourea NH protons. The chemical shifts indicating the presence of the SCH_3 group was not observed. This suggested that PA motif **6.16** had displaced SCH_3 to form compounds **6.24a-g.** Evidence for the formation of **6.24a-f** was also provided by the presence (^{13}C NMR) of thiourea carbon (C=S) signals at

δ 175.7-177.7 ppm as well as chemical shifts corresponding to iminic (C=N) and aliphatic carbons.

ESI-MS showed molecular ion peaks in each spectrum at *m/z* 1297.1724 (**6.24a**), 1337.1316 (**6.24b**), 1337.1259 (**6.248c**), 1393.1880 (**6.24d**), 1353.2444 (**6.24e**), 1397.3008 (**6.24f**), 1453.3694 (**6.24g**). Intense fragmentation peaks consistent with the sequential loss of TSC moiety provided further evidence of proposed structures. Microanalysis of all the compounds also appeared consistent with the atomic composition of **6.24a-g**.

6.7.4 Chemical Synthesis of Trithiosemicarbazones

This set of compounds was synthesised in the same manner (Scheme 12) as that for tetra(TSC) dendrimers. In contrast to **6.24a-g**, three equivalents of **6.23a-d** and **6.23g** as well as **6.17** were used in the reaction. Compounds **6.25a-e** were obtained as yellow to orange solids in moderate to good yields, Table 6.3. Figure 6.12 illustrates the chemical structure of dendritic TSC **6.25b**.

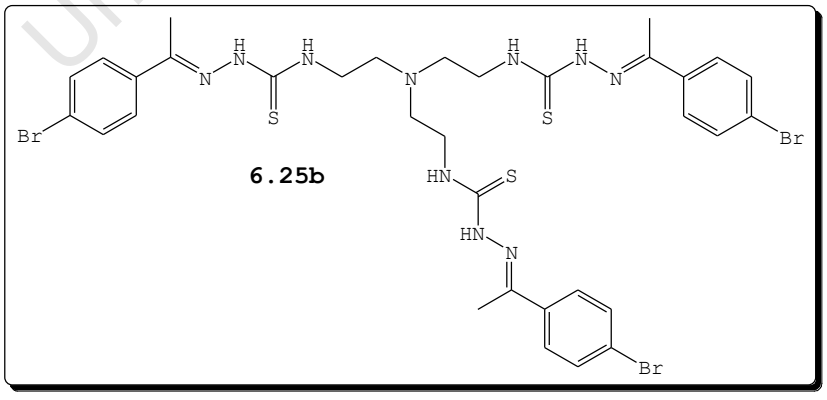

Figure 6.12: Chemical structure of PA-TSC dendrimer **6.25b**

Table 6.3: Isolated dendritic TSCs and yields.

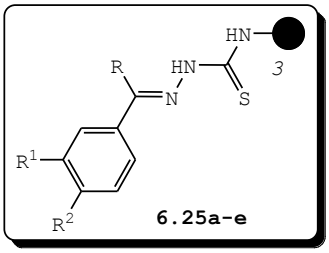

Entry	Code	Cmp. No.	R	R^1	R^2	Yield/[%]
1	**DK-153**	**6.25a**	CH_3	Br	H	72
2	**DK-154**	**6.25b**	CH_3	H	Br	74
3	**DK-155**	**6.25c**	CH_3	Cl	Cl	69
4	**DK-156**	**6.25d**	CH_3CH_2	Br	H	86
5	**DK-157**	**6.25e**	CH_3CH_2	Cl	Cl	85

6.7.4.1 Characterisations of Compounds 6.25a-e

^1H and ^{13}C NMR, FT-IR, MS, and elemental analysis were used to characterise compounds **6.25a-e**. In the ^1H NMR spectra, the chemical shifts of hydrazinic NH protons of **6.25a-e** appeared upfield at δ 8.47-8.50 ppm compared to thioesters **6.23a-d** and **6.23g** at δ 12.2-12.9 ppm. The ^{13}C NMR spectral data revealed thiourea (C=S) carbons at δ 176.5-178.1. The rest of the signals indicating the presence of iminic (C=N) and aliphatic carbons were also observed.

The ^1H and ^{13}C NMR spectral data were complemented by ESI-MS data, which showed molecular ion peaks in the spectrum of each compound at *m/z* 911.0126 (**6.25a**), 912.2995 (**6.25b**), 881.0412 (**6.25c**), 953.0519 (**6.25d**), 923.0916 (**6.25e**). The

fragmentation pattern of each structure appeared consistent with the sequential loss of TSC moiety in each structure.

6.8 BIOLOGICAL EVALUATION OF DENDRITIC TSCs

All the synthesised dendrimers were evaluated for *in vitro* growth inhibitory effects against the chloroquine-resistant (W2) strain of *P. falciparum*. The evaluation of non-conjugated thioesters **6.23a-g** as well as PA motifs **6.16** and **6.17** was conducted to determine the contribution of each component. In all the assays, CQ and ART were used as control drugs. The biological tests were carried out in collaboration with Professor P.J. Rosenthal, Department of Medicine, San Francisco General Hospital, University of California in San Francisco (UCSF).

6.8.1 Results

6.8.1.1 *In Vitro* Antiplasmodial Activity of Dendritic TSCs

The antiplasmodial activities of compounds **6.23a-g** against W2 (IC_{50} CQ = 49 nM, IC_{50} ART = 8.2 nM) were determined and the results are displayed in Table 6.4. It can be seen from the data that thioesters were not active against W2 strain at the maximum concentration tested (IC_{50} > 20 μM). On the other hand, compounds **6.23a** and **6.23d** showed antiplasmodial activities against 3D7 and K1 strains with ED_{50} values of (15.6 and 0.099 μM) and (7.84 and 23.5 μM), respectively.[44]

Table 6.4: Antiplasmodial activities of compounds **6.23a-g**

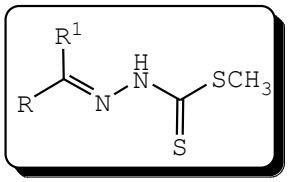

Entry	Compound No.	R	R^1	IC_{50} / μM
				W2
1	6.23a	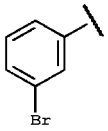	CH_3	>20
2	6.23b	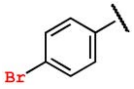	CH_3	>20
3	6.23c	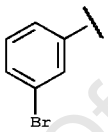	CH_3CH_2	>20
4	6.23d	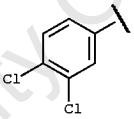	CH_3	>20
5	6.23e		H	>20
6	6.23f		CH_3	>20
7	6.23g	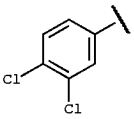	CH_3CH_2	>20

Dendritic TSCs **6.24a-g** were also tested *in vitro* against W2 strain and the data is summarised in Table 6.5. In this series TSC moieties were anchored on a branched PA scaffold **6.16** to establish the effects of this motif on the antiplasmodial activities of TSCs against W2.

Table 6.5: Antiplasmodial activities of compounds **6.24a-f**

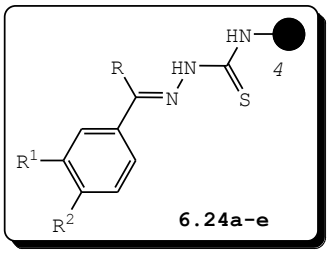

6.24a-e

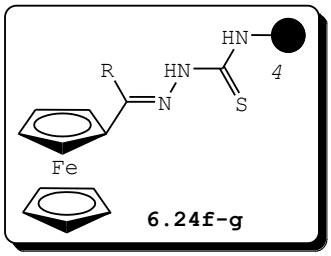

6.24f-g

Entry	Compound No.	R	R^1	R^2	IC_{50} / μM
					W2
1	**6.24a**	CH_3	Cl	Cl	1.33
2	**6.24b**	CH_3	Br	H	2.25
3	**6.24c**	CH_3	H	Br	0.79
4	**6.24d**	CH_3CH_2	Br	H	0.67
5	**6.24e**	CH_3CH_2	Cl	Cl	4.14
6	**6.24f**	H	Ferrocene		6.59
7	**6.24g**	CH_3	Ferrocene		1.79
8	**CQ**	-	-		0.049
9	**ART**	-	-		0.0082

From Table 6.5 it can be seen that dendrimers **6.24a-g** were generally more active against the W2 strain in comparison to unconjugated thioesters (Table 6.4). However, dendritic PA **6.16** was ineffective against W2 at the highest concentration tested (IC_{50} > 20μM). All tested dendritic TSCs **6.24a-g** displayed IC_{50} values below 7 μM. The most active compounds in this series were **6.24c** and **6.24d** with IC_{50} values below 1 μM against W2. However, these compounds were 13-803-fold less potent than CQ and ART as control drugs.

The antiplasmodial activity of the second series **6.25** was also determined and the results are summarised in Table 6.6. The data contained in this table also revealed that tris(TSCs) dendrimers generated from **6.17** were generally more active compared to unconjugated thioesters **6.23a-d** and **6.23g**. Unlike the PA motif **6.16,** compound **6.17** exhibited comparable activity (IC_{50} = 3.56 μM) with conjugates **6.25a, 6.25d** and **6.25e** against W2 strain (Table 6.6).

Table 6.6: Antiplasmodial activities of compounds **6.25a-e**

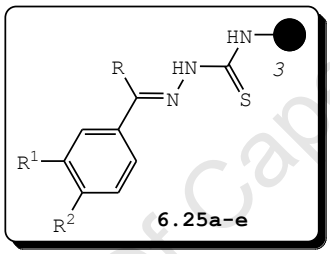

6.25a-e

Entry	Compound No.	R	R^1	R^2	IC_{50} / μM
					W2
1	**6.25a**	CH_3	Br	H	4.31
2	**6.25b**	CH_3	H	Br	1.51
3	**6.25c**	CH_3	Cl	Cl	1.37
4	**6.25d**	CH_3CH_2	Br	H	4.29
5	**6.25e**	CH_3CH_2	Cl	Cl	5.08
6	**CQ**	-	-	-	0.049
7	**ART**	-	-	-	0.0082

Although these compounds are more than 30-100 times less active compared to CQ and ART, they still retained activity in the low to mid micromolar range. The most active compounds in this series are **6.25b** (IC_{50} = 1.51 μM) and

6.25c (IC_{50} = 1.37 μM). However, this series was found to be relatively less active compared to series **6.24.**

6.8.2 Discussion

Previously, it was shown by *Bitonti et al.*[38] and *Klenke et al.*[45] that bis(benzyl)polamine and triazine-substituted PA conjugates displayed activity against malarial parasites within the range 0.2-14 μM range. In this study, series **6.24** and **6.25** are also active in the same range. Contrary to the reported PA-based compounds,[38,39] the series **6.24** and **6.25** displayed increased antimalarial potency against W2 with IC_{50} values below 7 μM. The observed antimalarial activity of each series could be due to selective uptake of **6.24a-g** and **6.25a-e** through PA transporters by infected erythrocytes. These have been shown to exhibit enhanced PA uptake.[8] The antimalarial activity of PA analogues, e.g. **6.14** and **6.15** (Fig. 6.8), was found to correlate with selective uptake by infected erythrocytes.[39]

It appears from this data that the poor activity of non-α-*N*-heterocyclic TSC derivatives is due to the limited accumulation in RBCs as their corresponding PA-TSC dendrimers exhibited significant antiplasmodial potencies than the corresponding mono-TSC scaffolds.

Although increasing the number of TSC moieties by using multivalent dendritic PA scaffolds **6.16** and **6.17** led to significant enhancement in the antiplasmodial activity, the difference in potencies between series **6.24** and **6.25** appeared to be small when considering the similarity of corresponding substituents (e.g. **6.24a** and **6.25c**). More

importantly, the formation of dendritic TSC structures led to enhanced antiplasmodial activities compared to mono analogues possibly due to dendritic effects (see section **6.4.1**).[33]

6.9 CONCLUSION

In conclusion, we have demonstrated the synthesis of novel dendritic TSCs. Most of the target molecules showed antiplasmodial activities in the low micromolar range. The ferrocenyl containing tetra(TSC) showed similar activity as aryl-based analogues. In general, dendritic TSCs displayed better antiplasmodial activities compared to their non-conjugated forms. From these results, dendritic PA scaffolds **6.16** and **6.17** appeared to have improved the antiplasmodial activity of TSCs possibly due to their enhanced accumulation in the infected erythrocytes.

6.10 REFERENCES

1. (a) D.C. Greenbaum, Z. Mackey, E. Hansell, P. Doyle, J. Gut, C.R. Cafrey, J. Lehman, P.J. Rosenthal, J.H. McKerrow, K. Chibale, *J. Med. Chem.*, **2004**, *47*, 3212-3219. (b) N. Fujii, J.P. Mallari, E.J. Hansell, Z. Mackey, P. Doyle, Y.M. Zhou, J. Gut, P.J. Rosenthal, J.H. McKerrow, R.K. Guy, *Bioorg. Med. Chem. Lett.*, **2005**, *15*, 121-123. (c) J.P. Mallari, W.A. Guiguemde, R.K. Guy, *Bioorg. Med. Chem. Lett.*, **2009**, *19*, 3546-3549.
2. D.L. Klayman, J.P. Scovill, T.S. Bartosevich, C.J. Griffin, C.J. Mason, *J. Med. Chem.*, **1979**, *22*, 1367-1373.
3. (a) Z.-Y. Tian, S.-Q. Xie, Z.-H. Mei, W.-Y. Gao, C.-J. Wang, *Org. Biomol. Chem.*, **2009**, *7*, 4651-4660. (b) J.J. Zhou, H. Huang, S.Q. Xie, Y.X. Wang, J. Zhao, C.J. Wang, *Chinese Chem. Lett.*, **2008**, *19*, 99-101. (c) C. Wang, J.-G. Delcros, J. Biggerstaff, O. Phanstiel IV, *J. Med. Chem.*, **2003**, *46*, 2663-2671.
4. (a) O. Phanstiel IV, N. Kaur, J.-G. Delcros, *Amino Acids*, **2007**, *33*, 305-313. (b) J.-G. Delcros, S. Tomasi, S. Carrington, B. Martin, J. Renault, I.S. Blagbrough, P. Uriac, *J. Med. Chem.*, **2002**, *45*, 5098-5111.
5. (a) H.M. Wallace, K. Niiranen, *Amino Acids*, **2007**, *33*, 261-265. (b) E.W. Gerner, F.L. Meyskens, Jr., *Nature Reviews: Cancer*, **2004**, *4*, 781-792
6. (a) T. Kusano, T. Berberich, C. Tateda, Y. Takahashi, *Planta*, **2008**, *228*, 367-381. (b) H. Tabor, C.W. Tabor, *Pharmacol. Rev.*, **1964**, *16*, 245-300.

7. I.B. Müller, R. Das Gupta, K. Lüersen, C. Wrenger, R.D. Walter, *Mol. Biochem. Parasitol.*, **2008**, *160*, 1-7.
8. S. Müller, G.H. Coombs, R.D. Walter, *Trends in Parasitology*, **2001**, *17*, 242-248 and references therein.
9. G.A. Ellestad, D.B. Cosulich, R.W. Broschard, J.H. Martin, M.P. Kunstmann, G.O. Morton, J.E. Lancaster, W. Fulmor, F.M. Lovell, *J. Am. Chem. Soc.*, **1978**, *100*, 2515-2524.
10. H.R. Mahler, G. Green, *Ann. N.Y. Acad. Sci.*, **1970**, *171*, 783-800.
11. M.K.-H. Doll, A. Guggisberg, M. Hesse, *Helv. Chim. Acta*, **1996**, *79*, 973-981.
12. (a) K. Hong, W. Zheng, A. Baker, D. Papahadjopoulos, *FEBS Letters*, **1997**, *400*, 233-237. (b) M. Merritt, M. Lanier, G. Deng, S.L. Regen, *J. Am. Chem. Soc.*, **1998**, *120*, 8494-8501.
13. T.P. Hettinger, Z. Kurylo-Borowska, L.C. Graig, *Ann. N.Y. Acad. Sci.*, **1970**, *171*, 1002-1009.
14. G. Karigiannis, D. Papaioannou, *Eur. J. Org. Chem.*, **2000**, 1841-1863 and references cited therein.
15. (a) J. Wang, S. Xie, Y. Li, Y. Guo, Y. Ma, J. Zhao, O. Phanstiel IV, *Bioorg. Med. Chem.*, **2008**, *16*, 7005-7012.
16. M.-Q. Klinkert, V. Heussler, *Mini-Rev. Med. Chem.*, **2006**, *6*, 131-143.
17. (a) J.-G. Delcros, S. Tomasi, S. Tomasi, S. Duhieu, M. Foucault, B. Martin, M. Le Roch, *J. Med. Chem.*, **2006**, *49*, 232-245. (b) F. Breitbeil III, N. Kaur, J.-G. Delcros, B. Martin, K.A. Abboud, O. Phanstiel IV, *J. Med. Chem.*, **2006**, *49*, 2407-2416.

18. N. Seiler, *Pharmacol. Therap.*, **2005**, *107*, 99-119.
19. R.A. Casero Jr., L.J. Marton, *Nature Reviews Drug Discovery*, **2007**, *6*, 373-390.
20. R.A. Casero Jr., P.M. Woster, *J. Med. Chem.*, **2009**, *52*, 4551-4573.
21. (a) R.J. Bergeron, G.W. Yao, W.R. Weimar, C.A. Sninsky, B. Raisler, Y. Feng, Q. Wu, F. Gao, *J. Med. Chem.*, **1996**, *39*, 2461-2471. (b) R.J. Bergeron, J. Wiegand, J.S. McManis, W.R. Weimar, R.E. Smith, S.E. Algee, T.L. Fannin, M.A. Slusher, P.S. Snyder, *J. Med. Chem.*, **2001**, *44*, 232-244.
22. (a) E. DeClercq, N. Yamamoto, R. Pauwels, J. Balzarini, M. Witvrouw, K. De Vreese, Z. Debyser, B. Rosenwirth, P. Peichl, R. Datema, D. Thornton, R. Skerlj, F. Gaul, S. Padmanabhan, G. Bridger, G. Henson, M. Abrams, *Antimicrob. Agents. Chemother.*, **1994**, *38*, 668-674. (b) J. Dessolin, P. Galea, P. Vlieghe, J.-C. Chermann, J.-L. Kraus, *J. Med. Chem.*, **1999**, *42*, 229-241.
23. N. Kaur, J.-G. Delcros, J. Imran, A. Khaled, M. Chehtane, N. Tschammer, B. Martin, O. Phanstiel IV, *J. Med. Chem.*, **2008**, *51*, 1393-1401.
24. P.M. Cullis, R.E. Green, L. Merson-Davies, N. Travis, *Chem. Biol.*, **1999**, *6*, 717-729.
25. (a) K.C. Nicolaou, W.-M. Dai, R.K. Guy, *Angew. Chem., Int. Ed. Engl.*, **1994**, *33*, 15-44. (b) E.K. Rowinski, Annu. Rev. Med., **1997**, *48*, 353-374.
26. A. Battaglia, A. Guerrini, E. Baldelli, G. Fontana, G. Varchi, C. Samorì, E. Bombardelli, *Tetrahedron Lett.*, **2006**, *47*, 2667-2670.

27. (a) E.M.M. de Brabander-van den Berg, E.W. Meijer, *Angew. Chem., Int. Ed. Engl.*, **1993**, *32*, 1308-1311. (b) M. Krämer, J.-F. Stumbé, G. Grimm, B. Kaufmann, U. Krüger, M. Weber, R. Haag, *ChemBioChem*, **2004**, *5*, 1081-1087.
28. E.R. Gillies, J.M.J. Fréchet, *Drug Discovery Today*, **2005**, *10*, 35-43.
29. (a) Y. Cheng, T. Xu, *Eur. J. Med. Chem.* (**2008**), 43, 2291-2297. (b) S.M. Grayson, J.M.J. Fréchet, *Chem. Rev.* **2001**, *101*, 3819-3867. (c) G.R. Newkome, C.N. Moorefield, F. Vögtle, *Dendritic Molecules: Concepts·Synthesis·Persepectives*, Ed. G. Walter, VHC Publishers, Inc., New York, **1996**, p 15-36.
30. S.-G. Sampathkumar, K.J. Yarema, *Nanotechnologies for the Life Sciences* Vol. 7: *Nanomaterials for Cancer Diagnosis*, Ed. C.S.S.R. Kumar, Wiley-VCH, Verlag GmbH & Co. KGaA, Weinheim, **2007**, p 1-43.
31. C.C. Lee, J.A. MacKay, J.M.J. Fréchet, F.C. Szoka, *Nature Biotechnology*, **2005**, *23*, 1517-1526.
32. (a) M. Mammen, S.K. Choi, G.M. Whitesides, *Angew. Chem. Int. Ed. Engl.*, **1998**, *37*, 2754-2794. (b) W.B. Turnbull, J.F. Stoddart, *Rev. Mol. Biotechnol.*, **2002**, *90*, 231-255. (c) J.J. Lundquist, E.J. Toone, *Chem. Rev.*, **2002**, *102*, 555-578.
33. U. Boas, P.M.H. Heegaard, *Chem. Soc. Rev.*, **2004**, *33*, 43-63 and references therein.
34. A. Agarwal, S. Saraf, A. Asthana, U. Gupta, V. Gajbhiye, N.K. Jain, *Int. J. Pharm.*, **2008**, *350*, 3-13.

35. S. Singh, S.K. Puri, S.K. Singh, R. Srivastava, R.C. Gupta, V.C. Pandey, *J. Biol. Chem.*, **1997**, *272*, 13506-13511.
36. T.N.C. Ramya, N. Surolia, A. Surolia, *Biochem. Biophys. Res. Commun.*, **2006**, *348*, 579-584.
37. R. Das Gupta, T. Krause-Ihle, B. Bergmann, I.B. Müller, A.R. Khomutov, S. Müller, R.D. Walter, K. Lüersen, *Antimicrob. Agents. Chemother.*, **2005**, *49*, 2857-2864.
38. A.J. Bitonti, J.A. Dumont, T.L. Bush, M.L. Edwards, D.M. Stemerick, P.P. McCann, A. Sjoerdsma, *Proc. Natl. Acad. Sci. USA*, **1989**, *86*, 651-655.
39. M.L. Edwards, D.M. Stemerick, A.J. Bitonti, J.A. Dumont, P.P. McCann, P. Bey, A. Sjoerdsma, *J. Med. Chem.*, **1991**, *34*, 569-574.
40. (a) L. Wang, H.L. Price, J. Juusola, M. Kline, O. Phanstiel IV, *J. Med. Chem.*, **2001**, *44*, 3682-3691. (b) O. Phanstiel IV, H.L. Price, L. Wang, J. Juusola, M. Kline, S.M. Shah, *J. Org. Chem.*, **2000**, *65*, 5590-5599.
41. B. Yingyongnarongkul, N. Apiratikul, N. Aroonrerk, A. Suksamrarn, *Arch. Pharm. Res.*, **2008**, *31*, 698-704.
42. D.M. Wiles, B.A. Gingras, T. Suprunchuk, *Can. J. Chem.*, **1967**, *45*, 1735-1743.
43. (a) T. Stringer, P. Chellan, B. Therrien, N. Shunmoogam-Gounden, D.T. Hendricks, G.S. Smith, *Polyhedron*, **2009**, *28*, 2839-2846. (b) M. Christlieb, A.R. Cowely, J.R. Dilworth, P.S. Donnelly, B.M. Paterson, H.S.R. Struthers, J.M. White, *Dalton Trans.*, **2007**, 327-331. (c) K.J. Duffy, A.N. Shaw, E. Delorme, S.B. Dillon, C. Erickson-Miller, L. Giampa, Y. Huang,

R.M. Keenan, P. Lamb, N. Liu, S.G. Miller, A.T. Price, J. Rosen, H. Smith, K.J. Wiggall, L. Zhang, J.I. Luengo, *J. Med. Chem.*, **2002**, *45*, 3573-3575.

44. F.M.M. Muganza, **MSc. Thesis**, University of Cape Town, **2006.**

45. B. Klenke, M.P. Barrett, R. Brun, I.H. Gilbert, *J. Antimicrob. Chemother.*, **2003**, *52*, 290-293.

CHAPTER 7

SUMMARY AND CONCLUSION

Simple principles of organic chemistry have led to the synthesis of a focused series of TSCs and pyrazoline analogues. From these ligand systems, a significant number of novel gold(I) and gold(III) TSC complexes has been synthesised. Due to easy access of gold(I) precursors, gold(I) TSC complexes form the bulk of compounds identified for pharmacological evaluation against *P. falciparum* strains. The ligands were prepared without further modification of their chemical structure as it was deemed necessary to avoid additional coordination sites.

Several gold precursors were used to synthesise the abovementioned gold complexes. All compounds reported in this dissertation were characterised using ^{1}H and ^{13}C NMR spectroscopy, infrared spectroscopy, mass spectrometry and elemental analysis (where possible). The X-ray crystal structures of two gold(I) complexes (**4.15** and **4.16**) were determined. In addition, interactions between molecules in crystal structures **4.15** and **4.16** were investigated using Hirshfeld surface analysis.[1] This tool revealed rare Cl...Cl interactions in **4.16**.[2]

The resulting gold TSC complexes along with parent ligands and gold precursors were tested for *in vitro* growth inhibition of *P. falciparum*, the causative agent of malaria. The coordination of gold ions to TSCs appeared advantageous as most gold(I) and gold(III) derivatives showed enhanced antiplasmodial activities compared to the

free ligands. It was also noted that the antiplasmodial activity of these compounds was independent of the nature of the complex. The introduction of different phosphine ligands (R_3P) to form complexes of the type $[Au^I(R_3P)TSC]X$ often led to compounds that showed similar activity against *P. falciparum* strains. The gold TSC complexes generally showed low cytotoxicity towards mammalian cells. These compounds presumably exert their antiplasmodial activities through multiple mechanism as no correlation was found between antiplasmodial activity and inhibition of FP-2.

On the other hand, TSCs were also incorporated into branched polyamine scaffolds (**6.16** and **6.17**) to form first generation dendrimers. These compounds were characterised using common analytical techniques. The preliminary antiplasmodial results clearly showed that the presence of dendritic polyamine scaffolds was beneficial. Most of dendritic TSCs displayed enhanced antiplasmodial activities against *P. falciparum*.

7.1 REFERENCES

1. M.A. Spackman, D. Yayatilaka, *CrystEngComm.*, **2009**, *11*, 19-32.
2. S.D. Khanye, N.B. Báthori, G.S. Smith, K. Chibale, *Dalton Trans.*, **2010**, 39, 2697-2700.

CHAPTER 8

EXPERIMENTAL PROCEDURE

8.1 CHEMICALS AND PURIFICATION OF SOLVENTS

All commercially available chemicals were purchased from either Sigma-Aldrich or Merck. All solvents were dried by appropriate techniques. Unless otherwise stated, all solvents used were anhydrous.

8.2 CHROMATOGRAPHIC SEPARATION

Merck Kieselgel 60: 70–230 mesh was used for all preparative and column chromatography. Reactions were monitored by thin layer chromatography (TLC) using Merck F254 aluminum-backed precoated silica gel plates and were visualized by the ultraviolet light.

8.3 PHYSICAL AND SPECTROSCOPIC INFORMATION

NMR spectra were recorded on either a Varian Mercury-300 (^{1}H 300.13, ^{31}P 121.5; ^{13}C 75.5 MHz) or a Varian Unity-400 (^{1}H 400.13; ^{31}P 161.9; ^{13}C 100.6 MHz) spectrometer. ^{1}H and ^{13}C NMR spectra were referenced internally, while the ^{31}P spectra were referenced externally to 85% H_3PO_4 using deuterated solvent ($CDCl_3$ or DMSO-d_6) at 298 K. Chemical shifts are reported on delta (δ) scale in parts per million (ppm). Coupling constants, J, are measured in Hertz (Hz). Abbreviations used in the assignment are as follows: broad (br), singlet (s), doublet (d), doublet of doublets (dd), multiplet (m), quartet (q), triplet (t).

Melting points were determined on a Reichert-Jung Thermovar hotstage microscope and are uncorrected. Infrared spectra were recorded on a Thermo Nicolete FT-IR instrument in the 4000–300 cm^{-1} range using KBr discs. Microanalyses were determined using a Fisons EA 1108 CHNO-S instrument. Mass spectra were recorded on a Waters API Q-TOF Ultima (ESI, 70 eV), University of Stellenbosch. At the University of Witwatersrand, SA, VG70-SEQ (FAB, 7 kV) instrument was used.

Crystal intensity data were collected on a Nonius Kappa CCD Single Crystal X-ray Diffractometer, using a graphite monochromated MoKα radiation (λ = 0.7107 Å, T = 173K) generated by a Nonius FR590 generator at 50 kV and 30 mV. Accurate unit cell parameters were refined on all data. The structures were solved using SHELXS-97[1] and refined using full-matrix least squares methods in SHELXL-97, with the aid of the program X-Seed.[2] The analysis of short contacts was carried out using PLATON.[3]

8.4 EXPERIMENTAL DETAILS FOR CHAPTER 3

A. General Procedure for the Synthesis of TSCs 3.28a-e

A mixture of an appropriate aldehyde/ketone (1.52 mmol), thiosemicarbazide (1.52 mmol) and catalytic amount of 1% acetic acid in MeOH (15 cm^3) was refluxed for 24 h. Cooling the solution to ambient temperature resulted in the formation of a precipitate, which was filtered, washed with cold MeOH and dried *in vacuo* to give the desired TSC. In some cases, the solvent was removed to give a crude product, which was purified by means of silica gel column

chromatography (SiO_2, EtOAc-Hex, 3:7) to afford desired TSCs.[4]

(*E*)-1-(1-(4-Bromophenyl)ethylidene)thiosemicarbazone, 3.28a

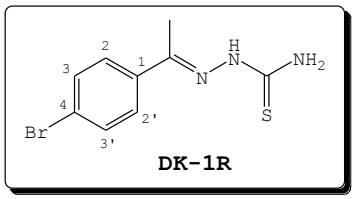

Off-white powder (1.41 g, 49%); R_f(EtOAc:Hex 3:7) 0.30; m.p. 193-194 °C (lit.[5] 190-192 °C); ν_{max} (KBr)/cm^{-1} 3412s, 3226s, 3191s, 3132s ν(NH), 1585s ν(C=N), 1501s ν(C=C), 1292s ν(C=S), 834s ν(CS, thioamide); δ_H (300 MHz, DMSO-d_6) 10.18 (1H, s, NH), 8.25 (1H, br s, NH*H*), 7.95 (1H, br s, N*H*H), 7.89 (2H, d, *J* 8.7 Hz, H2/H2′), 7.56 (2H, d, *J* 8.4 Hz, H3/H3′), 2.28 (3H, s, CH_3); δ_C (75 MHz, DMSO-d_6) 179.1, 146.5, 136.8, 131.1 (2C), 128.6 (2C), 122.6, 13.7.

(*E*)-1-(1-(3-Bromophenyl)ethylidene)thiosemicarbazone, 3.28b

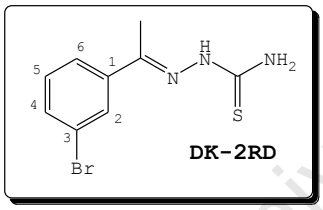

White powder (2.03 g, 60%); R_f(EtOAc:Hex 3:7) 0.30; m.p. 169-171 °C (lit.[4] 174.2-174.9 °C); ν_{max} (KBr)/cm^{-1} 3383s, 3208s, 3138 ν(NH), 1585s ν(C=N), 1512s ν(C=C), 1289s ν(C=S), 850s ν(CS, thioamide); δ_H (300 MHz, DMSO-d_6) 10.15 (1H, s, NH), 8.28 (1H, br s, NH*H*), 8.17 (1H, d, *J* 2.0 Hz, H2), 8.08 (1H, br s, N*H*H), 7.88 (1H, dd, *J* 2.1 and 8.0 Hz, H6), 7.56 (1H, dd, *J* 2.0 and 7.6 Hz, H4), 7.34 (1H, t, *J* 8.0 Hz, H5), 2.28 (3H, s, CH_3); δ_C (75 MHz, DMSO-d_6) 179.1, 146.1, 139.9, 131.7, 130.1, 128.8, 125.6, 121.9, 13.8.

(*E*)-1-(1-(3,4-Dichlorophenyl)ethylidene)thiosemicarbazone, 3.28c

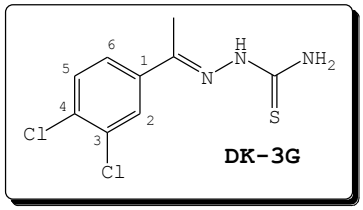

Off-white powder (2.62 g, 74%); R_f(EtOAc:DCM 3:7) 0.27; m.p. 193-194 °C (lit.[4] 196.0-197.9 °C); ν_{max} (KBr)/cm^{-1} 3395s, 3190s, 3138s ν(NH), 1593s ν(C=N), 1501s ν(C=C), 1291s ν(C=S), 805s ν(CS, thioamide); δ_H (300 MHz, DMSO-d_6) 10.21 (1H, s, NH), 8.28 (1H, br s, NH*H*), 8.24 (1H, d, *J* 1.8 Hz, H2), 8.13 (1H, br s, N*H*H), 7.87 (1H, dd, *J* 2.1 and 8.4 Hz, H6), 7.60 (1H, d, *J* 8.4 Hz, H5), 2.28 (3H, s, CH_3); δ_C (75 MHz, DMSO-d_6) 179.2, 145.2, 138.2, 131.5, 131.2, 130.1, 128.1, 126.6, 13.6.

(*E*)-1-(1-(3-Bromophenyl)propylidene)thiosemicarbazone, 3.28d

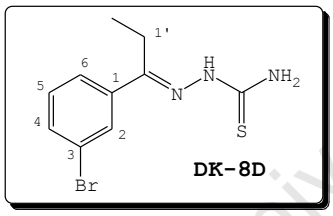

White crystalline needles (0.84 g, 30%); R_f(EtOAc:Hex 3:7) 0.45; m.p. 134-135 °C (lit.[4] 144.3-144.1 °C); ν_{max} (KBr)/cm^{-1} 3418s, 3208br, 3144s ν(NH), 1597s ν(C=N), 1507s ν(C=C), 1289s ν(C=S), 853s ν(CS, thioamide); δ_H (400 MHz, DMSO-d_6) 10.33 (1H, s, NH), 8.29 (1H, br s, NH*H*), 8.15 (1H, s, H2), 8.06 (1H, br s, N*H*H), 7.87 (1H, d, *J* 7.8 Hz, H6), 7.57 (1H, d, *J* 7.8 Hz, H4), 7.35 (1H, t, *J* 8.2 Hz, H5), 2.86 (2H, q, *J* 7.8 Hz, H1'), 1.0 (3H, t, *J* 7.8 Hz, CH_3); δ_C (101 MHz, DMSO-d_6) 179.4, 150.6, 139.1, 132.1, 130.7, 129.3, 126.1, 122.4, 19.4, 11.1.

(*E*)-1-(1-(3,4-Dichlorophenyl)propylidene)thiosemicarbazone, 3.28e

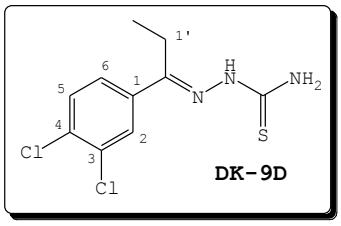

DK-9D

White solid (1.48 g, 54%); R_f (EtOAc:Hex 3:7) 0.40; m.p. 179-180 °C (lit.[4] 185.6-186.4 °C); ν_{max} (KBr)/cm^{-1} 3383s, 3249s, 3167s ν(NH), 1594s ν(C=N), 1506s ν(C=C), 1294m ν(C=S), 848s ν(CS, thioamide); δ_H (300 MHz, DMSO-d_6) 10.35 (1H, s, NH), 8.30 (1H, br s, NH*H*), 8.23 (1H, d, *J* 2.1 Hz, H2), 8.12 (1H, br s, N*H*H), 7.86 (1H, dd, *J* 2.1 and 8.7 Hz, H6), 7.61 (1H, d, *J* 8.4 Hz, H5), 2.87 (2H, q, *J* 7.8 Hz, H1'), 1.0 (3H, t, *J* 7.8Hz, CH_3); δ_C (75 MHz, DMSO-d_6) 178.6, 148.7, 136.5, 131.1, 130.9, 129.8, 127.8, 126.2, 18.4, 10.2.

1-Ferrocenemethylidenethiosemicarbazone, 3.28f

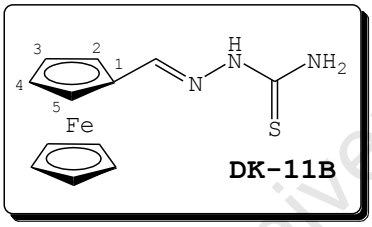

DK-11B

A mixture of ferrocenecarbaxaldehyde (0.21 g, 0.98 mmol), thiosemicarbazide (0.090 g, 0.99 mmol) and 32% HCl (*ca* 10 drops) in distilled water (20 cm^3) was stirred at ambient temperature for 4 h. During this time, an orange precipitate formed, and was filtered, washed with water and dried to give **3.28f** (0.23 g, 81%) as an orange solid;[6] m.p. 175-176 °C (lit.[7] 175 °C); ν_{max} (KBr)/cm^{-1} 3406s, 3348s, 3144s ν(NH), 1599s ν(C=N), 1559s ν(C=C), 1291s ν(C=S), 824s ν(CS, thioamide); δ_H (400 MHz, DMSO-d_6) 11.13 (1H, s, NH), 7.97 (1H, br s, NH*H*), 7.89 (1H, s, HC=N), 7.57 (1H, br s, N*H*H), 4.72 (2H, s, H2/H5), 4.41 (2H, s, H3/H4), 4.20 (5H, s, Cp); δ_C (101 MHz, DMSO-d_6) 176.8, 143.4, 78.8, 69.9 (5C), 68.9 (2C), 67.5 (2C).

1-(1-Ferrocenylethylidene)thiosemicarbazone, 3.28g

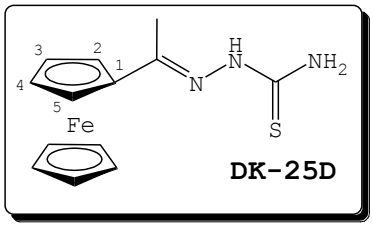

A mixture of thiosemicarbazide (0.067 g, 0.74 mmol) and 1-acetylferrocene (0.17 g, 0.73 mmol) in EtOH (15 cm^3) was refluxed for 2 h. Upon cooling to ambient temperature, a reddish precipitate was formed. The precipitate was filtered, washed with EtOH and dried *in vacuo* to give **3.28g** (0.16 g, 73%) as a red-brown solid; m.p. 170-172 °C (lit.[8] 169 °C); ν_{max} (KBr)/cm^{-1} 3401s, 3219s, 3138s ν(NH), 1587s ν(C=N), 1595s ν(C=C), 1286s ν(C=S), 833m ν(CS, thioamide); δ_H (400 MHz, DMSO-d_6) 9.91 (1H, s, NH), 8.06 (1H, s, NH*H*), 7.63 (1H, s, N*H*H), 4.79 (2H, t, *J* 2.0 Hz, H2/H5), 4.56 (2H, t, *J* 2.0 Hz, H3/H4), 4.17 (5H, s, Cp), 2.19 (3H, s, CH_3).

(*E*)-1-(4-Hydroxy-3-methoxybenzylidene)thiosemicarbazone, 3.28h

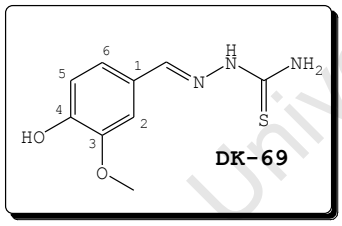

A mixture of 4-hydroxy-3-methoxybenzaldehyde (0.50 g, 3.32 mmol), thiosemicarbazide (0.30 g, 3.34 mmol) and catalytic amount of acetic acid (5 drops) in absolute EtOH (15 cm^3) was refluxed for 2 h. After consumption of starting materials (TLC), the reaction was cooled to ambient temperature, and solvent removed at reduced pressure to give a white solid residue. Drying the residue *in vacuo* afforded **3.28h** (0.76 g, 100%) as a white solid;[9] m.p. 194-196 °C (lit.[9] 175.3–177.5 °C); R_f(EtOAc:Hexane 3:7) 0.071; ν_{max} (KBr)/cm^{-1} 3438s (OH), 3278s, 3155s ν(NH), 1587s ν(C=N), 1517s ν(C=C), 1279s

ν(C=S), 838sh ν(CS, thioamide); δ_H 400 MHz, DMSO-d_6) 11.21 (1H, s, NH), 8.06 (1H, br s, NH*H*), 7.93 (1H, s, HC=N), 7.91 (1H, br s, N*H*H), 7.46 (1H, d, *J* 1.6 Hz, H2), 7.04 (1H, dd, *J* 1.6 and 8.0 Hz, H6), 6.77 (1H, d, *J* 7.6 Hz, H5), 3.83 (3H, s, OCH_3); δ_C (100 MHz, DMSO-d_6) 176.7, 148.1, 147.4, 142.2, 124.9, 121.6, 114.5, 108.7, 55.1.

B. General Procedure for the Synthesis of Mannich Bases 3.32a-f

A mixture of an appropriate ketone (10.0 mmol), dimethyl hydrochloride (13.1 mmol) and paraformaldehyde (13.1 mmol) in 96.4% EtOH (5 cm^3) was treated with 32% HCl (20 µl) at ambient temperature. The mixture was refluxed for 24 h under nitrogen. After cooling to ambient temperature, acetone (25 cm^3) was added and the resulting solution cooled to -20 °C to form a precipitate. The precipitate was filtered and dried to afford the desired hydrochloric salts.[4] *In some cases the solvent was concentrated to give solid residues. A few drops of HCl were added and the mixture worked-up with dichloromethane and water. The aqueous layer was adjusted to basic and extracted with dichloromethane. The organic layer was dried over $MgSO_4$ and filtered. The product was obtained as an oil following the removal of dichloromethane.*[4]

1-(3-Bromophenyl)-3-(dimethylamino)propan-1-one Hydrochloride, 3.32a

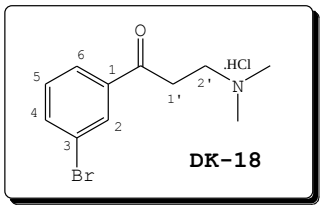

DK-18

White solid (1.82 g, 62%), δ_H (300 MHz, DMSO-d_6) 8.16 (1H, d, *J* 2.0 Hz, H2), 7.99

(1H, dd, *J* 1.8 and 7.4 Hz, H6), 7.89 (1H, d, *J* 8.4 Hz, H4), 7.54 (1H, t, *J* 8.0 Hz, H5), 3.64 (2H, t, *J* 7.2 Hz, H2′), 3.39 (2H, t, *J* 7.2 Hz, H1′), 2.80 (6H, s, $N(CH_3)_2$).

1-(4-Bromophenyl)-3-(dimethylamino)propan-1-one Hydrochloride, 3.32b

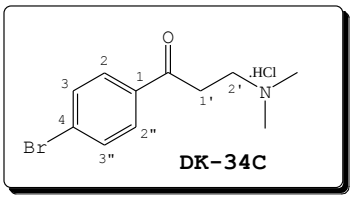

White crystalline needles (1.38 g, 47%), δ_H (300 MHz, DMSO-d_6) 10.88 (1H, br, HCl.$N(CH_3)_2$), 7.94 (2H, d, *J* 8.4 Hz, H2/H2″), 7.78 (2H, d, *J* 8.7 Hz, H3/H3″), 3.62 (2H, t, *J* 7.5 Hz, H2′), 3.39 (2H, t, *J* 7.5 Hz, H1′), 2.79 (6H, s, $N(CH_3)_2$).

1-(3,4-Dichlorophenyl)-3-(dimethylamino)propan-1-one Hydrochloride, 3.32c

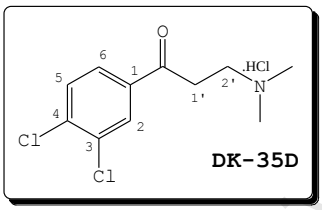

White solid (2.24 g, 74%), δ_H (400 MHz, DMSO-d_6) 11.08 (1H, br, HCl.$N(CH_3)_2$), 8.18 (1H, s, H2), 7.95 (1H, d, *J* 8.4 Hz, H6), 7.81 (1H, d, *J* 8.4 Hz, H5), 3.64 (2H, t, *J* 6.8 Hz, H2′), 3.39 (2H, t, *J* 7.2 Hz, H1′), 2.79 (6H, s, $N(CH_3)_2$).

1-(3-Bromophenyl)-3-(dimethylamino)-2-methylpropan-1-one, 3.32d

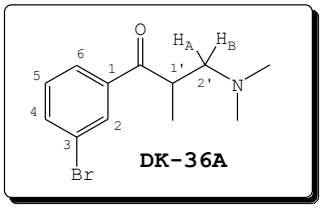

Colourless oil (0.88 g, 33%), δ_H (400 MHz, $CDCl_3$) 8.06 (1H, d, *J* 2.0 Hz, H2), 7.86 (1H, dd, *J* 2.0 and 8.8 Hz, H6), 7.64 (1H, d, *J* 8.4 Hz, H4), 7.31 (1H, t, *J* 8.0 Hz, H5), 3.54-3.63 (1H, m, H1′), 2.75 (1H, dd, *J* 4.4 and 7.6

Hz, H_A2'), 2.29 (1H, dd, *J* 6.0 and 6.8 Hz, H_B2'), 2.19 (6H, s, $N(CH_3)_2$), 1.16 (3H, d, *J* 7.2 Hz, CH_3)

1-(3-Bromophenyl)-3-(dimethylamino)propan-1-one Hydrochloride, 3.32e

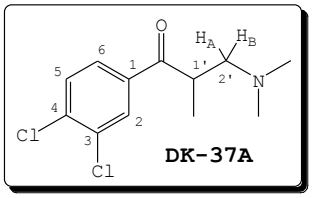

Yellowish oil (0.18 g, 15%), δ_H (400 MHz, $CDCl_3$) 8.02 (1H, d, *J* 2.0 Hz, H2), 7.77 (1H, dd, *J* 2.0 and 8.4 Hz, H6), 7.52 (1H, d, *J* 8.4 Hz, H5), 3.52-3.60 (1H, m, H1'), 2.76 (1H, dd, *J* 4.8 and 7.6 Hz, H_A2'), 2.29 (1H, dd, *J* 5.6 and 6.8 Hz, H_B2'), 2.19 (6H, s, $N(CH_3)_2$), 1.16 (3H, d, *J* 6.8 Hz, CH_3).

1-(4-Chlorophenyl)-3-(dimethylamino)propan-1-one Hydrochloride, 3.32f

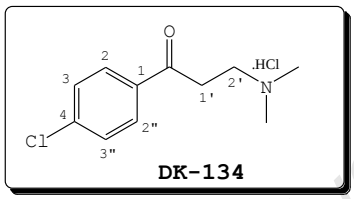

White solid (1.61 g, 65%), δ_H (300 MHz, (DMSO-d_6) 11.11 (1H, br, $HCl.N(CH_3)_2$), 8.03 (2H, d, *J* 8.4 Hz, H-2/H2"), 7.63 (2H, d, *J* 8.4 Hz, H3/H3"), 3.65 (2H, t, *J* 7.5 Hz, H2'), 3.40 (2H, t, *J* 7.5 Hz, H1'), 2.80 (6H, s, $N(CH_3)_2$).

C. General Procedure for the Synthesis of Pyrazoline TSCs 3.37a-f

Thiosemicarbazide (3.57 mmol) was dissolved in MeOH (10 cm^3) upon refluxing under nitrogen. A 50% NaOH solution was added to the reaction mixture followed by an appropriate Mannich base (3.57 mmol). The mixture was allowed to reflux for 48 h, and thereafter methanol concentrated.[10] The

resulting residue was dissolved in dichloromethane (25 cm^3) and washed with water. The organic layer was dried over $MgSO_4$, filtered and solvent evaporated to give a brown residue. The purification of the residue using silica gel column chromatography (98:2 DCM:MeOH) afforded the desired pyrazoline analogues.

3-(3-Bromophenyl)-2-pyrazoline-1-thiocarboxamide, 3.37a

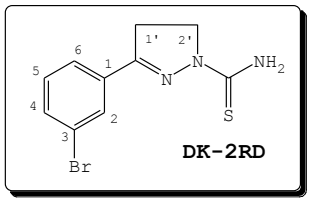

Light brown solid (0.11 g, 10%); R_f(DCM:MeOH 98:2) 0.17; m.p. 143-145 °C (Lit.[4] 172.9-174.5 °C, *Abid et al.*[11] 141 °C); ν_{max} (KBr)/cm^{-1} 3477m, 3353m, 3152s ν(NH), 2924s $\nu(CH_2)$, 1571s ν(C=N), 1502s ν(C=C), 914m ν(C=S); δ_H (300 MHz, $CDCl_3$) 8.35 (2H,s, NH_2), 7.88 (1H, s, H2), 7.61 (1H, d, *J* 7.8 Hz, H6), 7.58 (1H, d, *J* 8.7 Hz, H4), 7.30 (1H, t, *J* 7.8 Hz, H5), 4.39 (2H, t, *J* 10.2 Hz, H2'), 3.28 (2H, t, *J* 10.2 Hz, H1').

3-(3-Bromophenyl)-2-pyrazoline-1-thiocarboxamide, 3.37b

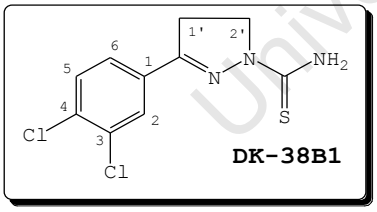

Yellow solid (0.29 g, 20%); R_f(DCM:MeOH 98:2) 0.55; m.p. 190-192 °C (Lit.[4] 199.3-201.4 °C); ν_{max} (KBr pellets)/cm^{-1} 3434s, 3233s, 3135s ν(NH), 2930w $\nu(CH_2)$, 1589s ν(C=N), 1467s ν(C=C), 807s ν(C=S); δ_H (300 MHz, $CDCl_3$) 7.79 (2H, m, H2 and N*H*H), 7.54-7.48 (3H, m, H5/H6 and NH*H*), 4.39 (1H, t, *J* 10.2 Hz, H2'), 3.26 (1H, t, *J* 10.5 Hz, H1'). Found: C, 45.1; H, 3.67; N, 13.9; S, 10.5%; Calc. for $C_{11}H_{13}Cl_2N_3S.CH_3OH$: C, 43.2; H, 4.28; N, 13.7; S 10.6%.

3-(4-*Bromophenyl*)-2-*pyrazoline*-1-*thiocarboxamide*, 3.37c

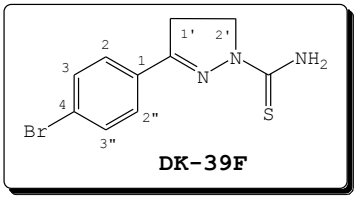

DK-39F

Yellow solid (0.49 g, 41%); R_f(DCM:MeOH 98:2) 0.64; m.p. 86-88 °C; ν_{max} (KBr pellets)/cm^{-1} 3431m, 3247s, 3144s ν(NH), 2924m ν(CH_2), 1583s ν(C=N), 1476s ν(C=C), 814s ν(C=S); δ_H (300 MHz, $CDCl_3$) 7.59-7.55 (6H, m, ArH and NHH), 4.37 (2H, t, *J* 10.2 Hz, H2′), 3.28 (2H, t, *J* 10.5 Hz, H1′). δ_C (400 MHz, $CDCl_3$) 176.9, 156.5, 133.4, 132.8 (2C), 128.2 (2C), 125.3, 48.6, 32.5; Found: C, 43.4; H, 3.90; N, 13.1; S, 9.84%; Calc. for $C_{10}H_{10}BrN_3S$: C, 42.3; H, 3.55; N, 14.8; S 11.3%.

3-(3,4-*Dichlorophenyl*)-4-methyl-2-*pyrazoline*-1-*thiocarboxamide*, 3.37d

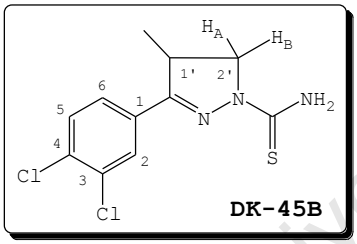

DK-45B

Yellow solid (0.49 g, 41%); R_f(DCM:MeOH 98:2) 0.64; m.p. 173-174 °C (Lit.[4] 171-172 °C; ν_{max} (KBr pellets)/cm^{-1} 3391m, 3175s ν(NH), 2975m ν(CH_2), 1595s ν(C=N), 1470s ν(C=C), 821s ν(C=S); δ_H (300 MHz, $CDCl_3$) 8.18 (2H, s, NHH), 7.75 (1H, s, H2), 7.43-7.49 (2H, m, H5/6), 4.39 (1H, t, *J* 11.6 Hz, H_A2′), 4.15 (1H, dd, *J* 6.1 and 12.0 Hz, H_B2′), 3.62-3.65 (1H, m, H1′), 1.09 (3H, d, *J* 7.2 Hz, CH_3); Found: C, 44.5; H, 4.27; N, 14.1; S, 11.1%; Calc. for $C_{11}H_{11}Cl_2N_3S$: C, 45.8; H, 3.85; N, 14.6; S 11.2%.

3-(3-*Bromophenyl*)-4-methyl-2-*pyrazoline*-1-*thiocarboxamide*, 3.37e

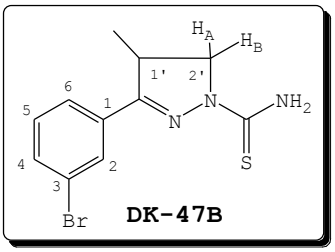

Yellow solid (0.81 g, 69%); R_f(DCM:MeOH 98:2) 0.64; m.p. 120-122 °C (Lit.[4] 107-109 °C, *Abid et al.*[11] 92 °C; ν_{max} (KBr pellets)/cm^{-1} 3416s, 3146s ν(NH), 2967m ν(CH_2), 1598s ν(C=N), 1468s ν(C=C), 856s ν(C=S); δ_H (300 MHz, $CDCl_3$) 8.98 (2H, s, NHH), 7.83 (1H, s, H2), 7.59 (1H, d, *J* 8.0 Hz, H6), 7.51 (1H, d, *J* 8.1 Hz, H4), 7.27 (1H, t, *J* 8.0 Hz, H5), 4.37 (1H, t, *J* 11.6 Hz, H_A2′), 4.15 (1H, dd, *J* 4.4 and 11.6 Hz, H_B2′), 3.65-3.71 (1H, m, H1′), 1.19 (3H, d, *J* 7.6 Hz, CH_3); Found: C, 43.1; H, 4.32; N, 14.1; S, 10.7%; Calc. for $C_{11}H_{12}BrN_3S$: C, 44.3; H, 4.06; N, 14.2; S 10.8%.

3-(3-*Chlorophenyl*)-2-*pyrazoline*-1-*thiocarboxamide*, 3.37f

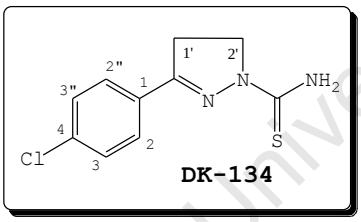

Yellow solid (0.33 g, 24%); R_f(DCM:MeOH 98:2) 0.67; m.p. 165-167 °C; ν_{max} (KBr pellets)/cm^{-1} 3364m, 3257s, 3154s ν(NH), 2923w ν(CH), 1583s ν(C=N), 1478s ν(C=C), 1378s ν(C=C), 793s ν(C=S); δ_H (300 MHz, $CDCl_3$) 7.64 (2H, d, *J* 8.4 Hz, H2/H2″), 7.38 (2H, d, *J* 8.8 Hz, H3/H3″), 4.37 (2H, d, *J* 9.6 Hz, H2′), 3.27 (2H, d, *J* 10.0 Hz, H1′); Found: C, 50.2; H, 4.45; N, 17.4; S, 13.3%; Calc. for $C_{10}H_{10}ClN_3S$: C, 50.1; H, 4.20; N, 17.5; S 13.4%.

8.5 EXPERIMENTAL DETAILS FOR CHAPTER 4

Synthesis of Hydrogen Tetrachloroauric Acid Tetrahydrate

Au (4.85 g) was added to a freshly prepared aqua regia (HCl_{conc}: HNO_{3conc}; 3:1) solution (40 cm^3) and stirred for 24 h under mild heating until all the gold had dissolved. After evaporating the solution at 40-45 °C for 48 h, the resulting yellow-orange residue was washed with concentrated HCl (2 × 10 cm^3) and dried *in vacuo* to give **$H[AuCl_4].4H_2O$** (8.56 g, 85%) as a yellow solid.[12]

Synthesis of Tetrahydrothiophene Gold(I)chloride 4.3

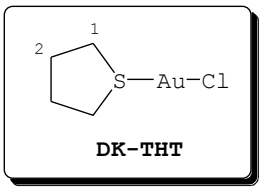

DK-THT

Tetrahydrothiophene (THT) (20 cm^3, 226.8 mmol), while stirring the mixture rapidly, was added dropwise to the solution of **$H[AuCl_4].4H_2O$** (3.18 g, 7.72 mmol) in 96.4% EtOH (25 cm^3). The reaction was accompanied by the formation a yellow precipitate ($AuCl_3$THT), which transformed into a white precipitate as more THT solution is continuously added. After stirring at ambient temperature for 20 minutes, the precipitate was filtered, washed with EtOH (3 × 10 cm^3) and dried *in vacuo* to give **4.3** (1.59 g, 64%) as a white solid;[13] δ_H (400 MHz, $CDCl_3$) 3.45 (4H, s, H1), 2.23 (4H, s, H2).

D. General Procedure for the Synthesis of Gold(I) Bis-TSC Complexes 4.12-4.18 and 4.20-4.23

A mixture of TSC (0.19 mmol) and **4.3** (0.093 mmol) in anhydrous MeOH (10 cm^3) was allowed to reflux for 2 h under nitrogen. After cooling to ambient temperature, the

solution was filtered through celite and solvent concentrated to give a semi-solid residue, which was dried *in vacuo* to afford the desired gold complexes.

***Bis(3-bromoacetophenone thiosemicarbazone-κS)-gold*(I) *chloride*, 4.12**

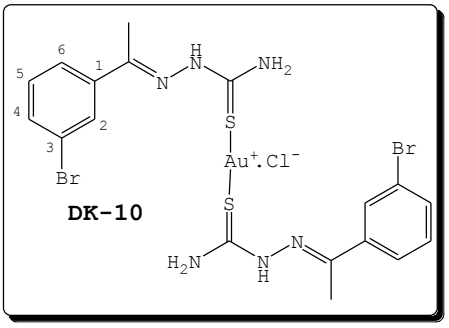

Light brown powder (0.069 g, 96%); m.p. 118-120 °C; ν_{max} (KBr)/cm^{-1} 3395m, 3226m, 3251m ν(NH), 1594s ν(C=N), 1518s ν(C=C), 1265s ν(C=S), 833m ν(CS, thioamide); δ_H (400 MHz, DMSO-d_6) 10.99 (2H, br s, NH), 9.12 (2H, br s, NH*H*), 8.69 (2H, br s, N*H*H), 7.93 (2H, d, *J* 7.2 Hz, H6), 8.23 (2H, s, H2), 7.61 (2H, d, *J* 8.0 Hz, H4), 7.37 (2H, t, *J* 7.6 Hz, H5), 2.37 (6H, s, CH_3); δ_C (101 MHz, DMSO-d_6) 173.6, 151.7, 139.2, 132.4, 130.2, 129.2, 126.0, 121.9, 14.7; *m/z* (FAB) 740.80 (100%, M^+); (Found: M^+ 740.80. $C_{18}H_{20}AuBr_2N_6S_2$ requires M^+ 740.92), 467.82 (22%, M^+-TSC); Found: C, 28.52; H, 2.81; N, 10.5; S, 8.56%; Calc. for $C_{18}H_{20}AuBr_2N_6S_2.Cl$: C, 27.83; H, 2.60; N, 10.82; S 8.26%.

***Bis(3-bromopropiophenone thiosemicarbazone-κS)-gold*(I) *chloride*, 4.13**

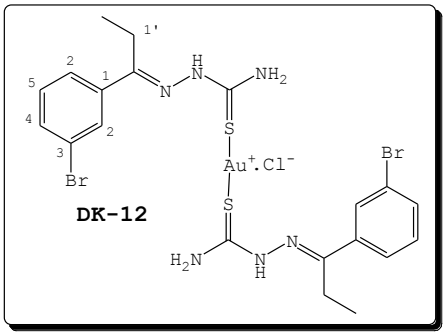

Greyish powder (0.023 g, 83%); m.p. 103-104 °C; ν_{max} (KBr)/cm^{-1} 3389m, 3231m, 3132w ν(NH), 1599s ν(C=N), 1518s ν(C=C), 1265s ν(C=S), 845m ν(CS, thioamide); δ_H (400 MHz, DMSO-d_6) 10.89 (2H, br s, NH), 8.88 (2H, br s, NH*H*), 8.55 (2H, br s, N*H*H), 8.19 (2H, s, H2), 7.91 (2H, d, *J* 8.0 Hz, H6), 7.62 (2H, d, *J* 7.6 Hz, H4), 7.38 (2H, t, *J* 7.6 Hz, H5), 2.91 (4H, q, *J* 7.6 Hz, H1′), 1.03 (6H, t, *J* 7.6 Hz, CH_3); δ_C (101 MHz, DMSO-d_6) 173.6, 154.3, 137.4, 131.7, 129.7, 128.7, 125.4, 121.4, 19.1, 10.1; *m/z* (FAB) 768.93 (80%, M^+); (Found: M^+, 768.93. $C_{20}H_{24}AuBr_2N_6S_2$ requires M^+, 768.95), 481.91 (44%, M^+-TSC); Found: C, 31.9; H, 3.38; N, 9.24; S, 7.50%; Calc. for $C_{20}H_{24}AuBr_2N_6S_2$: C, 31.2; H, 3.14; N, 10.9; S 8.33%.

***Bis(ferrocenylcarboxaldehyde thiosemicarbazone-κS) gold*(I) *chloride*, 4.14**

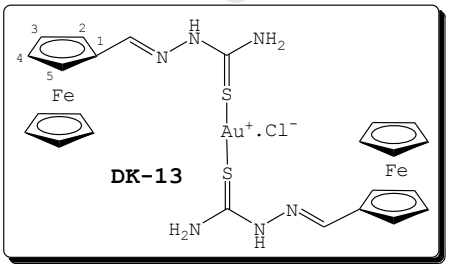

Dark-red powder (0.037 g, 89%); m.p. 176-177 °C; ν_{max} (KBr)/cm^{-1} 3389w, 3231w ν(NH), 1590s ν(C=N), 1544m ν(C=C), 1278m ν(C=S), 818s ν(CS, thioamide); δ_H (400 MHz, DMSO-d_6) 11.79 (2H, br s, NH), 8.70 (2H, br s, NH*H*), 8.18 (2H, br s, N*H*H), 8.10 (2H, s, HC=N), 4.78 (4H, s, H2/H5), 4.47 (4H, s, H3/H4), 4.23 (10H, s, Cp); δ_C (101 MHz, DMSO-

d_6) 171.2, 147.4, 77.5, 70.1 (2C), 68.6 (5C), 67.6 (2C); *m/z* (FAB) 770.95 (100%, M^+); (Found: M^+, 770.95. $C_{24}H_{22}AuFe_2N_6S_2$ requires, M^+, 767.98), 483.82 (20%, M^+-TSC); Found: C, 36.5; H, 3.43; N, 9.39; S, 8.80%; Calc. for $C_{24}H_{22}AuFe_2N_6S_2.H_2O$: C, 36.34; H, 3.40; N, 10.90; S 8.31%.

***Bis(4-bromoacetophenone thiosemicarbazone-κS)-gold*(I) *chloride*, 4.15**

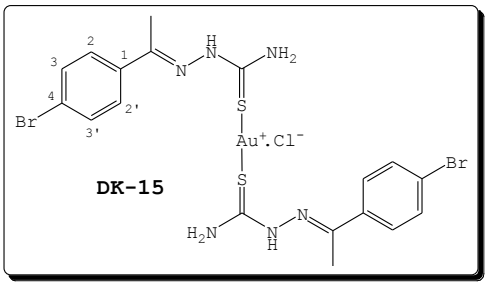

White powder (0.055 g, 96%); m.p. 136-137 °C; ν_{max} (KBr)/cm^{-1} 3389m, 3226w ν(NH), 3068m,br ν(NH), 1594s ν(C=N), 1521s ν(C=C), 1268s ν(C=S), 822s ν(CS, thioamide); δ_H (300 MHz, DMSO-d_6) 10.91 (2H, br s, NH), 8.96 (2H, br s, NH*H*), 8.52 (2H, br s, N*H*H), 7.94 (4H, d, *J* 8.4 Hz, H2/2′), 7.60 (4H, d, *J* 8.7 Hz, H3/3′), 2.35 (6H, s, CH_3); δ_C (75 MHz, DMSO-d_6) 173.9, 151.5, 136.0, 130.9 (2C), 128.8 (2C), 123.2, 14.3; *m/z* (FAB) 740.93 (100%, M^+) (Found: M^+, 740.92. $C_{18}H_{20}AuBr_2N_6S_2$ requires M^+, 740.92), 469.91 (42%, M^+-TSC); Found: C, 27.93; H, 2.96; N, 9.16; S, 8.12; Calc. for $C_{18}H_{20}AuBr_2ClN_6S_2$: C, 27.83; H, 2.60; N, 10.82; S, 8.26.

***Bis(3,4-dichloroacetophenone thiosemicarbazone-κS) gold*(I) *chloride*, 4.16**

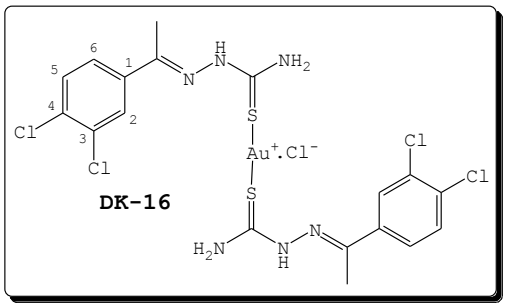

Light brownish powder (0.14 g, 97%); m.p. 65-67 °C; ν_{max} (KBr)/cm^{-1} 3395m, 3237w, 3062w ν(NH), 1599s ν(C=N), 1524s

ν(C=C), 1272s ν(C=S), 796m ν(CS, thioamide); δ_H (300 MHz, DMSO-d_6) 11.01 (2H, br s, NH), 9.10 (2H, br s, NH*H*), 8.77 (2H, br s, N*H*H), 8.32 (2H, s, H2), 7.93 (2H, d, *J* 8.7 Hz, H6), 7.66 (2H, d, *J* 8.7 Hz, H5), 2.36 (6H, s, CH_3); δ_C (75 MHz, DMSO-d_6) 173.1, 150.7, 137.0, 131.9, 130.9, 130.4, 129.7, 128.1, 14.0; *m/z* (FAB) 720.87 (93%, M^+); (Found: M^+, 720.87. $C_{18}H_{18}AuCl_4N_6S_2$ requires M^+, 720.94), 457.89 (49%, M^+-TSC); Found: C, 27.5; H, 2.70; N, 10.1; S, 8.72%; Calc. for $C_{18}H_{18}AuCl_5N_6S_2.H_2O$: C, 28.9; H, 2.81; N, 10.7; S, 8.13%.

***Bis*(3,4-*dichloropropiophenone thiosemicarbazone*-κS) *gold*(I) *chloride*, 4.17**

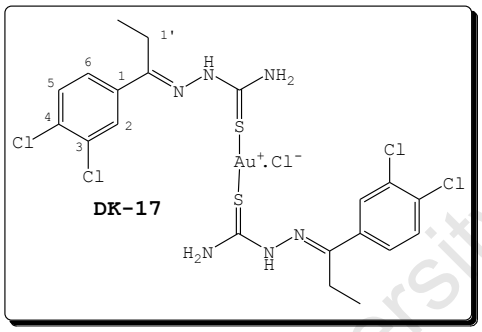

DK-17

Cream-white powder (0.047 g, 96 %); m.p. 115-116 °C; ν_{max} (KBr)/cm^{-1} 3395w, 3226w ν(NH), 1600s ν(C=N), 1521s ν(C=C), 1265s ν(C=S), 807w ν(CS, thioamide); δ_H (400 MHz, DMSO-d_6) 11.0 (2H, br s, NH), 8.99 (2H, br s, NH*H*), 8.68 (2H, br s, N*H*H), 8.28 (2H, s, H2), 7.91 (2H, d, *J* 8.4 Hz, H6), 7.67 (2H, d, *J* 8.8 Hz, H5), 2.91 (4H, q, *J* 7.6 Hz, H1′), 1.02 (6H, t, *J* 7.2 Hz, CH_3); δ_C (101 MHz, DMSO-d_6) 174.0, 153.9, 136.1, 132.0, 131.2, 130.1, 128.4, 126.9, 19.3, 10.5; *m/z* (FAB) 748.97 (80%, M^+); (Found: M^+, 748.97. $C_{20}H_{22}AuCl_4N_6S_2$ requires M^+, 748.92), 471.97 (53%, M^+-TSC); Found: C, 29.8; H, 3.15; N, 9.92; S, 8.77%; Calc. for $C_{20}H_{22}AuCl_5N_6S_2.H_2O$: C, 29.9; H, 3.01; N, 10.5; S, 7.99%.

***Bis(*acetylferrocene *thiosemicarbazone-*κS*) gold*(I) *chloride*, 4.18**

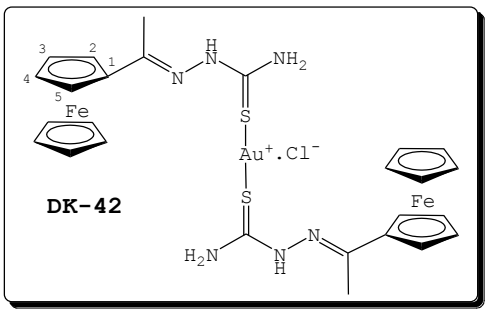

Dark-red powder (0.049 g, 95%); m.p. 125-127°C; ν_{max} (KBr)/cm^{-1} 3400m, 3212w, 3088m ν(NH), 1589s ν(C=N), 1469m ν(C=C), 1282s ν(C=S), 820s ν(CS, thioamide); δ_H (300 MHz, DMSO-d_6) 10.60 (2H, br s, NH), 8.68 (2H, br s, NH*H*), 8.06 (2H, br s, N*H*H), 4.84 (4H, s, H2/H5), 4.41 (4H, s, H3/H4), 4.19 (10H, s, Cp), 2.26 (6H, s, CH_3); δ_C (75 MHz, DMSO-d_6) 172.8, 155.8, 81.6, 69.8 (2C), 68.8 (5C), 67.2 (2C), 15.2; *m/z* (FAB) 798.7 (100%, M^+); (Found: M^+, 798.7, $C_{26}H_{26}AuFe_2N_6S_2$ requires M^+, 795.3), 496.1 (41%, M^+-FcTSC); Found: C, 38.3; H, 4.12; N, 6.62; S, 6.24; Calc. for $C_{26}H_{33}AuFe_2ClN_6S_2.H_2O.2MeOH$: C, 38.2; H, 4.81; N, 8.36; S, 9.57.

***Bis(*4*-hydroxy*-3*-methoxycarboxaldehyde thiosemicarbazone-*κS*) gold*(I) *chloride*, 4.19**

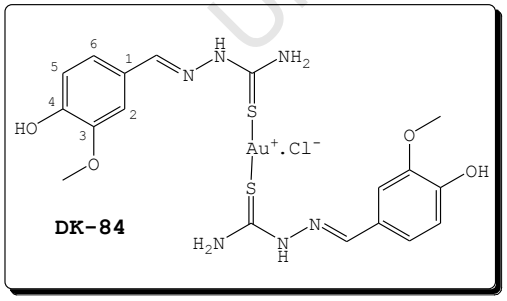

A solution of **3.28h** (0.051 g, 0.22 mmol) in anhydrous MeOH (10 cm^3) was treated with **4.3** (0.036 g, 0.11 mmol) at ambient temperature. The resulting cloudy solution was refluxed for 3 h. After cooling, the solution was filtered through celite and concentrated to give a brownish solid residue, which was dried *in vacuo* to afford **4.19** (0.074 g, 97%) as a light-brown powder; m.p. 163-165 °C; ν_{max} (KBr)/cm^{-1} 3400w ν(OH),

3251w ν(NH), 3127m ν(NH) 1587s ν(C=N), 1512s ν(C=C), 1281s ν(C=S), 823s ν(CS, thioamide); δ_H (400 MHz, DMSO-d_6) 11.79 (1H, br s, NH), 9.47 (1H, s, OH), 8.71 (1H, br s, NH*H*), 8.42 (1H, br s, N*H*H), 8.12 (1H, s, HC=N), 7.51 (1H, d, *J* 1.8 Hz, H2), 7.13 (1H, dd, *J* 2.1 and 8.1 Hz, H6), 6.82 (1H, d, *J* 8.1 Hz, H5), 3.84 (3H, s, OCH_3); δ_C (101 MHz, DMSO-d_6) 170.9, 149.3, 147.8, 147.3, 124.4, 122.9, 114.9, 109.5, 55.5; m/z (ESI) 647.0819 (100%, M^+); (Found: M^+, 647.0819. $C_{18}H_{22}AuN_6O_4S_2$ requires M^+, 647.0804); Found: C, 31.34; H, 3.11; N, 10.66; S, 9.22%; Calc. for $C_{18}H_{22}AuClN_6O_4S_2.CH_3OH$: C, 31.92; H, 3.67; N, 11.19; S, 8.97%.

***Bis(3-(3-bromophenyl)-2-pyrazoline-1-thiocarboxamide-κS) gold*(I) *chloride*, 4.20**

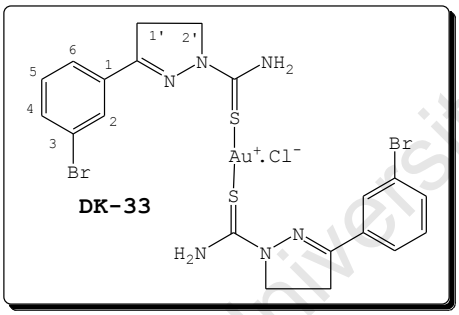

DK-33

Light brown solid (0.056 g, 77%); m.p. 160-163 °C; ν_{max} (KBr)/cm^{-1} 3408w, 3058m ν(NH), 1587s ν(C=N), 1534s, 1469m ν(C=C), 788s ν(C=S); δ_H (300 MHz, DMSO-d_6) 8.44 (4H, br, NHH), 8.18 (2H, s, H2), 7.81 (2H, d, *J* 7.8 Hz, H6), 7.70 (2H, d, *J* 8.1 Hz, H4), 7.45 (2H, t, *J* 8.1 Hz, H5), 4.23 (4H, t, *J* 9.6 Hz, H2′), 3.42 (4H, t, *J* 9.9 Hz, H1′); δ_C (75 MHz, DMSO-d_6) 173.2, 148.1, 133.2, 130.8, 130.3, 129.2, 126.3, 122.1, 48.6, 32.1; *m/z* (ESI) 764.90 (100%, M^+); (Found: M^+, 764.90. $C_{20}H_{20}AuBr_2N_6S_2$ requires M^+, 762.92); Found: C, 31.51; H, 3.82; N, 8.21; S, 5.34; Calc. for $C_{20}H_{20}AuBr_2N_6S_2$: C, 31.39; H, 2.63; N, 10.98; S, 8.38.

***Bis(3-(3,4-dichlorophenyl)-2-pyrazoline-1-thiocarboxamide-κS) gold*(I) *chloride*, 4.21**

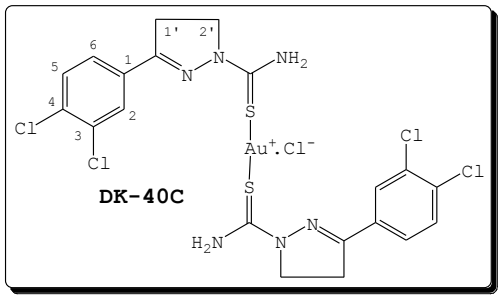

Tan solid (0.037 g, 51 %); m.p. 136-138 °C; ν_{max} (KBr)/cm^{-1} 3414w, 3224w, 3065m ν(NH), 1592s ν(C=N), 1529s, 1469s ν(C=C), 797m ν(C=S); δ_H (300 MHz, DMSO-d_6) 8.34 (4H, s, NHH), 8.19 (2H, s, H2), 7.82-7.73 (4H, m, H5/H6), 4.22 (4H, t, *J* 9.3 Hz, H2′), 3.39 (4H, t, *J* 9.9 Hz, H1′); δ_C (75 MHz, DMSO-d_6) 173.9, 150.3, 137.5, 132.2, 131.2, 130.2, 128.6, 127.1, 48.7, 32.3; *m/z* (ESI) 744.94 (100%, M$^+$); (Found: M$^+$, 744.94. $C_{20}H_{21}AuCl_4N_6S_2$ requires *M*$^+$, 742.95); Found: C, 32.41; H, 2.88; N, 7.87; S, 6.03; Calc. for : C, 32.23; H, 2.43; N, 11.28; S, 8.60%.

***Bis(3-(4-bromophenyl)-2-pyrazoline-1-thiocarboxamide-κS) gold*(I) *chloride*, 4.22**

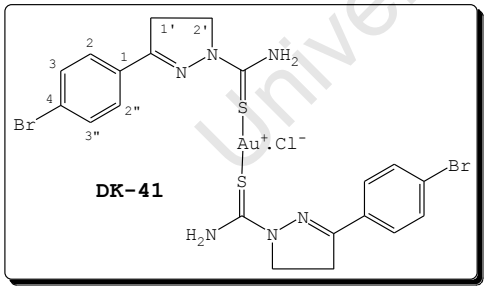

Yellow solid (0.066 g, 91%); m.p. 169-171 °C; ν_{max} (KBr)/cm^{-1} 3218s, ν(NH), 1589s ν(C=N), 1532 ν(C=C), 784s ν(C=S); δ_H (300 MHz, DMSO-d_6) 7.59-7.57 (8H, m, ArH), 4.33 (2H, t, *J* 9.6 Hz, H2′), 3.44 (2H, t, *J* 9.6 Hz, H1′); δ_C (1000.6 MHz, DMSO-d_6) 171.1, 150.3, 131.6 (2C), 131.1, 129.1 (2C), 124.3, 48.6, 32.3; *m/z* (ESI) 764.92 (100%, M$^+$); (Found: M$^+$, 764.92. $C_{20}H_{20}AuBr_2N_6S_2$ requires *M*$^+$, 762.92); Found: C, 30.7; H, 2.85; N, 8.64; S, 6.63; Calc. for $C_{20}H_{20}AuBr_2N_6S_2.CH_3OH$: C, 30.3; H, 2.90; N, 10.1; S, 7.70.

***Bis(3-(4-chlorophenyl)-2-pyrazoline-1-thiocarboxamide-κS) gold*(I) *chloride*, 4.23**

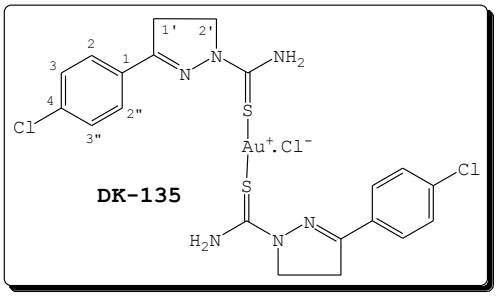

DK-135

Tan solid (0.041 g, 55%); m.p. 196-198 °C; ν_{max} (KBr)/cm^{-1} 3401w, 3075s ν(NH), 1594s ν(C=N), 1537s, 1490s ν(C=C), 787 ν(C=S); δ_H (400 MHz, $CDCl_3$) 7.67-7.63 (4H, m, ArH), 7.43-7.38 (4H, m, ArH), 4.34 (4H, t, *J* 10.0 Hz, H2'), 3.39 (4H, t, *J* 9.6 Hz, H1'); δ_C (100.6 MHz, DMSO-d_6) 175.1, 145.3, 136.1, 129.5 (2C), 129.3 (2C), 49.2, 32.9; *m/z* (ESI) 675.03 (100%, M^+); (Found: M^+, 675.03. $C_{20}H_{21}AuCl_2N_6S_2$ requires M^+, 675.02); Found: C, 31.8; H, 3.30; N, 11.1; S, 8.55; Calc. for $C_{20}H_{20}AuCl_3N_6S_2.2H_2O$: C, 32.12; H, 3.23; N, 11.2; S, 8.57%.

Synthesis of Triphenylphosphine Gold(I) Chloride 4.5

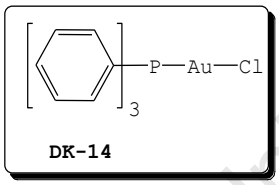

DK-14

A solution of **$H[AuCl_4].4H_2O$** (1.01 g, 2.45 mmol) in 96.4% EtOH (20 cm^3) was treated with triphenylphosphine (1.30 g, 4.97 mmol) at ambient temperature under nitrogen. After stirring for 1 h, a white precipitate that formed was filtered, washed with EtOH and dried *in vacuo* to afford **4.5** (1.19 g, 98%) as a white solid;[14] δ_P (121 MHz, DMSO-d_6) 34.02 ppm.

E. General Procedure for the Synthesis of Ph_3P Gold(I) TSC Complexes 4.29a-f

A mixture of $AgOSO_2CF_3$ (0.10 mmol) and **4.5** (0.10 mmol) in MeOH (5 cm^3) was stirred at ambient temperature for 1 h

under nitrogen.[15] During this time, a 'purple' precipitate formed; and was filtered through celite to give a colourless solution. Nitrogen gas was bubbled through the filtrate followed by addition of individual TSC (0.10 mmol). After stirring the reaction mixture for 4 h at ambient temperature, the colloidal solution was filtered and solvent concentrated to give a semi-solid residue, which was dried *in vacuo* to give the desired gold(I) complexes.

(3-*Bromoacetophinone-thiosemicarbazone*-κS)
(*triphenylphosphine*)*gold*(I) *triflate*, 4.26a

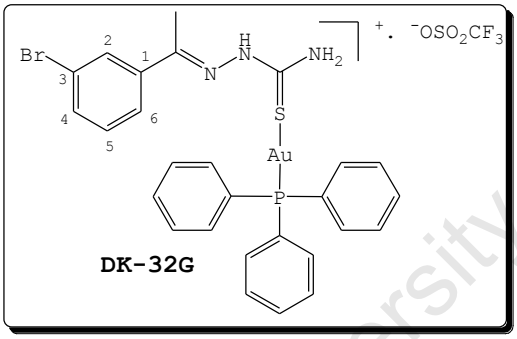

DK-32G

White solid (0.065 g, 73%); m.p. 86-88 °C; ν_{max} (KBr)/cm^{-1} 3402w br, 3286w, 3169m ν(NH), 1601s ν(C=N), 1531s ν(C=C), 1282s, 1245s ν(C=S), 1026sh ν(P-C), 831m ν(CS, thioamide); δ_H (300 MHz, DMSO-d_6) 11.33 (1H, s, NH), 9.49 (1H, br, N*H*H), 9.01 (1H, br, NH*H*), 8.23 (1H, s, H2), 7.94 (1H, d, *J* 7.8 Hz, H6), 7.67–7.63 (16H, m, 3 × Ph, H4), 7.38 (1H, t, *J* 8.4 Hz, H5), 2.36 (3H, s, CH_3); δ_C (75 MHz, DMSO-d_6) 171.3, 155.3, 138.9, 134.0, 132.4, 131.9, 130.5, 129.4, 128.6, 127.9, 126.5, 122.2, 15.3; δ_P (121 MHz, DMSO-d_6) 38.1 ppm; *m/*z (FAB) 731.9 (71%, M^+); (Found: M^+, 731.9. $C_{27}H_{25}AuBrN_3S$ requires M^+, 731.4), 459.0 (100%, Ph_3PAu^+); Found: C, 36.4; H, 3.21; N, 4.23; S, 7.63; Calc. for $C_{28}H_{25}AuBrF_3N_3O_3PS_2.2H_2O$: C, 36.7; H, 3.19; N, 4.58; S, 7.00.

(4-*Dichloroacetophinone-thiosemicarbazone*-κS)
(*triphenylphosphine*)*gold*(I)*triflate*, 4.26b

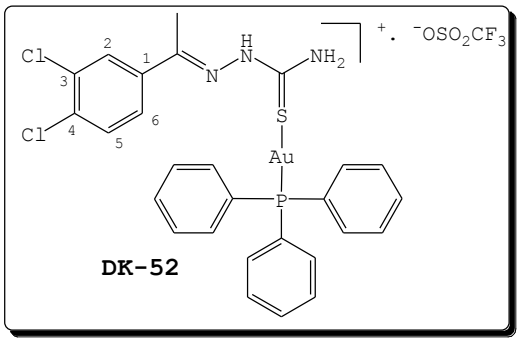

DK-52

White solid (0.060 g, 66%); m.p. 205-207 °C; ν_{max} (KBr)/cm^{-1} 3436m, 3172m ν(NH), 1603s ν(C=N), 1527s ν(C=C), 1275s, 1244s ν(C=S), 1028sh ν(P-C), 825w ν(CS, thioamide); δ_H (300 MHz, DMSO-d_6) 11.36 (1H, s, NH), 9.53 (1H, br, N*H*H), 9.05 (1H, br, NH*H*), 8.29 (1H, s, H2), 7.92 (1H, d, *J* 8.4 Hz, H6), 7.72-7.60 (16H, m, 3 × Ph, H5), 2.35 (3H, s, CH_3); δ_C (75 MHz, DMSO-d_6) 171.4, 154.1, 137.0, 133.7, 132.8, 132.1, 131.5, 130.2, 129.4, 128.7, 127.7, 127.2, 14.8; δ_P (121 MHz, DMSO-d_6) 38.3 ppm; *m/*z (FAB) 719.9 (60%, M^+); (Found: M^+, 719.9. $C_{27}H_{24}AuCl_2N_3S$ requires *M*$^+$, 721.4), 458.9 (100%, Ph_3PAu^+); Found: C, 37.8; H, 3.20; N, 4.15; S, 7.51; Calc. for $C_{28}H_{24}AuCl_2F_3N_3O_3PS_2.2H_2O$: C, 37.1; H, 3.11; N, 4.64; S, 7.07.

(3-*Bromopropiohenone-thiosemicarbazone*-κS)
(*triphenylphosphine*)*gold*(I)*triflate*, 4.26c

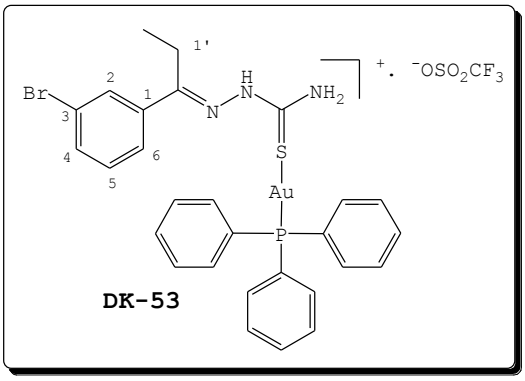

DK-53

Orange solid (0.074 g, 76%); m.p. 172-173°C; ν_{max} (KBr)/cm^{-1} 3414m br, 3272w, 3176m ν(NH), 1602s ν(C=N), 1528s ν(C=C), 1282s, 1245s ν(C=S), 1028sh ν(P-C), 791m ν(CS, thioamide); δ_H (300 MHz, DMSO-d_6) 11.23 (1H, s, NH), 9.30 (1H, br s, N*H*H), 8.84 (1H, br s, NH*H*), 8.17 (1H,

s, H2), 7.89 (1H, d, *J* 8.1 Hz, H6), 7.65–7.59 (16H, m, 3 × Ph, H4), 7.39 (1H, t, *J* 7.8 Hz, H5), 2.91 (2H, q, *J* 7.5 Hz, H1′), 1.0 (3H, t, *J* 7.5 Hz, CH_3); δ_C (75 MHz, DMSO-d_6) 170.2, 158.1, 137.6, 133.6, 132.6, 132.0, 130.2, 129.3, 128.4, 127.6, 126.1, 121.9, 20.0, 10.7; δ_P (121 MHz, DMSO-d_6) 37.7 ppm; *m/*z (FAB) 746.1 (70%, $[M+H]^+$); (Found: $[M+H]^+$, 746.1. $C_{28}H_{27}AuBrN_3PS$ requires M^+, 745.4), 459.0 (100%, Ph_3PAu^+); Found: C, 37.3; H, 3.73; N, 4.59; S, 8.11; Calc. for $C_{29}H_{27}AuBrF_3N_3O_3PS_2.2H_2O$: C, 37.4; H, 3.36; N, 4.52; S, 6.89.

(4-*Bromoacetophinone-thiosemicarbazone*-κS) (*triphenylphosphine*)*gold*(I)*triflate*, 4.26d

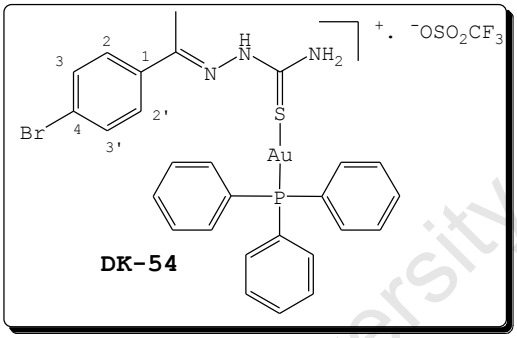

DK-54

White solid (0.065 g, 72%); m.p. 215-217 °C; ν_{max} (KBr)/cm^{-1} 3438m, 3274w, 3172m ν(NH), 1602s, 1587sh ν(C=N), 1528s ν(C=C), 1275s, 1247s ν(C=S), 1029sh ν(P-C), 829s ν(CS, thioamide); δ_H (300 MHz, DMSO-d_6) 11.25 (1H, s, NH), 9.41 (1H, br, N*H*H), 8.84 (1H, br, NH*H*), 7.94 (2H, d, *J* 8.4 Hz, H2/H2′), 7.63–7.59 (17H, m, 3 × Ph, H3/H3′), 2.36 (3H, s, CH_3); δ_C (75 MHz, DMSO-d_6) 171.6, 154.4, 135.3, 133.4, 131.7, 130.7 (2C), 129.0 (2C), 128.7, 128.1, 127.3, 123.4, 14.4; δ_P (121 MHz, DMSO-d_6) 38.6 ppm; *m/*z (FAB) 732.1 (70%, M^+); (Found: M^+, 732.1. $C_{27}H_{25}AuBrN_3S$ requires M^+, 731.4), 459.1 (100%, Ph_3PAu^+); Found: C, 37.7; H, 3.18; N, 4.65; S, 7.50; Calc. for $C_{28}H_{25}AuBrF_3N_3O_3PS_2.H_2O$: C, 37.4; H, 3.03; N, 4.68; S, 7.14.

(3,4-*Dichloroacetophinone-thiosemicarbazone*-κS)
(*triphenylphosphine*)*gold*(I) *triflate*, 4.26e

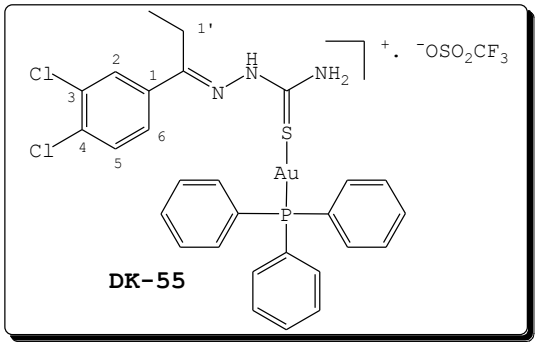

DK-55

White solid (0.068 g, 76%); m.p. 175-176°C; ν_{max} (KBr)/cm^{-1} 3419m, 3275w, 3178m ν(NH), 1602s ν(C=N), 1532s ν(C=C), 1273s, 1247s ν(C=S), 1028sh ν(P-C), 828w ν(CS, thioamide); δ_H (300 MHz, DMSO-d_6) 11.41 (1H, s, NH), 9.49 (1H, br, N*H*H), 9.01 (1H, br, NH*H*), 8.26 (1H, s, H2), 7.89 (1H, d, *J* 8.4 Hz, H6), 7.71–7.54 (16H, m, 3 × Ph, H5), 2.90 (2H, q, *J* 7.5 Hz, H1′), 1.0 (3H, t, *J* 7.5 Hz, CH_3); δ_C (75 MHz, DMSO-d_6) 171.6, 157.9, 135.7, 133.6, 132.7, 131.5, 130.2, 129.3, 128.8, 128.4, 127.6, 127.3, 19.9, 10.6; δ_P (121 MHz, DMSO-d_6) 38.0 ppm; *m/*z (FAB) 734.1 (70%, M^+); (Found: M^+, 734.1. $C_{28}H_{26}AuCl_2N_3PS$ requires M^+, 735.4), 459.0 (100%, Ph_3PAuP^+); Found: C, 37.9; H, 3.28; N, 4.30; S, 7.72; Calc. for $C_{29}H_{26}AuCl_2F_3N_3O_3PS_2.2H_2O$: C, 37.8; H, 3.28; N, 4.56; S, 6.97.

(*Ferronylcarboxaldehyde-thiosemicarbazone*-κS)
(*triphenylphosphine*)*gold*(I)*triflate*, 4.26f

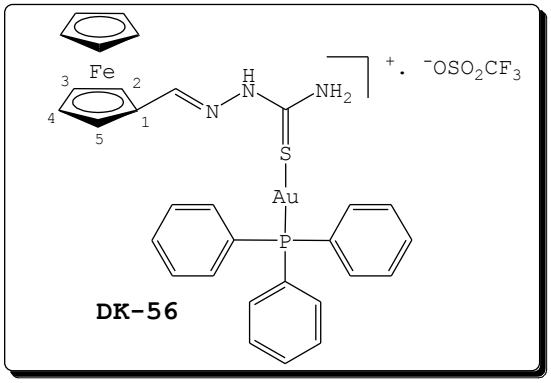

DK-56

Dark-red solid (0.079 g, 85%); m.p. 129-130 °C; ν_{max} (KBr)/cm^{-1} 3414m, 3277w, 3169m ν(NH), 1598s ν(C=N), 1282s, 1241s ν(C=S), 1027sh ν(P-C), 821s ν(CS, thioamide); δ_H (300 MHz,

DMSO-d_6) 12.12 (1H, s, NH), 9.18 (1H, br, NH*H*), 8.56 (1H, br, N*H*H), 8.15 (1H, s, HC=N), 7.66–7.60 (15H, m, 3 × Ph), 4.82 (2H, s, H2/H5), 4.52 (2H, s, H3/H4), 4.23 (5H, s, Cp); δ_C (75 MHz, DMSO-d_6) 168.5, 150.4, 133.5, 131.8, 129.2, 128.3, 76.7, 70.5 (5C), 68.7 (2C), 67.9 (2C); δ_P (121 MHz, DMSO-d_6) 37.6 ppm; *m/*z (FAB) 746.2 (90%, M^+); (Found: M^+, 746.2. $C_{30}H_{26}AuFeN_3PS$ requires M^+, 744.4), 459.0 (100%, Ph_3PAu^+); Found: C, 38.8; H, 3.48; N, 3.93; S, 7.17; Calc. for $C_{31}H_{28}AuF_3FeN_3O_4PS_2.3H_2O$: C, 38.6; H, 3.55; N, 4.35; S, 6.64.

Synthesis of

1,3,5-Triaza-7-phosphatricyclo[3.3.1.1^{3,7}]decane 4.28

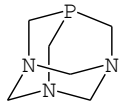

DK-99D

A mixture of tetrakis(hydroxymethyl)phosphonium chloride (80% solution in water, 17 cm^3, 95 mmol) and ice (12.4 g) was treated with a solution of NaOH (50% w/w, 6.39 g) solution, which was added slowly while manually stirring. After the resulting clear colourless solution reached ambient temperature, formaldehyde (37%, 40.0 g, 500 mmol) was added followed by hexamethylenetetramine (14.1 g, 100 mmol). The mixture was stirred at ambient temperature for 17 h followed by evaporation of water in the fume hood.[16] The resulting solid was then filtered, washed with several aliquots of cold ethanol and allowed to dry. Subsequently, the solid was dissolved in chloroform (150 cm^3) and the solution was gravity filtered and evaporated to complete dryness to give a white solid residue. Drying the residue *in vacuo* afforded **4.28** (9.11 g, 61%) as a white crystalline solid;[16] m.p. >

260 °C; δ_H (300 MHz, D_2O) 4.39 (6H, s, NCH_2N), 3.93 (6H, d, J_{H-P} 9.0 Hz, PCH_2N); δ_P (121.5 MHz, D_2O) -95.8 ppm.

1,3,5-Triaza-7-phosphatricyclo[3.3.1.1^{3,7}]decane-gold(I) Chloride, 4.24

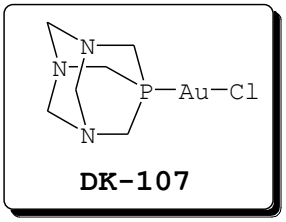

DK-107

A solution of **4.3** (0.37 g, 2.35 mmol) in $CHCl_3$ (10 cm^3) was treated with **4.28** (0.75 g, 2.34 mmol) dissolved in $CHCl_3$ (20 cm^3) at ambient temperature. After stirring the resulting mixture for 2 h, the precipitate was collected and washed with small portions of $CHCl_3$.[17] Drying the residue *in vacuo* afforded **4.24** (0.54 g, 59%) as a white powder; m.p. 255-256 °C (with decomposition);[18] δ_H (300 MHz, DMSO-d_6) 4.54 (1H, s, NCH_2N), 4.49 (2H, s, NCH_2N), 4.38 (3H, s, NCH_2N), 4.33 (6H, s, NCH_2P); δ_P (121.5 MHz, DMSO) -51.04 ppm.

F. General Procedure for the Synthesis of PTA Gold(I) TSC Complexes

A suspension of **4.24** (0.079 mmol) in MeOH (5 cm^3) at ambient temperature was treated with TSCs (**3.28a-h** and **3.37a-d**) (0.079 mmol) for 1½ h. The resulting cloudy or red solution was filtered through celite to give a colourless or red solution. The solvent was removed at reduced pressure to give a semi-solid residue, which was dried *in vacuo* to give the desired gold(I) complexes.

(4-*Bromoacetophinone-thiosemicarbazone*-κS)(1,3,5-*triaza*-7-*phosphatricyclo*[3.3.1.1^{3,7}]*decane*-κ*P*) *gold*(I), 4.29a

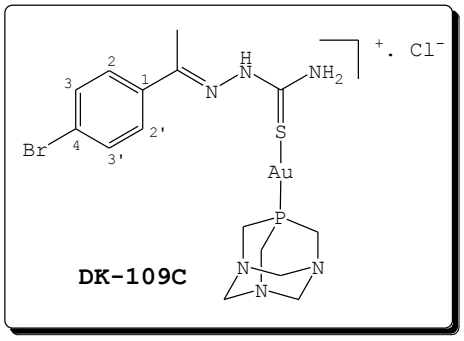

Tan solid (0.047 g, 87%); m.p. 124-126 °C; ν_{max} (KBr)/cm^{-1} 3365w, 3237w (NH), 1589s (C=N), 1522s (C=C), 1282s (C=S), 1245s (C-N), 968s (P-C), 822s, 736s (CS, thioamide), 322w (Au-S); δ_H (300 MHz, DMSO-d_6) 10.25 (1H, br, NH), 8.28 (1H, br, N*H*H), 7.99 (1H, br, NH*H*), 7.88 (2H, d, *J* 8.7 Hz, H2/H2′), 7.57 (2H, d, *J* 8.7 Hz, H3/H3′), 4.55 (2H, s, NCH_2N), 4.51 (2H, s, NCH_2N), 4.39 (2H, s, NCH_2N), 4.34 (6H, s, NCH_2P), 2.29 (3H, s, CH_3); δ_C (75 MHz, DMSO-d_6) 177.8, 147.1, 136.4, 130.6 (2C), 128.2 (2C), 122.2, 71.5 (3C), 50.7 (3C), 13.4; δ_P (121 MHz, DMSO-d_6) -50.8 ppm; *m/z* (ESI) 625.0219 (100%, M^+); (Found: 625.0219. $C_{15}H_{22}AuBrN_6PS$ requires *M*$^+$, 626.2847); Found: C, 28.4; H, 3.34; N, 11.7; S, 5.65%; Calc. for $C_{15}H_{22}AuBrN_6PSCl$: C, 28.8; H, 3.54; N, 13.4; S, 5.12.

(3-*Bromoacetophinone-thiosemicarbazone*-κS)(1,3,5-*triaza*-7-*phosphatricyclo*[3.3.1.1^{3,7}]*decane*-κ*P*)*gold*(I), 4.29b

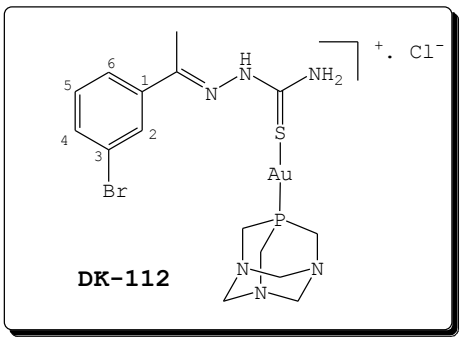

Light yellow solid (0.043 g, 84%); m.p. 117-119 °C; ν_{max} (KBr)/cm^{-1} 3378w, 3242w (NH), 1601s (C=N), 1526s (C=C), 1282s (C=S), 1245s (C-N), 971s (P-C), 841m, 786s (CS, thioamide), 326m (Au-S); δ_H (300 MHz, DMSO-d_6) 10.28 (1H, br, NH),

8.26 (2H, br, NHH), 8.15 (1H, s, H2), 7.88 (1H, d, *J* 7.8 Hz, H6), 7.58 (1H, d, *J* 8.1 Hz, H4), 7.35 (1H, t, *J* 8.1 Hz, H5), 4.55 (2H, s, NCH_2N), 4.51 (2H, s, NCH_2N), 4.39 (2H, s, NCH_2N), 4.34 (6H, s, NCH_2P), 2.30 (3H, s, CH_3); δ_C (100.6 MHz, DMSO-d_6) 176.6, 148.2, 139.6, 132.0, 130.2, 128.9, 125.8, 121.9, 71.8 (3C), 50.9 (3C), 14.2; δ_P (121 MHz, DMSO-d_6) -50.9 ppm; *m/z* (ESI) 625.0221 (100%, M^+); (Found: $C_{15}H_{22}AuBrN_6PS$ requires M^+, 626.2847); Found: C, 28.2; H, 3.47; N, 12.4; S, 6.47%; Calc. for $C_{15}H_{22}AuBrN_6PS$: C, 28.8; H, 3.54; N, 13.4; S, 5.12%.

(4-*Dichloroacetophinone-thiosemicarbazone*-κ*S*)(1,3,5-*triaza*-7-*phosphatricyclo*[3.3.1.1^{3,7}]*decane*-κ*P*)*gold*(I), 4.29c

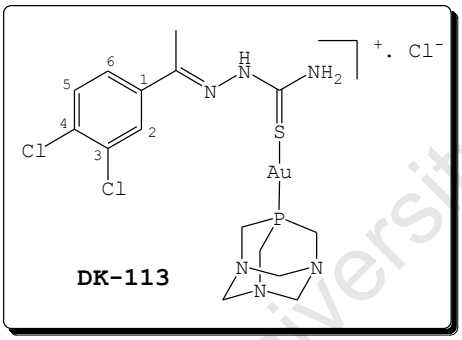

Light-yellow solid (0.041 g, 81%); m.p. 119-121 °C; ν_{max} (KBr)/cm^{-1} 3242w, 3133w (NH), 1601s (C=N), 1525s (C=C), 1281s (C=S), 1241s (C-N), 972s (P-C), 785m (CS, thioamide), 324m (Au-S); δ_H (300 MHz, DMSO-d_6) 10.33 (1H, s, NH), 8.24 (3H, s, H2, NHH), 7.88 (1H, d, *J* 8.4 Hz, H6), 7.61 (1H, d, *J* 8.7 Hz, H5), 4.55 (2H, s, NCH_2N), 4.51 (2H, s, NCH_2N), 4.39 (2H, s, NCH_2N), 4.34 (6H, s, NCH_2P), 2.30 (3H, s, CH_3); δ_C (75 MHz, DMSO-d_6) 177.6, 146.8, 137.8, 131.7, 131.2, 130.1, 128.2, 126.7, 71.8 (3C), 51.1 (3C), 13.8; δ_P (121 MHz, DMSO-d_6) -50.9 ppm; *m/z* (ESI) 615.0338 (100%, M^+); (Found: M^+, 615.0338. $C_{15}H_{21}AuCl_2N_6PS$ requires M^+, 616.2788); Found: C, 28.6; H, 3.31; N, 11.5; S, 6.21%; Calc. for $C_{15}H_{21}AuCl_2N_6PS$: C, 29.2; H, 3.43; N, 11.5; S, 5.20%.

(3-*Bromopropiohenone-thiosemicarbazone*-κ*S*)(1,3,5-*triaza*-7-*phosphatricyclo*[3.3.1.1^{3,7}]*decane*-κ*P*)*gold*(I), 4.29d

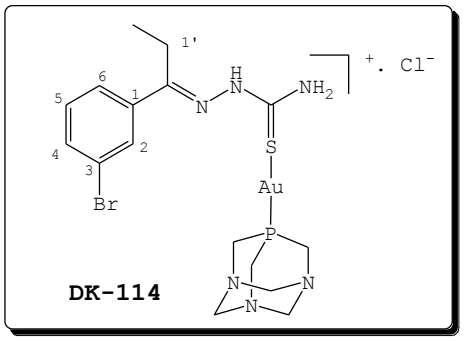

DK-114

Light yellow solid (0.044 g, 83%); m.p. 99-101 °C; ν_{max} (KBr)/cm^{-1} 3371w, 3242w (NH), 1598s (C=N), 1525s (C=C), 1279s (C=S), 1241s (C-N), 972s (P-C), 795s (CS, thioamide), 332m (Au-S); δ_H (300 MHz, DMSO-d_6) 10.45 (1H, s, NH), 8.34 (2H, br, NHH), 8.13 (1H, s, H2), 7.86 (1H, d, *J* 7.8 Hz, H6), 7.58 (1H, d, *J* 8.1 Hz, H4), 7.36 (1H, t, *J* 7.8 Hz, H5), 4.55 (2H, s, NCH_2N), 4.51 (2H, s, NCH_2N), 4.39 (2H, s, NCH_2N), 4.34 (6H, s, NCH_2P), 2.88 (2H, q, *J* 7.5 Hz, H1'), 1.02 (3H, t, *J* 7.2 Hz, CH_3); δ_C (75 MHz, DMSO-d_6) 176.4, 152.3, 138.1, 131.6, 129.9, 128.7, 125.4, 121.6, 71.5 (3C), 50.7 (3C), 19.0, 10.3; δ_P (121 MHz, DMSO-d_6) -50.9 ppm; *m/z* (ESI) 639.0355 (100%, M^+); (Found: M^+, 639.0355. $C_{16}H_{24}AuBrN_6PS$ requires M^+, 640.3113); Found: C, 29.7; H, 3.72; N, 11.9; S, 6.98; Calc. for $C_{16}H_{24}AuBrN_6PS$: C, 30.0; H, 3.78; N, 13.1; S, 5.01.

(3,4-*Dichloroacetophinone-thiosemicarbazone*-κS)(1,3,5-*triaza*-7-*phosphatricyclo*[3.3.1.1^{3,7}]*decane*-κ*P*)*gold*(I), 4.29e

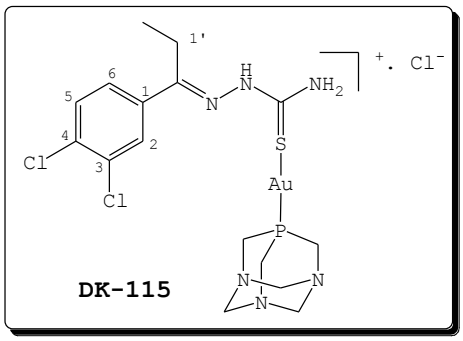

DK-115

Tan pellets (0.042 g, 80%); m.p. 109-112 °C; ν_{max} (KBr)/cm^{-1} 3371w, 3242w, 3145w (NH), 1603s (C=N), 1525s (C=C), 1279s (C=S), 1241s (C-N), 972s (P-C), 802w (CS, thioamide), 329m (Au-S); δ_H (300

MHz, DMSO-d_6) 10.45 (1H, s, NH), 8.34 (2H, br, NHH), 8.21 (1H, s, H2), 7.86 (1H, d, *J* 8.4 Hz, H6), 7.62 (1H, d, *J* 8.4 Hz, H5), 4.55 (2H, s, NCH_2N), 4.51 (2H, s, NCH_2N), 4.39 (2H, s, NCH_2N), 4.34 (6H, s, NCH_2P), 2.88 (2H, q, *J* 7.2 Hz, H1'), 1.01 (3H, t, *J* 7.5 Hz, CH_3); δ_C (75 MHz, DMSO-d_6) 177.4, 151.0, 136.8, 131.7, 131.4, 130.2, 128.3, 126.8, 71.8 (3C), 51.1 (3C), 19.1, 10.5; δ_P (121 MHz, DMSO-d_6) -50.9 ppm; *m/z* (ESI) 629.0517 (100%, M^+); (Found: M^+, 629.0517. $C_{16}H_{23}AuCl_2N_6PS$ requires M^+, 630.3053); Found: C, 30.9; H, 3.77; N, 11.9; S, 6.43%; Calc. for $C_{16}H_{23}AuCl_2N_6PS$: C, 30.5; H, 3.68; N, 13.3; S, 5.09%.

(3-*Hydroxy*-4-*methoxyformyl*-*thiosemicarbazone*-κ*S*)(1,3,5-*triaza*-7-*phosphatricyclo*[3.3.1.1^{3,7}]*decane*-κ*P*)*gold*(I), 4.29f

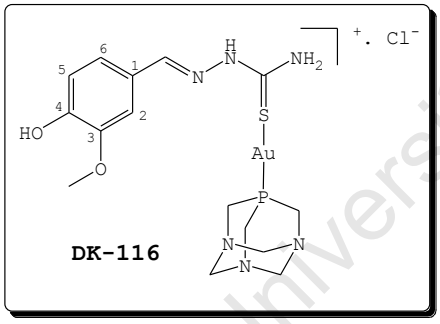

Yellow solid (0.047 g, 98%); m.p. 165-168 °C; ν_{max} (KBr)/cm^{-1} 3120m (NH), 1596s (C=N), 1512s (C=C), 1281s (C=S), 1236m (C-N), 970s (P-C), 798s (CS, thioamide), 324s (Au-S); δ_H (300 MHz, DMSO-d_6) 11.23 (1H, s, NH), 9.34 (1H, s, OH), 7.98 (1H, s, HC=N), 7.93 (2H, s, NHH), 7.45 (1H, d, *J* 1.5 Hz, H2), 7.06 (1H, dd, *J* 1.5 and 8.1 Hz, H6), 6.79 (1H, d, *J* 8.1 Hz, H5); 4.55 (2H, s, NCH_2N), 4.51 (2H, s, NCH_2N), 4.39 (2H, s, NCH_2N), 4.35 (6H, s, NCH_2P), 3.83 (3H, s, OCH_3); δ_C (101 MHz, DMSO-d_6) 175.9, 148.7, 143.5, 125.1, 122.2, 114.9, 109.2, 107.6, 71.5 (3C), 55.5, 50.7 (3C); δ_P (121 MHz, DMSO-d_6) -50.9 ppm; *m/z* (ESI) 579.1021 (100%, M^+); (Found: M^+, 579.1021 $C_{15}H_{22}AuBrN_6PS$ requires M^+, 579.3874); Found: C, 29.5; H, 4.21; N, 13.1; S,

5.11; Calc. for $C_{15}H_{23}AuN_6O_2$: C, 29.3; H, 3.77; N, 13.7; S, 5.22.

(*Ferronylcarboxaldehyde-thiosemicarbazone*-κS)(1,3,5-*triaza*-7-*phosphatricyclo*[3.3.1.1^{3,7}]*decane*-κ*P*)*gold*(I), 4.29g

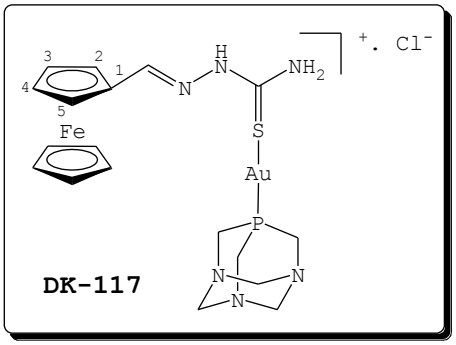

Red solid (0.051 g, 96%); m.p. 153-155 °C; ν_{max} (KBr)/cm^{-1} 3078m, (NH), 1595s (C=N), 1560m (C=C), 1279s (C=S), 1239s (C-N), 968s (P-C), 816s (CS, thioamide), 323m (Au-S); δ_H (300 MHz, DMSO-d_6) 11.17 (1H, s, NH), 7.94 (1H, s, HC=N), 7.59 (2H, br, NHH), 4.72 (2H, s, H2/H5), 4.55 (2H, s, NCH_2N), 4.51 (2H, s, NCH_2N), 4.42 (2H, s, H3/H4), 4.39 (2H, s, NCH_2N), 4.35 (6H, s, NCH_2P), 4.20 (5H, s, Cp); δ_C (101 MHz, DMSO-d_6) 175.7, 144.6, 78.7, 71.9 (3C), 70.1 (2C), 68.9 (5C), 67.7 (2C), 51.0 (3C); δ_P (121 MHz, DMSO-d_6) -50.9 ppm; *m/z* (ESI) 641.0628 (100%, M^+); (Found: M^+, 641.0628. $C_{18}H_{25}AuFeN_6PS$ requires M^+, 641.2816), Found: C, 32.6; H, 3.96; N, 11.3; S, 4.68%; Calc. for $C_{18}H_{25}AuClFeN_6PS.CH_3OH$: C, 32.2; H, 4.12; N, 11.9; S, 4.52%.

(*Ferronylcarboxaldehyde-thiosemicarbazone*-κS)(1,3,5-*triaza*-7-*phosphatricyclo*[3.3.1.1^{3,7}]*decane*-κ*P*)*gold*(I), 4.29h

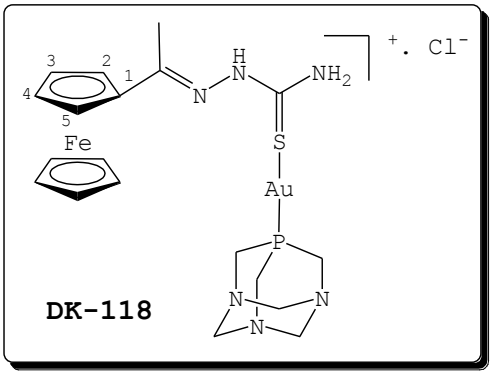

Red-brown solid (0.038 g, 70%); m.p. 96-98 °C; ν_{max} (KBr)/cm^{-1} 3365w, 3248w (NH), 1589s (C=N), 1533s (C=S), 1280 (C=S), 1240s (C=S), 972s (P-C), 820s (CS, thioamide), 327m (Au-S); δ_H (300 MHz, DMSO-d_6) 10.14 (1H, s, NH), 8.24 (1H, s, NHH), 7.79 (1H, s, NHH), 4.79 (2H, d, *J* 9.6 Hz, H2/H5), 4.56 (2H, s, NCH_2N), 4.52 (2H, s, NCH_2N), 4.39 (2H, s, NCH_2N), 4.35 (6H, s, NCH_2P), 4.24 (2H, s, H3/H4), 4.18 (5H, s, Cp), 2.22 (3H, s, CH_3); δ_C (75 MHz, DMSO-d_6) 177.1, 149.0, 71.7, 69.5, 69.3 (2C), 68.7 (5C), 67.0, 50.8, 14.8; δ_P (121 MHz, DMSO-d_6) -50.8 ppm; *m/z* (ESI) 655.0770 (100%, M^+); (Found: M^+, 655.0770. $C_{19}H_{27}AuFeBrN_6PS$ requires M^+, 655.30189).

***(3-(3-Bromophenyl)-2-pyrazoline-1-thiocarboxamide*-κS)(1,3,5-*triaza*-7-*phosphatricyclo*[3.3.1.1^{3,7}]*decane*-κ*P*)*gold*(I), 4.30a**

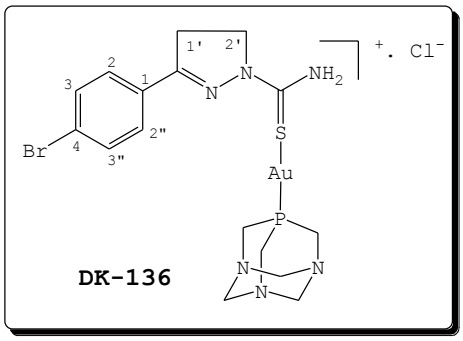

Tan solid (0.060 g, 50%); m.p. 138-140 °C; ν_{max} (KBr)/cm^{-1} 3246w, 3053w (NH), 1589s (C=N), 1533s, 1481s (C=C), 972s (P-C), 801s (C=S), 392m (Au-S); δ_H (300 MHz, DMSO-d_6) 7.99 (2H, br, NHH), 7.78 (2H, d, *J* 8.0 Hz, H2/H2″), 7.66 (2H, d, *J* 8.4 Hz, H3/H3″), 4.53 (2H, s, NCH_2N), 4.50 (2H, s, NCH_2N), 4.37 (2H, s,

NCH_2N), 4.34 (6H, s, NCH_2P), 4.15 (2H, t, *J* 10.0 Hz, H2′), 3.27 (2H, m, H1′); δ_C (100.6 MHz, DMSO-d_6) 176.3, 156.6, 132.1 (2C), 131.6, 130.9, 129.3 (2C), 72.3 (3C), 51.5 (3C), 49.0, 32.2; δ_P (121 MHz, DMSO-d_6) -51.1 ppm; *m/z* (ESI) 637.0228 (96%, M^+); (Found: M^+, 637.0228. $C_{16}H_{22}AuBrN_6PS$ requires M^+, 637.0213); Found: C, 31.1; H, 3.55; N, 11.1; S, 4.59%; Calc. for $C_{16}H_{22}AuBrN_6PS.2CH_3OH$: C, 30.5; H, 3.91; N, 12.5; S, 4.78%.

***(3-(3-Chlorophenyl)-2-pyrazoline-1-thiocarboxamide-κS)(1,3,5-triaza-7-phosphatricyclo[3.3.1.1^{3,7}]decane-κP) gold*(I), 4.30b**

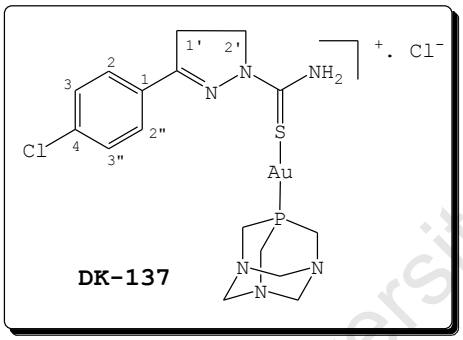

Tan solid (0.089 g, 67%); m.p. 112-114 °C; ν_{max} (KBr)/cm^{-1} 3247m, 3145w (NH), 1595s (C=N), 1538m, 1481s (C=C), 1364s (C-N), 973s (P-C), 801s, 740s (C=S), 392m (Au-S); δ_H (400 MHz, DMSO-d_6) 8.09 (2H, br, NHH), 7.85 (2H, d, *J* 8.0 Hz, H2/H2″), 7.53 (2H, d, *J* 8.0 Hz, H3/H3″), 4.53 (2H, s, NCH_2N), 4.50 (2H, s, NCH_2), 4.37 (2H, s, NCH_2N), 4.34 (6H, s, NCH_2P), 4.16 (2H, t, *J* 10.0 Hz, H2′), 3.29 (2H, t, *J* 10.4 Hz, H1′); δ_C (100.6 MHz, DMSO-d_6) 175.4, 156.0, 134.9, 129.9, 128.6 (2C), 128.5 (2C), 71.8 (3C), 50.9 (3C), 48.4, 31.6; δ_P (161.9 MHz, DMSO-d_6) -51.1 ppm; *m/z* (ESI) 593.07 (100%, M^+); (Found: M^+, 593.07. $C_{16}H_{22}AuClN_6PS$ requires M^+, 590.07); Found: C, 33.7; H, 3.99; N, 13.3; S, 5.95%; Calc. for $C_{16}H_{22}AuClN_6PS.CH_3OH$: C, 32; H, 4.19; N, 13.4; S, 5.12%.

(3-(3,4-Dichlorophenyl)-2-pyrazoline-1-thiocarboxamide-κS) **(1,3,5-*triaza*-7-*phosphatricyclo*[3.3.1.1^{3,7}]*decane*-κ*P*)*gold*(I), 4.30c**

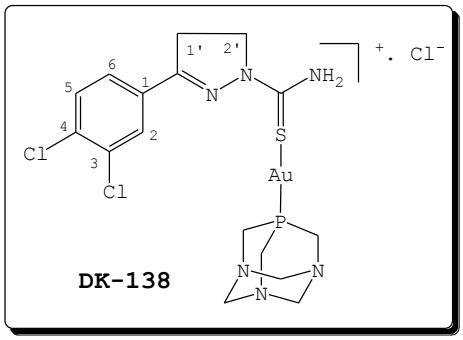

DK-138

Yellow solid (0.072 g, 60%); m.p.120-122 °C; ν_{max} (KBr)/cm^{-1} 3247m, 3140w (NH), 1591s (C=N), 1547m, 1461s (C=C), 1365s (C-N), 973s (P-C), 802s (C=S), 394w (Au-S); δ_H (300 MHz, DMSO-d_6) 8.15 (2H, s, H2), 7.92 (2H, br, NHH), 7.78-7.30 (2H, m, H5/H6), 4.55 (2H, s, NCH_2N), 4.51 (2H, s, NCH_2N), 4.38 (2H, s, NCH_2N), 4.34 (6H, s, NCH_2P), 4.18 (2H, t, *J* 10.5 Hz, H2′), 3.29 (2H, t, *J* 10.2 Hz, H1′); δ_C (75 MHz, DMSO-d_6) 175.9, 154.7, 132.5, 131.9, 131.5, 130.7, 128.2, 126.8, 71.8 (3C), 50.8 (3C), 48.5, 31.4; δ_P (121 MHz, DMSO-d_6) -50.9 ppm; *m/z* (ESI) 627.03 (100%, M^+); (Found: M^+, 627.03. $C_{16}H_{21}AuCl_2N_6PS$ requires M^+, 624.05); Found: C, 33.6; H, 3.51; N, 11.9; S, 5.52%; Calc. for $C_{16}H_{21}AuCl_2N_6PS$: C, 30.6; H, 3.37; N, 13.4; S, 5.10%.

G. General Procedure for the Synthesis of Et_3P Gold(I) TSC Complexes 4.31a-f

A solution of **3.28a** (0.050 g, 0.18 mmol) in anhydrous MeOH (5 cm^3) was reacted with Et_3PAuCl (0.065 g, 0.19 mmol) at ambient temperature.[19] After stirring the mixture for 4 h under nitrogen, the colourless solution was filtered through celite and solvent removed to give a semi solid residue, which was dried *in vacuo* to afford an off-white solid.

(4-*Bromoacetophinone-thiosemicarbazone*-κS)
(*triethylphosphine*)*gold*(I)*chloride*, 4.31a

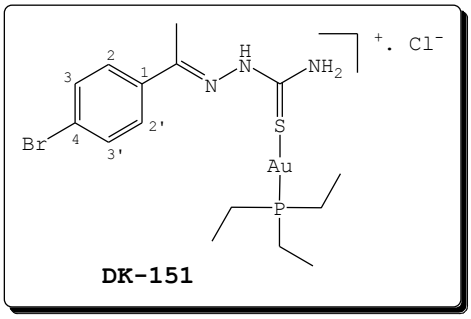

DK-151

Off-white solid (0.11 g, 92%); m.p. 45-47 °C; ν_{max} (KBr)/cm^{-1} 3237w ν(NH), 1587s ν(C=N), 1523s ν(C=C), 1265br, 828s ν(C=S, thioamide), 349m ν(Au-S); δ_H (300 MHz, DMSO-d_6) 10.21 (1H, s, NH), 8.37 (1H, br, N*H*H), 8.05 (1H, br, NH*H*), 7.87 (2H, d, *J* 8.7 Hz, H2/H2'), 7.55 (2H, d, *J* 8.7 Hz, H3/H3'), 2.29 (3H, s, CH_3), 1.97 (6H, m, P*CH*$_2$CH$_3$), 1.09 (9H, m, PCH$_2$*CH*$_3$); δ_P (121.5 MHz, DMSO-d_6) 35.2 ppm, *m*/z (ESI) 586.0344 (8%, M^+); (Found: M^+, 586.0344. $C_{15}H_{25}AuBrN_3PS$ requires M^+, 587.2884), 315.0520 (58%, Et_3PAu^+); Found: C, 27.2; H, 4.10; N, 5.38; S, 4.86; Calc. for $C_{15}H_{25}AuBrClN_3PS.2H_2O$: C, 27.4; H, 4.44; N, 6.38; S, 4.86.

(3-*Bromoacetophinone-thiosemicarbazone*-κS)
(*triethylphosphine*)*gold*(I), 4.31b

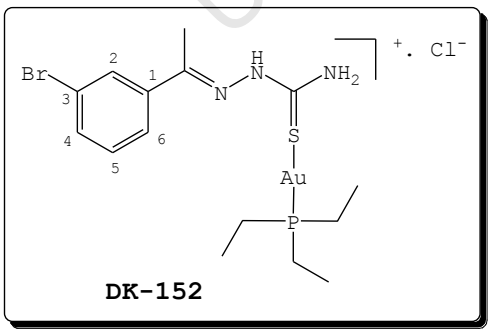

DK-152

Off white solid (0.12 g, 100%); m.p. 35-37 °C; ν_{max} (KBr)/cm^{-1} 3389w, 3237w ν(NH), 1601s ν(C=N), 1522s ν(C=C), 1264s ν(C=S), 839s ν(CS); δ_H (300 MHz, DMSO-d_6) 10.41 (1H, s, NH), 8.54 (1H, br, N*H*H), 8.28 (1H, br, NH*H*), 8.19 (1H, s, H2), 7.89 (1H, d, *J* 8.0 Hz, H6), 7.58 (1H, d, *J* 8.8 Hz, H4), 7.34 (1H, t, *J* 8.0 Hz, H5), 2.31 (3H, s, CH_3), 1.92 (6H, m, P*CH*$_2$CH$_3$), 1.09 (9H, m,

PCH_2CH_3); δ_P (161.9 MHz, DMSO-d_6) 35.2 ppm, *m/z* (ESI) 586.0369 (27%, M^+), 315.0531 (33%, Et_3PAu^+); Found: C, 27.7; H, 4.05; N, 5.28; S, 5.43; Calc. for $C_{15}H_{25}BrClN_3PS.2H_2O$: C, 27.4; H, 4.44; N, 6.38; S, 4.87.

(3,4-*Dichoroacetophinone-thiosemicarbazone*-κS) (*triethylphosphine*)*gold*(I), 4.31c

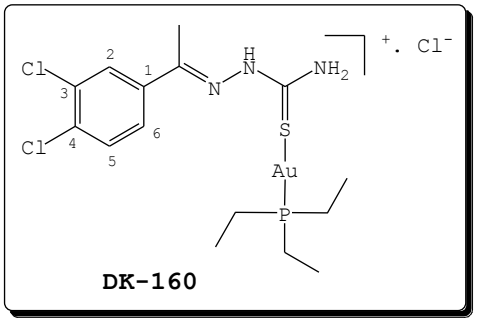

DK-160

White solid (0.12 g, 100%); m.p.53-55 °C; ν_{max} (KBr)/cm^{-1} 3236w ν(NH), 1603s ν(C=N), 1523s ν(C=C), 1297s ν(C=S), 821m ν(CS); δ_H (400 MHz, DMSO-d_6) 10.48 (1H, s, NH), 8.54 (1H, br, N*H*H), 8.32 (1H, br, NH*H*), 8.28 (1H, s, H2), 7.89 (1H, d, *J* 7.6 Hz, H6), 7.63 (1H, d, *J* 8.4 Hz, H5), 2.31 (3H, s, CH_3), 1.92 (6H, m, PCH_2CH_3), 1.09 (9H, m, PCH_2CH_3); δ_P (161.9 MHz, DMSO-d_6) 35.1 ppm, *m/z* (ESI) 576.0489 (53%, M^+); (Found: M^+, 576.0489. $C_{15}H_{24}AuCl_3N_3PS$ requires M^+, 577.2825), 315.0546 (23%, Et_3PAu^+); Found: C, 28.8; H, 3.88; N, 5.64; S, 5.60; Calc. for $C_{15}H_{24}AuCl_3N_3PS$: C, 29.4; H, 3.95; N, 6.86; S, 5.23.

(3-*Bromopropiophinone-thiosemicarbazone*-κS) (*triethylphosphine*)*gold*(I), 4.31d

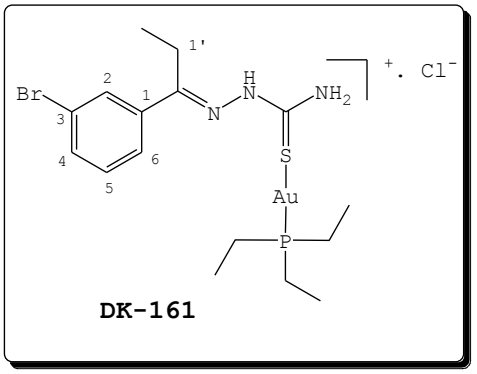

DK-161

White solid (0.11 g, 98%); ν_{max} (KBr)/cm^{-1} 3230w ν(NH), 1603s, 1568s ν(C=N), 1523s ν(C=C), 1266s ν(C=S), 774s ν(CS); δ_H (400 MHz, DMSO-d_6) 10.38 (1H, s, NH), 8.32

(2H, br, N*H*H), 8.14 (1H, s, H2), 7.86 (1H, d, *J* 8.0 Hz, H6), 7.56 (1H, d, *J* 8.8 Hz, H4), 7.35 (1H, t, *J* 8.0 Hz, H5), 2.86 (2H, q, *J* 7.6 Hz, H1'), 1.92 (6H, m, P*CH*$_2$CH$_3$), 1.09 (12H, m, PCH$_2$*CH*$_3$) 1.0 (3H, t, *J* 7.2 Hz, CH$_3$); δ_P (161.9 MHz, DMSO-d_6) 35.1 ppm, *m/*z (ESI) 602.0474 (70%, M^+); (Found: M^+, 602.0474. $C_{16}H_{27}AuBrN_3PS$ requires *M*$^+$, 601.3150), 315.0550 (35%, Et_3PAu^+); Found: C, 29.8; H, 4.26; N, 5.99; S, 5.69; Calc. for $C_{16}H_{27}AuBrN_3PS.H_2O$: C, 29.4; H, 4.46; N, 6.42; S, 4.90.

(3,4-*Dichloropropiophinone-thiosemicarbazone*-κS) (*triethylphosphine*)*gold*(I), 4.31e

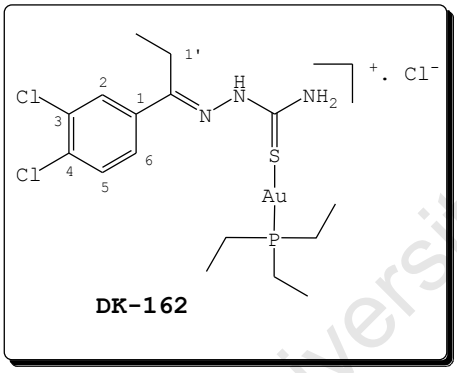

DK-162

White solid (0.11 g, 99%); m.p. 47-49 °C; ν_{max} (KBr)/cm^{-1} 3218w, ν(NH), 1603s ν(C=N), 1524s ν(C=C), 1272m ν(C=S), 825s ν(CS); δ_H (400 MHz, DMSO-d_6) 10.59 (1H, s, NH), 8.55 (1H, br, N*H*H), 8.32 (1H, br, NH*H*), 8.25 (1H, s, H2), 7.88 (1H, d, *J* 8.4 Hz, H6), 7.63 (1H, d, *J* 8.4 Hz, H5), 2.88 (2H, q, *J* 7.2 Hz, H1'), 1.92 (6H, m, P*CH*$_2$CH$_3$), 1.09 (9H, m, PCH$_2$*CH*$_3$), 1.00 (3H, t, *J* 7.6 Hz, CH$_3$); δ_P (161.9 MHz, DMSO-d_6) 35.1 ppm, *m/*z (ESI) 590.0621 (55%, M^+); (Found: M^+, 590.0621. $C_{16}H_{26}AuCl_2N_3PS$ requires *M*$^+$, 591.3091), 315.0584 (29%, Et_3PAu^+); Found: C, 29.6; H, 4.11; N, 5.10; S, 5.21; Calc. for $C_{16}H_{26}AuCl_2N_3PS.H_2O$: C, 29.8; H, 4.38; N, 6.52; S, 4.97.

(Formyl ferrone-*thiosemicarb*-κS)(*triethylphosphine*)*gold*(I), 4.31f

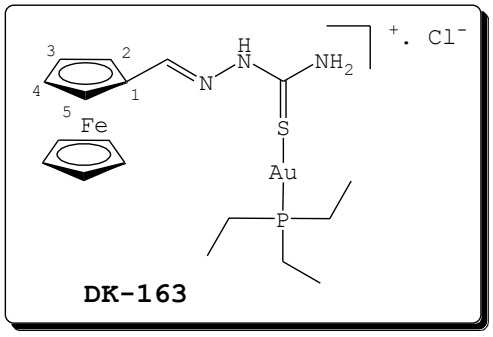

Red solid (0.12 g, 100%); m.p. 75-77 °C; ν_{max} (KBr)/cm^{-1} 3399w, 3237w ν(NH), 1594s ν(C=N), 1552s ν(C=C), 1276s ν(C=S), 821s ν(CS); δ_H (400 MHz, DMSO-d_6) 11.19 (1H, s, NH), 8.01 (1H, br, N*H*H), 7.91 (1H, s, HC=N), 7.61 (1H, br, NH*H*), 4.72 (2H, s, H2/H5), 4.41 (2H, s, H3/H4), 1.93 (6H, m, P*CH*$_2$CH$_3$), 1.10 (9H, m, PCH$_2$*CH*$_3$); δ_P (161.9 MHz, DMSO-d_6) 35.3 ppm; *m/*z (ESI) 602.0744 (100%, M$^+$); (Found: M$^+$, 602.0744. $C_{18}H_{28}AuFeN_3PS$ requires *M*$^+$, 602.2853), 315.0255 (20%, Et_3PAu^+); Found: C, 34.1; H, 4.46; N, 5.91; S, 4.50; Calc. for $C_{18}H_{28}AuClFeN_3PS$: C, 33.9; H, 4.43; N, 6.59; S, 5.03.

(4-*Chloroacetophinone-thiosemicarbazone*-κS) (*triethylphosphine*)*gold*(I), 4.32

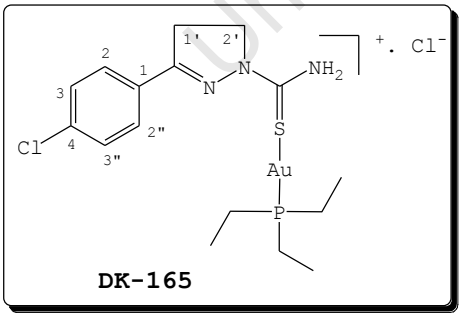

Yellow solid (0.12 g, 98%); m.p. 46-48 °C; ν_{max} (KBr)/cm^{-1} 3250w ν(NH), 1588s ν(C=N), 1538m ν(C=C), 1379s ν(C-N), 1251s ν(C=S), 771s ν(CS); δ_H (400 MHz, DMSO-d_6) 7.93 (2H, br, NH*H*), 7.78 (2H, d, *J* 8.4 Hz, H2/H2″), 7.66 (2H, d, *J* 8.4 Hz, H3/H3″), 4.15 (2H, t, *J* 9.6 Hz, H2′), 3.29 (2H, t, *J* 9.6 Hz, H1′), 1.92 (6H, m, P*CH*$_2$CH$_3$), 1.09 (9H, m, PCH$_2$*CH*$_3$); δ_P (161.9 MHz, DMSO-d_6) 35.1 ppm, *m/*z (ESI) 554.0851 (100%, M$^+$); (Found: M$^+$, 554.0851.

$C_{16}H_{25}AuCl_2N_3PS$ requires M^+, 554.8481), 315.0560 (33%, Et_3PAu^+); Found: C, 32.9; H, 4.52; N, 6.49; S, 5.43; Calc. for $C_{16}H_{25}AuCl_2N_3PS$: C, 32.6; H, 4.27; N, 7.12; S, 5.43.

(3-*Bromoacetophinone-thiosemicarbazone-*κS)(*triethylphosphine*)*gold*(I), 4.33

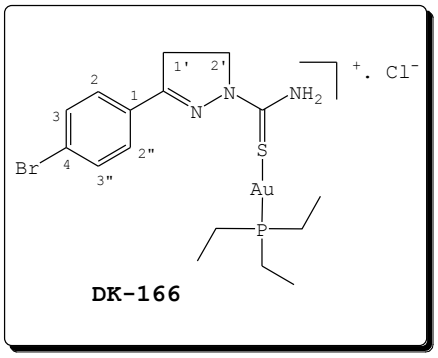

DK-166

Yellow solid (0.12 g, 95%); m.p. 53-55 °C; ν_{max} (KBr)/cm^{-1} 3250w, 3116s ν(NH), 1593s ν(C=N), 1538s ν(C=C), 1388s ν(C-N), 1257s ν(C=S), 773s ν(CS); δ_H (400 MHz, DMSO-d_6) 7.93 (1H, s, N*H*H), 7.83 (2H, d, *J* 8.4 Hz, H2/H2”), 7.75 (1H, br, NH*H*), 7.50 (2H, d, *J* 8.4 Hz, H3/H3”), 4.13 (2H, t, *J* 9.6 Hz, H2’), 3.27 (2H, t, *J* 9.6 Hz, H1’), 1.90 (6H, m, P*CH*$_2$CH$_3$), 1.07 (9H, m, PCH$_2$*CH*$_3$); δ_P (161.9 MHz, DMSO-d_6) 35.2 ppm, *m/*z (ESI) 598.0349 (100%, M^+); (Found: M^+, 598.0349. $C_{18}H_{28}AuBrN_3PS$ requires M^+, 599.2991), 315.0538 (42%, Et_3PAu^+); Found: C, 32.0; H, 4.66; N, 6.34; S, 5.18; Calc. for $C_{16}H_{25}AuBrN_3PS$: C, 32.1; H, 4.20; N, 7.01; S, 5.35.

Synthesis of Tetrahydrothiophene Gold(I) Pentafluorophenyl 4.34

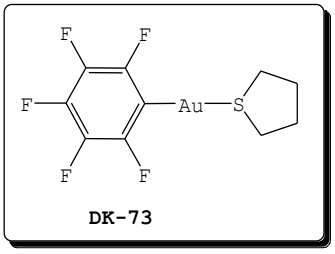

DK-73

A solution of bromopentafluorobenzene (0.50 g, 2.04 mmol) in freshly distilled diethyl ether (20 cm^3) was treated with *n*-butyllithium in hexane (2.5 M, 2.04 mmol) at -78 °C. The resulting mixture was stirred for 1 h upon which **4.3** (0.66 g, 2.05 mmol) was

added and the mixture stirred for further 15 minutes at -78 °C.[13] The mixture was allowed to warm to -30 °C over 30 minutes interval. After 15 minutes at -30 °C the cooler was removed and the white suspension stirred for additional 20 minutes. The solution was filtered through $MgSO_4$ and solvent evaporated *in vacuo* to yield **4.34** (934.3 mg, 90%) as a white solid.[13] Found: C, 26.2; H 1.89; Calc. for $C_{10}H_8AuF_5S$: C, 26.6; H, 1.78%.

H. General Procedure for the Synthesis of Pentaflourobenzyl gold(I) TSC Complexes 4.38a-f

A solution of **4.34** (0.51 g, 0.11 mmol) in DCM (15 cm^3) was treated with **3.28a** (0.30 g, 0.11 mmol) at ambient temperature.[20] The resulting clear solution was stirred for 1 h followed and then filtered through celite. The solvent was concentrated to give a white residue. Drying the residue *in vacuo* afforded the desired gold(I) complex as a yellow solid.

***(4-Bromoacetophenone-thiosemicarbazone-κS)(pentafluorobenzyl)gold*(I), 4.38a**

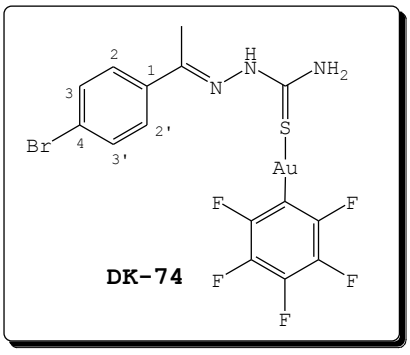

Yellow solid (0.077 g, 100%); m.p. 155-156 °C; ν_{max} (KBr)/cm^{-1} 3492m, 3373s (NH_2), 3262m (NH), 1593s (C=N), 1525s (C=C), 1486s δ(NSC), 1271m (C=S), 797m (CS, thioamide); δ_H (300 MHz, DMSO-d_6) 10.85 (1H, br s, NH), 9.15 (1H, br, N*H*H), 8.88 (1H, br, NH*H*), 7.95 (2H, d, *J* 8.4 Hz, H2/H2′), 7.60 (2H, d, *J* 8.7

Hz, H3/H3′), 2.36 (3H, s, CH_3); *m/z* (ESI) 467.95 (8%, $TSCAu^+$) ; Found: C, 29.0; H, 1.99; N, 5.54; S, 5.05; Calc. for $C_{15}H_{10}AuBrF_5N_3S$: C, 28.3; H, 1.58; N, 6.60; S, 5.04.

(3-*Bromoacetophenone-thiosemicarbazone*-κS)
(*pentafluorobenzyl*)*gold*(I), 4.38b

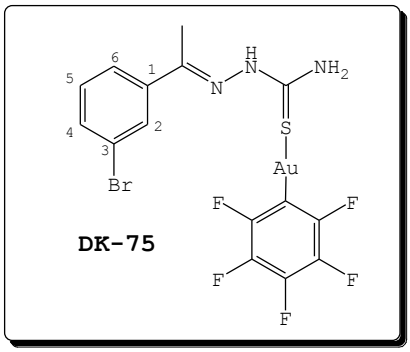

Yellow solid (0.073 g, 100%); m.p. 145-146 °C; ν_{max} (KBr)/cm^{-1} 3429s, 3380m, (NH), 3269m (NH), 1591s (C=N), 1519s (C=C), 1270s (C=S), 839m (CS, thioamide), 321w (Au-S); δ_H (300 MHz, DMSO-d_6) 10.80 (1H, br s, NH), 8.95 (2H, br, NHH), 8.23 (1H, s, H2), 7.93 (1H, d, *J* 7.8 Hz, H6), 7.62 (1H, d, *J* 7.5 Hz, H4), 7.37 (1H, d, *J* 7.8 Hz, H5), 2.36 (3H, s, CH_3); *m/z* (ESI) 467.94 (10%, $TSCAu^+$); Found: C, 28.5; H, 1.74; N, 5.83; S, 5.59; Calc. for $C_{15}H_{10}AuBrF_5N_3S$: C, 28.3; H, 1.58; N, 6.60; S, 5.04.

(3,4-*Dichloroacetophenone-thiosemicarbazone*-κS)
(*pentafluorobenzyl*)*gold*(I), 4.38c

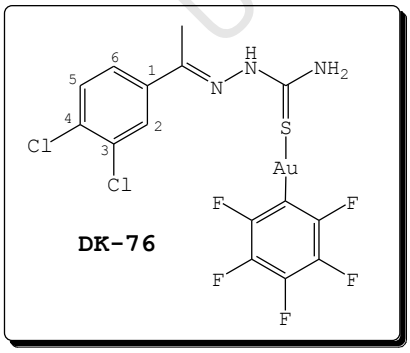

Yellow-organge solid (0.073 g, 100%); m.p. 160-161 °C; ν_{max} (KBr)/cm^{-1} 3429w, 3381s (NH), 3257m (NH), 1593s (C=N), 1517s (C=C), 1256s (C=S), 795sh (CS, thioamide), 319m (Au-S); δ_H (300 MHz, DMSO-d_6) 10.87 (1H, br, NH), 9.14 (2H, br, NH), 8.31 (1H, s, H2), 7.93 (1H, d, *J* 8.7 Hz, H6), 7.65 (1H, d, *J* 8.7 Hz, H5), 2.36 (3H, s, CH_3); Found: C, 28.6; H, 1.52; N, 5.70; S, 5.37;

Calc. for $C_{15}H_9AuCl_2F_5N_3S$: C, 28.8; H, 1.45; N, 6.71; S, 5.72.

(3-*Bromopropiophenone-thiosemicarbazone*-κS)
(*pentafluorobenzyl*)*gold*(I), 4.38d

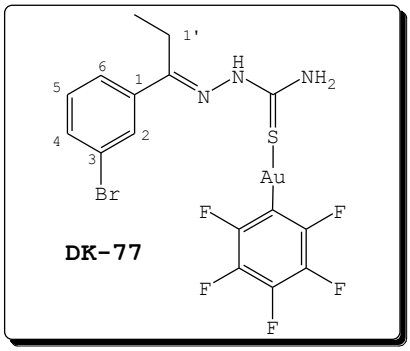

DK-77

Orange solid (0.062 g, 86%); m.p. 124-125 °C; ν_{max} (KBr)/cm^{-1} 3479m, 3360s (NH), 3284m (NH), 1587s (C=N), 1520s (C=C), 1268s (C=S), 797s (CS, thioamide), 371m (Au-S); δ_H (300 MHz, DMSO-d_6) 10.81 (1H, br s, NH), 8.85 (1H, br, NHH), 8.19 (1H, s, H2), 7.90 (1H, d, *J* 8.1 Hz, H6), 7.62 (1H, d, *J* 8.1 Hz, H4), 7.38 (1H, t, *J* 8.1 Hz, H5), 2.90 (2H, q, *J* 7.8 Hz, H1'), 1.04 (3H, t, *J* 7.8 Hz, CH_3); *m/*z (ESI) 650.97 (4%, M^+); (Found: M^+, 650.97. $C_{16}H_{12}AuBrF_5N_3S$ requires M^+ 650.21), 483.96 (12%, $TSCAu^+$); Found: C, 30.1; H, 1.80; N, 5.85; S, 6.61; Calc. for $C_{16}H_{12}AuBrF_5N_3S$: C, 29.6; H, 1.86; N, 6.46; S, 4.93.

(3,4-*Dichloropropiophenone-thiosemicarbazone*-κS)
(*pentafluorobenzyl*)*gold*(I), 4.38e

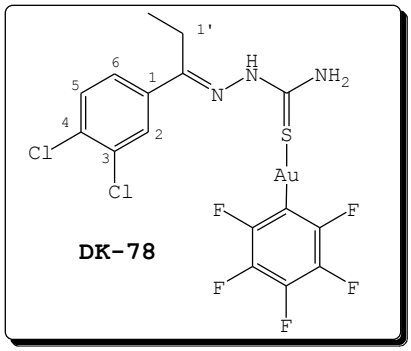

DK-78

White solid (0.073 g, 100%); m.p. 138-140 °C; ν_{max} (KBr)/cm^{-1} 3492m, 3373s (NH), 3262m (NH), 1593s (C=N), 1525s (C=C), 1271m (C=S), 797m (CS, thioamide); δ_H (400 MHz, DMSO-d_6) 10.88 (1H, br, NH), 8.92 (2H, br, NHH), 8.28 (1H, s, H2), 7.90 (1H, d, *J* 2.1 and 8.4 Hz, H6), 7.65 (1H, d, *J* 8.4 Hz, H5), 2.90 (2H, q, *J* 7.5 Hz, H1'),

1.03 (3H, t, *J* 7.5 Hz, CH_3); *m/*z (ESI) 471.97 (5%, $TSCAu^+$); Found: C, 31.1; H, 1.78; N, 5.82; S, 5.43; Calc. for $C_{16}H_{11}AuCl_2F_5N_3S$: C, 30.2; H, 1.73; N, 6.56; S, 5.01.

***(3-Hydroxy-4-methoxyformyl-thiosemicarbazone-κS)(pentafluorobenzyl)gold*(I), 4.38f**

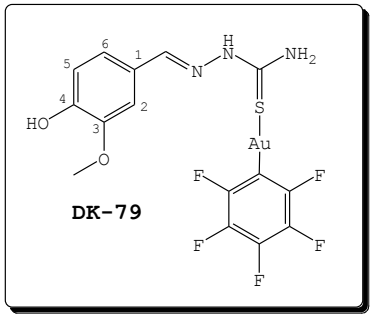

Yellow solid (0.077 g, 69%); ν_{max} (KBr)/cm^{-1} ; δ_H (300 MHz, DMSO-d_6) 12.02 (1H, br s, OH), 9.52 (1H, s, NH), 8.92 (1H, br s, N*H*H), 8.72 (1H, br s, NH*H*), 8.15 (1H, s, HC=N), 7.54 (1H, s, H2), 7.17 (1H, d, *J* 8.1 Hz, H6), 6.82 (1H, d, *J* 8.1 Hz, H5), 3.85 (3H, s, OCH_3); Found: C, 31.95; H, 1.82; N, 5.18; S, 5.50; Calc. for $C_{15}H_{10}AuBrF_5N_3S$: C, 30.57; H, 1.88; N, 7.13; S, 5.44.

Synthesis of [2-(Dimethylaminomethyl)phenyl]mercury(II)chloride 4.40

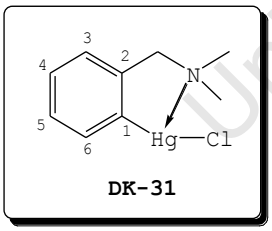

A solution of *N,N*-dimethylaminomethylbenzene (2.25 cm^3, 15.0 mmol) in dried Et_2O (20 cm^3) was treated with *t*-butylithium (2.5 M in hexane, 15.0 mmol), which was slowly added at 0 °C. The reaction mixture was allowed to warm to ambient temperature and stirred for 24 h under nitrogen. The mixture was cooled to -90 °C and $HgCl_2$ (4.05 g, 15.0 mmol) dissolved in THF (10 cm^3) was slowly added accompanied by the formation of a grey precipitate. After warming to ambient temperature, the resulting mixture was stirred 24 h. The yellow solution was filtered through

celite, solvent removed at reduced pressure to give a yellow semi-solid residue. Recrystallisation from pentane gave **4.40** (4.28 g, 77%) as a white-yellow crystals;[21,22] m.p. 67-68 °C (lit.[21] 76-77 °C); δ_H (400 MHz, $CDCl_3$) 7.39-7.31 (4H, m, ArH), 3.79 (2H, s, CH_2), 2.49 (6H, s, CH_3); Found: C, 28.51; H 3.57; N 3.11%; Calc for $C_9H_{12}ClHgN$: C, 29.20; H, 3.27; N, 3.78%.

Synthesis of methylammonium tetrachloroaurate 4.41

A mixture of **$H[AuCl_4].4H_2O$** (0.44 g, 1.08 mmol) and 32% HCl (6 cm^3) in water (10 cm^3) was cooled to 0 °C. A solution of Me_4NCl (0.12 g, 1.11 mmol) in water (2 cm^3) was slowly added with concomitant of a yellow precipitate. After 5 minutes, the yellow precipitate that formed was filtered, washed successively with water (5 cm^3) and Et_2O (5 cm^3). Drying the precipitate *in vacuo* afforded **4.41** (0.30 g, 68%) as a yellow powder;[23] Found: C, 11.9; H 3.98; N 3.14%; Calc. for $C_4H_{14}AuCl_4N.H_2O$: C, 11.3; H, 3.27; N, 3.25%.

Synthesis of
[2-(Dimethylaminomethyl)phenyl]gold(III)dichloride 2.15

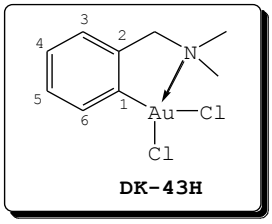

DK-43H

A mixture of **4.41** (0.20 g, 0.55 mmol), **4.40** (0.23 g, 0.56 mmol) and Me_4NCl (0.064 g, 0.58 mmol) in anhydrous acetonitrile (15 cm^3) was stirred at ambient temperature for 24 h. During this time a white precipitate, $Me_4N(Hg_2Cl_6)$, that formed was filtered and solvent evaporated to give a yellow solid residue. The residue was extracted with DCM (3 × 40 cm^3) and solvent evaporated to dryness. Drying the residue *in vacuo* afforded **2.15** (0.23 g,

95%) as a yellow solid;[24] m.p. 182-183 °C (lit. 185 °C); δ_H (300 MHz, $CDCl_3$) 7.63-7.54 (2H, m, ArH), 7.39-7.33 (2H, m, ArH), 4.43 (2H, s, CH_2), 3.34 (6H, s, NMe_2);[25] Found: C, 27.3; H, 3.17; N, 2.66; Calc. for $C_9H_{12}AuCl_2N.CH_2Cl_2$: C, 27.9; H, 3.52; N, 2.72.

I. General Procedure for the Synthesis of Mono-Gold(III) Chelates 4.42a-f

A solution of **3.28c** (0.021 g, 0.077 mmol) in dry acetone (20 cm^3) was treated with **2.15** (0.031 g, 0.077 mmol) at ambient temperature.[26] The mixture was allowed to reflux for 1 h; then stirred for further 5 h at ambient temperature. After the reaction, a yellow solution was filtered through celite and solvent concentrated to give yellow residue. Drying the residue *in vacuo* afforded **4.42a** as a yellow solid.

***Compound* 4.42a**

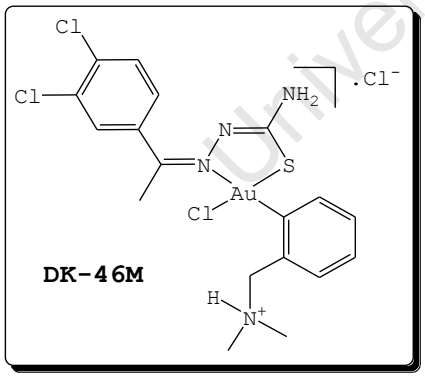

Yellow solid (0.050 g, 98%); m.p. 92-94 °C; ν_{max} (KBr)/cm^{-1} 3378w, 3060m ν(NH), 2667w ν(NH^+), 1624s, ν(C=N), 1547s ν(C=C), 798w ν(CS), 428w ν(Au-N), 357m ν(Au-S), 313s ν(Au-Cl); δ_H (300 MHz, DMSO-d_6) 10.35 (1H, br, $(CH_3)_2NH^+$), 8.27 (1H, s, H2), 7.90 (1H, d, *J* 8.1 Hz, H6), 7.64 (1H, d, *J* 8.4 Hz, H5), 7.51 (1H, m, ArH'), 7.27 (2H, m, ArH'), 7.15 (1H, m, ArH'), 4.62 (2H, s, CH_2), 3.20 (6H, s, $N(CH_3)_2$); *m/*z (ESI) 627.0275 (10%, M^+), (Found: M^+, 627.0275. $C_{18}H_{21}AuCl_3N_4S$ requires M^+, 627.0213), 591.0453 (100%, M^+-Cl); Found: C, 36.1; H, 4.04;

N, 7.40; S, 4.72; Calc. for $C_{18}H_{21}AuCl_3N_4S.(CH_3)_2CO$: C, 36.7; H, 3.96; N, 8.16; S, 4.72.

***Compound* 4.42b**

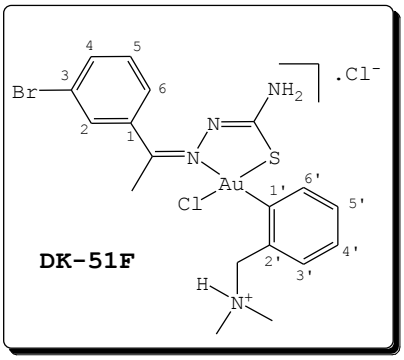

Yellow solid (0.081 g, 96%); m.p. 94-96°C; ν_{max} (KBr)/cm^{-1} 3277w, ν(NH), 1698s, 1625s ν(C=N), 1552s ν(C=C), 788s ν(CS), 426w ν(Au-N), 355w ν(Au-S), 329m ν(Au-Cl); δ_H (300 MHz, DMSO-d_6) 10.40 (1H, br s, NH$^+$), 8.19 (1H, s, H2), 7.90 (1H, d, *J* 7.5 Hz, H6), 7.61 (1H, d, *J* 7.2 Hz, H4), 7.48 (1H, m, ArH'), 7.36 (1H, t, *J*, 7.8 Hz, H5), 7.28 (2H, m, ArH'), 7.17-7.11 (1H, m, ArH'), 4.63 (2H, s, CH_2), 3.19 (6H, s, $N(CH_3)_2$), 2.34 (3H, s, CH_3); *m/z* (ESI) 637.0118 (8%, M$^+$); (Found: M$^+$, 637.0118. $C_{11}H_{22}AuBrClN_4S$ requires *M*$^+$, 637.0097), 601.0171 (100%, M$^+$-Cl); Found: C, 37.4; H, 4.49; N, 7.02; S, 4.38; Calc. for $C_{18}H_{22}AuBrClN_4S.2(CH_3)_2CO.H_2O$: C, 37.3; H, 4.49; N, 7.25; S, 4.15.

***Compound* 4.42c**

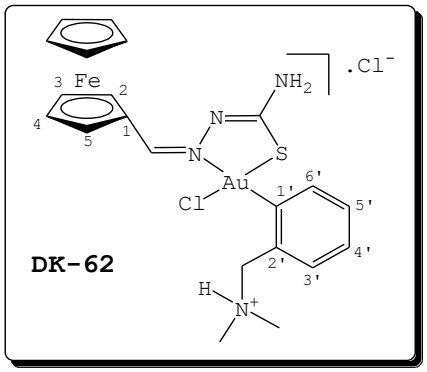

Dark-red solid (0.13 g, 98%); m.p. 142-143 °C (lit.[27] 179 °C); ν_{max} (KBr)/cm^{-1} 3264m, 3130m (NH), 2664-2466m ν(NH$^+$), 1599s, 1539s ν(C=N), 750sh ν(CS), 490s ν(Au-N), 356m,br ν(Au-S), 318m ν(Au-Cl); δ_H (400 MHz, DMSO-d_6) 10.44 (1H, br, NH$^+$), 8.17 (1H, s, HC=N), 7.73 (2H, br s, NH_2), 7.64-7.24 (4H, m,

ArH'), 5.40 (1H, s, C*H*H), 5.10 (1H, s, CH*H*), 4.69 (2H, s, H2/4), 4.46 (2H, s, H3/H5), 4.29 (5H, s, Cp), 2.74 (6H, s, $N(CH_3)_2$); *m/*z (FAB) 653.1 (100%, M^+); (Found: M^+, 653.1. $C_{21}H_{25}AuClFeN_4S$ requires M^+, 653.05), 617.1 (10%, M^+-Cl); Found: C, 38.0; H, 4.26; N, 5.90; S, 4.09; Calc. for $C_{21}H_{25}AuClFeN_4S.2CH_3OH$: C, 38.5; H, 4.63; N, 7.80; S, 4.47.

***Compound* 4.42d**

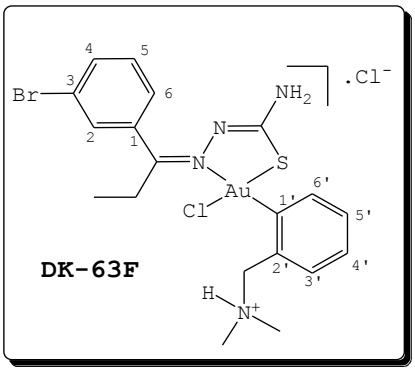

Orange-yellow solid (0.79 g, 93%); m.p. 80-82 °C; ν_{max} (KBr)/cm^{-1} 3237w ν(NH), 2683 ν(NH^+), 1698m, 1625s ν(C=N), 1537s ν(C=C), 791m ν(CS), 426w ν(Au-N), 352m ν(Au-S), 325m ν(Au-Cl); δ_H (300 MHz, DMSO-d_6) 10.83 (1H, br, NH^+), 8.16 (1H, s, H2), 7.88 (1H, d, *J* 7.2 Hz, H6), 7.62 (1H, d, *J* 7.5 Hz, H4), 7.48 (1H, m, ArH'), 7.38 (1H, t, *J* 7.8 Hz, H5), 7.27 (2H, m, ArH'), 7.17-7.11 (1H, m, ArH'), 4.62 (2H, s, CH_2), 3.18 (6H, s, $N(CH_3)_2$), 2.94 (2H, q, 7.5 Hz, CH_2), 1.0 (3H, t, *J* 7.5 Hz, CH_3), *m/*z (ESI) 651.0245 (10%, M^+); (Found: M^+, 651.0245. $C_{19}H_{24}AuBrClN_4S$ requires M^+, 651.0254), 617.0136 (100%, M^+-Cl); Found: C, 34.6; H, 4.44; N, 5.69; S, 5.33; Calc. for $C_{19}H_{24}AuBrClN_4S$: C, 34.9; H, 3.71; N, 8.58; S, 4.91.

***Compound* 4.42e**

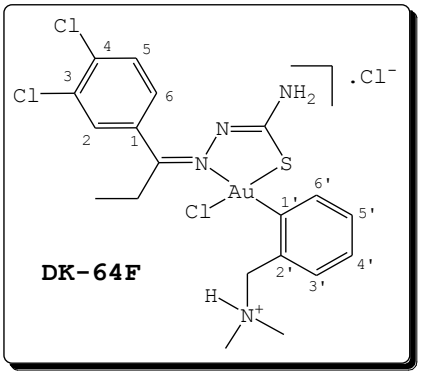

Yellow solid (0.088 g, 90%); m.p. 102-104 °C; ν_{max} (Kbr)/cm^{-1} 3237w ν(NH), 2683m ν(NH$^+$), 1698s, 1625s ν(C=N), 1543s ν(C=C), 785w ν(CS), 427w ν(Au-N), 361m ν(Au-S), 328s ν(Au-Cl); δ_H (300 MHz, DMSO-d_6) 10.77 (1H, br, NH$^+$), 8.25 (1H, s, H2), 7.88 (1H, d, *J* 7.5 Hz, H6), 7.64 (1H, d, *J* 8.4 Hz, H5), 7.48 (1H, ArH'), 7.27 (2H, m, ArH'), 7.16-7.14 (1H, m, ArH), 4.63 (2H, s, CH_2), 3.19 (6H, s, $N(CH_3)_2$), 2.94 (2H, q, *J* 7.5 Hz, CH_2), 1.0 (3H, t, *J* 7.2 Hz, CH_3); *m/*z (ESI) 641.0357 (10%, M$^+$); (Found: M$^+$, 641.0357. $C_{19}H_{23}AuCl_3N_4S$ requires *M*$^+$, 641.0369), 605.0240 (100%, M$^+$-Cl); Found: C, 37.7; H, 4.38; N, 6.85; S, 4.53; Calc. for $C_{19}H_{23}AuCl_3N_4S.2(CH_3)_2CO.2H_2O$: C, 37.8; H, 4.94; N, 7.05; S, 4.03.

***Compound* 4.42f**

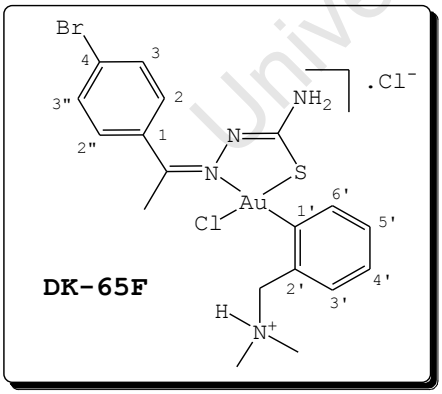

Orange-yellow powder (0.068 g, 91%); m.p. 97-99 °C; ν_{max} (Kbr)/cm^{-1} 3255w ν(NH), 1698s ν(C=N), 1585s ν(C=C), 829s ν(CS), 428w ν(Au-N), 360w ν(Au-S), 325m ν(Au-Cl); δ_H (300 MHz, DMSO-d_6) 10.45 (1H, br, NH$^+$), 7.91 (2H, d, *J* 7.8 Hz, H2/2″), 7.58 (2H, d, *J* 8.4 Hz, H3/3″), 7.51-7.47 (1H, m, ArH'), 7.27 (2H, m, ArH'), 7.16-7.13 (1H, m, ArH'), 4.62 (2H, s, CH_2), 3.19 (6H, s, $N(CH_3)_2$), 2.33 (3H, s, CH_3). *m/*z (ESI) 637.0110 (8%, M$^+$); (Found: M$^+$, 637.0110. $C_{18}H_{22}AuBrClN_4S$

requires M^+, 637.0097), 602.9982 (100%, M^+-Cl); Found: C, 36.1; H, 4.12; N, 7.52; S, 4.14; Calc. for $C_{18}H_{22}AuBrClN_4S.2(CH_3)_2CO.2H_2O$: C, 36.4; H, 4.84; N, 7.08; S, 4.05.

***Compound* 4.42g**

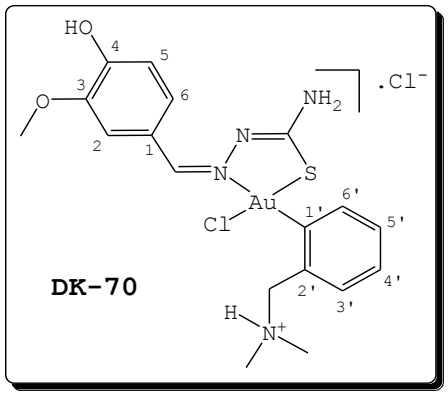

DK-70

A suspension of **3.24h** (0.079 mmol) in anhydrous MeOH (15 cm^3) was treated with **2.15** (0.23 mmol) at ambient temperature. The mixture was allowed to reflux for 2 h. The solution was filtered through celite and solvent concentrated to give an orange solid residue. Drying the residue *in vacuo* afforded **4.42g** (0.51 g, 96%) as an yellow solid;[28] m.p. 158-160 °C; ν_{max} (KBr)/cm^{-1} 3267m ν(NH), 3130br ν(OH), 2673br ν(NH^+), 1578s ν(C=N), 1533m ν(C=C), 784 ν(CS, thioamide), 366w ν(Au-S), 317w ν(Au-Cl); δ_H (300 MHz, DMSO-d_6) 10.45 (1H, br s, NH^+), 10.22 (1H, s, OH), 8.16 (1H, s, HC=N), 8.14 (2H, s, NHH), 7.81-7.76 (3H, m, H2/ArH'), 7.38 (1H, d, *J* 7.2 Hz, H6), 7.24-7.20 (2H, m, ArH'), 6.95 (1H, d, *J* 8.4 Hz, H5), 4.30 (2H, s, CH_2), 3.87 (3H, s, OCH_3), 2.65 (6H, s, $N(CH_3)_2$); *m/z* (FAB) 591.0 (65%, M^+); (Found: M^+, 591.0. $C_{18}H_{23}AuClN_4O_2S$ requires M^+, 591.09), 555.0 (30%, M^+-Cl); Found: C, 35.4; H, 4.36; N, 7.75; S, 4.05; Calc. for $C_{18}H_{23}AuClN_4O_2S.2CH_3OH$: C, 34.9; H, 4.88; N, 7.74; S, 4.43.

8.6 EXPERIMENTAL DETAILS FOR CHAPTER 6

Synthesis of Methyl Hydrazinecarbothioate 6.20

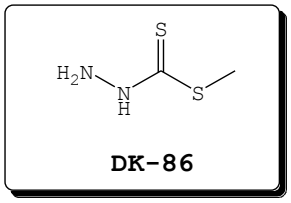

DK-86

A cooled solution of KOH (19.8 g, 300 mmol) in water (25 cm^3) and *i*PrOH (20 cm^3) was treated with hydrazine monohydrate (17 cm^3). Cold CS_2 was added dropwise to the stirred solution while maintaining the temperature below 10 °C. After 2.5 h, cold CH_3I (18.7 cm^3, 0.3 mol) was added over 2 h. After a further 90 min the white precipitate that formed was filtered, washed with cold water and recrystallised from DCM to give the **6.20** (16.0 g, 37%) as white needles,[29] m.p. 82-84 °C; ν_{max} (KBr)/cm^{-1} 3136 m (NH), 1599s δ(NH), 1283s (C=S), 709 (CS); δ_H (300 MHz, DMSO-d_6) 9.01 (br s, 1H, NH), 4.80 (br s, 1H, NH), 4.20 (br s, 1H, NH), 2.65 (s, 3H, SCH_3).

J. General Procedure for the Synthesis of TSC Thioesters 6.23a-g

A suspension of methyl hydrazinecarbodithioate **6.20** (4.11 mmol) in *i*PrOH (15 cm^3) was treated with an appropriate aldehyde and/or ketone (4.11 mmol) at ambient temperature. The mixture was stirred for 4 h accompanied by the formation of a precipitate. In some cases the precipitate formed by allowing the reaction to stir for 24 h.[29] The precipitate was filtered, washed with *i*PrOH and evaporated to afford the desired thioesters.

Methyl 3-[1-(3′-bromophenyl)ethylidene]-hydrazinecarbodithioate, 6.23a

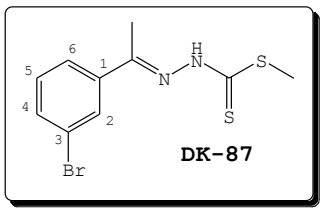

Yellowish powder (0.84 g, 68%);[30] m.p. 125-126 °C; ν_{max} (KBr)/cm^{-1} 3208s ν(NH), 1585m δ(NH), 1557s ν(C=N), 1473s ν(C=C), 1281s ν(C=S), 802s ν(C=S), 685s ν(C-S); δ_H (400 MHz, DMSO-d_6) 12.49 (1H, s, NH), 8.01 (1H, s, H2), 7.85 (1H, d, *J* 7.6 Hz, H6), 7.65 (1H, d, *J* 7.6 Hz, H4), 7.41 (1H, t, *J* 8.0 Hz, H5), 2.53 (3H, s, SCH_3), 2.38 (3H, s, CH_3).

Methyl 3-[1-(4′-bromophenyl)ethylidene]-Hydrazinecarbodithioate, 6.23b

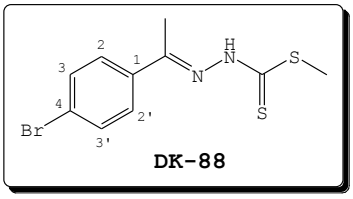

Tan powder (0.70 g, 56%);[31] m.p. 164-165 °C; ν_{max} (KBr)/cm^{-1} 3174s (NH), 1601w δ(NH), 1582m ν(C=N), 1474s ν(C=C), 1282s ν(C=S), 829s ν(C=S), 688sh ν(C-S); δ_H (400 MHz, DMSO-d_6) 12.45 (1H, s, NH), 7.80 (2H, d, *J* 8.4 Hz, H2/H2′), 7.65 (2H, d, *J* 8.4 Hz, H3/H3′), 2.52 (3H, s, SCH_3), 2.37 (3H, s, CH_3).

Ethyl 3-[1-(3′-bromophenyl)propylidene]-hydrazinecarbodithioate, 6.23c

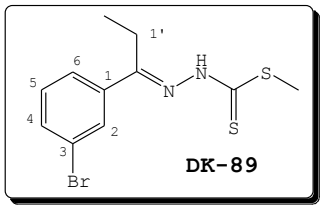

Light yellow powder (0.75 g, 58%); m.p. 100-102 °C; ν_{max} (KBr)/cm^{-1} 3168s (NH), 1585m δ(NH), 1557s (C=N), 1496s (C=C), 1288s (C=S), 816s (C=S), 692s (C-S); δ_H (400 MHz, DMSO-d_6) 12.62 (1H, s, NH), 8.01 (1H, s, H2), 7.84

(1H, d, *J* 8.0 Hz, H6), 7.65 (1H, d, *J* 8.0 Hz, H4), 7.42 (1H, t, *J* 8.0 Hz, H5), 2.94 (2H, q, *J* 7.6 Hz, H1'), 2.52 (3H, s, SCH_3), 1.03 (3H, t, *J* 7.2 Hz, CH_3).

Methyl 3-[1-(3',4'-dichlorophenyl)ethylidene]-hydrazine carbodithioate, 6.23d

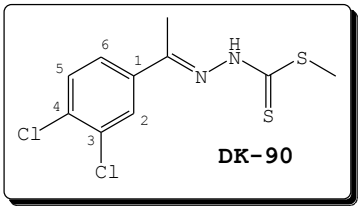

Tan powder (0.50 g, 41%); m.p. 148-149 °C; ν_{max} (KBr)/cm^{-1} 3158s (NH), 1611m δ(NH), 1552m (C=N), 1460s (C=C), 1269s (C=S), 811sh (C=S), 715sh (C-S); δ_H (400 MHz, DMSO-d_6) 12.51 (1H, s, NH), 8.02 (1H, d, *J* 2.0 Hz, H2), 7.81 (1H, dd, *J* 2.0 and 8.4 Hz, H6), 7.70 (1H, d, *J* 8.4 Hz, H5), 2.51 (3H, s, SCH_3), 2.37 (3H, s, CH_3).

Ferrocenemethylidene Hydrazinecarbothioate, 6.23e

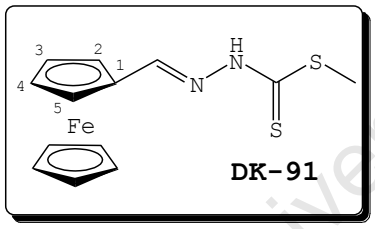

Red powder (1.12 g, 86%); m.p. 162-164 °C; ν_{max} (KBr)/cm^{-1} 3120s (NH), 1682m δ(NH), 1597s (C=N), 1522s (C=C), 1312s (C=S), 813s (C=S), 614sh (C-S); δ_H (400 MHz, DMSO-d_6) 12.99 (1H, s, NH), 8.12 (1H, s, HC=N), 4.67 (2H, s, H2/H5), 4.51 (2H, s, H3/H4), 4.24 (5H, s, Cp), 2.47 (3H, s, SCH_3).

Methyl-3-(Ferrocenyl)hydrazinecarbodithioate, 6.23f

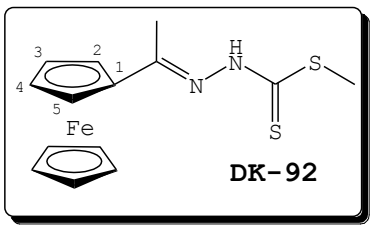

Brown powder (0.81 g, 58%);[32] m.p. 112-113 °C; ν_{max} (KBr)/cm^{-1} 3152s (NH), 1596s δ(NH), 1498s (C=N), 1460m (C=C), 1284s (C=S), 816s (C=S), 738s (C-S); δ_H (400 MHz, DMSO-d_6) 12.15 (1H, s, NH),

4.71 (2H, s, H2/H5), 4.44 (2H, s, H3/H4), 4.20 (5H, s, Cp), 2.48 (3H, s, SCH_3), 2.26 (3H, s, CH_3).

Ethyl 3-[1-(3′,4′-dichloropheny)propylidene]-Hydrazinecarbodithioate, 6.23g

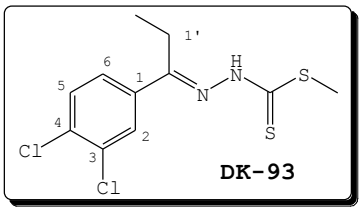

Tan powder (0.63 g, 50%); m.p. 143-145 °C; ν_{max} (KBr)/cm^{-1} 3152s (NH), 1552w δ(NH), 1497s (C=N), 1448s (C=C), 1286s (C=S), 810s (C=S), 705s (C-S); δ_H (400 MHz, DMSO-d_6) 12.65 (1H, s, NH), 8.03 (1H, d, *J* 2.0 Hz, H2), 7.81 (1H, dd, *J* 2.0 and 8.4 Hz, H6), 7.71 (1H, d, *J* 8.4 Hz, H5), 2.94 (2H, q, *J* 7.6 Hz, H1′), 2.52 (3H, s, SCH_3), 1.02 (3H, t, *J* 7.6 Hz, CH_3).

K. General Procedure for the Synthesis of Dendritic TSCs 6.24a-g

A suspension of hydrazinecarbodithioate, **6.23** (0.23 g, 0.80 mmol) in MeOH (10 ml) was treated with polypropylenimine tetraamine dendrimer (62.1 µl, 0.20 mmol) at room temperature. The mixture was allowed to reflux for 24 h. After cooling, the solution was concentrated to give a sticky yellow residue, which was dissolved in DCM (20 cm^3) and water (20 cm^3). The DCM layer was washed with water until the solution became clear and dried over Na_2SO_4. The solvent was concentrate to give from the filtrate to give a yellow semi-solid. Drying the residue *in vacuo* gave the desired dendrimer.

(2*E*,2′*E*,2″*E*,2‴*E*)-*N*,*N*′,*N*″,*N*‴-(3,3′3″,3‴)-*butane*-1,4-*diylbis*(*azanetriyl*))*tetrakis*(*propane*-3,1-*diyl*))*tetrakis*(2-(1-(3,4-*dichlorophenyl*)*ethylidene*)*hydrazinecarbothioamide*), 6.24a

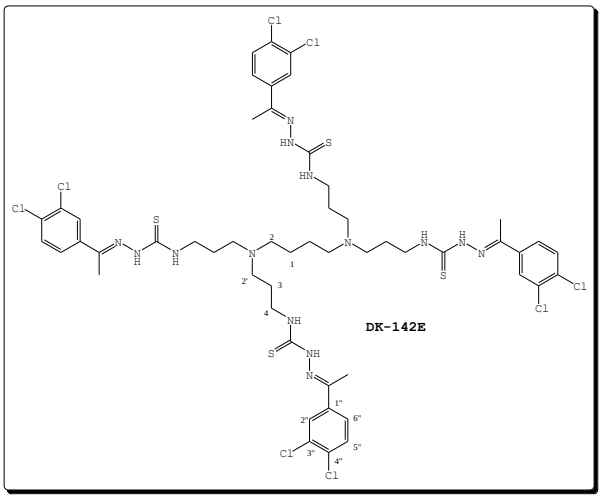

Yellow solid (0.20 g, 78%); m.p. 119-121 °C; ν_{max} (KBr)/cm^{-1} 3396m (NH), 1670s δ(NH), 1528s (C=N), 1468s (C=C), 820s (CS, thiourea); δ_H (400 MHz, DMSO-d_6) 8.64 (4H, s, HNN), 8.09-8.06 (8H, m, H2″/CH_2NH), 7.84-7.78 (4H, m, H6″), 7.59-7.56 (4H, m, H4″), 3.58 (8H, m t, H4), 2.42-2.38 (12H, m, H2/H2′), 1.70-1.68 (8H, m, H3), 1.42-1.39 (4H, m, H1); δ_C (100 MHz, DMSO-d_6) 177.3, 144.8, 137.8, 131.0, 130.7, 129.6, 127.5, 126.1, 53.1, 50.9, 42.5, 25.5, 23.8, 13.4; *m/z* (ESI) 1297.1724 (65%, M^+); (Found: M^+, 1297.1724. $C_{52}H_{64}Cl_8N_{14}S_4$ requires *M*, 1297.0424), 1051.213 (100%), 807.259 (39), 561.304 (5); Found: C, 48.1; H, 5.80; N, 14.8; S, 8.52; Calc. for $C_{52}H_{64}Cl_8N_{14}S_4$: C, 47.5; H, 5.06; N, 14.9; S, 9.75.

(2E,2E′,2E″,2E″′)-N,N′,N″,N″′-(3,3′,3″,3″′-butane-1,4-diylbis(azanetriyl))tetrakis(propane-3,1-diyl))tetrakis(2-(1-(3-bromophenyl)ethylidene)hydrazinecarbothioamide), 6.24b

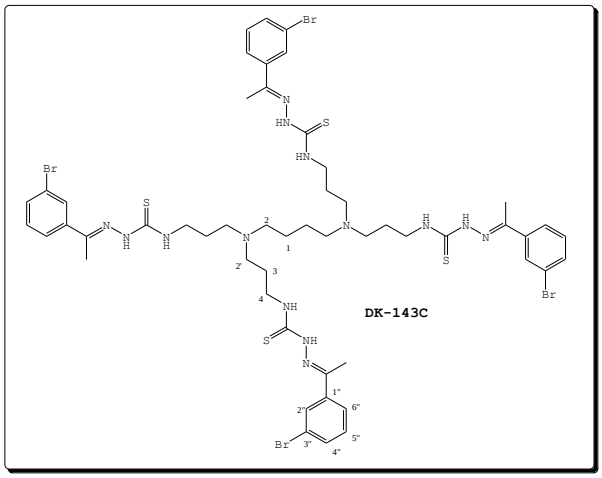

Yellow solid (0.18 g, 94%); m.p. 216-218 °C; ν_{max} (KBr)/cm^{-1} 3177m (NH), 1527s (C=N), 1466s (C=C), 834s (CS, thiourea); δ_H (400 MHz, DMSO-d_6) 8.62 (4H, s, HNN), 8.03 (8H, s, H2″/CH_2NH), 7.82 (4H, d, *J* 6.0 Hz, H6″), 7.54 (4H, d, *J* 8.0 Hz, H4″), 7.34 (4H, t, *J* 7.6 Hz, H5″), 3.61 (8H, t, *J* 4.4 Hz, H4), 2.35-2.32 (12H, m, H2/H2′), 2.28 (12H, s, CH_3), 1.71-1.68 (8H, m, H3), 1.42-1.40 (4H, m, H1); δ_C (101 MHz, DMSO-d_6) 177.7, 146.2, 140.1, 131.6, 130.1, 128.7, 125.4, 121.8, 53.5, 51.3, 43.0, 25.8, 24.2, 14.1; *m/z* (ESI) 1337.1316 (29%, M^+); (Found: M^+, 1337.1316. $C_{52}H_{68}Br_4N_{14}S_4$ requires *M*, 1337.0661), 1083.175 (100%), 827.228 (92), 571.663 (28); Found: C, 49.9; H, 6.14; N, 14.9; S, 9.10; Calc. for $C_{52}H_{68}Br_4N_{14}S_4.H_2O$: C, 46.1; H, 5.21; N, 14.5; S, 9.47.

***(2E,2′E,2″E,2″′E)-N,N′N″,N″′(3,3′3,″,3″′-(butane-1,4-diylbis(azanetriyl))tetrakis(propane-3,1-diyl))tetrakis(2-(1-(4-bromophenyl)ethylidene)hydrazinecarbothioamide,* 6.24c**

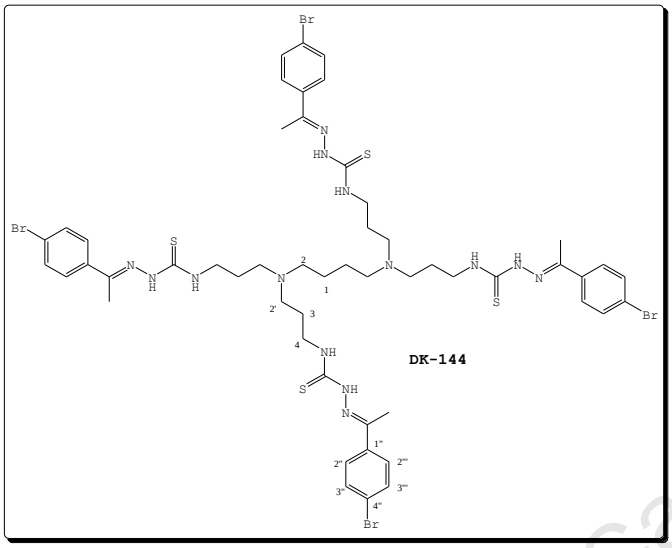

Yellow solid (0.21 g, 63%); m.p. 88-90 °C; ν_{max} (KBr)/cm^{-1} 3352w (NH), 1586w δ(NH), 1531s (C=N), 1482s (C=C), 826s (CS, thiourea); δ_H (300 MHz, DMSO-d_6) 8.49 (4H, s, HNN), 7.80 (4H, s, CH_2NH), 7.78 (8H, d, *J* 8.0 Hz, H2″/H2″′), 7.53 (8H, d, *J* 8.1 Hz, H3″/H3″′), 3.62 (8H, m, H4), 2.41 (12H, t, *J* 6.9 Hz, H2/H2″), 2.27 (12H, s, CH_3), 1.71 (8H, unresolved t, H3), 1.43 (4H, t, *J* 6.9 Hz, H1); δ_C (75.5 MHz, DMSO-d_6) 176.9, 145.6, 136.0, 130.1 (2C), 127.5 (2C), 121.6, 52.8, 50.5, 42.0, 25.1, 23.3; *m/z* (ESI) 1337.1259 (100%, M^+); (Found: M^+, 1337.1259. $C_{52}H_{68}Br_4N_{14}S_4$ requires 1337.0661), 1081.1851 (76%), 827.2379 (11), 573.2930 (8); Found: C, 47.9; H, 5.79; N, 14.6; S, 8.19; Calc. for $C_{52}H_{68}Br_4N_{14}S_4$: C, 46.71; H, 5.13; N, 14.7; S, 9.59.

(2E,2′E,2″,2″′E)-N,N′,N″,N″′-(3,3′,3″,3″′-(butane-1,4-diylbis(azanetriyl))tetrakis(propane-3,1-diyl))tetrakis(2-(1-(3-bromophenyl)propylidene)hydrazinecarbothioamide), 6.24d

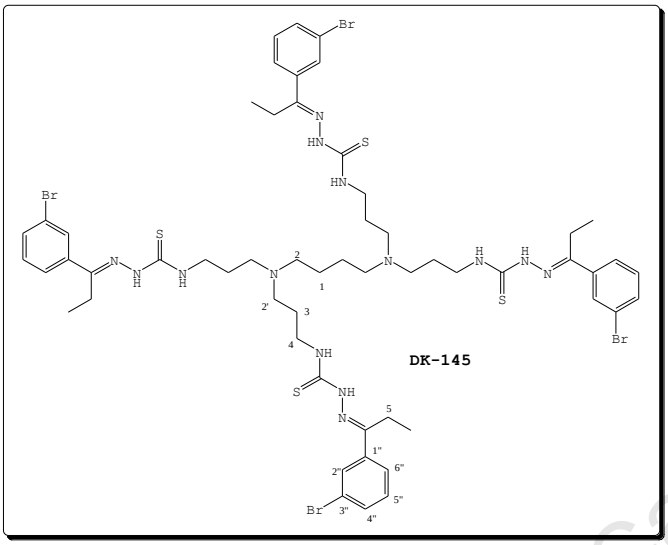

Yellow solid (0.27 g, 82%); m.p. 138-140 °C; ν_{max} (KBr)/cm^{-1} 3352w, 3177m (NH), 1527s (C=N), 1471s (C=C), 883w (CS, thiourea); δ_H (300 MHz, DMSO-d_6) 8.54 (4H, s, HNN), 7.96 (8H, s, H2″/CH_2NH), 7.79 (4H, d, *J* 7.2 Hz, H6″), 7.54 (4H, d, *J* 8.1 Hz, H4″), 7.34 (4H, m, H5″), 3.61 (8H, unresolved t, H4), 2.83 (8H, q, *J* 7.2 Hz, H5), 2.38 (12H, m, H2/H2′), 1.69 (8H, m, H3), 1.24-1.29 (4H, m, H1), 1.00 (12H, unresolved t, CH_3); δ_C (75.5 MHz, DMSO-d_6) 176.9, 149.4, 138.1, 130.7, 129.4, 127.9, 124.7, 121.0, 52.7, 50.5, 42.2, 25.0, 23.3, 18.6, 9.61; *m/z* (ESI) 1393.1880 (68%, M^+); (Found: M^+, 1393.1880. $C_{52}H_{76}Br_4N_{14}S_4$ requires M^+, 1393.1994), 1125.2191 (100%), 855.2638 (45); Found: C, 48.3; H, 5.97; N, 13.6; S, 9.70; Calc. for $C_{52}H_{64}Cl_8N_{14}S_4$: C, 48.4; H, 5.50; N, 14.1; S, 9.21.

(2*E*,2′*E*,2″*E*,2‴*E*)-*N*,*N*′,*N*″,*N*‴-(3,3′,3″,3‴-(*butane*-1,4-*diylbis*(*azanetriyl*))*tetrakis*(*propane*-3,1-*diyl*))*tetrakis*(2-(1-(3,4-*dichlorophenyl*)*propylidene*)*hydrazinecarbothioamide*), 6.24e

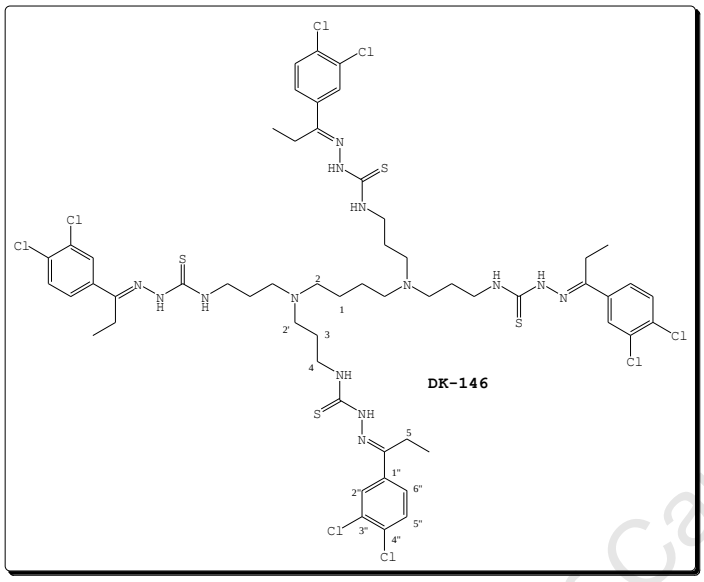

Yellow solid (0.21 g, 85%); m.p. 199-201 °C; ν_{max} (KBr)/cm^{-1} 3359w, 3167w (NH), 1527s (C=N), 1468s (C=C), 823w (CS, thiourea); δ_H (400 MHz, DMSO-d_6) 8.69 (4H, s, HNN), 8.09 (8H, s, CH_2NH/H2″), 7.83 (4H, m, H6″), 7.64 (4H, m, H5″), 3.63 (8H, m, H4), 2.88 (8H, m, H5), 2.37-2.35 (12H, m, H2/H2′), 1.72 (8H, m, H3), 1.44-1.30 (4H, m, H1), 1.0 (12H, m, CH_3); δ_C (101 MHz, DMSO-d_6) 177.7, 149.1, 137.2, 131.4, 131.3, 130.2, 128.1, 126.6, 53.5, 51.3, 42.9, 25.9, 24.2, 19.2, 10.5; *m/z* (ESI) 1353.2444 (33%, M^+); (Found: M^+, 1353.1487. $C_{56}H_{72}Cl_8N_{14}S_4$ requires M^+, 1353.1487), 1093.2708 (100%), 835.2927 (55), 575.6839 (13); Found: C, 51.3; H, 6.06; N, 15.1; S, 8.99; Calc. for $C_{56}H_{72}Cl_8N_{14}S_4$: C, 49.7; H, 5.36; N, 14.5; S, 9.48.

(2*E*,2′*E*,2″*E*,2‴*E*)-*N*,*N*′,*N*″,*N*‴-(3,3′,3″,3‴-(*butane*-1,4-*diylbis*(*azanetriyl*))*tetrakis*(*propane*-3,1-*diyl*))*tetrakis*(2-(1-(ferrocenyl)*methylidene*)*hydrazinecarbothioamide*), 6.24f

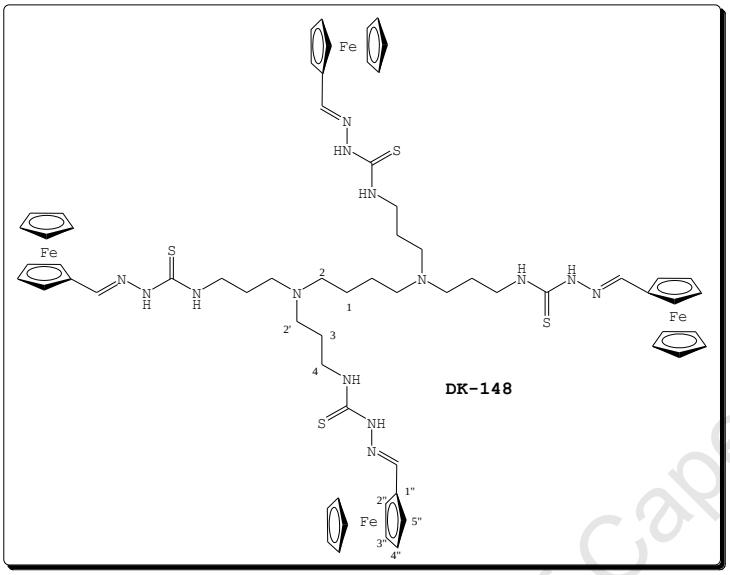

Red powder (0.28 g, 85%); m.p. 87-89 °C; ν_{max} (KBr)/cm^{-1} 3348w, 3093w (NH), 1603m δ(NH), 1531s (C=N), 1466m (C=C), 820s (CS, thiurea); δ_H (300 MHz, DMSO-d_6) 8.14 (4H, s, HNN), 7.92 (8H, s, CH_2NH/HC=N), 4.68 (8H, s, H2″/H5″), 4.41 (8H, s, H3″/H4″), 4.20 (20H, s, Cp), 3.58 (8H, t, *J* 4.8 Hz, H4), 2.46-2.40 (12H, m, H2/H2′), 1.71-1.69 (8H, m, H3), 1.51-1.49 (4H, m, H1); δ_C (75.5 MHz, DMSO-d_6) 175.7, 142.7, 78.5, 69.5 (2C), 68.4 (5C), 66.9 (2C), 53.2, 50.9, 42.2, 25.7, 24.0; *m/z* (ESI) 1397.3008 (10%, M^+); (Found: M^+, 1397.3008. $C_{64}H_{80}Fe_4N_{14}S_4$ requires M^+, 1397.0538), 1127.3112 (75%), 857.3220 (53), 584.1761 (75); Found: C, 54.9; H, 5.86; N, 11.8; S, 9.15; Calc. for $C_{64}H_{80}Fe_4N_{14}S_4$: C, 55.2; H, 5.77; N, 14.0; S, 9.18.

(2E,2′E,2″E,2″′E)-N,N′,N″,N″′-(3,3′,3″,3″′-(butane-1,4-diylbis(azanetriyl))tetrakis(propane-3,1-diyl))tetrakis(2-(1-(ferrocenyl)ethylidene)hydrazinecarbothioamide), 6.24g

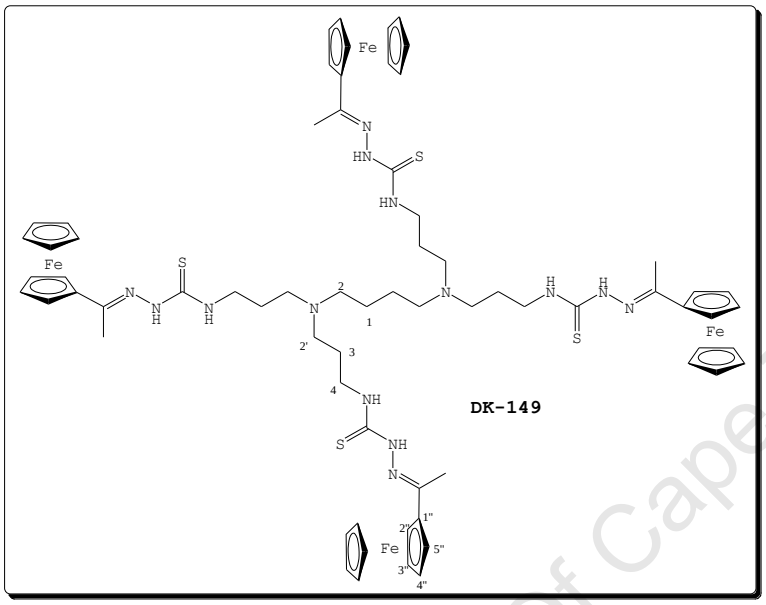

Brown pellets (0.22 g, 66%); m.p. 72-74 °C; ν_{max} (KBr)/cm^{-1} 3348w, 3079w (NH), 1626m δ(HN), 1528s (C=N), 819s (C=S); δ_H (300 MHz, DMSO-d_6) 8.21 (4H, s, HNN), 4.75 (8H, s, H2″/H5″), 4.37 (8H, s, H3″/H5″), 4.17 (20H, s, Cp), 3.84 (8H, m, H4), 2.61 (4H, s, CH_2NH), 2.42-2.34 (12H, m, H2/H2′), 2.20 (12H, s, CH_3), 1.70 (8H, m, H3), 1.48 (4H, unresolved t, H1); δ_C (75.5 MHz, DMSO-d_6) 177.3, 150.5, 83.0, 69.7 (2C), 69.0 (5C), 67.2 (2C), 53.7, 51.5, 42.7, 26.4, 24.6, 15.2; *m/z* (ESI) 1453.3694 (8%, M^+); (Found: M^+, 1453.3694. $C_{68}H_{88}Fe_4N_{14}S_4$ requires M^+, 1453.3597), 1169.0023 (80%), 885.3535 (73); Found: C, 58.4; H, 6.82; N, 12.1; S, 6.50; Calc. for $C_{68}H_{88}Fe_4N_{14}S_4$: C, 56.2; H, 6.10; N, 13.5; S, 8.83.

(2*E*,2′*E*,2″*E*)-*N*,*N*′,*N*″-(2,2′2″-*nitrilotris*(*ethane*-2,1-*diyl*)) *tris*(2-(1-(3-*bromophenyl*)*ethylidene*)*hydrazinecarbothioamide*, 6.25a

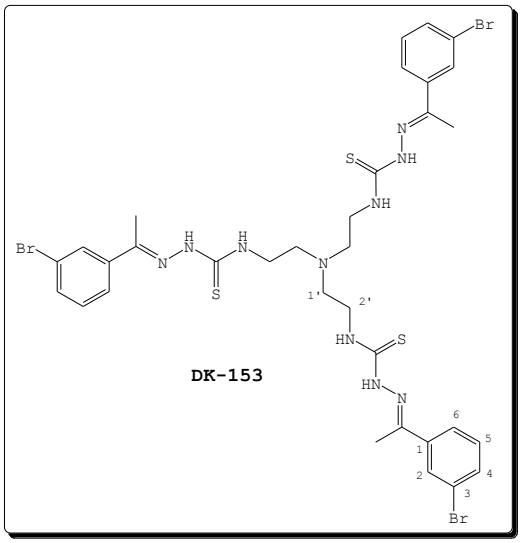

The compound was synthesised following the general procedure from **6.23a** (0.32 g, 1.04 mmol) and tris(2-aminoethyl)amine (0.05 g, 0.34 mmol), and was obtained (0.23 g, 72%) as a yellow-orange solid; m.p. 96-97 °C; ν_{max} (KBr)/cm^{-1} 3342w, (NH), 1528s (C=N), 1469m (C=C), 1286m (C=S), 784s (CS); δ_H (400 MHz, DMSO-d_6) 8.48 (3H, s, HNN), 8.02 (3H, s, H2), 7.84 (3H, d, *J* 8.0 Hz, H6), 7.57 (3H, d, *J* 7.2H, H4), 7.35 (3H, t, *J* 7.6 Hz, H5), 3.70 (6H, t, *J* 6.8 Hz, H-1′), 2.87 (6H, t, *J* 7.2, H2′), 2.27 (9H, s, CH_3); δ_C (101 MHz, DMSO-d_6) 177.8, 146.1, 139.9, 131.7, 130.2, 128.6, 125.3, 121.8, 52.4, 41.6, 13.9; *m/z* (ESI) 911.0126 (25%, M^+); (Found: M^+, 911.0126. $C_{33}H_{39}Br_3N_{10}S_3$ requires M^+, 911.6368), 657.0591 (100%); Found: C, 43.6; H, 5.03; N, 15.6; S, 8.89; Calc. for $C_{33}H_{39}Br_3N_{10}S_3$: C, 43.5; H, 4.31; N, 15.4; S, 10.6.

(2*E*,2′*E*,2″*E*)-*N*,*N*′,*N*″-(2,2′2″-*nitrilotris*(*ethane*-2,1-*diyl*)) *tris*(2-(1-(4-*bromophenyl*)*ethylidene*)*hydrazinecarbothioamide*, 6.25b

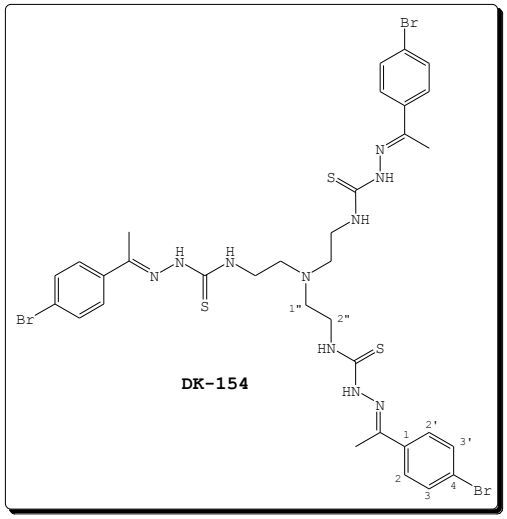

The compound was synthesised following the general procedure from **6.23b** (0.32 g, 1.04 mmol) and tris(2-aminoethyl)amine (0.05 g, 0.34 mmol), and was obtained (0.23 g, 74%) as an organge solid; m.p. 107-109 °C; ν_{max} (KBr)/cm^{-1} 3343m, 3173w (NH), 1530s (C=N), 1482s (C=C), 1288s (C=S), 824s (CS); δ_H (400 MHz, DMSO-d_6) 8.47 (3H, s, HNN), 7.81 (6H, d, *J* 8.4 Hz, H2/2′), 7.58 (6H, d, *J* 8.8 Hz, H3/3′), 3.68 (6H, t, *J* 6.8 Hz, H1″), 2.75 (6H, t, *J* 6.8 Hz, H2″), 2.25 (9H, s, CH_3); δ_C (101 MHz, DMSO-d_6) 177.8, 146.3, 136.7, 130.9 (2C), 128.3 (2), 122.4, 52.4, 41.8, 13.6; *m/z* (ESI) 912.2995 (20%, M^+); (Found: M^+, 912.2995. $C_{33}H_{39}Br_3N_{10}S_3$ requires M^+, 911.6360), 656.5025 (68); Found: C, 43.2; H, 5.18; N, 16.9; S, 9.96; Calc. for $C_{33}H_{39}Br_3N_{10}S_3.2CH_3OH$: C, 43.1; H, 4.86; N, 14.4; S, 9.86.

***(2E,2′E,2″E)-N,N′,N″-(2,2′2″-nitrilotris(ethane-2,1-diyl)) tris(2-(1-(3,4-dicholorophenyl)ethylidene) hydrazinecarbothioamide,* 6.25c**

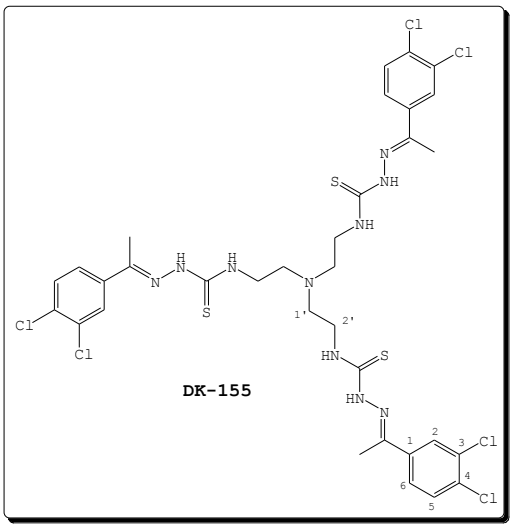

The compound was synthesised following the general procedure from **6.23d** (0.29 g, 1.04 mmol) and tris(2-aminoethyl)amine (0.05 g, 0.34 mmol), and was obtained (0.21 g, 69%) as an orange solid; m.p. 118-120 °C; ν_{max} (KBr)/cm^{-1} 3341w, 3155w (NH), 1528 (C=N), 1467s (C=C), 1291m (C=S), 817m (CS); δ_H (400 MHz, DMSO-d_6) 8.54 (3H, s, HNN), 8.06 (3H, d, *J* 1.6 Hz, H2), 7.82 (3H, dd, *J* 1.6 Hz, 8.4 Hz, H6), 7.62 (3H, d, *J* 8.8 Hz, H5), 3.69 (6H, t, *J* 6.8 Hz, H1′), 2.75 (6H, t, *J* 6.4 Hz, H2′), 2.26 (9H, s, CH_3); δ_c (100.6 MHz, DMSO-d_6) 177.9, 145.0, 138.1, 131.4, 130.1, 127.8, 126.2, 124.8, 52.3, 41.7, 13.6 *m/z* (ESI) 881.0412 (5%, M^+); (Found: M^+, 881.0412. $C_{33}H_{36}Cl_6N_{10}S_3$ requires *M*$^+$, 881.6189), 637.0580 (100%), 391.1178 (48); Found: C, 45.6; H, 4.60; N, 15.6; S, 10.9; Calc. for $C_{33}H_{36}Cl_6N_{10}S_3.CH_3OH$: C, 44.7; H, 4.41; N, 15.3; S, 10.5.

(2*E*,2′*E*,2″*E*)-*N*,*N*′,*N*″-(2,2′2″-*nitrilotris*(*ethane*-2,1-diyl)) tris(2-(1-(3-*bromophenyl*)*propylidene*)*hydrazinecarbothioamide*, 6.25d

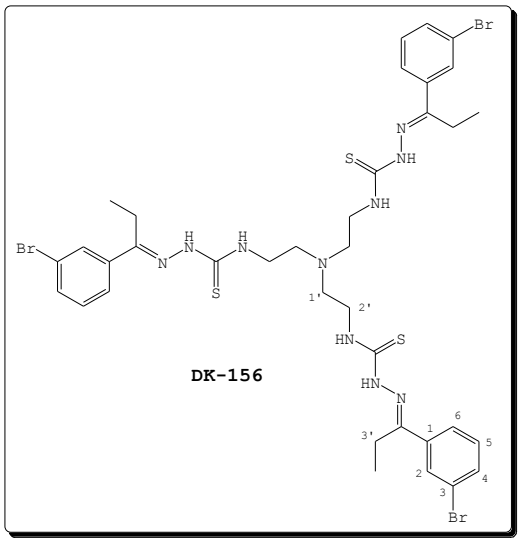

The compound was synthesised following the general procedure from **6.23c** (0.33 g, 1.04 mmol) and tris(2-aminoethyl)amine (0.05 g, 0.34 mmol), and was obtained (0.28 g, 86%) as a yellow solid, m.p. 85-87 °C; ν_{max} (KBr)/cm^{-1} 3349m, 3136m (NH), 1530s (C=N), 1284m (C=S), 784s (CS); δ_H (400 MHz, DMSO-d_6) 8.49 (3H, s, HNN), 7.98 (3H, m, H2), 7.84 (3H, m, H6), 7.55 (3H, m, H5), 7.36 (3H, m, H4), 3.75-3.70 (6H, m, H1′), 2.86-2.81 (8H, m, H2′ and H3′), 1.09-0.95 (9H, m, CH_3); δ_C (100.6 MHz, DMSO-d_6) 176.5, 148.5, 137.3, 130.1, 128.9, 127.2, 126.3, 123.9, 50.8, 40.3, 18.4, 9.14; *m/z* (ESI) 953.0519 (69%, M^+); (Found: M^+, 953.0519. $C_{36}H_{45}Br_3N_{10}S_3$ requires 953.7165), 685.0781 (100%); Found: C, 45.4; H, 4.86; N, 14.7; S, 11.2; Calc. for $C_{36}H_{45}Br_3N_{10}S_3$: C, 45.3; H, 4.76; N, 14.6; S, 10.1.

(2*E*,2′*E*,2″*E*)-*N*,*N*′,*N*″-(2,2′2″-*nitrilotris*(*ethane*-2,1-diyl))tris(2-(1-(3,4-*dichlorophenyl*)*propylidene*)*Hydrazinecarbothioamide*, 6.25f

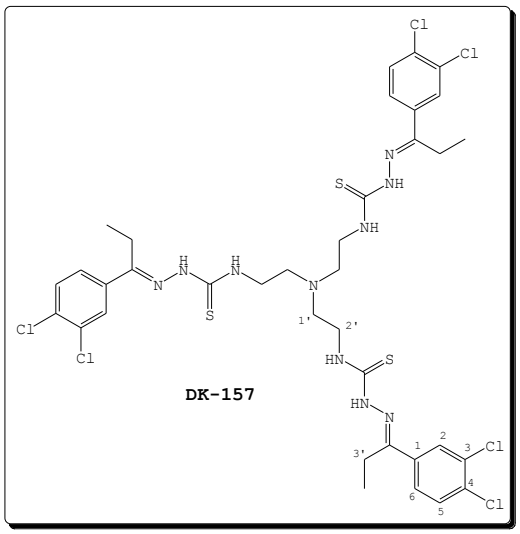

The compound was synthesised following the general procedure from **6.23g** (0.32 g, 1.04 mmol) and tris(2-aminoethyl)amine (0.05 g, 0.34 mmol), and was obtained (0.27 g, 85%) as a brownish solid; m.p. 83-85 °C; ν_{max} (KBr)/cm^{-1} 3351w, 3132w (NH), 1528s (C=N), 1471s (C=C), 1288m (C=S), 820m (CS); δ_H (400 MHz, DMSO-d_6) 8.50 (3H, s, HNN), 8.02 (3H, s, H2), 7.81 (3H, m, H6), 7.64-7.56 (3H, m, H5), 3.74-3.68 (6H, m, H1′), 2.87-2.79 (8H, m, H2′ and H3′); δ_C (100.6 MHz, DMSO-d_6) 178.1, 149.1, 137.2, 131.6, 130.4, 128.1, 126.6, 125.2, 52.4, 41.9, 19.7, 10.7; *m/z* (ESI) 923.0916 (33%, M^+); (Found: M^+, 923.0916. $C_{36}H_{42}Cl_6N_{10}S_3$ requires M^+, 923.6987), 665.1063 (100%), 405.1408 (13); Found: C, 46.9; H, 4.71; N, 16.0; S, 10.8; Calc. for $C_{36}H_{42}Cl_4N_{10}S_3$: C, 46.8; H, 4.58; N, 15.2; S, 10.4.

Synthesis of *Compound* 6.26

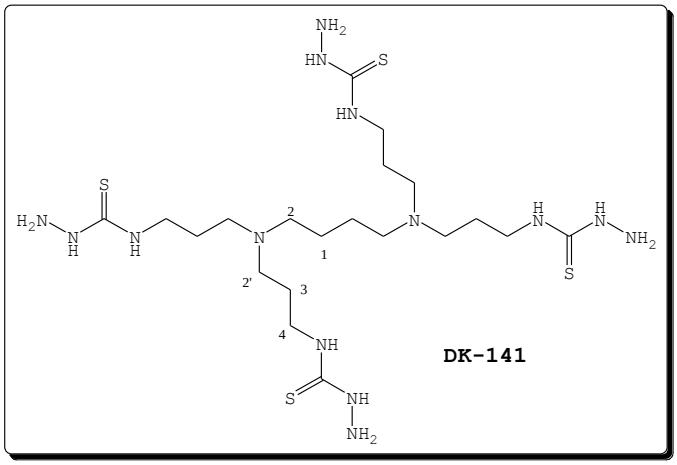

NaOH (0.77 g, 19.2 mmol) dissolved in water (40 cm^3) was treated with polypropylenimine tetraamine dendrimer (1.5 cm^3, 4.79 mmol) at room temperature. CS_2 (1.44 cm^3, 23.9 mmol) was added to the reaction mixture and allowed to stir for 4 h. The orange solution was reacted with chloroacetate (2.24 g, 19.3 mmol) and left stirring for 24 h at room temperature. The resulting brown solution was acidified (2 M HCl, 10 cm^3) followed by addition of $H_2NNH_2.H_2O$ (13 cm^3, 268.0 mmol). The mixture was heated at 90 °C for 2 h. After cooling, a 'gummy' yellow residue separated from the solution. The solution was decanted and the residue washed several times with aliquitos of water. Drying the residue *in vacuo* gave **6.26** (6.40 g, 65%) as a yellow solid; ν_{max} (KBr)/cm^{-1} ; δ_H (400 MHz, DMSO-d_6) 8.46 (4H, s, NH), 7.93 (4H, s, NH), 4.38 (8H, br, NHH), 3.45 (8H, t, *J* 6.0 Hz, H4), 2.37 (12H, t, *J* 6.0 Hz, H2/2'), 1.62 (8H, m, H3), 1.38 (2H, unresolved t, H1); δ_C (100.6 MHz, DMSO-d_6) 181.1, 53.3, 51.3, 41.9, 26.3, 24.1.

8.7 PROCEDURES FOR BIOLOGICAL ASSAYS

In Vitro Antiplasmodial Assays: D10 and W2 strains of *P. falciparum*

The test compounds were tested in duplicate against the chloroquine sensitive (CQS) strain of *P. falciparum* (D10). Continous in vitro cultures of asexual erythrocyte stages of *P. falciparum* were maintained using a modified method of Trager and Jensen.[33] Quantitative assessment of antiplasmodial activity in vitro was determined via the parasite lactate dehydrogenase assay using a modified method described by Maker.[34]

The samples were prepared to a 2 mg/ml stock solution in 10% methanol and sonicated to enhance solubility. Samples were tested as a suspension if not completely dissolved. Stock solutions were stored at -20 °C. Further dilutions were prepared on the day of the experiment. Chloroquine (CQ) was used as the reference drug in all experiments. A full dose-response was performed for all compounds to determine the concentration inhibiting 50% of parasite growth (IC_{50} – value). Test samples were tested at a starting concentration of 10 µg/ml, which was then serially diluted 2-fold in complete medium to give 10 concentrations; with the lowest concentration being 0.02 µg/ml. The same dilution technique was used for all samples. CQ was tested at a starting concentration of 100 ng/ml. The highest concentration of solvent to which the parasites were exposed to had no measurable effect on the parasite viability (data not shown). The IC_{50}-values were

obtained using a non-linear dose-response curve fitting analysis *via* Graph Pad Prism v.4.0 software.

W2-strain *P. falciparum* parasites (1% parasitaemia, 2% hematocrit) were cultured in 0.5 ml of medium in 48-well culture dishes. Appropriate inhibitors from 10 mM stocks in DMSO were added to cultured parasites to a final concentration of 20 µM. From 48-well plates, 125 µM of culture was transferred to two 96 well plates (duplicates). Serial dilutions (1%) of inhibitors were made to final concentrations of 10 µM, 2 µM, 0.4 µM, 80 nM, 16 nM and 3.2 nM. Cultures were maintained at 37 °C for 2 days after which the parasites were washed and fixed with 1% formaldehyde in PBS. After two days, parasitaemia was measured by flow cytometry using the DNA stain YOYO-1 as a marker for cell survival.[30]

***In Vitro* Assay: Falcipain-2**

IC_{50} values against the recombinant enzyme (falcipain-2) were determined as described by Du and coworkers.[30,35] Thus, equal amount of recombinant protein (*ca* 1 nM) was incubated with different concentrations of inhibitors (added from 100x stock solutions in DMSO) in 100 mM sodium acetate (pH 5.5)-10 mM dithiothreitol for 30 min at room temperature before addition of the substrate benzoxycarbonyl-Leu-Arg-7-amino-4-methyl-coumarin (final concentration = 25 µM). Fluorescence was continuously monitored for 30 min at room temperature in a Labsystems Fluoroskan® II spectrofluorometer. IC_{50} values were determined from plots of activity over inhibitor concentration with GraphPad

Prism® software. IC_{50}s for rhodesain were determined similarly at 3 nM.

In Vitro Antiplasmodial Assays: 3D7 and K1 strains of *P. falciparum*

Two clones of *P. falciparum* are used: (a) the 3D7 clone of NF_{54} which is known to be sensitive to all antimalarials, (b) the K1 strain originating from Thailand that is resistant to chloroquine and pyrimethamine, but sensitive to mefloquine. The cultures are naturally asynchronous (65 – 75% ring stage) and are maintained in continuous log phase growth in RPMI1640 medium supplemented with 5% washed human A+ erythrocytes, 25 mM Hepes, 32 nM $NaHCO_3$, and AlbuMAXII (lipid-rich bovine serum albumin) (GIBCO, Grand Island, NY) (CM). All cultures and assays are conducted at 37 °C under an atmosphere of 5% CO_2 and 5% O_2, with a balance of N_2.

Drug sensitivity assays

Stock drug solutions are prepared in 100% DMSO at 20 mg/ml unless otherwise suggested by the supplier. The compound is further diluted to the appropriate concentration using complete medium RPMI1640 supplemented with 15 nM cold hypoxanthine and AlbuMAXII. Assays are performed in sterile 96-well microtitre plates; each plate contains 100 µl of parasite culture (0.5% parasitaemia, 2.5% hematocrit). Each drug is tested in triplicate and parasite growth compared to control and blank (uninfected erythrocytes) wells. After 24 h of incubation at 37 °C, 3.7 Bq of [^{3}H]hypoxanthine is added to each well. Cultures are incubated for a further 24

h before they are harvested onto glass-fiber filter mats. The radioactivity is counted using a Wallac Microbeta 1450 scintillation counter. The results are recorded as counts per minute (CPM) per well at each drug concentration, control and blank wells. Percentage inhibition is calculated from comparison to blank and control wells, and IC_{50} values calculated using Microsoft *XL*Fit line fitting software (IDBS, UK).

Primary screen

The preliminary screen uses the 3D7 strain. The compounds are tested at 4 concentrations (30, 10, 3, 1, 0.3, and 0.1 µg/ml). If the compound does not affect parasite growth at 10 µg/ml it is classified as inactive, between 10 and 1 µg/ml, the compound is designated as partially active, and if <1 µg/ml, the compound is classified as active and is further evaluated by three-fold serial dilutions in a repeat test.

Secondary screen

Both the 3D7 clone and the K1 line are used. The compound is diluted three-fold over at 12 different concentrations with an appropriate starting concentration based on the preliminary screen. The IC_{50} is determined by a sigmoidal dose response analysis using Microsoft *XL*Fit™ (IDBS, UK). For each assay, the IC_{50} and IC_{90} values for each parasite line are determined against the known anti-malarial chloroquine, plus other standard compounds appropriate for the assay.

Cell cultures

KB cells – a cell line derived from a human carcinoma of the nasopharynx, typically used as an assay for antineoplastic agents. KB cells are maintained as monolayers in RPMI 1640 + 10% HIFCS. All cultures and assays are conducted at 37 °C under an atmosphere of 5% CO_2/95% air mixture.

Drug toxicity assays

Stock drug solutions are prepared in 100% DMSO unless otherwise suggested by the supplier at 20 mg/ml, and ball milled or sonicated if necessary. The stocks are kept at 4 °C. For the assays, the compound is further diluted to the appropriate concentration using complete medium.

Day 1: KB cells are harvested, counted and washed in serum-free medium (2000 rpm, 10 mins., 4 °C) and resuspended in fresh medium (RPMI 1640 + 10% HIFC) at a concentration of 4 × 104/ml. 100 µl is added to wells on a 96-well plate (4 × 103/well). The plate is incubated overnight at 37 °C, 5%CO_2/air mix to allow the cells to adhere.

Day 2: Test compounds are prepared in 100% DMSO 20 mg/ml and diluted down to a starting concentration of 600 µg/ml (2 × top concentration) with RPMI + 10% HIFCS. Control wells had no drug. A 10-fold serial dilution is performed across the plate – 300, 30, 3 etc. Podophyllotoxin is the control drug. The plate is incubated for 72 hours at 37 °C, 5%CO_2/air.

Day5: Each well is assessed by microscope observation. 20 µl Alamar Blue™ is then added to each well. Plates are incubated for a further 2-4 hours before reading (Gemini), EX/EM 530/580, cut-off 550 nm IC_{50} (IC_{90}) values are calculated using sigmoidal regression analysis (MS *xl*fit™).

8.8 REFERENCES

1. G.M. Sheldrick, *SHELXS-97 and SHELXL-97 Programs for crystal structure determination and refinement.* University of Gottingen, **1997**.
2. L.J. Barbour, *J. Supramol. Chem.*, **2001**, *1*, 189-191.
3. A.L. Spek, *J. Appl. Crystallogr.*, **2003**, *36*, 7-13.
4. X. Du, C. Guo, E. Hansell, P.S. Doyle, C.R. Caffrey, T.P. Holler, J.H. McKerrow, F.E. Cohen, *J. Med. Chem.*, **2002**, *45*, 2695-2707.
5. J. Liu, W. Yi, Y. Wan, L. Ma, H. Song, *Bioorg. Med. Chem.*, **2008**, *16*, 1096-1102.
6. M. Mariño, E. Gayoso, J.M. Antelo, L.A. Adrio, J.J. Fernández, J.M. Vila, *Polyhedron*, **2006**, *25*, 1449-1456.
7. J.S. Casas, M.V. Castaño, M.C. Cifuentes, J.C. García-Monteagudo, A. Sánchez, J. Sordo, U. Abram, *J. Inorg. Biochem.*, **2004**, *98*, 1009-1016.
8. J.S. Casas, M.V. Castano, M.C. Cifuentes, A. Sanchez, J. Sordo, *Polyhedron*, **2002**, *21*, 1651–1660.
9. P. Ren, T. Liu, J. Qin, C. Chen, *Spectrochimica Acta Part A*, **2003**, *59*, 1095–1101.
10. M. Abid, A.R. Bhat, F. Athar, A. Azam, *Eur. J. Med. Chem.*, **2009**, *44*, 417-425.
11. M. Abid, A. Azam, *Bioorg. Med. Chem. Lett.*, **2006**, *16*, 2812-2816.
12. G. Brauer, *Handbauch der Praparativen Anorganischen Chemie*, *Vol. 2*, 3rd ed., Verlag, Stuttgart, **1978**, 1014.
13. R. Uson, A. Laguna, M. Laguna, *Inorg. Synth.*, **1989**, *26*, 85-91.

14. P. Braunstein, H. Lehner, D. Matt, *Inorg. Synth.*, **1990**, *27*, 218.
15. A.M. Mueting, B.D. Alexander, P.D. Boyle, A.L. Casalnuovo, L.N. Ito, B.J. Johnson, L.H. Pignolet, *Inorg. Synth.*, **1992**, *29*, 279–299.
16. D.J. Daigle, A.B. Pepperman, Jr., *J. Heterocyclic Chem.*, **1974**, *11*, 407–408.
17. Z. Assefa, B.G. McBurnett, R.J. Staples, J.P. Fackler, B. Assmann, K. Angermaier, H. Schimidbaur, *Inorg. Chem.*, **1995**, *34*, 75-83.
18. D.J. Daigle, A.B. Pepperman, Jr., *J. Heterocyclic Chem.*, **1975**, *12*, 579–581.
19. J.S. Casas, E.E. Castellano, M.D. Couce, J. Ellena, A. Sanchez, J. Sordo, C. Taboada, *J. Inorg. Biochem.*, **2006**, *100*, 1858–1860.
20. M. Bardají, A. Laguna, M. Laguna, *Inorg. Chim. Acta*, **1994**, *215*, 215-218.
21. O. Bumbu, C. Silverstru, M.C. Gimeno, A. Laguna, *J. Organomet. Chem.*, **2004**, *689*, 1172–1179.
22. P.-A. Bonnardel, R.V. Parish, *J. Organomet. Chem.*, **1996**, *515*, 221–232.
23. W. R. Mason, H.B. Gray, *Inorg. Chem.*, **1968**, 7, 55–8.
24. J. Vicente, M.T. Chicote, M.D. Bermudez, *J. Organomet. Chem.*, **1984**, *268*, 191–195.
25. R.V. Parish, B.P. Howe, J.P. Wright, J. Mack, R.G. Pritchard, *Inorg. Chem.*, **1996**, *35*, 1659–1666.
26. A. Castiñeiras, S. Dehnen, A. Fuchs, I. García-Santos, P. Sevillano, *Dalton Trans.*, **2009**, 2731-2739.

27. J.S. Casas, M.V. Castaño, M.C. Cifuentes, J.C. García-Monteagudo, A. Sánchez, J. Sordo, U. Abram, *J. Inorg. Biochem.*, **2004**, *98*, 1009-1016.
28. (a) K. Ortner, U. Abram, *Inorg. Chem. Commun.* 1, **1998**, 251-253. (b) U. Abram, K. Ortner, R. Gust, K. Sommer, *J. Chem. Soc., Dalton Trans.*, **2000**, 735-744.
29. D.L. Klayman, J.P. Scovill, T.S. Bartosevich, C.J. Griffin, C.J. Mason, *J. Med. Chem.*, **1979**, *22*, 1367-1373.
30. D.C. Greenbaum, Z. Mackery, E. Hansell, P. Doyle, J. Gut, C.R. Caffrey, J. Lehman, P.J. Rosenthal, J.H. McKerrow, K. Chibale, *J. Med. Chem.*, **2004**, *47*, 3212-3219.
31. M. Munyololo, **M.Sc. Thesis**, University of Cape Town, **2006**.
32. C.-Y., Duan, Y.-P. Tian, Z.-H. Liu, X.-Z. You, T.C.W. Mak, *J. Organomet. Chem.*, **1998**, *570*, 155–162.
33. W. Trager, J.B. Jensen, *Science*, **1976**, *193*, 673-675.
34. M.T. Makler, J.M. Ries, J.A. Williams, J.E. Bancroft, R.C. Piper, B.L. Gibbins, D.J. Hinrichs, *Am. Soc. Trop. Med. Hyg.*, **1993**, *48*, 739–741.
35. (a) B.R. Shenai, P.S. Sijwali, A. Singh, P.J. Rosenthal, *J. Biol. Chem.*, **2000**, *275*, 29000-29010. (b) P.S. Sijwali; L.S. Brinen; P.J. Rosenthal, *Prot. Expr. Purif.*, **2001**, *22*, 128-134.

APPENDICES

Appendix A: Crystallographic data for compound **4.15**

Table A1: Crystal data of structure **4.15.**

Crystal Data			
Formula	$[C_{18}H_{20}N_6Au_1Br_2S_2].2(C_2H_3N).Cl^-$		
Formula Weight			858.86
Crystal System			Monoclinic
Space group		C2/c	(No. 15)
a, b, c [Angstrom]	11.846(2)	10.358(2)	24.577(5)
alpha, beta, gamma [deg]	90	101.89(3)	90
V [Ang**3]			2950.9(10)
Z			4
D(calc) [g/cm**3]			1.933
Mu(MoKa) [/mm]			7.952
F(000)			1648
Crystal Size [mm]		0.01 x 0.01 x 0.01	
Data Collection			
Temperature (K)			173
Radiation [Angstrom]		MoKa	0.71073
Theta Min-Max [Deg]			2.6, 25.3
Dataset		-14: 14 ; -12: 12 ; -29: 29	
Tot., Uniq. Data, R(int)		12752, 2705, 0.055	
Observed data [I > 2.0 sigma(I)]			2313
Refinement			
Nref, Npar			2705, 167
R, wR2, S		0.0321, 0.0688, 1.05	
w = 1/[\s^2^(Fo^2^)+(0.0282P)^2^+4.8300P] where P = (Fo^2^+2Fc^2^)/3			
Max. and Av. Shift/Error			0.00, 0.00

Min. and Max. Resd. Dens. [e/Ang^3] -0.83, 1.12

Table A2: Bond Distances (Angstrom) of **4.15.**

Au1	-S1	2.2825(13)	C5	-C6	1.387(7)
Au1	-S1_a	2.2825(13)	C6	-C7	1.378(7)
Br1	-C7	1.905(5)	C7	-C8	1.356(9)
S1	-C1	1.719(5)	C8	-C9	1.390(9)
N1	-C1	1.318(6)	C3	-H3B	0.9800
N2	-N3	1.399(5)	C3	-H3C	0.9800
N2	-C1	1.340(6)	C3	-H3A	0.9800
N3	-C2	1.287(6)	C5	-H5	0.9500
N1	-H1A	0.8800	C6	-H6	0.9500
N1	-H1B	0.8800	C8	-H8	0.9500
N2	-H2	0.8800	C9	-H9	0.9500
N4	-C10	1.127(8)	C10	-C11	1.444(8)
C2	-C3	1.496(7)	C11	-H11A	0.9800
C2	-C4	1.481(7)	C11	-H11B	0.9800
C4	-C5	1.397(7)	C11	-H11C	0.9800
C4	-C9	1.386(7)			

Table A3: Bond angles (degrees) of **4.15.**

S1	-Au1	-S1_a	170.24(6)	C7	-C8	-C9	119.8(5)
Au1	-S1	-C1	109.59(17)	C4	-C9	-C8	120.8(6)
N3	-N2	-C1	116.4(4)	C2	-C3	-H3A	109.00
N2	-N3	-C2	117.6(4)	C2	-C3	-H3B	109.00
H1A	-N1	-H1B	120.00	C2	-C3	-H3C	109.00
C1	-N1	-H1A	120.00	H3A	-C3	-H3B	109.00
C1	-N1	-H1B	120.00	H3A	-C3	-H3C	109.00
N3	-N2	-H2	122.00	H3B	-C3	-H3C	110.00
C1	-N2	-H2	122.00	C4	-C5	-H5	120.00

S1	-C1	-N1	118.2(3)	C6	-C5	-H5	120.00
S1	-C1	-N2	122.5(4)	C5	-C6	-H6	121.00
N1	-C1	-N2	119.2(4)	C7	-C6	-H6	120.00
N3	-C2	-C3	125.7(4)	C7	-C8	-H8	120.00
C3	-C2	-C4	119.2(4)	C9	-C8	-H8	120.00
N3	-C2	-C4	115.1(4)	C4	-C9	-H9	120.00
C2	-C4	-C9	121.6(5)	C8	-C9	-H9	120.00
C5	-C4	-C9	118.2(5)	N4	-C10	-C11	178.6(6)
C2	-C4	-C5	120.2(4)	C10	-C11	-H11A	109.00
C4	-C5	-C6	120.8(5)	C10	-C11	-H11B	109.00
C5	-C6	-C7	119.1(5)	C10	-C11	-H11C	109.00
Br1	-C7	-C6	120.0(4)	H11A	-C11	-H11B	109.00
C6	-C7	-C8	121.3(5)	H11A	-C11	-H11C	109.00
Br1	-C7	-C8	118.7(4)	H11B	-C11	-H11C	110.00

Table A4: Selected torsion angles (deg.) of **4.15.**

Au1	-S1	-C1	-N1	166.5(3)
Au1	-S1	-C1	-N2	-11.6(4)
C1	-N2	-N3	-C2	-170.6(4)
N3	-N2	-C1	-S1	-178.2(3)
N3	-N2	-C1	-N1	3.7(6)
N2	-N3	-C2	-C3	1.0(7)
N2	-N3	-C2	-C4	-178.6(4)
N3	-C2	-C4	-C5	22.5(7)
N3	-C2	-C4	-C9	-157.0(5)
C3	-C2	-C4	-C5	-157.2(5)
C3	-C2	-C4	-C9	23.4(7)
Br1	-C7	-C8	-C9	177.8(4)

Table A5: Hydrogen Bonds (angstrom, deg.) of **4.15.**

N1	--	H1A	N3	0.8800	2.2500	2.609(6)	104.00
N1	--	H1A	N4	0.8800	2.2800	3.030(7)	144.00
N1	--	H1B	Cl1	0.8800	2.3700	3.237(4)	168.00 5_545
N2	--	H2	Cl1	0.8800	2.5600	3.242(4)	135.00
C3	--	H3C	N2	0.9800	2.3900	2.809(6)	105.00

Appendix B: Crystallographic data for compound **4.16**

Table B1: Crystal data for structure **4.16.**

Crystal Data

Formula	$[C_{18}H_{18}N_6S_2AuCl_4].2(C_2H_3N_1).Cl^-$		
Formula Weight	838.83		
Crystal System	Monoclinic		
Space group	C2/c (No. 15)		
a, b, c [Angstrom]	11.776(2)	10.658(2)	24.515(5)
alpha, beta, gamma [deg]	90	96.79(3)	90
V [Ang**3]	3055.3(10)		
Z	4		
D(calc) [g/cm**3]	1.824		
Mu(MoKa) [/mm]	5.417		
F(000)	1632		
Crystal Size [mm]	0.05 x	0.05 x	0.05

Data Collection

Temperature (K)	173		
Radiation [Angstrom]	MoKa 0.71073		
Theta Min-Max [Deg]	2.6, 25.7		
Dataset	-14: 13 ; -11: 12 ; -28: 29		
Tot., Uniq. Data, R(int)	9300,	2889,	0.040
Observed data [I > 2.0 sigma(I)]	2377		

Refinement

Nref, Npar	2889, 176
R, wR2, S	0.0330, 0.0702, 1.07
w = 1/[\s^2^(Fo^2^)+(0.0275P)^2^+5.3451P] where P = (Fo^2^+2Fc^2^)/3	
Max. and Av. Shift/Error	0.00, 0.00
Min. and Max. Resd. Dens. [e/Ang^3]	-1.18, 1.74

Table B2: Bond distances (Angstrom) of **4.16.**

Au1	-S1	2.2818(13)	C4	-C5	1.391(7)
Au1	-S1_a	2.2818(13)	C5	-C6	1.373(7)
Cl2	-C6	1.730(5)	C6	-C7	1.382(7)
Cl3	-C7	1.737(5)	C7	-C8	1.380(7)
S1	-C1	1.729(5)	C8	-C9	1.393(7)
N1	-C1	1.314(6)	C3	-H3B	0.9800
N2	-N3	1.389(5)	C3	-H3C	0.9800
N2	-C1	1.329(6)	C3	-H3A	0.9800
N3	-C2	1.286(6)	C5	-H5	0.9500
N1	-H1A	0.8800	C8	-H8	0.9500
N1	-H1B	0.8800	C9	-H9	0.9500
N2	-H2	0.8800	C10	-C11	1.451(8)
N4	-C10	1.137(8)	C11	-H11A	0.9800
C2	-C4	1.479(6)	C11	-H11B	0.9800
C2	-C3	1.501(7)	C11	-H11C	0.9800
C4	-C9	1.391(7)			

Table B3: Bond angles (deg.) of **4.16.**

S1	-Au1	-S1_a	169.66(6)	C6	-C7	-C8	119.8(5)
Au1	-S1	-C1	109.52(17)	Cl3	-C7	-C8	118.9(4)
N3	-N2	-C1	116.5(4)	C7	-C8	-C9	120.2(5)
N2	-N3	-C2	118.7(4)	C4	-C9	-C8	120.4(4)
C1	-N1	-H1A	120.00	C2	-C3	-H3A	109.00
C1	-N1	-H1B	120.00	C2	-C3	-H3B	109.00
H1A	-N1	-H1B	120.00	C2	-C3	-H3C	109.00
C1	-N2	-H2	122.00	H3A	-C3	-H3B	110.00
N3	-N2	-H2	122.00	H3A	-C3	-H3C	109.00
S1	-C1	-N2	122.3(4)	H3B	-C3	-H3C	110.00
N1	-C1	-N2	120.2(4)	C4	-C5	-H5	119.00
S1	-C1	-N1	117.5(3)	C6	-C5	-H5	119.00
N3	-C2	-C3	126.1(4)	C7	-C8	-H8	120.00
N3	-C2	-C4	114.7(4)	C9	-C8	-H8	120.00
C3	-C2	-C4	119.2(4)	C4	-C9	-H9	120.00
C5	-C4	-C9	118.1(4)	C8	-C9	-H9	120.00
C2	-C4	-C9	121.3(4)	N4	-C10	-C11	178.5(6)
C2	-C4	-C5	120.6(4)	C10	-C11	-H11A	109.00
C4	-C5	-C6	121.6(4)	C10	-C11	-H11B	109.00
Cl2	-C6	-C5	119.4(4)	C10	-C11	-H11C	109.00
C5	-C6	-C7	119.9(4)	H11A	-C11	-H11B	109.00
Cl2	-C6	-C7	120.8(4)	H11A	-C11	-H11C	109.00
Cl3	-C7	-C6	121.3(4)	H11B	-C11	-H11C	109.00

Table B4: Selected torsion angles (deg.) in **4.16.**

Au1	-S1	-C1	-N1	162.4(3)
Au1	-S1	-C1	-N2	-16.3(4)
C1	-N2	-N3	-C2	-166.0(4)
N3	-N2	-C1	-S1	-179.8(3)

N3	-N2	-C1	-N1	1.5(6)
N2	-N3	-C2	-C3	3.1(6)
N2	-N3	-C2	-C4	-177.4(4)
N3	-C2	-C4	-C5	17.1(6)
N3	-C2	-C4	-C9	-162.9(4)
C3	-C2	-C4	-C5	-163.3(4)
C5	-C6	-C7	-Cl3	-178.7(4)
C5	-C6	-C7	-C8	1.4(7)
Cl3	-C7	-C8	-C9	178.3(4)
C6	-C7	-C8	-C9	-1.8(8)
C7	-C8	-C9	-C4	1.0(8)

Table B5: Hydrogen Bonds (Angstrom, deg.) in **4.16.**

N1	-- H1A	N3	0.8800	2.2700	2.612(5)	103.00
N1	-- H1A	N4	0.8800	2.2800	3.040(6)	144.00
N1	-- H1B	Cl1	0.8800	2.3800	3.254(4)	173.00 5_545
N2	-- H2	Cl1	0.8800	2.4700	3.221(4)	144.00
C3	-- H3C	N2	0.9800	2.4200	2.837(6)	105.00